

**Whole-cell redox biocatalysis driven by photosynthesis – an  
integrated bioprocess design for phototrophic biocatalysts**

Von der Fakultät für Lebenswissenschaften  
der Universität Leipzig  
genehmigte

**D I S S E R T A T I O N**

zur Erlangung des akademischen Grades

**Doktor der Naturwissenschaften**

**Dr. rer. nat.**

vorgelegt von

M. Sc. Anna Hoschek

geboren am 12.11.1989 in Marl

Dekan: Prof. Dr. Tilo Pompe

Gutachter: Prof. Dr. Andreas Schmid (Universität Leipzig)  
Prof. Dr. Frank Hollmann (TU Delft)

Tag der Verteidigung: 15.02.2019



## Acknowledgements

First, I would like to express gratitude to Prof. Andreas Schmid for being my doctoral father. Thank you for giving me the opportunity to work in this exceptional research and social environment. Thank you for providing me guidance and simultaneously freedom and trust in my work. You taught me to see the “big picture“ of scientific research.

Especially I want to thank Prof. Bruno Bühler for providing me the scientific supervision. You always shared your experience and gave me your support for assembling the research results to answer the key research questions.

I am grateful and happy to had the opportunity to work together with Dr. Rohan Karande. Thank you for sharing your numerous precious ideas with me which finally provided a strong basis for this thesis. I hope I can pick up some of your scientific creativity and (almost) endless enthusiasm for my future work.

I am very thankful to Prof. Dr. Katja Bühler for giving me the opportunity to make an excursion to the interesting research topic of biocatalytic biofilms. It was a pleasure and joy to experience your productive and comfortable working atmosphere.

I also thank Prof. Frank Hollmann for his willingness to be the second reviewer of my doctoral thesis and the members of the committee Prof. Christian Wilhelm, Prof. Hauke Harms, and Prof. Wolfgang Zimmermann.

I am deeply indebted to my collaborating colleagues Dr. Linde Debor and Dr. Jörg Toepel and students Adrian Hochkeppel and Tobias Kaufer who, not only, helped me with valuable hands-on experimental work but also created a joyful working atmosphere.

Very special thanks I want to express to my colleagues Magda and Marcel who became real friends of mine. Thank you so much for your succor and the great time not only at but also outside work. A sorrow shared is a sorrow halved.

The comfortable and joyful atmosphere in the SoMa and former BT group provided a valuable contribution to my work. Therefore, I would like to thank all the (former) colleagues and SoManians (Adrian, Anja, Babu, Bart, Bin, Bruno, Carolin, Caroline, Diego, Eleni, Fabian, Heiko, Inge, Jenny, Jens (Krömer and Appel), Jochen, Jörg, Kamila, Karolin, Katja, Katrin, Kerstin, Klaus, Kristin, Linde, Lisa, Magda, Mahir, Mani, Marcel, Martin (Schirmer and Lindmeyer), Marvin, Mattijs, Michael, Michelle, Olli, Paul, Peter, Rohan, Ron, Samuel, Sebastian, Stephan, the three Christians (David, Dusny, Willrodt), Tobias, Verena, and Vu).

Importantly, I would like to thank my family: Danke, Mama und Papa, für eure Unterstützung und den unentwegten Zuspruch. Danke, Christian mit Caro, Scadi und Vicky für eure Lebensfreude, die ihr mir trotz der Ferne immer zukommen lasst. Danke Oma, Edith, Axel, Thomas und Ulrich, für jegliche Unterstützung, die weltbesten Plätzchen, den Ausritt in die Natur und dafür, dass ihr meine Familie seid.

Finally, I want to express my gratitude to Christian. Thank you so much for sharing your strength and giving me support not only for accomplishing this thesis but also for the ups and downs outside work. Thank you for being part of my life and your undeviating love.



**Sunshine, sunshine reggae**

**Let the good vibes get a lot stronger**

„*Sunshine reggae*“ from Laid Back. 1983.



# Table of contents

<b>Acknowledgements</b> .....	<b>I</b>
<b>Table of contents</b> .....	<b>V</b>
<b>Summary</b> .....	<b>VII</b>
<b>Zusammenfassung</b> .....	<b>XI</b>
<b>List of abbreviations</b> .....	<b>XV</b>
<b>Chapter 1</b> General introduction.....	<b>1</b>
<b>Chapter 2</b> Materials & Methods .....	<b>31</b>
<b>Chapter 3</b> Overcoming the gas-liquid mass transfer of oxygen by coupling photosynthetic water oxidation with biocatalytic oxyfunctionalization.....	<b>45</b>
<b>Chapter 4</b> Stabilization of photosynthesis-driven whole-cell hydroxylation of nonanoic acid methyl ester by two-liquid phase biotransformation .....	<b>55</b>
<b>Chapter 5</b> Light-dependent and aeration-independent gram-scale hydroxylation of cyclohexane to cyclohexanol by CYP450 harboring <i>Synechocystis</i> sp. PCC 6803.....	<b>75</b>
<b>Chapter 6</b> Super-high cell density cultivation of <i>Synechocystis</i> sp. PCC 6803 in a mixed-trophies biofilm-based capillary reactor .....	<b>95</b>
<b>Chapter 7</b> General discussion - <i>In situ</i> O <sub>2</sub> generation for biocatalytic oxyfunctionalization reactions .....	<b>109</b>
<b>Chapter 8</b> Conclusions & Outlook.....	<b>121</b>
<b>Chapter 9</b> References .....	<b>127</b>
<b>Chapter 10</b> Appendix.....	<b>145</b>
<i>Curriculum vitae</i> .....	<b>187</b>





## Summary

Oxygenic photosynthesis constitutes a milestone of natural evolution and manifested in phototrophic organisms, such as cyanobacteria, algae, and plants. In nature, photosynthetic water oxidation served as new source for activated reduction equivalents while O<sub>2</sub>, initially a by-product, accumulated in the environment. Redox enzymes utilizing O<sub>2</sub> as electron acceptor and/ or oxygen donor developed and increased the evolutionary fitness of microorganisms harnessing these enzymes by providing them access to previously inaccessible carbon sources. Today, biocatalysis profits from these enzymes for the selective and specific conversion of substrates to fuels and value-added chemicals under mild reaction conditions. Thus far, redox biotransformations mainly rely on the application of isolated enzymes or chemoheterotrophic whole-cell biocatalysts such as *E. coli* or *Pseudomonas*. In these organisms, energy and reduction equivalents are accessed by the catabolism of carbohydrates such as glucose.

This thesis builds on a new research field that takes advantage of photosynthesis as the milestone of natural evolution. By the use of photoautotrophic organisms as biocatalytic host systems, redox reactions such as the reduction of protons to hydrogen or the oxyfunctionalization of hydrocarbons are fueled with O<sub>2</sub> and/ or reduction equivalents deriving from photosynthetic water oxidation. Photobiocatalysis therefore allows atom-efficient biotransformations and enables catalyst (re)generation based on an inorganic and abundant carbon source via CO<sub>2</sub> fixation. In the present work, recombinant cyanobacterial strains harboring different oxygenases acting as redox enzymes were generated and investigated for photosynthesis-driven biocatalysis. Subsequently, biocatalyst, reaction, and process engineering strategies were approached for the bioprocess intensification of hydrocarbon oxyfunctionalizations.

A recombinant photobiocatalyst was constructed by the genetic introduction of the three-component alkane monooxygenase AlkBGT into the cyanobacterium *Synechocystis* sp. PCC 6803 (= Syn6803\_BGT). The strain catalyzed the hydroxylation of nonanoic acid methyl ester (NAME) to 9-hydroxynonanoic acid methyl ester (H-NAME) at a rate of 1.5 U g<sub>CDW</sub><sup>-1</sup>. Under exclusion of external O<sub>2</sub> supply, Syn6803\_BGT channeled 25% of the photosynthetically generated O<sub>2</sub> *in situ* into the hydroxylation of NAME. Thus far, oxygen gas-liquid mass transfer constituted a key limitation in O<sub>2</sub> dependent bioprocesses. The developed concept of *in situ* O<sub>2</sub> generation in the liquid phase overcomes this technical limitation and thus enables the implementation of fast hydrocarbon oxyfunctionalization processes that otherwise suffer from limited O<sub>2</sub> mass transfer.

After the first proof of catalytic oxyfunctionalization activity, an integrated bioprocess engineering strategy comprising reaction and process engineering was pursued. Optimization of expression and reaction conditions, e.g., by the supplementation of the

reaction medium with  $\text{NaHCO}_3$ , enhanced the initial NAME oxyfunctionalization activity of Syn6803\_BGT to  $3.0 \text{ U g}_{\text{CDW}}^{-1}$ . In addition, specific activities were shown to be independent of the light-intensity applied during biotransformation. Thus, AlkB was assumed to indirectly couple with the photosynthetic water oxidation, potentially via the catabolism of storage compounds. Productive biotransformations with a recombinant strain lacking the electron transferring enzyme rubredoxin reductase AlkT pointed to an electron transfer from the photosynthetic metabolism to AlkB via endogenous proteins.

Continuously decreasing oxyfunctionalization activities and low biotransformation stabilities with a product yield on biomass of  $0.5 \text{ mmol}_{\text{H-NAME}} \text{ g}_{\text{CDW}}^{-1}$  were observed during long-term biotransformation with Syn6803\_BGT. Growth experiments using non-recombinant *Synechocystis* sp. PCC 6803 cells supplied with pure NAME revealed high rates of substrate hydrolysis to nonanoic acid (NA) and severe cell toxification by both reactants NAME and NA. Diisononyl phthalate (DINP) was identified as a suitable organic carrier solvent for an *in situ* substrate supply approach, because it did not, in contrast to ethyl oleate, influence the cyanobacterial cell growth negatively. Subsequent, two-liquid phase biotransformations reduced cell toxification and simultaneously enhanced substrate mass transfer and reduced NAME hydrolysis. This resulted in enhanced initial NAME hydroxylation activities of  $5.6 \text{ U g}_{\text{CDW}}^{-1}$  and prolonged biotransformation stabilities with specific yields on biomass of  $3.8 \text{ mmol}_{\text{H-NAME}} \text{ g}_{\text{CDW}}^{-1}$ . Finally, scaling of the biocatalyst cultivation and two-liquid phase biotransformation from mL scale to a multi-liter photobioreactor demonstrated the technical applicability of Syn6803\_BGT for photobiocatalytic oxyfunctionalizations of unactivated hydrocarbons.

The scope of photosynthesis-driven hydrocarbon oxyfunctionalization was broadened by the construction of another recombinant cyanobacterial strain. A cytochrome P450 cyclohexane monooxygenase originating from *Acidovorax* sp. CHX100 was genetically introduced into *Synechocystis* sp. PCC 6803, resulting in Syn6803\_CYP. The strain converted cyclohexane to cyclohexanol at high rates of  $24 \text{ U g}_{\text{CDW}}^{-1}$ , which was as fast as the recombinant heterotrophic biocatalyst *Pseudomonas* sp. VLB120 harboring the very same enzyme system. In contrast to the oxyfunctionalization activity of Syn6803\_BGT, the oxyfunctionalization rate of Syn6803\_CYP was shown to be dependent on the light-intensity, indicating a direct electron transfer from the photosynthetic light reaction to the CYP enzyme, potentially via ferredoxins or ferredoxin reductases. Also here, two-liquid phase biotransformations enhanced substrate mass transfer rates and reduced substrate toxicity. This resulted in substantially higher initial oxyfunctionalization rates of nearly  $40 \text{ U g}_{\text{CDW}}^{-1}$ . Furthermore, the biotransformation stability was prolonged from 5 to 24 h, yielding  $4.5 \text{ g g}_{\text{CDW}}^{-1}$  of the oxyfunctionalized products cyclohexanol and cyclohexanone. During scaling of the reaction system from mL scale to a multi-liter stirred tank photobioreactor,

substrate evaporation was overcome by a process operation without aeration. This process operation was enabled by the *in situ* O<sub>2</sub> generation from photosynthetic water oxidation. Finally, Syn6803\_CYP produced 2.6 g cyclohexanol from cyclohexane, water, and light and thus for the first time demonstrated the gram-scale production of oxyfunctionalized hydrocarbons with a photobiocatalytic host.

The implementation of bioprocesses on industrial scales requires high productivities and titers and thus the generation and utilization of high biomass concentrations. The technical requirements for efficient growth and use of photobiocatalysts basically rely on sufficient light input and distribution. However, scaling of established standard bioreactors, such as the applied stirred tank bioreactor, results in decreased surface to volume ratios which, in turn, lead to a diminished light availability within the reactor. Capillary reactors constitute a promising alternative reactor technology, providing high surface to volume ratios and thus efficient light input. Applying the microbial catalyst in a biofilm format further intensifies this technology, featuring self-immobilization, biocatalyst regeneration and high biomass retention. However, cultivation of *Synechocystis* sp. PCC 6803 in a biofilm-based capillary reactor was shown to result in low surface coverage and oxidative stress response due to elevated O<sub>2</sub> concentrations within the aqueous medium. In analogy to microbial mats occurring in nature, a new cultivation concept via the co-cultivation of *Synechocystis* sp. PCC 6803 with the biofilm supporting, heterotrophic strain *Pseudomonas* sp. VLB120 was established. This technology enabled stable and continuous cultivation at high cyanobacterial biomass concentrations. Furthermore, respiration of citrate by the heterotrophic strain reduced the oxidative stress resulting from supersaturated O<sub>2</sub> concentrations. Finally, cultivation of the mixed-species biofilm in a capillary reactor system enabled the retention of high biomass concentrations at 48 g<sub>BDW</sub> L<sup>-1</sup> composed of 85% (v/v) cyanobacterial cells. Such high biomass concentrations have not been reached before using standard reactor technologies like the stirred tank photobioreactor.

The results of this thesis show that photosynthesis-driven whole-cell oxyfunctionalization holds a huge potential to reach high, industrially relevant oxyfunctionalization productivities. To quantify the extent of photosynthetic water oxidation contributing to oxyfunctionalization bioprocesses, theoretical maximum productivities in the context of *in situ* O<sub>2</sub> supply in the liquid phase are discussed. For standard large-scale bioreactors a gas-liquid mass transfer constant  $k_{La}$  of 200 h<sup>-1</sup> is considered feasible, allowing maximum possible productivities of 9 g L<sup>-1</sup> h<sup>-1</sup>. Heterotrophic biocatalysts respire O<sub>2</sub> and thus inherently reduce this productivity to 5.6 g L<sup>-1</sup> h<sup>-1</sup>. In contrast, photoautotrophic biocatalysts alleviate the technical process limitation theoretically enabling productivities of up to 30 g L<sup>-1</sup> h<sup>-1</sup>. Thus, O<sub>2</sub> evolving biocatalysts bear a fundamental advantage over established, O<sub>2</sub>-respiring heterotrophic biocatalysts.

In conclusion, *Synechocystis* sp. PCC 6803 was shown to be a well suited phototrophic biocatalytic host, supplying activated reduction equivalents and O<sub>2</sub> for hydrocarbon oxyfunctionalizations. For the first time, a reaction engineering strategy demonstrated the technical applicability of cyanobacteria for the conversion of toxic and volatile compounds. The mixed-species biofilm-based capillary reactor system demonstrated a promising process technology for the application of photobiocatalysts at high biomass concentrations. Future applications may comprise the coupling of other redox reactions with the photosynthetic water oxidation. For instance, the reduction of protons using e.g., hydrogenases, constitutes a valuable strategy for the eco-efficient production of hydrogen as zero-emission fuel gas using the energy of light. By the integration of biocatalyst, reaction, and process engineering strategies, this study paves the way for the implementation of photobiocatalysts for photosynthesis-driven and eco-efficient redox reactions.

## Zusammenfassung

Die oxygene Photosynthese stellt einen Meilenstein in der natürlichen Evolution dar und manifestierte sich in phototrophen Organismen wie zum Beispiel Cyanobakterien, Algen oder Pflanzen. Die photosynthetische Wasseroxidation diente der Natur als neue Quelle für aktivierte Reduktionsäquivalente. Sauerstoff, zunächst ein Nebenprodukt, reicherte sich auf der Erde an und bildete somit die Grundlage für die Entwicklung von Redoxenzymen, welche  $O_2$  als Elektronenakzeptor und/ oder Sauerstoffdonor verwerteten. Die Nutzung dieser Enzyme ermöglichte Mikroorganismen zum Beispiel Zugang zu bisher unzugänglichen Kohlenstoffquellen, was zu einer Erhöhung ihrer evolutionären Fitness führte. Heute profitiert die Biokatalyse von solchen Redoxenzymen für die selektive und spezifische Umsetzung diverser Substrate unter milden Reaktionsbedingungen zu Kraftstoffen und hochwertigen Chemikalien. Bisher basieren Redoxbiotransformationen hauptsächlich auf dem Einsatz isolierter Enzyme sowie chemoheterotropher Ganzzellbiokatalysatoren wie *E. coli* oder *Pseudomonas*. Diese Organismen gewinnen Energie und Reduktionsäquivalente aus dem Abbau von Kohlenhydraten wie Glukose.

Die vorliegende Dissertation baut auf einem neuen Forschungsbereich auf, der sich die Vorteile der Photosynthese als Meilenstein der natürlichen Evolution zu Nutze macht. Durch den Einsatz von photoautotrophen Organismen als Biokatalysoren werden Redoxreaktionen, wie die Reduktion von Protonen zu Wasserstoff oder die Oxyfunktionalisierung von Kohlenwasserstoffen, mit  $O_2$  und/ oder Reduktionsäquivalenten aus der photosynthetischen Wasseroxidation angetrieben. Somit ermöglicht die Photobiokatalyse atom-effiziente Biotransformationen und Katalysator(re-)generation basierend auf der anorganischen und abundant verfügbaren Kohlenstoffquelle  $CO_2$ . In dieser Arbeit wurden rekombinante cyanobakterielle Stämme zur Synthese verschiedener Oxygenase-Enzymssysteme erzeugt und anschließend für die Photosynthese-getriebene Biokatalyse eingesetzt. Integrierte Biokatalysator-, Reaktions- und Prozessentwicklungsstrategien erzielten anschließend eine Intensivierung der Photosynthese-getriebenen Oxyfunktionalisierung von Kohlenwasserstoffen.

Durch die heterologe Expression der Alkanmonooxygenase AlkBGT aus *Pseudomonas putida* GpO1 in das Cyanobakterium *Synechocystis* sp. PCC 6803 wurde ein rekombinanter Photobiokatalysator erzeugt (= Syn6803\_BGT). Der Stamm katalysierte die Hydroxylierung von Pelargonsäuremethylester (PSME) zu 9-Hydroxypelargonsäuremethylester (H-PSME) mit einer Rate von  $1.5 \text{ U}_{g_{TG}^{-1}}$ . Unter Ausschluss externer  $O_2$  Zufuhr konnten 25% des photosynthetisch erzeugten  $O_2$  *in situ* für die Hydroxylierung von PSME genutzt werden. Bisher stellte der Gas-flüssig Massentransfer von  $O_2$  eine entscheidende Limitation der Skalierung von  $O_2$ -abhängigen Bioprozessen dar. Das entwickelte Konzept der photosynthetischen *in situ*  $O_2$  Erzeugung in der Flüssigphase umgeht diese technische

Limitation und ermöglicht somit die Implementierung von bisher O<sub>2</sub>-Massentransfer limitierten Prozessen zur schnellen Oxyfunktionalisierung von Kohlenwasserstoffen.

Unter Betrachtung eines integrierten Konzeptes zur Bioprozessentwicklung wurden im Anschluss die Expressions- und Reaktionsbedingungen, wie zum Beispiel die Komplementierung des Reaktionsmediums mit NaHCO<sub>3</sub>, optimiert. Dies erhöhte die initiale Rate der PSME Hydroxylierung auf 3 U g<sub>ZTG</sub><sup>-1</sup>. Syn6803\_BGT zeigte unter den eingesetzten Reaktionsbedingungen eine von der Lichtintensität unabhängige spezifische Reaktionsrate. Demnach wurde eine indirekte Kopplung der photosynthetischen Wasseroxidation mit AlkB vermutet, welches möglicherweise über den Abbau von Speicherstoffen wie Glykogen erfolgt. Die Hydroxylierung von PSME mit einem AlkB-enthaltenden cyanobakteriellen Stamm, welcher das elektronenübertragende Enzym Rubredoxin Reduktase AlkT nicht synthetisiert, belegte schließlich, dass endogene Proteine den Elektronentransfer von dem photosynthetischen Stoffwechsel zu AlkBG ermöglichen.

Die PSME Biotransformation mit Syn6803\_BGT über einen längeren Zeitraum von 30 min bis über 24 h zeigte eine kontinuierlich sinkende spezifische Aktivität und somit Reaktionsstabilität mit einem spezifischen Ausbeute von 0.5 mmol<sub>H-PSME</sub> g<sub>ZTG</sub><sup>-1</sup>. Wachstumsversuche mit nicht-rekombinanten *Synechocystis* sp. PCC 6803 Zellen zeigte eine signifikante Substrathydrolyse zu Pelargonsäure (PS), sowie eine starke Zelltoxifizierung durch die beiden Reaktanden PSME und PS. Zur Umgehung der Substrattoxizität sowie der Substratlimitierung wurde eine Strategie zur *in situ* Substratzufuhr über eine organische Trägerphase entwickelt. Diisononylphthalat (DINP) erwies sich dabei als geeignete organische Trägerphase da es, im Gegensatz zu Ethyloleat, keinen negativen Einfluss auf das Zellwachstum von *Synechocystis* sp. PCC 6803 zeigte. Anschließende Biotransformation mit organischer Trägerphase reduzierte die Zelltoxifizierung bei gleichzeitiger Erhöhung des PSME Massentransfers und reduzierter PSME Hydrolyse. Dies führte zu einer hohen initialen, spezifischen Rate der PSME Hydroxylierung von 5.6 U g<sub>ZTG</sub><sup>-1</sup> und einer verlängerten Biokatalysatorstabilität mit einer spezifischen Ausbeute von 3.8 mmol<sub>H-PSME</sub> g<sub>ZTG</sub><sup>-1</sup>. Letztlich demonstrierte die Skalierung der Biokatalysatorkultivierung sowie der Biotransformation mit organischer Trägerphase vom mL-Maßstab in den multiliter Rührkessel-Photobioreaktor die technische Anwendbarkeit von Syn6803\_BGT für die photobiokatalytische Oxyfunktionalisierung von nicht-aktivierten Kohlenwasserstoffen.

Der Umfang der Photosynthese-getriebenen Oxyfunktionalisierung von Kohlenwasserstoffen wurde durch die Entwicklung eines weiteren Photobiokatalysators erweitert. Hierzu wurde eine Cytochrom P450 Cyclohexan-Monooxygenase aus *Acidovorax* sp. CHX100 genetisch in *Synechocystis* sp. PCC 6803 eingebracht (= Syn6803\_CYP). Der Stamm katalysierte die Hydroxylierung von Cyclohexan zu Cyclohexanol mit einer spezifischen Rate von 24 U g<sub>ZTG</sub><sup>-1</sup>. Dies entspricht der Hydroxylierungsrate des rekombinanten heterotrophen Biokatalysators

*Pseudomonas* sp. VLB120, welcher das gleiche Enzymsystem trägt. Im Gegensatz zu Syn6803\_BGT zeigte Syn6803\_CYP eine Lichtintensität-abhängige spezifische Aktivität. Dies wies somit auf einen direkten Elektronentransfer von der photosynthetischen Lichtreaktion zu der Monoxygenase hin. Auch hier konnte durch die Nutzung einer organischen Trägerphase der Substratmassentransfer erhöht und die Substrattoxizität reduziert werden. Dies erhöhte die initiale, spezifische Hydroxylierungsrate auf etwa  $40 \text{ U g}_{\text{ZTG}}^{-1}$  und verlängerte die Biokatalysatorstabilität von 5 auf 24 h, was in einer spezifischen Ausbeute von  $4.5 \text{ g g}_{\text{ZTG}}^{-1}$  Cyclohexanol und Cyclohexanon resultierte. Während der anschließenden Skalierung der Biotransformation in den Rührkessel-Photobioreaktor konnte die Evaporation des leicht flüchtigen Substrates Cyclohexan durch eine Prozesskontrolle ohne Begasung, ermöglicht durch die *in situ*  $\text{O}_2$ -Bildung, verhindert werden. Schließlich produzierte Syn6803\_CYP 2.6 g Cyclohexanol aus Cyclohexan, Wasser und Licht und demonstrierte somit erstmals die Produktion von oxyfunktionalisierten Kohlenwasserstoffen im Gramm-Maßstab mithilfe eines photobiokatalytischen Hostsystems. Die Realisierung von Bioprozessen im industriellen Maßstab benötigt hohe Produktivitäten und Titer, und somit die Erzeugung und den Einsatz von hohen Biomassekonzentrationen. Die technischen Anforderungen für effizientes Wachstum und Nutzung von Photobiokatalysatoren basiert unter Anderem auf einem ausreichenden Lichteintrag. Die Skalierung von etablierten Bioreaktoren, wie dem hier eingesetzten Rührkessel Bioreaktor, führt jedoch zu einem verringerten Oberflächen zu Volumen Verhältniss, welches im Weiteren zu einem verminderten Lichteintrag in den Reaktor führt. Kapillarreaktoren stellen eine vielversprechende alternative Reaktortechnologie dar, indem sie ein hohes Oberflächen zu Volumen Verhältnis und somit maximalen Lichteintrag ermöglichen. Der Einsatz von mikrobiellen Katalysatoren im Biofilmformat erlaubt eine kontinuierliche Prozessführung, die durch die selbständige Biokatalysator Immobilisierung und Regenerierung sowie die Aufrechterhaltung hoher Biomassekonzentrationen bestärkt wird. Die Kultivierung von *Synechocystis* sp. PCC 6803 im Biofilm-basierten Kapillarreaktor wurde bereits etabliert, zeigte jedoch eine niedrige Besiedlung der Kapillaroberfläche und Reaktionen auf oxidativen Stress durch die Entwicklung von erhöhten  $\text{O}_2$  Konzentrationen in der Flüssigphase. In Anlehnung an die in der Natur vorkommenden mikrobiellen Matten („microbial mats“) wurde ein neues Kultivierungskonzept über die Co-Kultivierung von *Synechocystis* sp. PCC 6803 mit dem Biofilm-bildendend, heterotrophen Stamm *Pseudomonas* sp. VLB120 etabliert. Die Veratmung von Citrat durch *Pseudomonas* sp. VLB120 reduzierte die Sauerstoffkonzentration und verhinderte somit den oxidativen Stress auf den phototrophen Organismus. Die neue Technologie ermöglichte schließlich die stabile und kontinuierliche Kultivierung von *Synechocystis* sp. PCC 6803 mit einer hohen Biomasse von  $48 \text{ g}_{\text{ZTG}} \text{ L}^{-1}$  bestehend aus etwa 85% (v/v) cyanobakteriellen Zellen. Biomassekonzentrationen in dieser

Höhe konnten bisher nicht mit Standard-Reaktortechnologien wie dem Rührkessel-Photobioreaktor erreicht werden.

Die Ergebnisse dieser Dissertation zeigen, dass die Photosynthese-getriebene Ganzzell-Oxyfunktionalisierung von Kohlenwasserstoffen ein großes Potential für das Erreichen von industriell relevanten Produktivitäten aufweist. In einem übergeordneten Diskussionskapitel wurde das Potential der photosynthetischen Wasseroxidation für O<sub>2</sub>-abhängige Bioprozesse im Zusammenhang der *in situ* O<sub>2</sub> Erzeugung in der Flüssigphase diskutiert und über theoretisch mögliche maximale Produktivitäten veranschaulicht. Heterotrophe Biokatalysatoren veratmen O<sub>2</sub> und reduzieren somit die maximal mögliche Produktivität auf 5,6 g<sub>Produkt</sub> L<sup>-1</sup> h<sup>-1</sup> bei einer vorausgesetzten Gas-flüssig Massentransferkonstanten k<sub>La</sub> von 200 h<sup>-1</sup> für großtechnische Rührkesselreaktoren. Im Gegensatz dazu erhöhen photoautotrophe Biokatalysatoren die maximale Produktivität auf 30 g<sub>Produkt</sub> L<sup>-1</sup> h<sup>-1</sup> durch die *in situ* Erzeugung von O<sub>2</sub>. Damit erhalten O<sub>2</sub>-generierende Photobiokatalysatoren einen fundamentalen Vorteil gegenüber etablierten O<sub>2</sub>-verbrauchenden heterotrophen Biokatalysatoren.

Zusammenfassend wurde gezeigt, dass *Synechocystis* sp. PCC 6803 ein geeigneter phototropher Biokatalysator für den Zugang zu aktivierten Reduktionsäquivalenten und O<sub>2</sub> für die Oxyfunktionalisierung von Kohlenwasserstoffen darstellt. Erstmals demonstrierte eine Strategie zur Reaktionsentwicklung die technische Anwendbarkeit von Cyanobakterien zur Umsetzung von toxischen und leicht-flüchtigen Verbindungen. Der Co-Einsatz zweier Spezies aus zwei unterschiedlichen Trophien (heterotroph und phototroph) im System des biofilmbasierten Kapillarreaktors schaffte den Zugang zu hohen Biomassekonzentrationen des phototrophen Mikroorganismus *Synechocystis* sp. PCC 6803.

Zukünftige Anwendungen von Photobiokatalysatoren umfasst die Kopplung der photosynthetischen Wasseroxidation mit weiteren Redoxreaktionen. Zum Beispiel stellt die Reduktion von Protonen mithilfe von Hydrogenasen und Licht eine wertvolle Strategie zur Produktion von Wasserstoff als emissionsfreier Energieträger dar. Durch die Integration von Stamm-, Reaktions-, und Prozessentwicklungsstrategien ebnet diese Arbeit den Weg zur Implementierung von Photobiokatalysatoren für Photosynthese-getriebene und ökoeffiziente Redoxreaktionen.



## List of abbreviations

3-HP	3-hydroxypropionic acid
3-PG	3-Phosphoglycerate
a	Area
AlkB	Alkane Monooxygenase
AlkG	Rubredoxin
AlkJ	Alcohol dehydrogenase
AlkT	Rubredoxin Reductase
aq.	aqueous phase
ATP	Adenosine triphosphate
BDW	Biofilm dry weight
BEHP	Bis(2-ethylhexyl)phthalate
BVMO	Baeyer-Villiger monooxygenase
C3H	p-Coumarate-3-hydroxylase
CDH	Cyclohexanol dehydrogenase
CDW	Cell dry weight
CHXON	Cyclohexanone monooxygenase
CYP	Cytochrome P450 monooxygenase
CYPchx	Cyclohexane monooxygenase
Cyt b6f	Cytochrome b6f complex
DBMIB	2,5-Dibromo-3-methyl-6-isopropylbenzoquinone
DCMU	3-(3,4-Dichlorophenyl)-1,1-dimethylurea
DCPK	Dicyclopropyl ketone
DINP	Diisononyl phthalate
DMSO	Dimethyl sulfoxide
DSP	Downstream processing
E	Einstein ( $\mu\text{mol}_{\text{photons}}$ )
EDTA	Ethylenediaminetetraacetic acid
FAD	Flavin adenine dinucleotide
FAME	Fatty acid methyl ester
Fd	Ferredoxin
FdR	Ferredoxin reductase
FID	Flame ionization detector
FMN	Flavin mononucleotide
GAP	Glyceraldehyde 3-phosphate
GC	Gas chromatography
H <sub>cc</sub>	Henry volatility
HEPES	4-(2-Hydroxyethyl)-1-piperazinethanesulfonic acid
H-NAME	9-Hydroxynonanoic acid methyl ester
HPLC	High performance liquid chromatography
H-PSME	9-Hydroxypelargonsäuremethylester
IAM	Iodoacetamide
IPTG	Isopropyl $\beta$ -D-1-thiogalactopyranoside
ISPR	<i>In situ</i> product removal
ISSS	<i>In situ</i> substrate supply
K <sub>cat</sub>	Catalytic constant ( $\text{s}^{-1}$ )
k <sub>L</sub>	Mass transfer coefficient
k <sub>L</sub> a	Mass transfer constant
K <sub>m</sub>	Michaelis constant
Km	Kanamycin
KPi	Potassium phosphate buffer
lacI	Lac repressor
LED	Light-emitting diode
logP	Logarithmic octanol-water coefficient
MMO	Methane monooxygenase

## List of abbreviations

---

NA	Nonanoic acid
NAD(P/H)	(reduced) Nicotinamide adenine dinucleotide (phosphate)
NAME	Nonanoic acid methyl ester
OD <sub>450</sub>	Optical density at 450 nm
OD <sub>750</sub>	Optical density at 750 nm
OER	Oxygen evolution rate
OM	Outer membrane
org.	organic phase
ORR	Oxygen respiration rate
OTR	Oxygen transfer rate
P <sub>alk</sub>	Alk promoter
PAR	Photosynthetically active radiation ( $\mu\text{E m}^{-2} \text{s}^{-1}$ )
PC	Plastocyanin
Pdx	Putidaredoxin
PHA	Polyhydroxyalkanoate
PM	Plasma membrane
PMSF	Phenylmethylsulfonyl fluorid
PnrsB	NrsB promoter
PQ	Plastoquinone
PQH <sub>2</sub>	Plastoquinol
P <sub>mpB</sub>	RnpB promoter
PS	Photosystem
Ps.	<i>Pseudomonas</i> sp. VLB120
PSME	Pelargonsäuremethylester
P <sub>tac</sub>	Tac promoter
P <sub>trc</sub>	Trc promoter
PTV	Programmed temperature vaporizer
R-1,5-BP	Ribulose 1,5-bisphosphate
RBS	Ribosomal binding site
RBS*	Optimized ribosomal binding site
RT	Room temperature
RubisCO	Ribulose bisphosphate carboxylase
SDS PAGE	Sodium dodecyl sulphate-polyacrylamide gel electrophoresis
sp.	Species
STR	Stirred tank bioreactor
StyAB	Styrene Monooxygenase
Syn6803	<i>Synechocystis</i> sp. PCC 6803
T	Temperature
T <sub>An</sub>	Annealing temperature
TBS	Tris buffered saline
t <sub>elong</sub>	Elongation time
Term	Terminator
TM	Thylakoid membrane
TN	Turnover number
TTN	Total turnover number
U	Unit ( $\mu\text{mol min}^{-1}$ )
XylMO	Xylene monooxygenase
ZTG	Zelltrockengewicht

## **Chapter 1**    General introduction

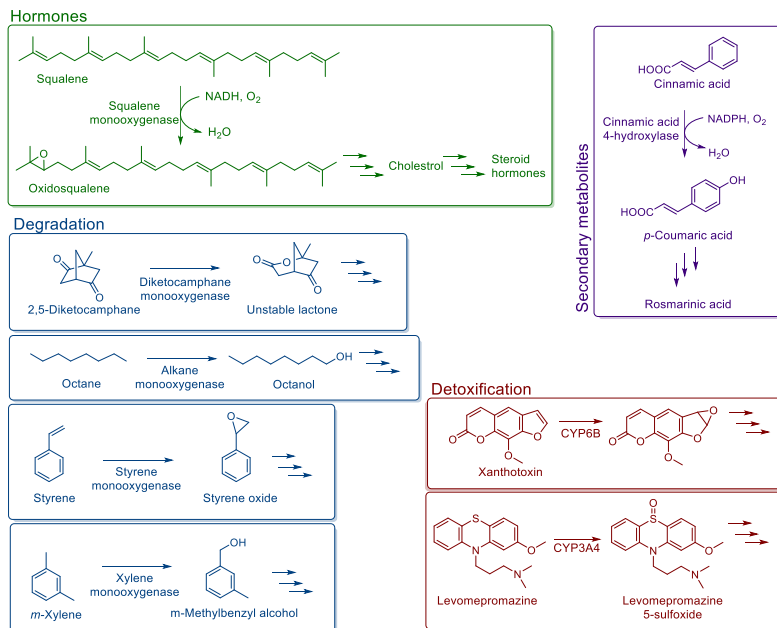
### 1.1 Photosynthesis as a driver for eco-efficient oxygenase-based biotransformations

Oxygenic photosynthesis triggered a milestone in natural evolution, occurring 2-3 billion years ago (Madigan and Martinko, 2006). The photosynthetic water oxidation provided a new source for reduction equivalents accessed by the energy of light. Oxygen, initially a by-product, accumulated in the atmosphere after oxidizing abundant reduced substances such as FeS and drove the establishment of aerobic organisms. Various enzymes catalyzing a multitude of chemical reactions developed as a result of evolutionary adaptation to the oxic atmosphere. Oxygenases make use of O<sub>2</sub> as oxygen donor and catalyze the oxyfunctionalization of diverse substrates. These enzymes increased the evolutionary fitness of microorganisms by enabling them to utilize previously inaccessible molecules as an organic carbon source. Today, organic chemistry profits from oxygenases which selectively and specifically catalyze, inter alia, hydrocarbon oxyfunctionalization reactions under mild conditions, generating value-added chemicals (Bühler and Schmid, 2004). Thus far, bioprocesses mainly rely on isolated enzymes or chemoheterotrophic whole-cell biocatalysts such as *E. coli* or Pseudomonads (Wachtmeister and Rother, 2016). In these organisms, energy and reduction equivalents are accessed by the catabolism of carbohydrates such as glucose. Although high reaction efficiencies, as well as the use of renewable organic carbons, contribute to the development of eco-efficient production processes, the implementation of such bioprocesses on industrial scales is rare.

The present study builds on a new research field that takes advantage of photosynthesis as the milestone of natural evolution. Photosynthetic water oxidation is coupled with oxygenases fueling oxyfunctionalization reactions with reduction equivalents and O<sub>2</sub> derived from water. The use of photoautotrophic host systems, therefore, enables atom-efficient bioprocesses and catalyst (re)generation based on the inorganic and abundant carbon source CO<sub>2</sub>. The following introduction briefly reviews the state of the art of oxyfunctionalization bioprocess development and outlines the new concept of photosynthesis-driven redox biotransformations. First, types and reaction mechanisms of oxygenase enzymes are explained. The following sections specify aspects relevant for industrial implementations and introduce the concept of integrated bioprocess design. The boundaries of current redox bioprocesses are then defined and followed by sections focusing on the new concept of photosynthesis-driven redox biotransformations. Oxygenic photosynthesis in general and the photosynthetic light reaction in detail are described, and trapping positions for heterologous redox enzymes are specified. Subsequently, the state of the art of photo-biotechnology is comprised. In the scope of the thesis, the current lack in developing photosynthesis-driven redox bioprocesses leads to the main research question and the key strategies used in the present dissertation.

## 1.2. Scope and mechanism of oxygenase enzymes

In nature, oxygenases ubiquitously occur in microorganisms, plants, fungi, and animals, and play a key role in numerous physiological mechanisms. As a subclass of oxidoreductases, they catalyze the transfer of electrons and oxygen, resulting in reduction and oxidation of atoms within respective substrates (**Figure 1.1**).

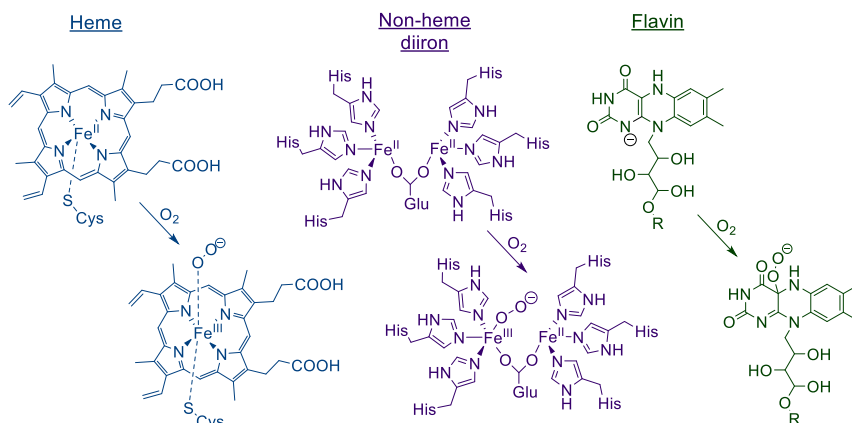


**Figure 1.1:** Scope of oxyfunctionalization reactions catalyzed by oxygenases. In nature, these enzymes harbor ubiquitous roles, e.g., in the synthesis of hormones and secondary metabolites, in the degradation/ catabolism of organic compounds, or in the detoxification of otherwise toxic chemicals.

Organic carbon sources, such as camphor (Jones *et al.*, 1993), octane (van Beilen *et al.*, 1994), styrene (Mooney *et al.*, 2006), or xylene (Harayama and Reki, 1990), are accessed by the enzymatic activation of hydrocarbon bonds. Plant toxicants, such as the furanocoumarin xanthotoxin (Schuler, 2011), or synthetic drugs, such as the neuroleptic levomepromazine (Wójcikowski *et al.*, 2014), are deactivated by initiating their catabolism. Steroid hormones are synthesized from cholesterol participated by various oxygenase enzymes (Payne and Hales, 2004), whereas cholesterol biosynthesis itself comprises an oxygenase enzyme (Laden *et al.*, 2000; Michal, 1999). In addition, various secondary metabolites, such as rosmarinic acid, are synthesized by this enzyme class (Petersen *et al.*, 2009).

### 1.2.1 What is the molecular mechanism of oxygenases?

The first experimental step towards revealing the mechanism of oxygenases took place in 1955 and was conducted independently by the two scientists Howard S. Mason (Monooxygenase Phenolase) (Mason *et al.*, 1955) and Osamu Hayaishi (Dioxygenase Pyrocatechase) (Hayaishi *et al.*, 1955). Both proved the introduction of one (monooxygenase) or two (dioxygenase) oxygen atoms from  $O_2$  into an organic substrate yielding oxyfunctionalized hydrocarbon bonds. This was in contrast to the earlier assumption that  $H_2O$  is an exclusive oxygen donor in enzymatic catalysis. The main function of oxygenase enzymes lays in the activation of oxygen driven by the donation of electrons. These enzymes act as single or as multi-component systems, rely on redox partners, and receive electrons from cofactors such as NAD(P)H. Recognition, distance, electrostatic interactions between the partners, as well as redox potentials, are essentials for successful electron transfer. Nature developed different oxyfunctionalization mechanisms that are assigned to different enzyme subclasses by the architecture of their active site (**Figure 1.2**).



**Figure 1.2:** Core active sites of heme-dependent, non-heme, and flavin-dependent oxygenases. Next to the shown diiron(II, III)-superoxo complex in the non-heme diiron oxygenase active site, also diiron(III, IV)-oxo and diiron(IV)-oxo species are possible. Flavin-dependent oxygenases: Riboflavin R=H, Flavin mononucleotide FMN R=PO<sub>3</sub><sup>2-</sup>, Flavin adenine dinucleotide FAD R=ADP.

**Heme-dependent oxygenases.** Iron-coordinated active sites characterize one of the main subclasses of oxygenases, although also copper, manganese, cobalt, and nickel-dependent oxygenases are known (Fiedler and Fischer, 2017; Liang *et al.*, 2018b; Pazmino *et al.*, 2010). Heme-dependent monooxygenases are ubiquitous enzymes and occur in eukaryotes, archaea, and bacteria. Cytochrome P450 monooxygenases (CYPs) build the major fraction in this subclass. They were named by their specific light absorption ability at 450 nm resulting from the reduced CO-bound heme-complex which is used for enzyme quantification. In the

core of the active site, an iron atom is bound to protoporphyrin IX, while a cysteine acts as the fifth ligand. Upon reduction, the iron atom binds and activates O<sub>2</sub> and substrate oxyfunctionalization can occur. Three-component monooxygenases composed of the heme-containing hydroxylase, a ferredoxin moiety that transfers electrons via Fe<sub>2</sub>S<sub>2</sub> clusters and a FAD-containing ferredoxin reductase that receives electrons from NADH are referred to class I CYPs. In contrast, class II type CYPs consist of a membrane-bound hydroxylase and a Flavin-containing ferredoxin reductase. Class III CYPs assemble the heme-containing hydroxylase as well as the Flavin-containing ferredoxin reductase moiety on a single polypeptide forming a self-sufficient protein. Recently, also a class IV CYP category was discovered that assembles the three components of heme-hydroxylase, Fe<sub>2</sub>S<sub>2</sub>-ferredoxin and Flavin-ferredoxin reductase in one protein.

Peroxygenases constitute another heme-dependent oxygenase subclass that is structurally related to CYPs and make use of H<sub>2</sub>O<sub>2</sub> as oxygen donor (Bormann *et al.*, 2015; Wang *et al.*, 2017). The reaction mechanism is independent of nicotinamide cofactors and other electron supplying proteins and resembles the peroxide shunt of CYPs.

**Non-heme iron oxygenases.** Non-heme iron oxygenases have evolved in parallel with cytochrome P450s (Jasniewski and Que Jr, 2018; Pazmino *et al.*, 2010). Both, mono- and di-nuclear iron centers coordinated within the enzyme active site are known. Mono-nuclear active sites often occur in dioxygenases and lipoxygenases (Salomon *et al.*, 2013). Di-iron catalytic centers are bridged, e.g., by a glutamate residue, while glutamate or histidine residues arrange the octahedral coordination of the iron atoms and are complemented by solvent-derived water and hydroxide ions. Well studied non-heme diiron monooxygenases are the three-component soluble methane monooxygenase MMO (Dalton, 1980; Merx *et al.*, 2001), the membrane-bound three-component alkane monooxygenase AlkBGT (Austin and Groves, 2011; Peterson *et al.*, 1966a), as well as the membrane-bound two-component xylene monooxygenases XylMO (Suzuki *et al.*, 1991).

**Flavin-based oxygenases.** The active site of oxygenases can also be built on carbon-based catalytic centers such as Flavin-containing (covalent = prosthetic) or Flavin-dependent (external Flavin = coenzyme) oxygenases (Liang *et al.*, 2018b; Pazmino *et al.*, 2010). Flavin-based enzymes are abundant in prokaryotic organisms and make use of Flavin Mononucleotide (FMN) or Flavin adenine dinucleotide (FAD) as cofactors. Examples are the FAD-containing squalene monooxygenase (Laden *et al.*, 2000), the external flavoprotein styrene monooxygenase StyAB (Hartmans *et al.*, 1990), and the Baeyer-Villiger diketocamphane monooxygenase (Jones *et al.*, 1993).

### 1.2.2 Why are oxygenases interesting for the chemical industry?

As already highlighted by the physiological mechanisms in nature, both the reaction as well as the substrate variety covered by the oxygenase subclass is huge. Non-activated **hydrocarbons**, such as the alkanes octane (Peterson *et al.*, 1966a) and xylene (Suzuki *et al.*, 1991) are **hydroxylated**, while unsaturated hydrocarbons, such as styrene (Hartmans *et al.*, 1990) or squalene (Laden *et al.*, 2000) are **epoxidized**. Aldehydes and ketones are converted to the respective esters by **Baeyer-Villiger** Monooxygenases, as for example known for the oxidation of the cyclic ketone diketocamphane (Jones *et al.*, 1993) to the corresponding lactone. Next to hydrocarbons, also compounds containing heteroatoms such as sulfides or amines can be oxygenated to **sulfoxides** (Wójcikowski *et al.*, 2014) or **oximes** (Zhu *et al.*, 2013).

In addition to the huge chemical variety concerning the substrate scope, oxygenase enzymes act incomparably regio-, chemo-, and enantioselective by embedding their substrate in a well-aligned binding pocket (Liang *et al.*, 2018b). This, together with the fact that enzymes operate under mild conditions (neutral pH, low temperature, low pressure, aqueous solvents), turns oxygenases into a highly promising catalyst for the chemical industry. Oxygenated compounds are ubiquitous in all product classes of pharma, fine and bulk chemicals. Structural complex molecules are found in pharmaceutical compounds, such as the cholesterol-derived anti-inflammatory drug cortisone, and can be accessed by the application of oxygenases (Hudlicky and Reed, 2009). Chiral building blocks, such as chiral alcohols, complement the fine chemical industry. Oxygenated hydrocarbons function as building blocks for the polymer industry (Evonik Industries AG, 2013; Karande *et al.*, 2017; Ladkau *et al.*, 2016).

### 1.3 Development of oxygenation bioprocesses

#### 1.3.1 Targets for industrial implementation

Referring to the Darwinian evolutionary theory, the driver for natural evolution is 'survival of the fittest'. Oxygenase-catalyzed oxygenation reactions evolved within the framework of physiological mechanisms with the target of maximizing the efficiency of maintenance, growth, and reproduction. In contrast, chemical synthesis aims at maximum (oxygenated) product formation, irrespective of being driven by chemical, enzymatic or whole-cell (bio-) catalysis. Thus, bioprocess development tasks the change of the microbial objective from exclusive survival to the maximized production of target compounds.

The ambition of developing new processes relies on both, economic as well as ecologic aspects summarized by the descriptor 'eco-efficiency' as done, e.g., by the World Business Council for Sustainable Development (WBCSD, 2000). On the one hand, economic feasibility refers to the margin between production cost and product value and is explicitly determined



by the capital investment costs (CapEx, e.g., equipment), the operational costs (OpEx, e.g., raw materials, utilities, waste, maintenance) and the manufacturability (Tufvesson *et al.*, 2010). On the other hand, ecologic aspects refer to a sustainable design of a chemical production process, being manifested in the twelve principles of Green Chemistry: Prevention, Atom Economy, Less Hazardous Chemical Synthesis, Designing Safer Chemicals, Safer Solvents and Auxiliaries, Design for Energy Efficiency, Use of Renewable Feedstocks, Reduce Derivatives, Catalysis, Design for Degradation, Real-Time Analysis for Pollution Prevention, Inherently Safer Chemistry for Accident Prevention (Anastas and Eghbali, 2010). Importantly, although often associated with the term “green”, biocatalysis per se does not account for green chemistry, and careful quantification of the environmental impacts is essential (Ni *et al.*, 2014). In general, process efficiency directly affects the production costs and the raw material input, therefore being a crucial parameter in tuning the eco-efficiency during process development. Three key metrics determine the process efficiency (Straathof *et al.*, 2002):

- Productivity, space-time yield ( $\text{g L}^{-1} \text{h}^{-1}$ )
- product titer ( $\text{g L}^{-1}$ ), and
- product yield ( $\text{g g}_{\text{substrate}}^{-1}$  or  $\text{g g}_{\text{catalyst}}^{-1}$ )

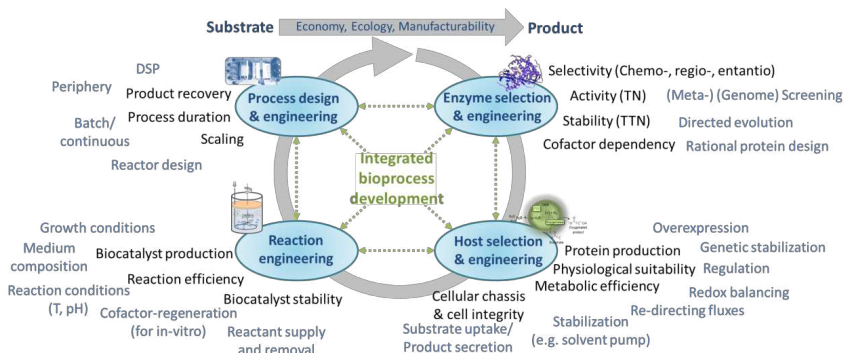
The very consideration of economic viability requires productivities and titer of at least  $0.001 \text{ g L}^{-1} \text{h}^{-1}$  and  $0.1 \text{ g L}^{-1}$ , respectively, for high-priced compounds mainly found in the pharmaceutical industries (Julsing *et al.*, 2008). For mid-priced chemicals, seen in the fine and the bulk chemical industry, the demand for efficiency further increases. Productivities and titers should be as high as  $0.1 \text{ g L}^{-1} \text{h}^{-1}$  and  $1 \text{ g L}^{-1}$ , respectively. Concerning whole-cell biocatalytic applications, product yields on biocatalysts should range from  $10 \text{ g g}_{\text{CDW}}^{-1}$  (pharmaceutical compounds) to  $2000 \text{ g g}_{\text{CDW}}^{-1}$  (bulk chemicals) (Tufvesson *et al.*, 2010). Thus, biocatalytic activity, as well as stability, are two main parameters determining the successful implementation of a bioprocess.

### 1.3.2 Concept of integrated bioprocess design

The eco-efficient use of oxygenases, irrespective of applied as isolated enzymes or in whole-cells, meeting requirements of economy, ecology, and manufacturability is possible with a process design taking numerous different aspects into account. In a rational approach, the development of a bioprocess can pass four levels of engineering addressing enzyme, host, reaction, and process (**Figure 1.3**) (Karande *et al.*, 2016b; Schmid *et al.*, 2001; Willrodt *et al.*, 2015b). Within each level, the optimization of distinct targets is addressed by numerous strategies/ parameters. Thereby, the selection and technological implementation of these strategies is governed by the mutual interconnection of the four engineering levels.

The transfer of a microbial cell from its natural status to a well-functioning biocatalyst in a

technical setting changes the objective from survival to maximizing product formation (Volmer *et al.*, 2015). Deciphering these differences and similarities allows the optimization and particularly exploitation of technologies that were designed by nature's evolution for chemical synthesis.



**Figure 1.3:** Concept of integrated bioprocess design. The development of bioprocesses meeting requirements of economy, ecology, and manufacturability necessitates the integrated consideration of the four levels of enzyme, host, reaction, and process engineering. Within each level, the optimization of distinct targets is addressed by numerous strategies/ parameters. Thereby, the selection and technological implementation of these strategies is governed by the mutual interconnection of the four engineering levels. Figure adapted from Schmid *et al.* 2001 (Schmid *et al.*, 2001).

Holistic biocatalysis cycles were developed guiding towards individual objectives such as aligning bioprocess development with physicochemical properties of the reactants or hydrocarbon oxyfunctionalization (Bühler and Schmid, 2004; Willrodt *et al.*, 2015b). Although each development step requires in-depth knowledge of particular engineering technologies, the early integration of analysis as well as optimization strategies on all levels of engineering strengthens and accelerates bioprocess design. During (isolated enzyme or whole-cell) biocatalyst development, the optimization towards the final reaction and process setting is of high importance as, for instance, the microenvironment changes from mL-scale shake flask to m<sup>3</sup>-scale bioreactors which may result in fundamental changes concerning the process performance. Today, the process setup is designed to match the biocatalyst requirements. However, the reverse handling, e.g., by directed evolution of the biocatalysts under real process conditions, allows for selecting and engineering the biocatalyst to match the existing process design (Burton *et al.*, 2002; Hibbert *et al.*, 2005; Woodley, 2018). Particular technologies such as single-cell analysis support the evaluation of the performance of individual cells under reaction and process conditions and enable the identification and optimization of bottlenecks in the process efficiency induced for instance by heterogeneity and population dynamics (Rosenthal *et al.*, 2017). Systems biology, which is the quantitative

description of cellular functions, e.g., using omics tools, becomes an integrating engineering tool by implementing the knowledge on reaction and process requirements of a targeted bioprocess with the rational engineering of the biocatalyst (Kuhn *et al.*, 2010a). A systematic understanding and the ability to address problems on all levels of bioprocess development enables prolonged and thus more efficient bioprocesses with enhanced yields and titers (Kadisich *et al.*, 2017b).

The following section introduces engineering strategies applied for improving the oxygenase bioprocess efficiency and is clustered according to the four levels of bioprocess design just introduced.

### **1.3.3 Enzyme selection and engineering**

Selectivity, activity, and stability are the key targets for enzyme selection and engineering and are quantified by the product composition, turnover number, and total turnover number. When starting bioprocess development, the choice of the right enzymatic catalyst is crucial. Screening and isolation of enzymes from natural sources with a microenvironment fitting to the intended bioprocess is very promising (Watts *et al.*, 2005). One example is the catalyst CYP450chx used for cyclohexane oxyfunctionalization, which was identified from a bacterial strain isolated from a biotrickling filter applied for cleaning air containing cyclohexane as contaminant (Salamanca and Engesser, 2014; Salamanca *et al.*, 2015). In case, the portfolio of the naturally available enzyme does not fit the required reaction requirements concerning selectivity, activity, or stability, enzyme engineering can be pursued to optimize the performance (Bloom *et al.*, 2005; Bornscheuer *et al.*, 2012; Kuchner and Arnold, 1997). The prospects of enzyme engineering technologies are studied extensively at one of the best-known oxygenases, P450 BM3 (= CYP102A1) (Whitehouse *et al.*, 2012). This class III CYP is the third isolated oxygenase from *Bacillus megaterium*. The non-engineered enzyme hydroxylates medium- to long-chain fatty acids (C<sub>12</sub>-C<sub>20</sub>) at the sub-terminal positions using NADPH as a cofactor. P450 BM3 shows the highest known oxygenase activity ( $k_{\text{cat}} = 285 \text{ s}^{-1}$  determined via arachidonate-induced NADPH oxidation) (Noble *et al.*, 1999). Protein engineering efforts can facilitate broader substrate diversity, higher activities towards non-natural substrates, and increased catalyst lifetimes (Whitehouse *et al.*, 2012). Rational design by molecular modeling and site-directed evolution of P450 BM3, for instance, enabled hydroxylation of the aromatic isoflavone daidzein at distinct positions (Ko *et al.*, 2015). Random mutagenesis resulted in an enzyme capable of the hydroxylation of alkanes (Glieder *et al.*, 2002). Site-directed mutagenesis enhanced the oxidation rate of polycyclic aromatic hydrocarbons 200-fold. Increasing product formation rates often goes along with increased unproductive NAD(P)H oxidation rates (uncoupling), mainly derived from the un-proper fitting of the substrate within the active site (Carmichael and Wong, 2001). Protein engineering can enhance the coupling efficiency and therefore the protein stability regarding the total turnover

number (Fasan *et al.*, 2007). Another simple but efficient method of protein engineering is the design of synthetic fusion proteins (Yu *et al.*, 2015b). Electron transferring components, such as the reductase domain of P450 BM3, can be fused to oxygenase enzymes, enhancing the electron transfer efficiency (Scheeps *et al.*, 2013). Multi-step reactions can profit from enzymes brought in spatial proximity resulting in the conversion of otherwise accumulating intermediates (Willrodt *et al.*, 2015a). In addition to the protein efficiency-determining metrics, the cofactor dependency of oxygenases influences the subsequent bioprocess design. This is especially important for whole-cell applications, where the scope of available cofactors varies among the microbial species. Using protein engineering, the NADPH – NADH cofactor dependency can be modulated as likewise shown for the P450 BM3 (Girvan *et al.*, 2011; Neeli *et al.*, 2005).

### 1.3.4 Host selection and engineering

Once an appropriate (oxygenase) enzyme is chosen and, if necessary and successfully engineered, subsequent catalysis requires a suitable host system. Thereby, protein production, physiological suitability, metabolic efficiency, and cellular chassis, as well as cell integrity, are key targets that require special consideration and, if needed, optimization. Whether the microbial cell functions as protein production host only or as a whole-cell biocatalyst for the catalytic reaction is one of the first choices made during the bioprocess development. In the case of oxygenase-based catalysis, numerous advantageous for *in vivo* or *in vitro* applications, respectively, exist (de Carvalho, 2011). Whole-cells provide an endogenous cofactor as well as protein regeneration system. The microbial cell presents a natural environment, protecting the proteins from destabilizing conditions such as organic solvents. Inherently, *in vivo* application avoids the purification of, potentially membrane-bound, (multi-component) oxygenases. In contrast, the use of isolated enzymes provides high flexibility, e.g., for combining specific catalytic reactions for multi-step catalysis. Substrate and product mass transfer remain unlimited, and no side-reactions occur from microbial host intrinsic enzymes. Protein engineering enabled the stable use of oxygenases in organic media or ionic liquids. In-situ cofactor regeneration is possible, e.g., by enzymatic, chemical or electrochemical approaches.

**Host selection.** Natural sources already provide optimized microbial systems as a result of elaborate evolution. The native organism synthesizes the enzyme of choice in a correctly folded and therefore active conformation. Posttranslational modifications, such as glycosylation, and support of protein folding, e.g., by chaperones, are well-established in these organisms. In contrast to the natural host systems, the technical use of proteins demands high concentrations accompanied by simple cultivation technology (reducing production costs) and ease of manipulation (Carvalho, 2017). Typical organisms for biocatalytic enzyme production and application are prokaryotic microorganisms such as

*E. coli*, Pseudomonads, *Bacillus* sp., and eukaryotic yeasts such as *Saccharomyces cerevisiae* or *Pichia pastoris*. Yeasts possess organelles providing compartmentalization and much space for the incorporation of membrane proteins as frequently the case of oxygenases. Some extremophile bacteria, often *Pseudomonas* species, show an increased tolerance towards solvents such as cyclohexane or styrene (Sardessai and Bhosle, 2004). This is beneficial for the application of such organic solvents as carrier phase for hydrophobic and therefore low water-soluble compounds, e.g., testosterone, as they predominantly occur as substrates for oxyfunctionalization catalysis (Kuhn *et al.*, 2012a; Ruijssenaars *et al.*, 2007). Given heme-containing oxygenases, host systems that endogenously synthesize aminolevulinic acid for porphyrin biosynthesis are preferred (Julsing *et al.*, 2008; van Beilen *et al.*, 2005). Different organisms can provide altered yields of product based on the same carbon source. During styrene epoxidation catalyzed by StyAB, for instance, 1.5 times higher yields of styrene oxide on glucose was observed using *E. coli* JM101 as host system in comparison to *Pseudomonas* sp. VLB120 (0.87 vs. 0.55 g<sub>product</sub> g<sub>glucose</sub><sup>-1</sup>) (Kuhn *et al.*, 2012a). Host intrinsic side reactions often occur and can be both adverse as well as beneficial for the desired reaction. Limonene hydroxylation using the CYP153A6, for instance, resulted in perillyl aldehyde and perillyl acid overoxidation catalyzed by a pseudomonas intrinsic dehydrogenase. A change of the biocatalytic chassis to *E. coli* W3110 supported the production of mainly perillyl alcohol by host intrinsic reduction of perillyl aldehyde back to perillyl alcohol (Cornelissen *et al.*, 2013).

**Protein production.** Genetic manipulation and engineering of the selected microbial host system is the basis for successful overexpression of genes for heterologous protein production. Knowledge and use of methodologies on all levels of protein biosynthesis, including replication, transcription, translation, and posttranslational modification strengthen the control over protein production. While the use of plasmids as vectors for foreign genes is simple and fast, genome integration enables more stable genetic incorporation. A broad range of promoters, comprising constitutive as well as inducible expression systems, allow for the defined transcription of the genetic material at desired time-scales. In addition, the applied codon usage and ribosomal binding sites control the strength of translation. Modularization of genes in different operons tunes the ratio of multi-component protein systems. Introduction of specific helper proteins, such as chaperones or the maltose binding protein, support the proper and soluble protein folding. Overexpression of the glutamyl-tRNA reductase, a key enzyme catalyzing the rate-limiting reaction in heme biosynthesis, allows for proper cofactor incorporation also in *E. coli* (Harnastai *et al.*, 2006).

**Physiological suitability and metabolic efficiency.** Biocatalytic applications sometimes rely on more than one enzyme and connect to the microbial metabolism in different complexity (Schrewe *et al.*, 2013). Whereas the use of isolated enzymes is inherently

independent of the microbial host system, whole-cell biotransformations make use of the endogenous cofactor- or even co-substrate regeneration. Therefore, the physiological background has to be suitable to accommodate the desired enzyme performance. When applying oxygenases in whole-cells, host-intrinsic side-reactions often interfere with the target reaction. In such cases, pathway engineering on endogenous enzymes is required. Identification and subsequent knock-out of the esterase BioH in *E. coli*, for instance, reduced the fatty acid methyl ester (FAME) hydrolysis by a factor of 22, enhancing the product yield for FAME hydroxylation (Kadisich *et al.*, 2017a).

The use of oxygenases implies the supply with electrons from respective cofactors. When applying whole-cell reaction systems, the supply with cofactors is highly dependent on the endogenous consumption of such. Metabolic engineering is a highly useful tool for optimizing the catalytic performance of a cell (Lin and Tao, 2017). Systems biology, comprising *in silico* modeling and multi-omics data analysis, allows for the identification of rate-limiting steps and following definition of targets for maximizing and balancing the (electron) flux towards the desired product. The genetic introduction of additional enzymes can increase fluxes. The co-expression of the alcohol dehydrogenase AlkJ, for instance, with the alkane monooxygenase enzyme system AlkBGT supported the irreversible oxidation of the hydroxylated fatty acid methyl ester to the targeted aldehyde compounds (Schrewe *et al.*, 2014). Also, cofactor regeneration can be accelerated, e.g., by introducing an orthogonal cofactor re-regeneration system. The incorporation of a glucose uptake and NADP<sup>+</sup>-dependent glucose dehydrogenase system in *E. coli*, for instance, 9-times increased the  $\alpha$ -pinene to  $\alpha$ -pinene oxide oxyfunctionalization rate catalyzed by P450 BM-3 (Schewe *et al.*, 2008). The knock-out of non-efficient cofactor generating pathways, such as the glycolytic pathway, increases the flux through the pentose phosphate pathway and thus improves the cofactor generation yield on glucose (Fasan *et al.*, 2011). The same effect could be achieved by the partial inactivation of competing pathways, such as endogenous respiration and fermentative pathways (Fasan *et al.*, 2011).

Microorganisms often provide either NADH or NADPH as the main cofactor. A simple but effective metabolic engineering tool, if the applied oxygenase does not match the cellular cofactor supply, is the genetic introduction of a transhydrogenase that catalyzes the hydride transfer between the two nicotinamide dinucleotides (Blank *et al.*, 2010). Co-expression of an L-lactate dehydrogenase and a soluble transhydrogenase, for instance, increased the lactate production rate and yield in the cyanobacterium *Synechocystis* sp. PCC 6803 (Angermayr *et al.*, 2012).

**Cellular chassis & cell integrity.** The application of oxygenases in whole-cell biocatalysts relies on a biocatalytic host functioning as reaction chassis. Although the microbial metabolism can be optimized by metabolic engineering regarding balanced fluxes directing

towards the chemical product, the whole-cell embodiment itself affects the reaction performance, inter alia, by the presence of cell membranes (and cell walls). Cellular engineering re-structures the microbial chassis, e.g., for the improved substrate uptake, product secretion, or toxic reactant export. The outer membrane of microbial cells functions as a barrier for hydrophobic compounds. Outer membrane pore proteins such as AlkL (Julsing *et al.*, 2012b), OprG (Touw *et al.*, 2010), OmpW (Hong *et al.*, 2006), or FadL (van Den Berg *et al.*, 2004) facilitate the uptake of oxyfunctionalization substrates by providing hydrophobic channels. Co-expression of AlkL in recombinant *Pseudomonas putida* KT2440 harboring CYP153A6, for instance, increases the hydroxylation activity of (S)-limonene to (S)-perillyl alcohol by a factor of five (Cornelissen *et al.*, 2013). In addition, hydrophobic substrate uptake can be enhanced by engineering the lipopolysaccharide acylation state (Vorachek-Warren *et al.*, 2002). Thus, lipopolysaccharide mutant strains of *E. coli* W3110 harboring P450 BM3 enabled the whole-cell oxyfunctionalization of the hydrophobic substrate linoleic acid (Lee *et al.*, 2011). The secretion of oxyfunctionalized products is not inherently hampered as the oxyfunctionalization process itself increases the hydrophilicity of the respective substrates. In contrast, too much uptake of reactants, e.g. of organic solvents, is detrimental to the cells resulting in decreased bioprocess stability by microbial inactivation. Solvent extrusion, supported by efflux pumps such as TtgABC, TtgGHI, or SrpABC identified in various Pseudomonads, keeps the intracellular toxicant concentration low and therefore enables the survival or even growth of microorganisms under exposure of solvent compounds. Constitutive synthesis of the efflux pump TtgGHI in *Pseudomonas* sp. VLB120ΔC reduced the adaptation time to respective reaction conditions and, also, doubled the specific styrene epoxidation activity (Volmer *et al.*, 2014).

The application of (oxygenase) enzymes in isolated form overcomes the need for reactant mass transfer. A sophisticated way of facilitating the direct contact between the catalyst and the substrate by the simultaneous preservation of enzyme stability and regeneration is the display of enzymes on the microbial surface (Schüürmann *et al.*, 2014). Also, the well-studied cytochrome P450BM3 was displayed on the cell surface of *E. coli* and enabled the hydroxylation of lauric acid, palmitic acid and arachidonic acid independent from membrane mass-transfer (Yim *et al.*, 2010). Easy separation from the reaction mixture and re-usability strengthened this method (Ströhle *et al.*, 2016). Exclusion of the enzyme from the microbial metabolism challenges the cofactor supply, although external supply with NAD(P)H via electrochemical, chemical and enzymatic regeneration systems were already developed successfully.

### **1.3.5 Reaction engineering**

Key optimization targets within the level of reaction engineering are biocatalyst production, reaction efficiency, and biocatalyst stability. Nature adapted its mechanisms according to the

present microenvironment. In contrast, biocatalyst generation and chemical conversion necessitate altered/ optimized growth and reaction conditions. Temperature, pH, and media composition (including, inter alia, ionic strength) are of high importance for both, the catalyst production and the chemical reaction. In the case of whole-cell biotransformations, the reaction medium does not only affect the oxyfunctionalization reaction itself, but also the state of the cellular metabolism. The depletion of nutrients, for instance, induces a non-growing state of the cell. Such resting cells can provide increased cofactor supply on the given energy source, as shown for the epoxidation of styrene to (S)-styrene oxide catalyzed by recombinant *E. coli* harboring a styrene monooxygenase (Julsing *et al.*, 2012a).

Throughout the whole reaction time, reactant concentrations have to match the enzyme or whole-cell kinetics, respectively. Michaelis-Menten kinetics, including product inhibition and reactant toxicity, are key aspects to be considered (Ringborg and Woodley, 2016). Oxyfunctionalization substrates often are hydrophobic and therefore lowly water soluble. Intercalation of such chemical compounds in the membranes of whole-cell biocatalysts results in cell disintegration, and therefore destabilization of the bioprocess (Sikkema *et al.*, 1994). Solvents with a logarithmic octanol-water coefficient logP between 1 and 4 are considered to be highly toxic to cells (de Bont, 1998). On the one hand, a continuous substrate feed can prevent from supplying the toxic substrate in excess. Importantly, the feed rate has to match the oxyfunctionalization rate to keep the substrate concentration constantly low. In the example of fluorobenzene oxyfunctionalization to fluorocatechol catalyzed by *Pseudomonas putida* whole-cells, reactant inhibition was successfully overcome by such a substrate feeding strategy (Lynch *et al.*, 1997). On the other hand, organic carrier solvents can be used to continuously provide the substrate to the aqueous phase, regulated by the organic:aqueous phase partitioning coefficient. The oxyfunctionalization of  $\alpha$ -pinene to  $\alpha$ -pinene-oxide catalyzed by recombinant *E. coli* harboring a cytochrome P450 BM3 variant, for instance, revealed an optimal substrate concentration of 30% (v/v)  $\alpha$ -pinene dissolved in the organic carrier solvent diisononyl phthalate (DINP) resulting in high initial specific activities and prolonged biotransformation stability (Schewe *et al.*, 2009).

Oxyfunctionalization intermediates and products accumulating at concentrations toxic to the biocatalysts constitute another source of reduced biotransformation stability. The accumulation of hydrophobic compounds in the microbial membranes was estimated to induce cell breakdown at concentrations of 300 - 400 mM (Kratzer *et al.*, 2015). *In situ* product removal (ISPR) is a useful technique to retain low reactant concentrations (Lye and Woodley, 1999). Examples for ISPR comprise, amongst many others, liquid-liquid extraction, and solid-phase adsorption. Solid-phase *in situ* product extraction by adsorption to the hydrophobic Optipore L-493 resin, for instance, enhanced the rate and yield of the Baeyer-Villiger oxidation of bicyclo[3.2.0]hept-2-en-6-one to the corresponding lactones catalyzed by



recombinant *E. coli* harboring a cyclohexanone monooxygenase (Simpson *et al.*, 2001). The use of bis(2-ethylhexyl)phthalate (BEHP) as liquid extraction solvent during *E. coli* Xylene monooxygenase (XylMO) biotransformation, for instance, allowed for stable oxyfunctionalization of pseudocumene to the respective aldehydes and acids at high concentrations (Bühler *et al.*, 2002).

In addition to the prevention of catalyst inactivation and retention of highly volatile reactants in the reaction system, *in situ* substrate supply and product extraction also allow for the kinetic control of multi-step oxyfunctionalizations. Thus, the defined use of 2-liquid phase biotransformation directed the product formation pattern of the *E. coli* XylMO reaction system to the accumulation of 3,4-dimethylbenzaldehyde (Bühler *et al.*, 2003b). Organic-carrier solvents are not only applicable for whole-cell applications, but also for the use of isolated oxygenase enzyme systems. Cytochrome P450 BM3 variants, for instance, could successfully be applied with cyclohexane as an organic carrier solvent for the hydroxylation of octane or myristic acid (Maurer *et al.*, 2005).

Next to the substrate supply and product extraction, the co-substrate O<sub>2</sub> is one of the most critical parameters during oxyfunctionalization catalysis. The dissolved oxygen concentration influences the oxyfunctionalization rate and can affect the regioselectivity of the reaction. For instance, the impact of oxygen on the oxyfunctionalization of pentadecanoic acid catalyzed by cytochrome P450 BM-3 was investigated in both, isolated enzyme and whole-cell applications (Schneider *et al.*, 1999). Excess of oxygen resulted in the formation of hydroxypentadecanoic acids as well as ketohydroxy- and dihydroxypentadecanoic acids with an oxyfunctionalization rate of 2.1 U g<sub>CDW</sub><sup>-1</sup> (*in vivo*) and 100 U g<sub>protein</sub><sup>-1</sup> (*in vitro*), respectively. In contrast, oxygen-limited conditions resulted in decreased oxyfunctionalization rates of 1.25 U g<sub>CDW</sub><sup>-1</sup> (*in vivo*) and 60 U g<sub>protein</sub><sup>-1</sup> (*in vitro*), respectively, with hydroxypentadecanoic acids as the main hydroxy products.

### 1.3.6 Process design & engineering

Process engineering focuses on the transfer of a developed bioprocess into a technical setting with special consideration of scaling, process duration, and product recovery. The technical setting is highly dependent on whether the process runs continuously or in batch mode. Scalability and the scale-up progress maintaining the reaction efficiency are prerequisites for the successful process development and, eventually, implementation.

**Scaling & process duration.** Optimal growth of the host system and efficient protein biosynthesis determine the catalyst production performance. On fermenter-scale, defined cultivation conditions of the recombinant expression systems are crucial for generating high catalyst concentrations. Development and optimization of a fed-batch strategy, for instance, allowed for the synthesis of the cytochrome P450 BM3 to a concentration of ~ 11% per g<sub>CDW</sub> of recombinant *E. coli* (Pflug *et al.*, 2007). Both, enzymes and whole cells can be applied for

catalysis in suspended or immobilized format (Eş *et al.*, 2015). Suspended biocatalysts avoid labor and cost-intensive development and preparation techniques. Existing production settings can be used for the industrial application. Mixing and therefore mass transfer is not limited by supporting materials, and the catalyst preserves its conformational freedom. Immobilization often possesses high stability, good storage possibilities, simplified catalyst recovery, and recyclability and thus mediates an increased yield on biocatalyst. Various immobilization techniques exist and are extensively applied in industry. Immobilization materials comprise, e.g., the nature-derived polymers collagen and alginate, or the synthetic polymer polyacrylamide. In view of whole-cell biocatalysts, certain bacteria, such as *Pseudomonas* sp. VLB120 (Gross *et al.*, 2007), feature self-immobilization into a biofilm format (Halan *et al.*, 2012). High catalyst density and enhanced resistance towards destabilizing environmental conditions allow for efficient bioprocessing (Gross *et al.*, 2010). During the actual reaction process, the bioreactor facilitates efficient interaction of the biocatalyst with the (co-)substrate and, if required during the biotransformation process, adequate product extraction. In general, a bioreactor can be operated in batch or continuous mode and raises particular demands on the reactor design. Examples of bioreactor types comprise, inter alia, stirred tank reactors, fixed-bed reactors, or membrane reactors, mainly differing in the biocatalyst application format and the mixing type. Scaling under retention of the reaction parameters is crucial. The following paragraphs describe two examples of different bioreactor types and operation modes.

The stirred-tank bioreactor (STR) constitutes an industrial standard for fermentation and biocatalytic processes. The core of the STR represents a reaction vessel equipped with a stirring device for sufficient mixing of the reaction mixture (agitation). Often, the biocatalyst is applied in suspended format. The exchange between the gas and liquid phase mainly occurs via aeration. In batch mode, the reaction medium containing all necessary nutrients and, if required, the carbon source is provided to the biocatalyst right from the start of the reaction process. In a fed-batch mode, the substrate (e.g., an organic carbon source or the reaction substrate) is provided during the biotransformation process to avoid inhibition effects. During the discontinuous operation, the reactant concentrations continuously change over time. Laboratory scaling of a developed two-liquid phase bioprocess to a 30 L stirred-tank bioreactor, for instance, enabled the production 3,4-dimethylbenzaldehyde from pseudocumene with a productivity of 31 L<sup>-1</sup> d<sup>-1</sup> and a final product titer of 37 g L<sup>-1</sup> catalyzed by recombinant *E. coli* harboring a XylMO (Bühler *et al.*, 2003a).

Capillary reactors comprise miniaturized reaction chambers combined with microfluidic devices. Continuous operation favors the use of biocatalysts immobilized on the inner surface of the capillary reactor, e.g., as a self-immobilized biofilm. The reaction medium and the substrate are continuously supplied, while the reaction product is continuously obtained

at the reactor outlet. The application of air segments (plug flow) facilitates the exchange with the gas phase (Karande *et al.*, 2016b). On a laboratory scale, the application of *Pseudomonas* sp. VLB120ΔC in a biofilm-based capillary reactor, for instance, allowed for the stable oxyfunctionalization of styrene to styrene-oxide for at least 50 days with an average volumetric productivity of 24 g L<sup>-1</sup> day<sup>-1</sup> (Gross *et al.*, 2010). Scaling takes place by numbering-up and comprises a, not yet industrially applied, promising alternative to stirred-tank reactor processes enabling high product yields on biomass (Gross *et al.*, 2013).

**Product recovery.** Downstream processing (DSP) includes the separation of the product from the catalyst (cell harvest and disruption for whole-cell applications if the product accumulates intracellularly), product recovery, product concentration, product purification, and packing (Chmiel, 1991). Next to centrifugation and filtration this comprises, *inter alia*, precipitation, adsorption, solvent extraction, electrophoretic, and chromatographic methodologies. Often, *in situ* product removal (ISPR) strategies such as adsorption or solvent extraction are used for a continuous and stabilized bioprocess control. Although the DSP is a highly cost intensive (usually more than half of the total costs) part of a bioprocess, and therefore an indispensable element for the development of an eco-efficient bioprocess, academic research on the systematic optimization of appropriate oxyfunctionalized product purification methodologies is rare.

## 1.4 Towards photosynthesis-driven redox biotransformations

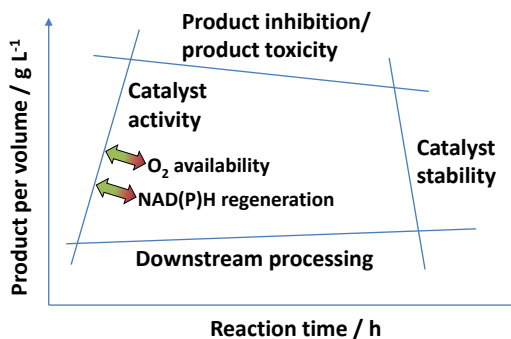
### 1.4.1 Boundaries of current oxyfunctionalization bioprocesses and the potential of photosynthesis

The introduced integration of strategies addressing the key targets for the development of efficient bioprocess leads to a complex interconnection of process parameters. In principle, constraints of the process efficiency within each process development level go back to catalyst activity, product inhibition/ toxicity, catalyst stability, and product recovery. The graphical visualization in a window of operation helps to classify the actual state of bioprocess development and to define the future engineering targets for achieving an eco-efficient production process (**Figure 1.4**) (Woodley and Titchener-Hooker, 1996).

In general, the left-hand site process boundary arises from the catalyst activity (determined by, e.g., the turnover number). The enzyme or whole-cell kinetics for product inhibition and product toxicity limit the maximum product titer and form an upper process boundary. The biocatalyst stability (determined by, e.g., the total turnover number) restricts the duration of a bioprocess. The lower process boundary is defined by the downstream processing methodology which becomes viable at a specific minimum product titer and the minimum amount of product per volume which is targeted in the process.

In a detailed view of the left-hand site process boundary of oxygenase biocatalysis,

especially the co-substrate supply restricts the maximum catalyst activity. Thus, the limited availability of  $O_2$  via gas-liquid mass transfer and the regeneration of NAD(P)H cofactors challenge the development of viable bioprocesses. Chemoheterotrophic whole-cell reaction systems provide reduction equivalents by the catabolism of organic carbon-based sources, such as glucose. However, high energy demand for growth and maintenance reduces the level of reduction equivalents that are accessible for the catalytic reaction (Blank *et al.*, 2008; Bühler *et al.*, 2008). In addition, microbial respiration reduces the amount of  $O_2$  available in the reaction system and technically challenges the reaction setup (Hilker *et al.*, 2006; Law *et al.*, 2006).



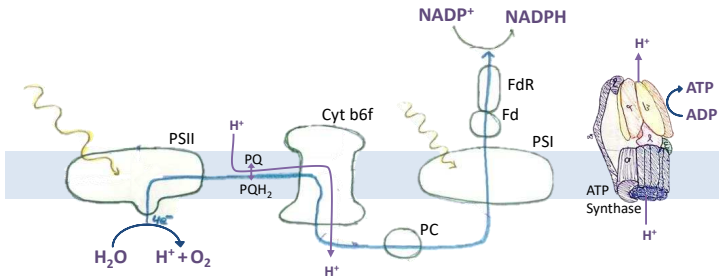
**Figure 1.4:** Window of operation with process boundaries for biocatalytic processes. In oxyfunctionalization processes, the catalyst specific activity is confined by the  $O_2$  availability and NAD(P)H regeneration rate. While heterotrophic whole-cell biocatalysts are prone to limit both, photosynthetic water oxidation provides an extensive source of electrons and  $O_2$ . Figure adapted from Schrewe *et al.* 2013 (Schrewe *et al.*, 2013).

Oxygenic photosynthesis provides an extensive source of both,  $O_2$  and reduction equivalents. Thus, by changing the biocatalytic host system from chemoheterotrophic to photoautotrophic organisms, in theory, allows for the unlimited exploitation of the oxygenase activity. Water serves as a carbon-independent source of both co-substrates accessed by the energy of light. The uncoupled fixation of inorganic carbon ( $CO_2$ ) enables cheap and sustainable catalyst (re)generation. Coupling of oxygenases to the photosynthetic water oxidation is highly promising for the development of eco-efficient production processes that are currently  $O_2$  and electron-limited but require high productivities. Especially when the production costs are essential, e.g., for low-cost products, the replacement of organic carbon sources such as glucose by  $CO_2$  is favorable.

### 1.4.2 The mechanism of oxygenic photosynthesis

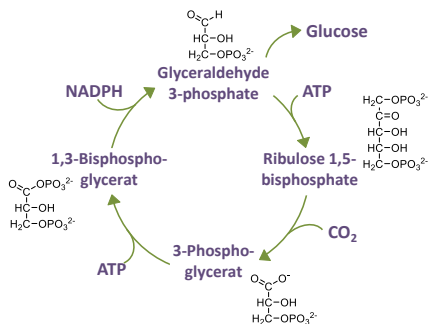
The application and development of photobiocatalytic host systems require an understanding of the underlying photosynthetic metabolism. Therefore, the following sections introduce the

mechanism of oxygenic photosynthesis, with focus on the photosynthetic water oxidation reaction and possible trapping positions for oxygenase enzymes.



**Figure 1.5:** Schematic representation of the photosynthetic light reaction. With the energy of light water is oxidized and electrons are transferred through the electron transport chain towards the cofactor NADPH, resulting in a proton motive force and the subsequent generation of ATP. Both, NADPH and ATP are used for the fixation of CO<sub>2</sub> via the Calvin-cycle. PSII = photosystem II, PQ = plastoquinone (PQ), PQH<sub>2</sub> = plastoquinol, Cyt b6f = cytochrome b6f complex, PC = plastocyanin, PSI = photosystem I, Fd = ferredoxin, FdR = ferredoxin reductase.

Photoautotrophic organisms such as plants, algae, and cyanobacteria, convert light energy into chemical energy by the oxidation of water and fix CO<sub>2</sub> for the generation of carbohydrates. In the primary, light-driven reaction the energy and electron carrier ATP and NADPH are generated via an electron transport chain (**Figure 1.5**). In the secondary reaction, ATP and NADPH are used for the fixation of CO<sub>2</sub> and the generation of carbohydrates (**Figure 1.6**).



**Figure 1.6:** Schematic representation of the Calvin-cycle. ATP and NADPH derived from the photosynthetic light reaction and are used to fix CO<sub>2</sub>.

The uptake of light quanta (a physical unit for light energy) occurs by photopigments located within the thylakoid membranes. Various photopigments with different characteristics and

absorption spectra exist, allowing for the efficient usage of the whole range of light energy (Madigan and Martinko, 2006). Chlorophyll constitutes one of the main photopigments. It assembles a porphyrin scaffold with a coordinated magnesium ion in its centrum. Absorption of red and blue light results in a green color. In proteins, chlorophyll forms complexes of 50 to 300 molecules functioning as energy funnel directed towards the reaction center. The electron transport chain of the photosynthetic light reaction comprises two of such protein complexes:

- photosystem PSII containing chlorophyll P680 (absorption of far-red light)
- photosystem PSI containing chlorophyll P700 (absorption of near red light)

Phycobilins form another group of light-harvesting and light-energy transferring antenna pigments. The aggregates of open-chain tetrapyrroles, such as phycoerythrin (red), phycocyanin (blue), or allophycocyanin (blue), are closely linked to chlorophyll reaction centers. With decreasing light intensity, the phycobillin content increases. Carotenoids conduct a photoprotective role by quenching reactive oxygen species and absorption of harmful light. The long chain hydrocarbons with a conjugated double-bond system absorb blue light and thus appear yellow, red, brown, or green.

The photosynthetic light reaction is initiated at the photosystem PSII by the oxidation of water into  $O_2$ , protons and electrons. Subsequent absorption of light facilitates the electron excitation and thus transport through the electron transport chain. Second light absorption and electron excitation takes place at the photosystem PSI before the electron transfer proteins ferredoxin and ferredoxin reductase and finally the cofactor  $NADP^+$  are reduced. Location of the electron transport chain within the thylakoid membranes results in the formation of a proton gradient with high proton concentrations within the thylakoid lumen. Finally, this proton motive force drives the ATP synthase.

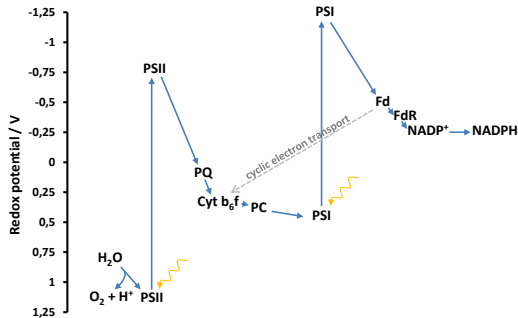
Generated ATP and NADPH then are used for the fixation of  $CO_2$  by the Calvin-cycle. In the first step,  $CO_2$  is fixed in ribulose 1,5-bisphosphate (R-1,5-BP) catalyzed by the ribulose bisphosphate carboxylase (RubisCO) resulting in two molecules of 3-phosphoglycerate (3-PG). Subsequently, the  $C_3$ -molecule 3-PG is reduced to glyceraldehyde 3-phosphate (GAP) under consumption of ATP and NADPH. Finally, GAP molecules are either regenerated to R-1,5-BP by the consumption of ATP or taken up by reversed glycolysis for the generation of carbohydrates. Fixed carbon is either directly taken up by the metabolism for growth and maintenance or stored in storage compounds such as glycogen. In the absence of light (e.g., in the night), these polysaccharides then are catabolized again.

### 1.4.3 Trapping electrons from the photosynthetic light reaction for redox biocatalysis

Redox biocatalysis, such as catalyzed by oxygenase enzymes, requires the efficient coupling of the photosynthetic light reaction with the heterologous redox enzyme that makes use of

the activated reduction equivalents. The mainly reduced cofactor of photosynthesis is NADPH. However, the photosynthetic light reaction offers a multitude of positions for trapping the light-excited electrons by redox enzymes (Mellor *et al.*, 2017). Importantly, the transfer of electrons necessitates the interaction with electron transferring enzymes that match respective redox potentials. The Z-scheme of photosynthesis explains the redox pathway of, the by light, excited electrons and discloses the trapping positions for heterologous oxygenases (**Figure 1.7**).

Due to the spatial accessibility, PSI, ferredoxins, flavodoxins, and ferredoxin reductases are the most suitable trapping positions. In contrast, the localization of the copper-containing plastocyanin/ heme-containing cytochrome c<sub>6</sub> in the thylakoid lumen places these proteins to hardly accessible trapping positions for heterologous redox enzymes. The fast exchange between electron transferring enzymes occurs if the distance between the central redox cofactors is below 14 Å. The relatively weak interactions rely on hydrophobic and electrostatic interactions, resulting in an unspecific binding pattern, allow the transfer of electrons to various downstream acceptor proteins. Ferredoxins, flavodoxins, plastocyanin, and cytochrome c<sub>6</sub> are negatively charged and thus interact with the positively charged sites of the cytochrome b<sub>6</sub>f complex and the photosystem PSI.



**Figure 1.7:** Z-scheme representing the electron transfers within the photosynthetic light reaction. Electrons are transferred from proteins with a high redox potential to those with a low redox potential. Electrons are excited by the energy of light which takes place in the photosystems PSII and PSI. PSII = photosystem II, PQ = plastoquinone, Cyt b<sub>6</sub>f = cytochrome b<sub>6</sub>f complex, PC = plastocyanin, PSI = photosystem I, Fd = ferredoxin, FdR = ferredoxin reductase.

Downstream of the photosystem PSI, ferredoxins are the primary electron transferring enzymes. They distribute the reducing power within the metabolism of the photosynthetic organism. Electron transfer occurs via iron-sulfur clusters (Fe<sub>2</sub>S<sub>2</sub>, Fe<sub>3</sub>S<sub>4</sub>, Fe<sub>4</sub>S<sub>4</sub>). Rubredoxins have the same function but contain a single iron center. Both are one electron carriers. Thus the reduction of NADPH requires two electron transfer steps. Absent in plants, flavodoxins comprise functional homologs to ferredoxins. The FMN-based, one-electron carrier proteins

share a comparable redox potential but interact with even lower specificity than ferredoxins. Redox enzymes, such as oxygenases, often rely on functionally related electron transferring enzyme systems. Thus the exchange of these systems with those derived from the photosynthetic machinery is reasonable and facilitated by their promiscuity (Goñi *et al.*, 2009; Lacour and Ohkawa, 1999).

Numerous studies already conceptually investigated the exploitation of the photosynthetic water oxidation for redox reactions (**Table 1.1**). The different possibilities for trapping photosynthesis-derived electrons are explained best on the example of hydrogen production, which is the take-up of electrons for the reduction of protons to hydrogen. Hydrogenases can be coupled to the PSI by localizing both enzymes in spatial proximity (Ihara *et al.*, 2006b). Connection of both central Fe<sub>4</sub>S<sub>4</sub> clusters via a thiolated molecular wire enables a direct electron transfer (Lubner *et al.*, 2011). Alternatively, mediation of the electrons deriving from PSI to the hydrogenase, for instance, results from the fusion of PSI with a cytochrome c<sub>3</sub> (Ihara *et al.*, 2006a). In addition, hydrogen production is facilitated by the fusion of hydrogenases with photosynthesis deriving ferredoxins (Yacoby *et al.*, 2011). In general, the abstraction of electrons competes with the endogenous metabolism, such as CO<sub>2</sub> fixation (main part), nitrogen, and sulfur assimilation. Down-regulation of competing pathways and orthogonal re-direction of electrons, therefore, might be crucial.

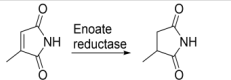
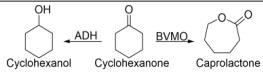
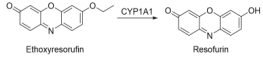
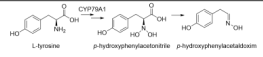
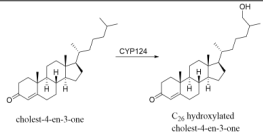

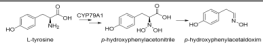
### 1.4.4 Current state of photobiotechnology

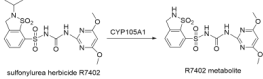
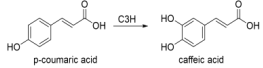
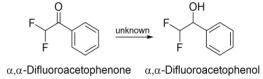
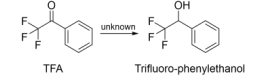
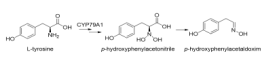
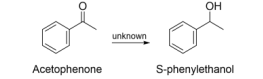
Thus far, substantial effort was dedicated to the proof-of-concept studies coupling the photosynthetic light reaction with redox enzymes, and great success was achieved. The implementation of eco-efficient photosynthesis-driven redox biotransformations into suitable process settings, however, requires the identification of key limitations and engineering targets. Therefore, the following section briefly reviews the current state-of-the-art in photobiotechnology in analogy to the approach of addressing the levels of process development described above.

**Selection of phototrophic host systems.** The group of phototrophic organisms covers plants, algae, and cyanobacteria. Referring to the theory of endosymbiosis, ancestors of cyanobacteria stably incorporated into primitive eukaryotic cells, resulting in the development of chloroplasts present in plants and algae. Due to enhanced cell growth and genetic accessibility in comparison to plants and algae, cyanobacteria comprise promising host systems for photosynthesis driven biotechnological applications. *Synechocystis* sp. PCC 6803 presents a cyanobacterial model organism for which few engineering methodologies were already established (Ruffing, 2011). *Synechococcus elongatus* PCC 7942 constitutes another unicellular model organism, while various filamentous strains such as *Anabaena* sp. or *Nostoc* sp. are mostly studied in the context of hydrogen production.



**Table 1.1:** Photosynthesis-driven electron demanding reactions. DCMU = 3-(3,4-dichlorophenyl)-1,1-dimethylurea, specific inhibitor of photosystem II (PSII) electron transport; IAM = Iodoacetamide; DBMBI = 2,5-dibromo-3-methyl-6-isopropylbenzoquinone; C3H = p-coumarate-3-hydroxylase.

Reaction	Host system	Information on mechanism	Rate	Ref
 <p>2-methylmaleimide → 2-methylsuccinimide</p>	<i>Synechocystis</i> sp. PCC 6803 recombinant	DCMU reduces activity Light-dependent activity Low activity with DCMU in the absence of light	123 U g <sub>CDW</sub> <sup>-1</sup>	(Köninger <i>et al.</i> , 2016)
$2\text{H}^+ + 2\text{e}^- \xrightarrow{\text{Hydrogenase}} \text{H}_2$	<i>Tetraspora</i> sp. CU2551 wildtype	-	20 U g <sub>CDW</sub> <sup>-1</sup>	(Maswana <i>et al.</i> , 2018)
 <p>Cyclohexanol → Cyclohexanone → Caprolactone</p>	<i>Synechocystis</i> sp. PCC 6803 recombinant	DCMU reduces activity Light-dependent activity Low activity with DCMU in the absence of light	6 U g <sub>CDW</sub> <sup>-1</sup>	(Böhmer <i>et al.</i> , 2017)
 <p>Ethoxyresorufin → Resorufin</p>	<i>Synechococcus</i> sp. PCC 7002 recombinant	Active without native reductase DCMU reduces activity Light-dependent activity Almost no activity in the absence of light	31 mU g <sub>CDW</sub> <sup>-1</sup>	(Berepiki <i>et al.</i> , 2016)
 <p>L-tyrosine → p-hydroxyphenylacetamide → p-hydroxyphenylacetaboinam</p>	<i>Synechococcus</i> sp. PCC 7002 recombinant	Fused to photosystem I subunit PsaM → localization in the thylakoid membrane	27 U mg <sub>chlorophyll</sub> <sup>-1</sup>	(Lassen <i>et al.</i> , 2014a)
$2\text{H}^+ + 2\text{e}^- \xrightarrow{\text{Nitrogenase}} \text{H}_2$	<i>Nostoc</i> sp. PCC 7120 Δ <i>hupW</i> knock-out of uptake hydrogenase	-	14 U mg <sub>chlorophyll</sub> <sup>-1</sup>	(Nyberg <i>et al.</i> , 2015)
 <p>cholest-4-en-3-one → C<sub>3</sub> hydroxylated cholest-4-en-3-one</p>	<i>In vitro</i> CYP124 + PSI + Ferredoxin	Light-driven activity Catalase was added to prevent ROS deriving from CYP	7 U mg <sub>chlorophyll</sub> <sup>-1</sup>	(Jensen <i>et al.</i> , 2012)
 <p>7-ethoxycoumarin → 7-hydroxycoumarin</p>	<i>In vitro</i>	isolated cactus chloroplasts + yeast microsomes containing CYP1A1 fused with ferredoxin reductase	2.3 U mg <sub>chlorophyll</sub> <sup>-1</sup>	(Hara <i>et al.</i> , 1997)
 <p>L-tyrosine → p-hydroxyphenylacetamide → p-hydroxyphenylacetaboinam</p>	<i>Synechocystis</i> sp. PCC 6803 recombinant	Localization of CYP to thylakoid membranes	10 mU mg <sub>chlorophyll</sub> <sup>-1</sup>	(Włodarczyk <i>et al.</i> , 2015)

Reaction	Host system	Information on mechanism	Rate	Ref
$2\text{H}^+ + 2\text{e}^- \xrightarrow{\text{Hydrogenase}} \text{H}_2$	<i>In vitro</i> Hydrogenase fused to PSI	Light-driven activity	9.7 mU mg <sub>chlorophyll</sub> <sup>-1</sup>	(Ihara <i>et al.</i> , 2006b)
 <p>sulfonurea herbicide RT402 <math>\xrightarrow{\text{CYP105A1}}</math> RT402 metabolite</p>	<i>Nicotiana tabacum</i> transgenic	Active only when targeted to chloroplasts	0.012 mU g <sub>leaf</sub> <sup>-1</sup>	(Okeefe <i>et al.</i> , 1994)
 <p>p-coumaric acid <math>\xrightarrow{\text{C3H}}</math> caffeic acid</p>	<i>Synechocystis</i> sp. PCC 6803 recombinant	-	9.4 mU L <sup>-1</sup>	(Xue <i>et al.</i> , 2013)
 <p><math>\alpha, \alpha</math>-Difluoroacetophenone <math>\xrightarrow{\text{unknown}}</math> <math>\alpha, \alpha</math>-Difluoroacetophenol</p>	<i>Synechococcus elongatus</i> PCC 7942 wildtype	DCMU inhibits activity	active	(Nakamura and Yamanaka, 2002)
 <p>TFA <math>\xrightarrow{\text{unknown}}</math> Trifluoro-phenylethanol</p>	<i>Synechococcus elongatus</i> PCC 7942 wildtype	Activity inhibited by DCMU (PSII), enhanced by IAM (Calvin-cycle) and DBMIB (Cytb6f) Low activity in the absence of light	active	(Yamanaka <i>et al.</i> , 2011)
 <p>L-tyrosine <math>\xrightarrow{\text{CYP79A1}}</math> p-hydroxyphenylacetamide + p-hydroxyphenylacetaldoxim</p>	<i>In vitro</i> Isolated chloroplasts containing CYP79A1 fused to Ferredoxin	active without soluble Ferredoxin	active	(Mellor <i>et al.</i> , 2016)
 <p>Acetophenone <math>\xrightarrow{\text{unknown}}</math> S-phenylethanol</p>	<i>Synechocystis</i> sp. PCC6803 wildtype	Enhanced yield via overexpression of FdR	active	(Luo <i>et al.</i> , 2018)

**Engineering of photobiocatalytic hosts.** Yet, genetic modification of cyanobacteria lacks a powerful genetic engineering toolbox. Genetic modifications either rely on a broad host range replicative plasmid (RSF origin of replication) or chromosomal integration into several neutral sites. Introduction of genetic materials is possible via natural transformation, electroporation or conjugation (Ruffing, 2011). *Synechocystis* sp. PCC 6803 and many other cyanobacteria contain multiple genome copies, necessitating full segregation of genetic insertions/ knock-outs for stable genetic manipulation. In consequence of varying copy numbers and folding structures, the different insertion positions result in altered expression strengths. For *Synechocystis* sp. PCC 6803, the highest expression of a fluorescent reporter protein was achieved by integration into its endogenous plasmid (Ng *et al.*, 2015). In general, the codon usage of *Synechocystis* sp. PCC 6803 is similar to other bacteria such as *E. coli*. The overexpression of genes can be performed via native promoter systems, such as the light-inducible  $P_{sbA2}$  promoter (Heidorn *et al.*, 2011). The promoter natively controls the synthesis of a photosystem PSII subunit and results in a strong and, under standard cultivation conditions, constitutive expression. In addition, metal ion inducible promoter systems are used. The  $P_{nrsB}$  promoter, for instance, natively controls nickel, cobalt, and zinc efflux pumps, and constitutes a highly tunable system with a relatively silent expression under non-induced conditions (Englund *et al.*, 2016). Metal ions such as  $Ni^{2+}$  are highly toxic to the bacterial cells and necessitate a well-balanced addition to the culture medium. Orthogonal expression systems, such as  $P_{trc}$  (Huang *et al.*, 2010) or  $P_{tac}$  (Albers *et al.*, 2015), mainly rely on the IPTG-inducible lac expression system. However, its functionality is not comparable to established heterotrophic host systems such as *E. coli*, resulting in expression even in the absence of the inducing agent.

Analysis of all native *Synechocystis* sp. PCC 6803 ribosomal binding site (RBS) sequences resulted in an optimized RBS\* with 9 base pairs between the Shine–Dalgarno core sequence and start codon (Heidorn *et al.*, 2011). Evaluation of RBS\* with fluorescent reporter proteins showed high translation efficiency. Synthetic biology is required for the development of controllable and strong genetic engineering tools.

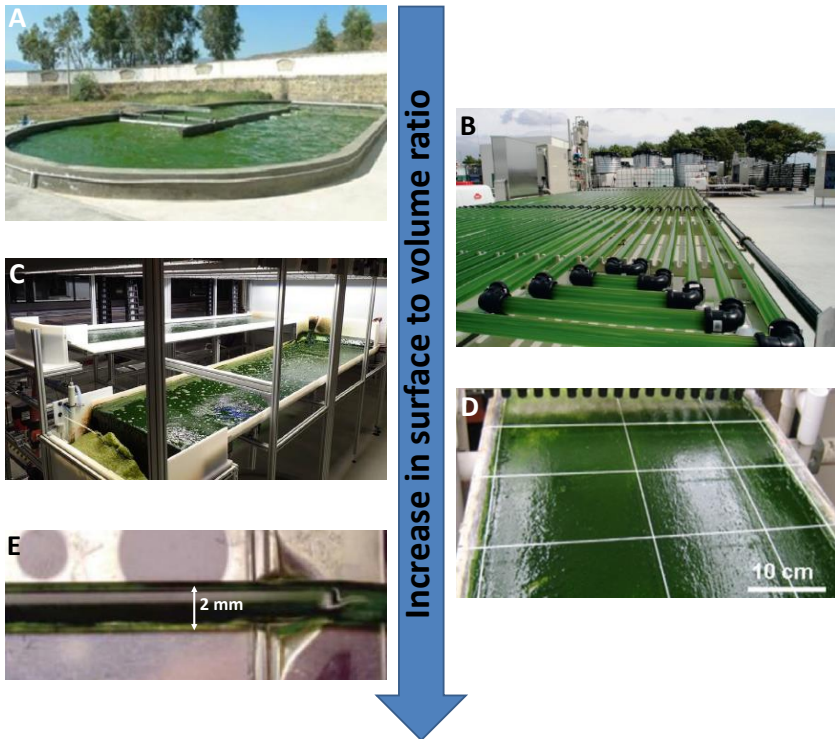
In contrast to the use of phototrophic organisms for biotransformation reactions, much research was already conducted on the development of fermentative production systems for hydrocarbon-based chemicals. Numerous photosynthesis-driven catalysts were generated and engineered to produce various compounds, such as ethanol (Liang *et al.*, 2018a), lactate (Angermayr *et al.*, 2012), isobutanol (Varman *et al.*, 2013), fatty acids (Ruffing, 2014), isoprene (Pade *et al.*, 2016), ethylene (Veetil *et al.*, 2017), itaconic acids (Chin *et al.*, 2015), carbohydrates (glucose, fructose) (Niederholtmeyer *et al.*, 2010), glycerol (Savakis *et al.*, 2015), erythritol (van der Woude *et al.*, 2016), or propandiol (David *et al.*, 2018; Li and Liao, 2013), from  $CO_2$ . In addition, the feature of naturally synthesizing terpenoids and

isoprenoids renders them well suited as biocatalysts for pharmaceuticals, cosmetics, colorants, disinfectants, fragrances, flavorings, and agro-chemicals (Pattanaik and Lindberg, 2015). The production of 3-hydroxypropionic acid (3-HP) represents an example for extensive metabolic engineering of a phototrophic metabolism (Wang *et al.*, 2016b). First, the heterologous introduction of the malonyl-CoA reductase from *Chloroflexus aurantiacus* into *Synechocystis* sp. PCC 6803 and optimization of culture conditions enabled the CO<sub>2</sub>-based production of 32 mg L<sup>-1</sup> 3-HP. Subsequent change of the expression system, including inter alia the promoter strength, significantly enhanced the product titer to 692 mg L<sup>-1</sup>. Overexpression of the endogenous acetyl-CoA carboxylase and biotinilase, as well as the NAD(P) transhydrogenase, increased the supply of the precursor malonyl-CoA as well as the cofactor NADPH, respectively, achieving the production of 745 and 752 mg L<sup>-1</sup> 3-HP. The same product titers were observed after the inactivation of the competing pathways for PHA and acetate biosynthesis, respectively. Finally, the combination of these metabolic engineering approaches in one strain resulted in the production of ca. 837 mg L<sup>-1</sup> 3-HP from CO<sub>2</sub>.

**Cultivation and process technologies.** Numerous photobiotechnological processes were already developed for the generation of algal biomass for animal and human nutrition products, cosmetics, or for the extraction of high-value molecules such as fatty acids or pigments (Chaumont, 1993; Grobbelaar, 2009; Pulz, 2001; Singh and Sharma, 2012; Spolaore *et al.*, 2006; Weissman *et al.*, 1988). Traditional algal cultivation systems comprise open pond reactor systems (**Figure 1.8 A**). The production of lipids as biodiesel using the microalgae *Graesiella* sp. WBG-1, for instance, was carried out in a 40000 L raceway open pond bioreactor, comprising a surface area of 200 m<sup>2</sup> (20 x 10 x 0.2 m) (Wen *et al.*, 2016). After 15 days of cultivation, the final biomass concentration was 138 g m<sup>-2</sup> corresponding to ca. 0.7 g<sub>CDW</sub> L<sup>-1</sup> and contained ca. 33% of the target lipids. In contrast to open systems, closed tubular photobioreactors reduce the risk of contaminations and thus, in theory, support the cultivation of genetically modified organisms (Wijffels *et al.*, 2013). In addition, tubular photobioreactors, such as built at the AlgaePARC in Wageningen, Netherlands, increase the light input by increased surface to volume ratios (**Figure 1.8 B**) (Wijffels *et al.*, 2013). A 500 km long tubular photobioreactor (700 m<sup>3</sup>) in Klötze, Germany, for instance, enables the production of 130 – 150 t<sub>CDW</sub> of the algae *Chlorella* per year (average productivity of 6.2 g<sub>CDW</sub> m<sup>-2</sup> day<sup>-1</sup>) (Spolaore *et al.*, 2006).

By further increasing the surface area to volume ratio, an open thin-layer photobioreactor was developed recently (**Figure 1.8 C**) (Apel *et al.*, 2017). With this system, cultivation of the saline microalgae *Nannochloropsis salina* on a technical scale of 8 m<sup>2</sup> resulted in high final biomass concentrations of 50 g<sub>CDW</sub> L<sup>-1</sup> within 25 days (313 g<sub>CDW</sub> m<sup>-2</sup>). In addition to biomass production, photosynthetically active algae are applied during waste-water treatment as well.

Here, algal biofilms are grown on open surfaces such as polystyrene foam (Johnson and Wen, 2010) or concrete (Ozkan *et al.*, 2012) (**Figure 1.8 D**). Evaluation of the biofilm formation of the green alga *Botryococcus braunii* on concrete with a cultivation area of 0.275 m<sup>2</sup>, for instance, showed a biomass formation of ca. 25 g m<sup>-2</sup>, corresponding to a biomass concentration of ca. 96 g L<sup>-1</sup> (Ozkan *et al.*, 2012). Recently, the principle of miniaturization was intensified further and allowed for the cultivation of the model cyanobacterium *Synechocystis* sp. PCC 6803 as biofilm in a capillary reactor (**Figure 1.8 E**) (David *et al.*, 2015). This reaction system now awaits further evaluation of biomass concentrations and applicability for biocatalytic purposes.



**Figure 1.8:** Photobioreactor concepts with increasing surface-to-volume area. **A**) Open raceway pond, figure from (Wen *et al.*, 2016), **B**) Closed tubular photobioreactor, figure from (Wijffels *et al.*, 2013), **C**) Open thin-layer photobioreactor, figure from (Apel *et al.*, 2017), **D**) Biofilm-based cultivation on concrete, figure from (Ozkan *et al.*, 2012), **E**) Biofilm-based cultivation in a capillary reactor, figure from (David *et al.*, 2015).

### 1.5 Scope of the thesis

Much success was already achieved for the development of efficient oxyfunctionalization bioprocesses by the application of oxygenases in heterotrophic whole-cell host systems. However, several restrictions such as the technically limited O<sub>2</sub> supply and carbohydrate-based electron supply still limit their implementation on an industrial scale concerning production rates and costs. The use of phototrophic organisms as whole-cell biocatalysts for oxygenase-based biotransformations provides an alternative and promising technology for the eco-efficient production of oxyfunctionalized value-added chemicals. While numerous cyanobacterial or microalgal bioprocesses were already developed for CO<sub>2</sub>-derived fermentations, biotransformation processes relying on the generation of activated reduction equivalents as well as O<sub>2</sub> derived from photosynthetic water oxidation are rare. In this context, research mainly focuses on the demonstration of engineered catalysts with emphasis on the production of hydrogen (Das and Veziroğlu, 2001). Yet, an integrated bioprocess design for the application of phototrophic organisms in redox biotransformations beyond the proof-of-concept catalyst development is lacking (Fresewinkel *et al.*, 2014).

This thesis aims at the integrated application of biotechnological methods and strategies for the development of eco-efficient photosynthesis-driven oxyfunctionalization processes. The main research question combines the conceptual evaluation of photosynthetic electron and O<sub>2</sub> supply with the technical applicability of cyanobacteria as phototrophic host organisms in a hydrocarbon oxyfunctionalization bioprocess. Using the guide of integrated bioprocess design depicted in **Figure 1.3**, biocatalyst, reaction, and process engineering tools are applied for the establishment of new, photosynthesis-driven bioprocesses.

**Chapter 3** comprises the development of a *Synechocystis* sp. PCC 6803 strain, heterologously synthesizing the alkane monooxygenase AlkBGT originating from *Pseudomonas putida* GPo1 (Syn6803\_BGT). This chapter presents the novel concept of *in situ* supply of O<sub>2</sub> from photosynthetic water oxidation for the hydroxylation of nonanoic acid methylester (NAME) to 9-hydroxynonanoic acid methylester (H-NAME). **Chapter 4** further details the Syn6803\_BGT photobiocatalyst in long-term biotransformations, exercises substrate mass transfer and reactant toxicity in a reaction engineering approach via two-liquid phase biotransformation and describes the applicability of the photobiocatalyst in a lab-scale stirred tank photobioreactor. **Chapter 5** shows the development and application of a *Synechocystis* sp. PCC 6803 strain, heterologously synthesizing the cytochrome P450 enzyme system originating from *Acidovorax* sp. CHX100 (Syn6803\_CYP) for the hydroxylation of the volatile and toxic substrate cyclohexane to cyclohexanol. **Chapter 6** addresses the key limitation of cultivation systems to achieve high cyanobacterial biomass concentrations and focuses on the application of *Synechocystis* sp. PCC 6803 in a high-cell density format. This is realized via a mixed-trophies biofilm-based capillary reactor setting

using *Synechocystis* sp. PCC 6803 in combination with *Pseudomonas* sp. VLB120. **Chapter 7** generally discusses the potential of phototrophic bacteria as host organisms for O<sub>2</sub>-dependent reactions with a particular focus on *in situ* O<sub>2</sub> supply via photosynthetic water oxidation in relation to other concepts facilitating the *in situ* O<sub>2</sub> generation in the liquid phase. **Chapter 8** summarizes the outcome of this thesis and provides prospects for the development of eco-efficient whole-cell redox processes. In addition, the chapter gives further insights into how the results of this thesis may be implemented into a conceptual framework addressing O<sub>2</sub>-sensitive reactions such as the production of hydrogen functioning as zero-emission fuel gas.





## **Chapter 2    Materials & Methods**

## 2.1 Chemicals

**Chemicals.** Nonanoic acid methyl ester (NAME,  $\geq 97\%$ ), cyclohexanone (Cone, 99.5%), and diisononyl phthalate (DINP, technical grade) were purchased from Sigma-Aldrich (Steinheim, Germany). 9-hydroxynonanoic acid methyl ester (H-NAME,  $> 95\%$ ) was purchased from TCI Europe N.V. (Zwijndrecht, Belgium). Cyclohexane (Chx,  $\geq 99.8\%$ ) and cyclohexanol (Col,  $\geq 99\%$ ) were purchased from Merck (Darmstadt, Germany). Nonanoic acid (NA,  $\geq 97\%$ ) was obtained from Fluka Chemie GmbH (Buchs, Switzerland). All other chemicals were purchased from Carl-Roth GmbH (Karlsruhe, Germany), Merck (Darmstadt, Germany) or Sigma-Aldrich (Steinheim, Germany) in the highest purity available.

## 2.2 Bacterial strains and cultivation conditions

**Bacterial strains.** All cyanobacterial and *E. coli* strains and plasmids used in this thesis are listed in **Table 2.1**. Kanamycin was used as selection at a final concentration of  $50 \mu\text{g mL}^{-1}$ .

**Table 2.1:** Strains/ plasmids used in this thesis.

Strain/ Plasmid	Description	Reference
<i>E. coli</i> DH5 $\alpha$	F <sup>-</sup> $\Phi 80\text{lacZ}\Delta\text{M15 } \Delta(\text{lacZYA-argF})$ U169 recA1 endA1 hsdR17 (rK <sup>-</sup> , mK <sup>+</sup> ) phoA supE44 $\lambda\text{B}^-$ thi-1 gyrA96 relA1	(Hanahan, 1983)
<i>Synechocystis</i> sp. PCC 6803	Geographical origin: California, USA; Received from Pasteur Culture Collection of Cyanobacteria (PCC, Paris, France)	(Stanier <i>et al.</i> , 1971)
<i>E. coli</i> W3110	F <sup>-</sup> , $\lambda^-$ , rph-1, IN( <i>rrnD-rrnE</i> )1	(Bachmann, 1996)
<i>Pseudomonas</i> sp. VLB120	Wild-type <i>Pseudomonas</i> ; styrene prototroph	(Panke <i>et al.</i> , 1998)
pSB1AC3_Ptrc10:GFPmut3B	pMB1, P <sub>trc10</sub> promoter, <i>GFPmut3B</i> (BBa_E0040)	(Huang <i>et al.</i> , 2010)
pSB1AC3_PrnpB:lacI	pMB1, P <sub>mpB</sub> (constitutive promoter), lac repressor (lacI)	(Huang <i>et al.</i> , 2010)
pPMQAK1	Broad host range plasmid (RSF), mob genes, empty cloning vector	(Huang <i>et al.</i> , 2010)
pRSF_PrnpB:lacI_Ptrc10 (= pAH032)	RSF, lacI under control of P <sub>mpB</sub> promoter, P <sub>trc10</sub> promoter, empty expression vector	<b>Chapter 3</b>
pBT10	ColE1, pRO1600, alkane monooxygenase enzyme system <i>alkBFG</i> , <i>alkST</i> (originating from <i>Pseudomonas putida</i> GPo1) under control of P <sub>alk</sub> promoter	(Schrewe <i>et al.</i> , 2011)
pRSF_Ptrc10:BGtII (= pAH042)	RSF, lacI under control of P <sub>mpB</sub> , <i>alkBGT</i> genes under control of P <sub>trc10</sub> promoter (genes in a row, optimized RBS, C-terminal Strep-tag II), with central terminator (biobrick #BBa_B0015)	<b>Chapter 3</b>

pSEVA251	Broad host range plasmid (RSF), empty cloning vector	(Martínez-García <i>et al.</i> , 2014)
pRSF_nAlk (=pAH010)	RSF, alkane monooxygenase enzyme system <i>alkBFG</i> , <i>alkST</i> under control of P <sub>Alk</sub> promoter	<b>Chapter 4</b>
pRSF_PAik (=pAH008)	RSF, Palk regulatory system	<b>Chapter 4</b>
pRSF_PAik:BGT (=pAH039)	RSF, <i>alkBGT</i> genes under control of P <sub>Alk</sub> promoter (genes in a row, optimized RBS, C-terminal Strep-tag II)	<b>Chapter 4</b>
pRSF_Ptrc10:BGT (= pAH038)	RSF, <i>lacI</i> under control of P <sub>mpB</sub> promoter, <i>alkBGT</i> genes under control of P <sub>trc10</sub> promoter (genes in a row, optimized RBS, w/o C-terminal Strep-tag II), with central terminator (biobrick #BBa_B0015)	<b>Chapter 4</b>
pRSF_Ptrc10:BGTII_2x (= pAH048)	RSF, <i>lacI</i> under control of P <sub>mpB</sub> promoter, two copies of the operon containing the <i>alkBGT</i> under control of P <sub>trc10</sub> promoter	<b>Chapter 4</b>
pRSF_Ptrc10:BI (= pAH044)	RSF, <i>lacI</i> under control of P <sub>mpB</sub> promoter, <i>alkB</i> gene under control of P <sub>trc10</sub> promoter (optimized RBS, C-terminal Strep-tag II), with central terminator (biobrick #BBa_B0015)	<b>Chapter 4</b>
pRSF_Ptrc10:BGII (= pAH047)	RSF, <i>lacI</i> under control of P <sub>mpB</sub> promoter, <i>alkBG</i> genes under control of P <sub>trc10</sub> promoter (genes in a row, optimized RBS, C-terminal Strep-tag II), with central terminator (biobrick #BBa_B0015)	<b>Chapter 4</b>
pCom10_capro	ColE1, pRO1600, CypP450 monooxygenase (CYPchx), ferredoxin reductase (FdR), ferredoxin (Fd), cyclohexanone monooxygenase (CHXON) and cyclohexanol dehydrogenase (CDH) (originating from <i>Acidovorax</i> sp. CHX100) under control of P <sub>alk</sub> promoter	(Karande <i>et al.</i> , 2017)
pRSF_Ptrc10:CYP (= pAH050)	Based on pAH032; <i>CYPchx</i> , <i>FdR</i> , and <i>Fd</i> genes under control of P <sub>trc10</sub> promoter (genes in a row, optimized RBS in front of CYP)	<b>Chapter 5</b>
pRSF_Ptrc10:BVMO (= pAH049)	Based on pAH032; BVMO (CHXON originating from <i>Acidovorax</i> sp. CHX100) under control of P <sub>trc10</sub> promoter (optimized RBS, C-terminal Strep-tag II)	<b>Chapter 6</b>

**Cultivation of *E. coli* strains.** Overnight cultures were inoculated from cryo-stocks and grown in LB medium at 37 °C and 180 rpm (2.5 cm amplitude) (Sambrook and Russell, 2001). Pre-cultures were inoculated with 500 µL from this overnight culture and grown in 50 mL M9\* medium (US<sup>Fe</sup> trace elements) in a 250 mL baffled shake flask at 30 °C and 180 rpm (2.5 cm amplitude) (Bühler *et al.*, 2003b; Panke *et al.*, 1999). M9\* main-cultures were grown as described before by inoculating with the M9\* pre-cultures to an OD<sub>450</sub> of 0.2. Gene expression was induced 4 h after inoculation using 0.025% (v/v) DCPK (P<sub>alk</sub> promoter system) or 1 mM IPTG (P<sub>trc10</sub> promoter system) for another 4 h. The correlation factor

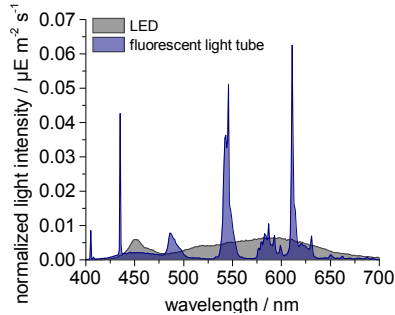
0.166 g<sub>CDW</sub> L<sup>-1</sup> OD<sub>450</sub><sup>-1</sup> was used for the calculations of cell dry weight concentrations (Blank *et al.*, 2008).

**Standard cultivation of *Synechocystis* sp. PCC 6803 strains.** *Synechocystis* sp. PCC 6803 was grown in YBG11 medium based on Shcolnick *et al.* 2007 containing 50 mM HEPES (Shcolnick *et al.*, 2007). Standard cultivation was performed using 20 mL YBG11 medium in 100 mL baffled Erlenmeyer shaking flasks in an orbital shaker (Multitron Pro shaker, Infors, Bottmingen, Switzerland) at 30 °C, 150 rpm (2.5 cm amplitude), 50 µE m<sup>-2</sup> s<sup>-1</sup> light intensity (LED), ambient CO<sub>2</sub> (0.04%) and 75% humidity. Growth was monitored by measuring the optical density at a wavelength of 750 nm using a spectrophotometer (Libra S11, Biochrom Ltd, Cambridge, UK). Pre-cultures were inoculated using 200 µL of a cryo-stock and grown under standard conditions for 4 - 6 days. Main cultures were inoculated from this pre-culture, starting with an OD<sub>750</sub> of 0.08 and, if not stated otherwise, grown for 3 days under standard conditions before gene expression was induced using 2 mM IPTG.

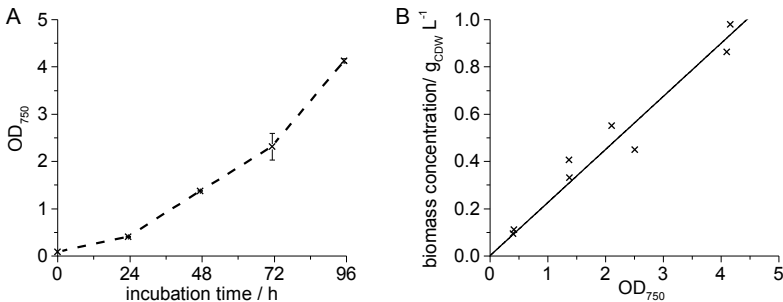
**YBG11 medium composition.** 1.49 g L<sup>-1</sup> NaNO<sub>3</sub>, 0.074 g L<sup>-1</sup> MgSO<sub>4</sub> · 7 H<sub>2</sub>O, 0.031 g L<sup>-1</sup> K<sub>2</sub>HPO<sub>4</sub>, 10 mL L<sup>-1</sup> YBG11 trace elements (100x), 0.019 g L<sup>-1</sup> Na<sub>2</sub>CO<sub>3</sub>, 50 mM HEPES (pH 7.2); YBG11 trace elements (100x): 3.6 g L<sup>-1</sup> CaCl<sub>2</sub> · 2 H<sub>2</sub>O, 0.63 g L<sup>-1</sup> citric acid, 0.28 g L<sup>-1</sup> boric acid, 0.11 g L<sup>-1</sup> MnCl<sub>2</sub> · 4 H<sub>2</sub>O, 0.02 g L<sup>-1</sup> ZnSO<sub>4</sub> · 7 H<sub>2</sub>O, 0.039 g L<sup>-1</sup> Na<sub>2</sub>MoO<sub>4</sub> · 2 H<sub>2</sub>O, 0.007 g L<sup>-1</sup> CuSO<sub>4</sub> · 5 H<sub>2</sub>O, 0.005 g L<sup>-1</sup> Co(NO<sub>3</sub>)<sub>2</sub> · 6 H<sub>2</sub>O, 0.16 g L<sup>-1</sup> FeCl<sub>3</sub> · 6 H<sub>2</sub>O, 0.6 g L<sup>-1</sup> Na<sub>2</sub>EDTA · 2 H<sub>2</sub>O

**Light intensity and light spectra.** The light intensity was measured by means of photosynthetically active radiation (PAR) in µE m<sup>-2</sup> s<sup>-1</sup>, determined using a universal light meter (ULM-500, Heinz Walz GmbH, Effeltrich, Germany) equipped with a MQS-B mini quantum sensor. Light spectra were measured using a light spectrometer (Tristan, m-u-t GmbH, Wedel, Germany) in the orbital shaker used for cultivation of *Synechocystis* sp. PCC 6803 (LED, Multitron Pro shaker, Infors, Bottmingen, Switzerland), for oxyfunctionalization activity measurements (fluorescence light tubes, Multitron, Infors HT, Bottmingen, Switzerland) and in the growth chamber used for cultivation on agar plates (fluorescence light tubes, poly klima GmbH, Freising, Germany) (Figure 2.1).

**Correlation factor OD<sub>750</sub> - cell dry weight (CDW).** The correlation of the optical density OD<sub>750</sub> to the cell dry weight (CDW) was determined for the recombinant strain *Synechocystis* sp. PCC 6803 pAH042 (= Syn6803\_BGT) grown under standard conditions. At respective time-points 30 mL of grown culture was harvested by centrifugation (15 min, 3180 g, 4 °C), washed once in 15 mL H<sub>2</sub>O, resuspended in 1.5 mL H<sub>2</sub>O, and dried in pre-dried and pre-weighted glass tubes at 70 °C for 10 days. The cell dry weight was determined and correlated to the optical density with a resulting correlation factor of 0.2246 g<sub>CDW</sub> L<sup>-1</sup> OD<sub>750</sub><sup>-1</sup> (Figure 2.2).



**Figure 2.1.** Light spectra measured in incubators equipped with LED panels or fluorescent light tubes, respectively.



**Figure 2.2:** Determination of the correlation factor regarding biomass concentrations ( $\text{g}_{\text{CDW}} \text{L}^{-1}$ ) at various optical densities  $\text{OD}_{750}$ . **(A)** Growth curve of *Synechocystis* sp. PCC 6803 pRSF\_Ptr10:BGTTII, **(B)** Biomass concentrations measured as  $\text{g}_{\text{CDW}} \text{L}^{-1}$  at various optical densities.

### 2.3 Plasmid constructions

Plasmid constructions were performed via *E. coli* DH5 $\alpha$  using the primer given in **Table 2.2** and the following protocols and cloning steps.

**Restriction** endonucleases used in this study were obtained from Thermo Scientific – Germany GmbH (Schwerte, Germany) and used according to the manufactures’ user guide.

**Amplification** of DNA fragments was performed by PCR applying the Phusion High Fidelity (HF) DNA polymerase from Thermo Scientific – Germany GmbH (Schwerte, Germany) according to the 3-step protocol described in the manufactures’ user guide using primers purchased from Eurofins MWG (Ebersberg, Germany) listed in **Table 2.2**. Respective annealing temperatures ( $T_{\text{An}}$ ) and elongation times ( $t_{\text{Elong}}$ ) are given below. **Overlap-Extension PCR** (OE-PCR) was performed by applying 50 ng of each DNA Fragment to be fused in 100  $\mu\text{L}$  of the standard PCR mix, initially missing the respective primer as these

were added after 5 PCR cycles. **Dephosphorylation** of plasmid DNA was performed using the FastAP Thermosensitive Alkaline Phosphatase from Thermo Scientific – Germany GmbH (Schwerte, Germany) according to the manufactures’ user guide. **Purification** of plasmid DNA and amplified DNA fragments was performed using the PCR clean-up gel extraction kit from MACHERY-NAGEL GmbH & Co. KG (MACHEREY-NAGEL GmbH & Co. KG, Düren, Germany). **Gibson cloning** was performed by an one-step isothermal in vitro recombinant cloning method described by Gibson *et al.*, 2009 (Gibson *et al.*, 2009). **Ligation** was performed using the T4 DNA Ligase from Thermo Scientific – Germany GmbH (Schwerte, Germany) according to the manufactures’ user guide. **Verification** of cloning results was performed by sequencing by Eurofins MWG (Ebersberg, Germany).

**Table 2.2:** Primer used during cloning procedure for plasmids constructions. **binding region**, **fusion**, **overlap to vector**, **restriction site**, **appendix(P<sub>trc10</sub>)**, **scar**, **RBS\***, **Strep-tag II**, **stop**

Primer#	Function	Sequence 5' → 3'
PAH006	AlkT rev	GCATCATTGCTAATCAGG
PAH029	AlkG rev	TCACTTTTCCTCGTAGAGC
PAH030	nAlk rev	TGCAGGTCGACTCTAGAGGATCCCCGGGTCACTTTTCCTCGTAGAGC
PAH037	nAlk fwd	CCGCGCGAATTCGAGCTCGGTACCCGCATCATTGCTAATCAGG
PAH043	P <sub>alk</sub> fwd	ATAACAATTTACACAGGAGGCCGCCTTAGATAAATTCCTTGACGC
PAH044	P <sub>alk</sub> rev	AAGCTTGCATGCCTGCAGGTCGACTCTCAAGCATATGGAATCTC
PAH055	P <sub>trc10</sub> :Term Part I fwd	TCCGGCTCGTATAATGTGTGGAATTGTGAGCGGATAACAATTTACACATACTAGTACCAGGCATCAAATAAAACG
PAH056	P <sub>trc10</sub> :Term PartI rev	TATAAACGCAGAAAGGCC
PAH057	P <sub>trc10</sub> :Term Part II fwd	TGATTTCTGGAATTCGCGGCCGCTTCTAGATTGACAATTAATCATCCGGCTCGTATAATGTG
PAH058	P <sub>trc10</sub> :Term PartII rev	ACACCTTGCCCGTTTTTTTGCCGGACTGCAGTATAAACGCAGAAAGGCC
PAH059	oAlkBII fwd	TGAGCGGATAACAATTTACACATACTAGAGTAGTGGAGTTACTAGATGCTTGAGAAACACAGAG
PAH060	AlkB rev	CTACGATGCTACCCGAC
PAH061	AlkG fwd	GAGTACCTCTGCGGTAGCATCGTAGTACTAGAGTAGTGGAGGTTACTAGATGGCTAGCTATAAATGCC
PAH062	AlkT fwd	CTATGTGCTCTACGAGGAAAAGTGATACTAGAGTAGTGGAGGTTACTAGATGGCAATCGTTGTTGTTG
PAH063	Fusion oBGTII fwd	TGAGCGGATAACAATTTTC
PAH064	AlkBGT fusion rev	CTTTCGTTTTATTGATGCCTGGTACTCTAGTAGCATCATTGCTAATCAGG
PAH067	oAlkBII rev	CTATTTTTCGAACTCGGGTGGCTCCAAGCGCTCGATGCTACGCAGAGG
PAH068	oAlkGII fwd	GAGCCACCCGCGATTCGAAAAATAGTACTAGAGTAGTGGAGGTTACTAGATGGCTAGCTATAAATGCC
PAH069	oAlkGII rev	CTTTTCCTCGTAGAGCAC

PAH070	oAlkTII fwd	GAGCCACCCGAGTTCGAAAAATAGTACTAGAGTAGTGGAG GTTACTAGATGGCAATCGTTGTTGTTG
PAH071	oAlkTII rev	ATCAGGTAATTTTATACTCCC
PAH072	Fusion oBGII rev	CTATTTTTCGAACTGCGGGTGGCTCCAAGCGCTCTTTTCCTC GTAGAGCAC
PAH073	Fusion oBGTII rev	CTTTGTTTTATTGATGCCTGGTACTATTTTTCGAACTGCGG GTGGCTCCAAGCGCTATCAGGTAATTTATACTCCC
PAH074	AlkB fwd	ATGCTTGAGAAACACAGAG
PAH075	AlkBGT fusion fwd	GCGACTAATTTAATAAAAAATTGGAGCTAGAGTAGTGGAGGTT ACTAGATGCTTGAGAAACACAGAG
PAH076	AlkBGT fusion rev	TGCAGGTCGACTCTCAAGCATATGGCTCTAGTAGCATCATTG CTAATCAGG
PAH077	Terminator fwd	GGGAGGTATTGGACCGCATTGAACTCTAGTATATAACGCAG AAAGGCC
PAH078	Terminator rev	ACGAGCCGGATGATTAATTGTCAATCTAGAGCCAGGCATCAA ATAAAACG
PAH079	AlkB rev	CTTTGTTTTATTGATGCCTGGTACTATTTTTCGAACTGCGG GTGGCTCCAAGCGCTCGATGCTACCGCAGAGG
PAH087	P <sub>trc10</sub> :BGT fwd	ATCAGCTCACTCAAAGGCGGTAATCTTGACAATTAATCATCC GGC
PAH090	P <sub>trc10</sub> :BGT rev	ATTCGGCTGAGGGTAAAAGAACTCAATTGCGAGGAAGCCT GCATAAC
PAH091	BVMO fwd	TGAGCGGATAACAATTTACACATACTAGAGTAGTGGAGGTT ACTAGATGAAAAAACCCAACATCTGG
PAH092	BVMO rev	TCGTTTTATTGATGCCTGGCTGCACTATTTTTCGAACTGCG GGTGGCTCCAAGCGCTCTGGAATACGAAACCCTCG
PAH093	CYP fwd	TGAGCGGATAACAATTTACACATACTAGAGTAGTGGAGGTT ACTAGATGACTCAGACTGCTGGCGG
PAH094	CYP rev	CTTTGTTTTATTGATGCCTGGTACAGTGCTGCCCTTGGC
SPA017	Verification fwd	CCATCAAACAGGATTTTCG
SPA023	Verification rev	TGCCACCTGACGTCTAAGAA

### Construction of pRSF\_P<sub>trc10</sub>:BGTII (=pAH042)

a) Construction of empty expression vector pAH032

Restriction: pSB1AC3\_P<sub>trc10</sub>:GFPmut3B (XbaI + PstI) → pSB1AC3 (XbaI, PstI)

Amplification: *P<sub>trc10</sub>:Term* part I from pSB1AC3\_P<sub>trc10</sub>:GFP  
(PAH055 + PAH056 → 186 BP, T<sub>An</sub>: 60 °C, t<sub>Elong</sub>: 10 sec)  
*P<sub>trc10</sub>:Term* part II from part I  
(PAH057 + PAH058 → 262 BP, T<sub>An</sub>: 72 °C, t<sub>Elong</sub>: 10 sec)

Gibson cloning: pSB1AC3 (XbaI, PstI) + *P<sub>trc10</sub>:Term* part II  
→ pSB1AC3\_P<sub>trc10</sub>:Term

Restriction: pSB1AC3\_P<sub>trc10</sub>:Term (XbaI)

Dephosphorylation: pSB1AC3\_P<sub>trc10</sub>:Term (XbaI) (FastAP, Thermo)

Restriction: pSB1AC\_P<sub>trn</sub>B:lacI with (XbaI + SpeI)

Ligation: pSB1AC3\_P<sub>trc10</sub>:Term (XbaI) + P<sub>trn</sub>B:lacI (XbaI\_SpeI) (1:2)  
→ pSB1AC3\_P<sub>trn</sub>B:lacI\_P<sub>trc10</sub>:Term

Verification by PCR: Clones with the *PmpB:lacI* fragment incorporated in the intended direction were determined by PCR

(SPA017 + SPA023 → 500 BP,  $T_{An}$ : 61 °C,  $t_{Elong}$ : 15 sec)

Restriction: pPMQAK1 (EcoRI + PstI)

Restriction: pSB1AC3\_PmpB:lacI\_Ptrc1O:Term (EcoRI + PstI)

Ligation: pPMQAK1 (EcoRI, PstI) + PmpB:lacI\_Ptrc1O:Term (EcoRI, PstI) ( 1:5)  
→ pPMQAK1\_PmpB:lacI\_Ptrc1O:Term = pAH032

b) Construction of pRSF\_Ptrc1O:BGTII (pAH042)

Restriction: pPMQAK1\_PmpB:lacI\_Ptrc1O:Term (SpeI)

Amplification: *oAlkBII* from pBT10

(PAH059 + PAH067 → 1283 BP,  $T_{An}$ : 65 °C,  $t_{Elong}$ : 25 sec)

*oAlkGII* from pBT10

(PAH068 + PAH069 → 568 BP,  $T_{An}$ : 60 °C,  $t_{Elong}$ : 25 sec)

*oAlkTII* from pBT10

(PAH070 + PAH071 → 1204 BP,  $T_{An}$ : 65 °C,  $t_{Elong}$ : 25 sec)

OE-PCR: *oAlkBII*+ *oAlkGII* → *oAlkBGI*

(PAH063 + PAH072 → 1859 BP,  $T_{An}$ : 65 °C,  $t_{Elong}$ : 60 sec)

*oAlkBGI* + *oAlkTII* → *oAlkBGTII*

(PAH063 + PAH073 → 3096 BP,  $T_{An}$ : 57 °C,  $t_{Elong}$ : 90 sec)

Gibson cloning: pPMQAK1\_PmpB:lacI\_Ptrc1O:Term (SpeI) + *oAlkBGTII*  
→ pPMQAK1\_PmpB:lacI\_Ptrc1O:BGTII\_pre (w/o  $T_{central}$ )

Restriction: pPMQAK1\_PmpB:lacI\_Ptrc1O:BGTII\_pre (XbaI)

Amplification: *Term* from pSB1AC3\_Ptrc1O:GFP

(PAH077 + PAH078 → 191 BP,  $T_{An}$ : 60 °C,  $t_{Elong}$ : 5 sec)

Gibson cloning pPMQAK1\_PmpB:lacI\_Ptrc1O:BGTII\_pre (XbaI) + *Term*  
→ pRSF\_Ptrc1O:BGTII = pAH042

### Construction of pRSF\_nAlk (= pAH010)

Restriction: pSEVA251 with SmaI

Amplification: native *alk* expression system from pBT10 (=nAlk)

(PAH037+ PAH030 → 6747 BP,  $T_{An}$ : 58 °C,  $t_{Elong}$ : 210 sec)

Gibson cloning: pSEVA251 (SmaI) + nAlk → pRSF\_nAlk = pAH010

### Construction of pRSF\_Palk:BGT (= pAH039)

a) Construction empty expression vector pAH008

Restriction: pSEVA251 with XmaI + XbaI

Amplification: Promoter system *P<sub>alkS</sub>alkS\_P<sub>alkB</sub>* from pBT10 (=Palk)

(PAH043+ PAH044 → 3157 BP,  $T_{An}$ : 65 °C,  $t_{Elong}$ : 60 sec)

Gibson cloning: pSEVA251 (XmaI, XbaI) + *Palk* → pRSF\_Palk = pAH008



b) Construction of pRSF\_Palk:BGT (= pAH039)

Restriction: pRSF\_Palk with EcoRI

Amplification: *AlkB* from pBT10  
 (PAH074 + PAH060 → 1206 BP, T<sub>An</sub>: 60 °C, t<sub>Elong</sub>: 60 sec)  
*AlkG* from pBT10  
 (PAH061 + PAH029 → 571 BP, T<sub>An</sub>: 65°C, t<sub>Elong</sub>: 25 sec)  
*AlkT* from pBT10  
 (PAH062 + PAH006 → 1216 BP, T<sub>An</sub>: 65°C, t<sub>Elong</sub>: 25 sec)

OE-PCR: *AlkB* + *AlkG* → *AlkBG*  
 (PAH074 + PAH029 → 1752 BP, T<sub>An</sub>: 60 °C, t<sub>Elong</sub>: 35 sec)  
*AlkBG* + *AlkT* → *AlkBGT*  
 (PAH075 + PAH076 → 3023 BP, T<sub>An</sub>: 60 °C, t<sub>Elong</sub>: 80 sec)

Gibson cloning: pSEVA251\_Palk (EcoRI) + *AlkBGT* → pRSF\_Palk:BGT = pAH039

**Construction of pRSF\_Ptrc10:BGT (= pAH038)**

Restriction: pAH032 with SpeI

Amplification: *AlkB* from pBT10  
 (PAH059 + PAH060 → 1253 BP, T<sub>An</sub>: 65°C, t<sub>Elong</sub>: 25 sec)  
*AlkG* from pBT10  
 (PAH061 + PAH029 → 571 BP, T<sub>An</sub>: 65°C, t<sub>Elong</sub>: 25 sec)  
*AlkT* from pBT10  
 (PAH062 + PAH006 → 1216 BP, T<sub>An</sub>: 65°C, t<sub>Elong</sub>: 25 sec)

OE-PCR: *AlkB* + *AlkG* → *AlkBG*  
 (PAH063 + PAH029 → 1799 BP, T<sub>An</sub>: 65°C, t<sub>Elong</sub>: 60 sec)  
*AlkBG* + *AlkT* → *AlkBGT*  
 (PAH063 + PAH064 → 3023 BP, T<sub>An</sub>: 57°C, t<sub>Elong</sub>: 90 sec)

Gibson cloning: pAH032 (SpeI) + *AlkBGT* → pRSF\_Ptrc10:BGT\_pre (w/o T<sub>central</sub>)

Restriction: pRSF\_Ptrc10:BGT\_pre with XbaI

Amplification: *Term* from pSB1AC3\_Ptrc10:GFPmut3B  
 (PAH077 + PAH078 → 191 BP, T<sub>An</sub>: 60 °C, t<sub>Elong</sub>: 5 sec)

Gibson cloning: pRSF\_Ptrc10:BGT\_pre (XbaI) + *Term*  
 → pRSF\_Ptrc10:BGT = pAH038

**Construction of pRSF\_Ptrc10:BGTII\_2x (= pAH048)**

Restriction: pRSF\_Ptrc10:BGTII with MunI

Amplification: *Ptrc10:BGTII* from pRSF\_Ptrc10:BGTII  
 (PAH087+ PAH090 → 3387 BP, T<sub>An</sub>: 72°C - 0.3°C cycle<sup>-1</sup>, t<sub>Elong</sub>: 60 sec)

Gibson cloning: pRSF\_Ptrc10:BGTII (MunI) + *Ptrc10:BGTII*  
 → pRSF\_Ptrc10:BGTII\_2x = pAH048

**Construction of pRSF\_Ptrc1O:BIl (= pAH044)**

Restriction: pAH032 with SpeI  
Amplification: *alkB* from pBT10  
(PAH059+ PAH079 → 1308 BP, T<sub>An</sub>: 64 °C, t<sub>Elong</sub>: 40 sec)  
Gibson cloning: pAH032 (SpeI) + *AlkB* → pRSF\_Ptrc1O:BIl\_pre (w/o T<sub>central</sub>)  
Restriction: pRSF\_Ptrc1O:BIl\_pre with XbaI  
Amplification: *Term* from pSB1AC3\_Ptrc1O:GFPmut3B  
(PAH077 + PAH078 → 191 BP, T<sub>An</sub>: 60 °C, t<sub>Elong</sub>: 5 sec)  
Gibson assembly: pRSF\_Ptrc1O:BIl\_pre (XbaI) + *Term* → pRSF\_Ptrc1O:BIl = pAH044

**Construction of pRSF\_Ptrc1O:BGII (=pAH047)**

Restriction: pAH032 with SpeI  
Amplification: *alkB* from pBT10  
(PAH074+ PAH067 → 1236 BP, T<sub>An</sub>: 67°C, t<sub>Elong</sub>: 25 sec)  
*alkG* from pBT10  
(PAH068+ PAH069 → 568 BP, T<sub>An</sub>: 61°C, t<sub>Elong</sub>: 25 sec)  
OE-PCR: *alkB* + *alkG* → *alkBG*  
(PAH059+ PAH072 → 1884 BP, T<sub>An</sub>: 56°C, t<sub>Elong</sub>: 45 sec)  
Gibson cloning: pAH032 (SpeI) + *alkBG* → pRSF\_Ptrc1O:BGII\_pre (w/o T<sub>central</sub>)  
Restriction: pRSF\_Ptrc1O:BGII\_pre with XbaI  
Amplification: *Term* from pSB1AC3\_Ptrc1O:GFPmut3B  
(PAH077 + PAH078 → 191 BP, T<sub>An</sub>: 60 °C, t<sub>Elong</sub>: 5 sec)  
Gibson cloning: pRSF\_Ptrc1O:BGII\_pre (XbaI) + *Term*  
→ pRSF\_Ptrc1O:BGII = pAH047

**Construction of pRSF\_Ptrc1O:CYP (= pAH050)**

Restriction: pAH032 with SpeI  
Amplification: *CYP-FdR-Fd* from pCom10\_capro  
(PAH093 + PAH094 → 2970 BP, T<sub>An</sub>: 72 °C, t<sub>Elong</sub>: 60 sec)  
Gibson cloning: pAH032 (SpeI) + *CYP-FdR-Fd*  
→ pRSF\_Ptrc1O:CYP\_pre (w/o T<sub>central</sub>)  
Restriction: pRSF\_Ptrc1O:CYP\_pre with XbaI  
Amplification: *Term* from pSB1AC3\_Ptrc1O:GFPmut3B  
(PAH077 + PAH087 → 191 BP, T<sub>An</sub>: 60 °C, t<sub>Elong</sub>: 5 sec)  
Gibson cloning: pRSF\_Ptrc1O:CYP\_pre (XbaI) + *Term*  
→ pRSF\_Ptrc1O:CYP = pAH050

**Construction of pRSF\_Ptrc10:BVMO (= pAH049)**

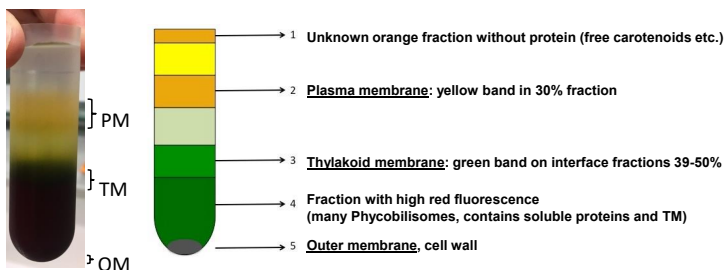
Restriction: pAH032 with SpeI  
 Amplification: BVMO from pCom10\_capro  
 (PAH091 + PAH092 → 1689 BP,  $T_{An}$ : 72 °C,  $t_{Elong}$ : 45 sec)  
 Gibson cloning: pAH032 (SpeI) + BVMO → pRSF\_Ptrc10:BVMO\_pre (w/o  $T_{central}$ )  
 Restriction: pRSF\_Ptrc10:BVMO\_pre with XbaI  
 Amplification: Term from pSB1AC3\_Ptrc10:GFPmut3B  
 (PAH077 + PAH087 → 191 BP,  $T_{An}$ : 60 °C,  $t_{Elong}$ : 5 sec)  
 Gibson cloning: pRSF\_Ptrc10:BVMO\_pre (XbaI) + Term  
 → pRSF\_Ptrc10:BVMO = pAH049

**Transformation.** Transformation of *Synechocystis* sp. PCC 6803 was performed by electroporation based on a method described by Ferreira, 2014 (Ferreira, 2014). Electro-competent cells were produced by growing a 50 mL YBG11 main culture (in 100 mL baffled shaking flask) to an  $OD_{750}$  of 0.5 – 1. Cells were harvested by centrifugation (10 min, 3180 g, 4 °C), washed three times in 10 mL ice-cold HEPES buffer (1 mM, pH 7.5) and resuspended in 1 mL HEPES buffer (1 mM, pH 7.5). Electro-competent cells were stored at -80 °C in 5% (v/v) DMSO. For electroporation 0.2 - 1.0 µg of plasmid DNA were added to 60 µL of cells in an electroporation cuvette (2 mm electrode gap), pulsed with 2500 V for 5 ms (12.5 kV cm<sup>-1</sup>) (Eppendorf Eporator, Eppendorf Vertrieb Deutschland GmbH, Wesseling-Berzdorf, Germany) and subsequently transferred to 50 mL YBG11 medium (100 mL baffled shanking flask). After cultivation at standard conditions for 24 h, cells were harvested by centrifugation (10 min, 3180g, RT), resuspended in 100 µL YBG11 medium and plated on BG11 agar supplemented with 0.3% of sodium thiosulfate and 50 µg mL<sup>-1</sup> kanamycin. Plates were cultivated in a growth chamber for 4-6 days at 30 °C, 20-50 µE m<sup>-2</sup> s<sup>-1</sup> light intensity (fluorescence light tubes), ambient CO<sub>2</sub> (0.04%) and 80% humidity (poly klima GmbH, Freising, Germany). Single colonies were picked, plated on fresh BG11 agar and incubated as described before. The grown biomass was used to inoculate a 20 mL YBG11 pre-culture until cryo stocks were prepared from this pre-culture and stored in 5% (v/v) DMSO at -80 °C.

**BG11 agar plates:** 1.5 g L<sup>-1</sup> NaNO<sub>3</sub>, 0.075 g L<sup>-1</sup> MgSO<sub>4</sub> · 7 H<sub>2</sub>O, 0.036 g L<sup>-1</sup> CaCl<sub>2</sub> · 2 H<sub>2</sub>O, 0.006 g L<sup>-1</sup> citric acid, 0.04 g L<sup>-1</sup> K<sub>2</sub>HPO<sub>4</sub>, 0.006 g L<sup>-1</sup> ferric ammonium citrate, 0.001 g L<sup>-1</sup> Na<sub>2</sub>EDTA, 0.02 g L<sup>-1</sup> Na<sub>2</sub>CO<sub>3</sub>, 1 mL L<sup>-1</sup> BG11 trace elements (1000x), 0.3% Na<sub>2</sub>S<sub>2</sub>O<sub>3</sub>, 10 mM HEPES (pH 8), 1.5% agar; BG11 trace elements (1000x): 2.86 g L<sup>-1</sup> boric acid, 1.8 g L<sup>-1</sup> MnCl<sub>2</sub> · 4 H<sub>2</sub>O, 0.22 g L<sup>-1</sup> ZnSO<sub>4</sub> · 7 H<sub>2</sub>O, 0.39 g L<sup>-1</sup> Na<sub>2</sub>MoO<sub>4</sub> · 2 H<sub>2</sub>O, 0.08 g L<sup>-1</sup> CuSO<sub>4</sub> · 5 H<sub>2</sub>O, 0.05 g L<sup>-1</sup> Co(NO<sub>3</sub>)<sub>2</sub> · 6 H<sub>2</sub>O

## 2.4 Biochemical analysis of recombinant strains

**Membrane fractionation of Syn6803\_BGT using sucrose density gradient centrifugation.** Membrane fractionation of Syn6803\_BGT was performed using a protocol adapted from Omata and Murata et al. (Murata and Omata, 1988; Omata and Murata, 1983; Omata and Murata, 1984). If not stated otherwise, all steps were performed on ice. 50 mL of cyanobacterial cell culture ( $OD_{750} > 40$ ) were washed twice in 50 mL of buffer A (5 mM HEPES, pH 7 – sterile filtered, 1 mM phenylmethylsulfonyl fluorid (PMSF) - added just before use), resuspended in 100 mL lysis buffer (10 mM HEPES, pH 7, 600 mM sucrose, 5 mM EDTA, 50 mM NaCl, 2.5 g L<sup>-1</sup> lysozyme – added just before use) and incubated in a 250 mL baffled shake flask for 2 h at 50  $\mu\text{E m}^{-2} \text{s}^{-1}$ , 30 °C, and 200 rpm (2.5 cm amplitude). After centrifugation (10 min, 5000 g, 4 °C), the pellet was washed twice in 50 mL buffer B (20 mM HEPES, pH 7, 600 mM sucrose, 1 mM PMFS – added just before use), resuspended in 50 mL buffer B and supplemented with 50  $\mu\text{L}$  DNase I (final 5 U mL<sup>-1</sup>, stock: 5000 U mL<sup>-1</sup>, 1.3 mg mL<sup>-1</sup> DNase I à 3755 U mg<sup>-1</sup> in 20 mM Tris pH 7.5, 1 mM MgCl<sub>2</sub> · 6 H<sub>2</sub>O, 50% glycerol). Cell disruption was conducted using FrenchPress (3 x 1900 Psi). After centrifugation (5 min, 5000 g, 4 °C), the supernatant was collected as total protein fraction and supplemented with 0.74 volumes of 90% sucrose dissolved in buffer B (= 50% total sucrose concentration). Sucrose density centrifugation was performed in thin wall polypropylene tubes (total volume 38.5 mL, Beckmann Coulter GmbH, Krefeld, Germany) using the following gradient: 15 mL of sample (50% sucrose), 10 mL 10% sucrose (in buffer B), 3 mL 30% sucrose (in buffer B), and 10 mL 10% sucrose (in buffer B). Ultracentrifugation was conducted at 130,000 g and 4 °C for 18 h. Fractions for plasma membrane (PM), thylakoid membrane (TM), and the red fraction were collected as depicted in **Figure 2.3**.



**Figure 2.3:** Picture (left) and schematic view (right) of membrane fractions containing respective proteins obtained after sucrose density centrifugation.

The outer membrane (OM) proteins in the pellet were resuspended in 250  $\mu\text{L}$  buffer C (20 mM HEPES, pH 7). PM and TM fractions were diluted 3-fold in buffer C, centrifuged again at 120,000g, 4 °C for 1 h and resuspended in 250  $\mu\text{L}$  buffer C. The red fraction was further separated by centrifugation (30 min, 10,000g, 4 °C). Protein concentrations were

measured using Bradford analysis (Bradford, 1976). All samples were stored at -20 °C for Western blot analysis.

**Strep-tag purification of recombinant *Synechocystis* sp. PCC 6803 strains.** Ca. 200 mL of cyanobacterial cell culture (OD<sub>750</sub> ca. 2) were harvested by centrifugation (5000g, 4 °C, 10 min), washed in 25 mL TBS buffer (100 mM Tris-HCl pH 7.5, 150 mM NaCl, 1 mM phenylmethylsulfonyl fluorid (PMSF) - added just before use), and resuspended in 3 mL TBS buffer containing 100 µL of DNase I (final 167 U, stock: 5000 U mL<sup>-1</sup>, 1.3 mg mL<sup>-1</sup> DNase I à 3755 U mg<sup>-1</sup> in 20 mM Tris pH 7.5, 1 mM MgCl<sub>2</sub> · 6 H<sub>2</sub>O, 50% glycerol). Cell disruption was conducted using FrenchPress (2 x 1200 Psi). The total protein fraction in the supernatant was collected by centrifugation (5,000g, 4 °C, 10 min). Protein concentrations were quantified by the method of Bradford (Bradford, 1976). AlkB, AlkG, and AlkT were separated from the total protein fraction using Strep-Tactin Superflow chromatography according to the manufactory manual (IBA GmbH, Göttingen, Germany). 1.5 mL of the total protein sample were loaded to a pre-conditioned Strep-Tactin purification column (2 mL of 50% Strep-Tactin Superflow suspension, equilibrated with 2 mL buffer W (100 mM Tris-HCl pH 8.0, 150 mM NaCl, 1 mM EDTA)). Proteins were washed using 3 x 1 mL TBS buffer before Strep-tag proteins were eluted using 2 x 0.75 mL elution buffer (2.5 mM Desthiobiotin in TBS buffer). If required, proteins were 5x concentrated by acetone precipitation by adding 800 µL acetone to 200 µL of proteins, and incubation at -20 °C for ca. 16 h. Proteins were collected by centrifugation (17,000g, 4 °C, 10 min) and resuspended in 20 µL of SDS buffer.

**Cell disruption of *Synechocystis* sp. PCC 6803 using glass beads.** *Synechocystis* sp. PCC 6803 cells were cultivated as described before, harvested by centrifugation (10 min, 4 °C, 5000g) and stored at -20 °C. Cell disruption was performed with a homogenizer (Precellys Evolution Super Homogenizer, BERTIN TECHNOLOGIES, Saint Quentin en Yvelines Cedex, France) using glass beads in TBS-buffer (0.1 M Tris, 0.15 M NaCl, pH 7.5) containing 1 mM PMSF at an OD<sub>750</sub> of 20 (4 x 30 s at 17,000g, cooling with liquid nitrogen). Proteins in the supernatant were treated with 2x SDS-buffer at 99 °C for 10 min before 20 µL of each sample was loaded on SDS-gels.

**SDS PAGE analysis and Western blot analysis.** Protein separation was performed as described by Laemmli with a 3.6% acrylamide stacking and a 12% acrylamide separating gel (Laemmli, 1970). For Western blot analysis, proteins were transferred from acrylamide gels to a nitrocellulose membrane (0.45 µm) using semi-dry blotting for 30 min at 0.8 mA cm<sup>-2</sup>. Detection of Strep-tagII-tagged proteins was performed using a Strep-Tactin-HRP antibody (IBA Lifesciences, Göttingen, Germany). Analysis of the purity of the plasma membrane protein fraction after membrane fractionation was performed using anti NrtA antibody. Visualization was followed using chemiluminescence (SuperSignal West Pico PLUS Chemiluminescent Substrate, ThermoFisher Scientific, Waltham, USA) and X-ray development.



## **Chapter 3      Overcoming the gas-liquid mass transfer of oxygen by coupling photosynthetic water oxidation with biocatalytic oxyfunctionalization**

Bruno Bühler and Andreas Schmid coordinated the project and corrected the manuscript.

Published in:

*Angewandte Chemie International Edition*, **2017**, 56 (47), 15146 – 15149

### **3.1 Abstract**

Gas-liquid mass transfer of gaseous reactants is a major limitation for high space-time yields, especially for O<sub>2</sub>-dependent (bio)catalytic reactions in aqueous solutions. Herein, oxygenic photosynthesis was used for homogeneous O<sub>2</sub> supply via *in situ* generation in the liquid phase to overcome this limitation. The phototrophic cyanobacterium *Synechocystis* sp. PCC 6803 was engineered to synthesize the alkane monooxygenase AlkBGT from *Pseudomonas putida* GPo1. With light, but without external addition of O<sub>2</sub>, the chemo- and regioselective hydroxylation of nonanoic acid methyl ester to 9-hydroxynonanoic acid methyl ester was driven by O<sub>2</sub> generated through photosynthetic water oxidation. Photosynthesis also delivered the necessary reduction equivalents to regenerate the Fe<sup>2+</sup> center in AlkB for oxygen transfer to the terminal methyl group. The *in situ* coupling of oxygenic photosynthesis to O<sub>2</sub>-transferring enzymes now enables the design of fast hydrocarbon oxyfunctionalization reactions.

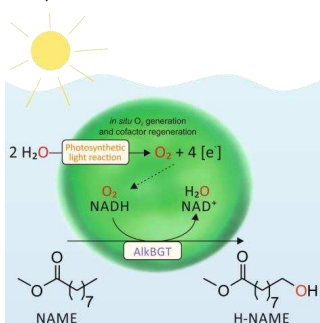


### 3.2 Introduction

Gas-liquid mass transfer defines the performance and efficiency of reactions in liquids with gaseous reactants. This is especially true for (bio)catalysts operating in aqueous solutions (Chaudhari *et al.*, 1995; Cornils and Herrmann, 2004; Law *et al.*, 2006; Park, 2007; Wachsen *et al.*, 1998). O<sub>2</sub> is one of the most prominent gaseous reactants. As an oxidant for oxidative catalysis, O<sub>2</sub> is of great importance for the production of value-added chemicals and pharmaceuticals (Bühler *et al.*, 2003a; Gavriilidis *et al.*, 2016; Piera and Bäckvall, 2008; Shi *et al.*, 2012). For the efficient use of O<sub>2</sub> as a reactant, harsh reaction conditions with high temperatures and/or pressures are typically necessary. Such conditions may lead to severe safety and selectivity issues, often resulting in low reaction yields. They typically also necessitate highly regulated, elaborate, and thus expensive process control regimes (Gavriilidis *et al.*, 2016; Osterberg *et al.*, 2014; Schuchardt *et al.*, 2001). Mild reaction conditions, high selectivities, and high yields are generally desirable for oxidative production processes and achieved most efficiently by enzyme catalysis (Bordeaux *et al.*, 2012; Schmid *et al.*, 2001). However, low gas-liquid mass transfer rates unfortunately constitute major limitations under such mild conditions (Law *et al.*, 2006). Furthermore, the application of enzymes in whole cells, which is advantageous for oxygenases, suffers from a competition for O<sub>2</sub> between the target reaction and respiration (Duetz *et al.*, 2001; Schrewe *et al.*, 2013). A technical solution for increasing the O<sub>2</sub> gas-liquid mass transfer rate under ambient conditions is the utilization of O<sub>2</sub>-enriched air (Hilker *et al.*, 2006). Yet, O<sub>2</sub> mass transfer is basically limiting the space-time yields of processes with high oxidation rates, especially in the production of bulk chemicals (Duetz *et al.*, 2001; Garcia-Ochoa and Gomez, 2009; Gemoets *et al.*, 2016; Law *et al.*, 2006). To improve O<sub>2</sub> mass transfer, various reactor concepts with different modes of gaseous reactant supply have been proposed (Gavriilidis *et al.*, 2016). Examples include the utilization of bubble columns, gas-permeable membranes, segmented flow microreactors, or falling film microreactors (Bolivar *et al.*, 2016; Gemoets *et al.*, 2016; Greene *et al.*, 2015; Kantarci *et al.*, 2005; Karande *et al.*, 2011; Tomaszewski *et al.*, 2014).

Herein, we report a novel concept based on oxygenic photosynthesis for the homogeneous supply of O<sub>2</sub> to an oxidation reaction. To date, several studies have investigated the coupling of light-driven electron activation to (enzymatic) reactions, both chemically and biotechnologically (Balcerzak *et al.*, 2014; Hisatomi *et al.*, 2014; Hollmann *et al.*, 2007; Köninger *et al.*, 2016; Lassen *et al.*, 2014b; Mifsud *et al.*, 2014; Okeefe *et al.*, 1994; Yu *et al.*, 2013). However, light-driven water oxidation has not been considered for the homogeneous supply of O<sub>2</sub>. Photosynthesis generates O<sub>2</sub> *in situ* within an aqueous liquid phase from water. This has the potential to basically overcome gas-liquid mass transfer limitations. Light-driven photosynthetic water oxidation is the core of our concept, delivering O<sub>2</sub> homogeneously

within cells to the catalytically active oxygenase enzyme, thus driving the oxyfunctionalization reaction (**Figure 3.1**). The well-studied phototrophic cyanobacterium *Synechocystis* sp. PCC 6803 was chosen as the source for delivering O<sub>2</sub>. It was engineered for the synthesis of alkane monooxygenase AlkBGT originating from *Pseudomonas putida* GPo1 (hereinafter referred to as Syn6803\_BGT) (Peterson *et al.*, 1966b). The highly regioselective terminal oxyfunctionalization of nonanoic acid methyl ester served as the model oxidation reaction. It constitutes an industrially relevant example for the production of polymer building blocks from renewables (**Figure 3.1**) (Evonik Industries AG, 2013; Ladkau *et al.*, 2016; Schaffer and Haas, 2014; Schrewe *et al.*, 2014).



**Figure 3.1:** Homogenous O<sub>2</sub> evolution coupled to an oxygenase-catalyzed oxyfunctionalization reaction. Water is oxidized by the photosynthetic cyanobacterium *Synechocystis* sp. PCC 6803, yielding O<sub>2</sub> and activated reduction equivalents. The heterologously introduced alkane monooxygenase system AlkBGT captures both O<sub>2</sub> and the reduction equivalents, and catalyzes the regioselective oxyfunctionalization of nonanoic acid methyl ester (NAME) to 9-hydroxynonanoic acid methyl ester (H-NAME).

### 3.3 Materials and methods

**Chemicals and cultivation procedures.** Chemicals and cultivation procedures used in this study are described in **Chapter 2**.

**Bacterial strain.** The genetic introduction of the *alkBGT* genes encoding the alkane monooxygenase AlkB, the rubredoxin AlkG and the rubredoxin reductase AlkT into *Synechocystis* sp. PCC 6803 was achieved via an expression system located on the broad host range plasmid pPMQAK1 (Huang *et al.*, 2010). The cloning procedure for the resulting plasmid pAH042 is given in **Chapter 2**. Gene expression was based on the IPTG inducible P<sub>trc10</sub> promoter system (Huang *et al.*, 2010) and translation was initiated via optimized ribosomal binding sites in front of each gene (Heidorn *et al.*, 2011); each gene sequence encoded a C-terminal Strep-tag II (Schmidt *et al.*, 1996) (**Figure 3.2**). *Synechocystis* sp. PCC 6803 harboring the plasmid pAH042 is hereinafter referred to as Syn6803\_BGT.



**Figure 3.2:** Schematic representation of the constructed expression system of the plasmid pAH042. RBS\* = ribosomal binding site optimized for *Synechocystis* sp. PCC 6803 (Heidorn *et al.*, 2011), STII = Strep-tag II (Schmidt *et al.*, 1996), T<sub>double</sub> = double terminator (biobrick #BBa\_B0015).

**Whole-cell oxyfunctionalization using Syn6803\_BGT.** Oxyfunctionalization activity measurements were performed 24 hours after induction of gene expression. Cells were harvested by centrifugation (15 min, 2000 g, 4 °C) and resuspended in YBG11 medium (50 mM HEPES) to a final cell concentration of ca. 2 g<sub>CDW</sub> L<sup>-1</sup>. To 1 mL cell suspension in 11 mL screw cap glass tubes, the substrate NAME was added to a final concentration of 10 mM from a 2 M stock in ethanol. The biotransformation reaction was performed at 30 °C, 220 rpm (2.5 cm amplitude) in an orbital shaker equipped with fluorescence light tubes set to a light intensity of 30 μE m<sup>-2</sup> s<sup>-1</sup> (Multitron, Infors HT, Bottmingen, Switzerland). The biotransformation reaction was quenched after respective time-points by addition of 1 mL of ice-cold diethylether containing 0.2 mM hexadecane as internal standard. After thorough mixing for 1 min (vortex) and phase separation performed by centrifugation (5 min, 3180 g, 4 °C), the organic phase was dried over anhydrous Na<sub>2</sub>SO<sub>4</sub> and analyzed via gas chromatography. Activity assays under anaerobic conditions were performed by degassing the cell suspension from oxygen by bubbling with nitrogen gas at 70 mL min<sup>-1</sup> for 10 minutes, followed by substrate addition in an anaerobic chamber in N<sub>2</sub> atmosphere (100 ppm O<sub>2</sub>, 1.6 ppm H<sub>2</sub>, 25 °C, 65% humidity). Afterwards the gas tight screwed glass tubes were treated as described above, except for a changed light intensity from 30 to 50 μE m<sup>-2</sup> s<sup>-1</sup>. The light spectrum applied for the determination of oxyfunctionalization activities under anaerobic conditions might vary as light tubes with the same specifications were used covered by a plastic hood (L18W/840, Lumilux Cool White, Osram, München, Germany).

**Whole-cell oxyfunctionalization using *E. coli* W3110 (pAH042).** Cells were grown as described before, harvested by centrifugation (5000g, 4 °C, 10 min) and resuspended in KPi buffer containing 1% glucose (pH 7.4) to respective biomass concentrations. Aliquots of 0.8 mL culture were provided in 2 mL reaction tubes and pre-warmed for 5 min at 30 °C and 1500 rpm (ThermoMixerC, Eppendorf, Wesseling-Berzdorf). The biotransformation reaction was started by adding 5 mM NAME (5 μL of 0.8 M stock in ethanol). After 15 minutes of incubation time, the reaction was quenched using 0.8 mL ice-cold diethyl ether containing 200 μM of hexadecane as internal standard and vortexing for 1 min before centrifugation (17000g, 4 °C, 5 min). The supernatant was dried over anhydrous Na<sub>2</sub>SO<sub>4</sub> and applied for GC analysis.

**Quantification of product formation.** The oxyfunctionalized product H-NAME was quantified using gas chromatography (GC Trace 1310, Thermo Fisher Scientific, Waltham, USA) equipped with a TG-5MS capillary column (5% diphenyl / 95% dimethyl polysiloxane, 30 m, I.D.: 0.25 mm, film thickness: 0.25  $\mu\text{m}$ , ThermoFisher Scientific, Waltham, USA) and a flame ionization detector (FID) operating at 320  $^{\circ}\text{C}$ , 350  $\text{mL min}^{-1}$  air flow, 30  $\text{mL min}^{-1}$  makeup gas flow and 35  $\text{mL min}^{-1}$  hydrogen gas flow. Nitrogen gas was applied as carrier gas with a constant flow of 1.5  $\text{mL min}^{-1}$ . The injection volume was set to 1  $\mu\text{L}$  using a PTV injector, programmed with a temperature gradient of 10  $^{\circ}\text{C s}^{-1}$  from 90-300  $^{\circ}\text{C}$ . Split transfer was applied after 0.5 min with a split ratio of 7. The oven temperature profile was: 1) 80  $^{\circ}\text{C}$  for 1 min, 2) 80-160  $^{\circ}\text{C}$  with 50  $^{\circ}\text{C min}^{-1}$ , 3) 160-220  $^{\circ}\text{C}$  with 15  $^{\circ}\text{C min}^{-1}$ , 4) 220-300  $^{\circ}\text{C}$  with 50  $^{\circ}\text{C min}^{-1}$  and 5) 300  $^{\circ}\text{C}$  for 3.8 min.

**Oxygen evolution measurement.** Oxygen evolution measurements were performed using a Clark-type sensor, measuring the oxygen partial pressure (OX-MR microsensor, 400  $\mu\text{m}$  tip diameter, Unisense, Aarhus, Denmark) equipped with the respective microsensor amplifier (Microsensor multimeter, Unisense, Aarhus, Denmark) applied in gas tight glass chambers (MicroRespiration System, Unisense, Aarhus, Denmark). Oxygen evolution rates were calculated within 5 minutes of illumination at a light intensity of 50  $\mu\text{E m}^{-2} \text{s}^{-1}$  (fluorescence light tube).

### 3.4 Results

Syn6803\_BGT produced ca. 65  $\mu\text{M}$  9-hydroxynonanoic acid methyl ester (H-NAME) from 10 mM nonanoic acid methyl ester (NAME) within 20 min under constant illumination. This translates into a specific oxidation rate of  $1.5 \pm 0.2 \text{ U g}_{\text{CDW}}^{-1}$  (**Table 3.1**) and demonstrates the functionality of the biocatalyst. However, a specific oxidation rate of  $1.3 \pm 0.1 \text{ U g}_{\text{CDW}}^{-1}$  was still measured in the dark, showing that reduction equivalents were supplied at almost the same rate with and without light (**Table 3.1**). Obviously, the catabolism of storage compounds enabled substantial NAD(P)H regeneration in the dark.

Upon successful construction of the functional phototrophic whole-cell biocatalyst, we evaluated the oxidation reaction for exclusive utilization of photosynthetically generated O<sub>2</sub>. The terminal hydroxylation of NAME by Syn6803\_BGT was studied under anaerobic, but otherwise identical conditions. H-NAME formation depended directly upon illumination and thus water oxidation. Product formation was not observed in the absence of light (**Figure 3.3**). The specific oxidation rate obtained under anaerobic conditions and illumination was  $0.9 \pm 0.1 \text{ U g}_{\text{CDW}}^{-1}$  (**Table 3.1**) de facto driven by O<sub>2</sub> generated in the photosynthetic light reaction.

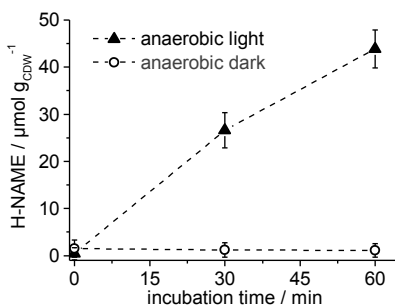
The specific O<sub>2</sub> evolution rate of Syn6803\_BGT was determined separately in the absence of the substrate NAME, for assessing the fraction of photosynthetically generated O<sub>2</sub> captured by the monooxygenase (**Table 3.1**). With an O<sub>2</sub> evolution rate of  $3.7 \pm 0.5 \text{ U g}_{\text{CDW}}^{-1}$ ,

corresponding to 100% of O<sub>2</sub> available in the system (assuming no photorespiration), nearly 25% of the photosynthetically generated O<sub>2</sub> was captured for terminal hydroxylation of NAME.

**Table 3.1:** Specific rates for the hydroxylation of nonanoic acid methyl ester to 9-hydroxynonanoic acid methyl ester and O<sub>2</sub> evolution of Syn6803\_BGT.

Conditions	Specific production reaction rate / U g <sub>CDW</sub> <sup>-1</sup>
Aerobic, irradiated [a]	1.5 ± 0.2
Aerobic, in the dark [a]	1.3 ± 0.1
Anaerobic, irradiated [b]	0.9 ± 0.1
Anaerobic, in the dark [b]	0.0
Anaerobic, irradiated, OER [c]	3.7 ± 0.5

Specific product formation rates are given with respect to the product formed after [a] 20 or [b] 30 min. [c] The specific O<sub>2</sub> evolution rate (OER) was determined within the aqueous phase in a sealed, gas-free glass chamber in the absence of substrate. U = μmol min<sup>-1</sup>. Average values and standard deviations of at least two independent biological replicates are given.



**Figure 3.3.** *In situ* supply of photosynthetically generated O<sub>2</sub> to the oxidizing enzyme AlkBGT in Syn6803\_BGT. The biotransformation experiment was performed under anaerobic conditions under irradiation (-▲-) or in the dark (-○-). Average values and standard deviations of two independent biological replicates are given. CDW = cell dry weight.

### 3.5 Discussion

Diffusion of photosynthetically generated O<sub>2</sub> may affect the reaction efficiency of the terminal hydroxylation and theoretically results in gas-liquid mass transfer processes within the assay system. The specific O<sub>2</sub> accumulation rate in the aqueous phase was calculated to be 0.01 μmol min<sup>-1</sup> g<sub>CDW</sub><sup>-1</sup> assuming immediate O<sub>2</sub> diffusion from the aqueous to the gaseous phase (aqueous/gaseous ratio 1:10, Henry volatility for O<sub>2</sub> in water:  $H_{cc}=c_{aq}/c_{gas}=0.0297$  at 25 °C) (Sander, 2015). Thus the effective O<sub>2</sub> concentration does not exceed 0.6 μM within

30 min of reaction time (applied biomass concentration: 2 g<sub>CDW</sub> L<sup>-1</sup>). In contrast, Michaelis constants ( $K_M$ ) of oxygenases with respect to O<sub>2</sub> are typically in the range of 10-60 μM (Duetz *et al.*, 2001). This, together with the high fraction of O<sub>2</sub> captured by the monooxygenase (25%), suggests that the photosynthetically generated O<sub>2</sub> is concentrated within the microbial cell and captured *in situ* by the monooxygenase before diffusing out of the cell. Although O<sub>2</sub> can in principle diffuse across cellular membranes, the lipid bilayer system seems to pose a physical barrier that is beneficial for the intracellular oxidation process. These results are proof of concept for the *in situ* coupling of photosynthetic O<sub>2</sub> evolution to O<sub>2</sub>-dependent oxidation reactions. The photosynthetic light reaction was used for the intracellular supply of both activated reduction equivalents and O<sub>2</sub>.

### 3.6 Conclusions & Outlook

These results might be the starting point for the development of various efficient photosynthesis-driven oxyfunctionalization reactions. In the present case, future optimizations include an increase in the AlkBGT level in the cyanobacterial whole-cell biocatalyst (Oliver and Atsumi, 2014; Ruffing, 2011). This is obvious from comparing the transformation rates of NAME into H-NAME catalyzed by *E. coli* W3110 carrying the very plasmid pAH042 (10.0 ± 0.1 U g<sub>CDW</sub><sup>-1</sup>; **Figure 10.1**) with those of *E. coli* that strongly express *alkBGT* (104 - 128 U g<sub>CDW</sub><sup>-1</sup>) (Julsing *et al.*, 2012b; Schrewe *et al.*, 2011). Other targets are electron channeling and improved cultivation and bioreactor concepts. The cyanobacterial photosynthetic metabolism supports the supply of activated reduction equivalents at high rates (123 U g<sub>CDW</sub><sup>-1</sup>) (Königer *et al.*, 2016). Yet, the O<sub>2</sub> evolution rate determined in this study implies a photosynthetic activity of only 3.7 U g<sub>CDW</sub><sup>-1</sup>. This corresponds to a specific NAD(P)H regeneration rate of 7.4 U g<sub>CDW</sub><sup>-1</sup>. The theoretical maximum of this rate was estimated to be 850 U g<sub>CDW</sub><sup>-1</sup> (assumptions for PSII:  $k_{cat}=1000$  s<sup>-1</sup>, 10 mg g<sub>CDW</sub><sup>-1</sup>,  $M_W = 350$  kDa) (Dismukes *et al.*, 2009; Königer *et al.*, 2016; Shen, 2015). With high biomass concentrations (40 g<sub>CDW</sub> L<sup>-1</sup>), a theoretical maximum of 2040 mmol L<sup>-1</sup> h<sup>-1</sup> would be possible for the oxygen supply rate. This translates into a volumetric mass transfer coefficient  $k_{L,a}$  of 4533 h<sup>-1</sup> for a bioreactor operated at 2.5 atm, 30 °C, and a residual O<sub>2</sub> concentration of 100 μM (typical conditions for large-scale bioreactor operation) (Duetz *et al.*, 2001). In contrast, the  $k_{L,a}$  values of large-scale bioreactors are on the order of 200 h<sup>-1</sup> (Duetz *et al.*, 2001). In addition, the use of photoautotrophic instead of chemoheterotrophic organisms largely relieves the competition for O<sub>2</sub> between oxygenation and respiration.

The development of photobioreactors enabling the generation of high biomass concentrations with high oxygen evolution activity is key for the future applicability of the presented concept (Kumar *et al.*, 2011). Biofilm cultivation in capillary microreactors constitutes one possible solution to increase the cyanobacterial biomass concentration (David *et al.*, 2015). Stable cyanobacterial biofilm cultivation has recently been achieved over

several weeks with retention of the photosynthetic activity throughout the biofilm. Reaction optimization addressing the key issue of photobioreactor development has the potential to facilitate currently oxygen-transfer-limited selective hydroxylation processes for the biocatalytic functionalization of hydrocarbons (Duetz *et al.*, 2001; Schrewe *et al.*, 2013). In summary, the *in situ* coupling of oxygenic photosynthesis to oxidizing enzymes provides a novel and safe access to O<sub>2</sub> as a reactant for designing new reactions for oxidation catalysis.

#### **2.7 Acknowledgements**

We thank Birke Brumme, Lisa-Marie Bangen (DBFZ, Leipzig, Germany), and Dr. Sabine Kleinsteuber (UMB, UFZ, Leipzig, Germany) for assistance and laboratory infrastructure. The group of Victor de Lorenzo (Madrid, Spain) and Prof. Peter Lindblad (Uppsala University, Sweden) kindly provided the plasmids pSEVA251 + pPMQAK1 and pSB1AC3\_PrnpB:lacI + pSB1AC3\_Ptrc1O:GFP, respectively. We acknowledge the use of the facilities of the Centre for Biocatalysis (MiKat) at the Helmholtz Centre for Environmental Research, which is supported by European Regional Development Funds (EFRE, Europe funds Saxony) and the Helmholtz Association.





## **Chapter 4      Stabilization of photosynthesis-driven whole-cell hydroxylation of nonanoic acid methyl ester by two-liquid phase biotransformation**

Bruno Bühler and Andreas Schmid coordinated the project and corrected the manuscript.

Parts published in:

*Biotechnology and Bioengineering*, **2019**, DOI: 10.1002/bit.27006

### 4.1 Abstract

Photoautotrophic organisms are promising hosts for biocatalytic oxyfunctionalizations because they supply reduction equivalents as well as O<sub>2</sub> via photosynthetic water oxidation. Thus far, research on photosynthesis-driven bioprocesses mainly focuses on strain development and the proof of principle in small-scale biocatalytic reaction setups. This study investigates the long-term applicability of the previously developed cyanobacterial strain *Synechocystis* sp. PCC 6803\_BGT harboring the alkane monooxygenase system AlkBGT catalyzing terminal alkyl group oxyfunctionalization. For nonanoic acid methyl ester (NAME) hydroxylation, the biocatalyst showed light intensity-independent hydroxylation activity and substantial hydrolysis of NAME to nonanoic acid. Substrate mass transfer limitation, substrate hydrolysis, as well as substrate toxicity were overcome via *in situ* substrate supply by means of a two-liquid phase system. Usage of diisononyl phthalate as organic carrier solvent enabled 1.7-fold increased initial specific activities ( $5.6 \pm 0.1 \text{ U g}_{\text{CDW}}^{-1}$ ) and 7.6-fold increased specific yields on biomass ( $3.8 \pm 0.1 \text{ mmol}_{\text{H-NAME}} \text{ g}_{\text{CDW}}^{-1}$ ) as compared to single aqueous phase biotransformation. Finally, the whole-cell biotransformation system was successfully scaled from 1 mL glass tube to 3 L stirred tank photo-bioreactor scale. This is the first study reporting on the application of the two-liquid phase concept for efficient phototrophic whole-cell biocatalysis.

## 4.2 Introduction

Oxygenases are powerful enzymes for regio-, chemo-, and stereoselective C-H oxyfunctionalization. Whole-cell biocatalysis systems based on chemoheterotrophic host organisms like *E. coli* or Pseudomonads have successfully been developed reaching titers and rates feasible for the chemical industries (Evonik Industries AG, 2013; Ladkau *et al.*, 2016; Panke *et al.*, 2002). Recently, photoautotrophic organisms such as cyanobacteria have been tested as alternative biocatalytic host systems for such biotransformations (Böhmer *et al.*, 2017; Lassen *et al.*, 2014b; Włodarczyk *et al.*, 2015; Yamanaka *et al.*, 2015). Photosynthesis-driven NAD(P)H regeneration relies on electrons derived from water oxidation empowered by light energy. In contrast to chemoheterotrophic biocatalysts, which depend on organic carbon-based electron and energy sources like glucose, cofactor, biocatalyst, and enzyme (re)generation in photoautotrophic biocatalysts only requires water, inorganic CO<sub>2</sub>, and light. Furthermore, *in situ* O<sub>2</sub> generation upon photosynthetic water oxidation advances the applicability of whole-cell biocatalysts for oxyfunctionalization reactions by overcoming gas-liquid O<sub>2</sub> mass transfer limitations (**Chapter 3, Chapter 7**).

The oxyfunctionalization of fatty acid methyl esters (FAMEs) to respective alcohols, aldehydes, and acids, catalyzed by the alkane monooxygenase system AlkBGT, is a well-developed example for the use of chemoheterotrophic cells as host system for oxygenases. This three-component enzyme system originates from *Pseudomonas putida* GPo1 and consists of a rubredoxin reductase (AlkT), a rubredoxin (AlkG), and the monooxygenase component AlkB (McKenna and Coon, 1970; Peterson *et al.*, 1966b). In 2011, Schrewe *et al.* developed a recombinant *E. coli* strain, catalyzing the terminal hydroxylation of nonanoic acid methyl ester (NAME) to 9-hydroxynonanoic acid methyl ester (H-NAME) at high specific rates (100 U g<sub>CDW</sub><sup>-1</sup>) (Schrewe *et al.*, 2011). Subsequent reaction engineering involving *in situ* product removal via a two-liquid phase approach enabled efficient terminal oxy- and aminofunctionalization of FAMEs at bioprocess relevant scales (Evonik Industries AG, 2013; Ladkau *et al.*, 2016; Schrewe *et al.*, 2014). Recently, we transferred the AlkBGT system via the plasmid pAH042 into the photoautotrophic host *Synechocystis* sp. PCC 6803 (henceforth referred to as Syn6803\_BGT) and experimentally proved the concept of photosynthesis-driven FAME oxyfunctionalization (**Chapter 3**).

In this study, the hydroxylation performance of Syn6803\_BGT was investigated in more detail, focusing on CO<sub>2</sub> and light availabilities as influencing factors during biocatalyst growth and biotransformation. Further, the long-term operational stability of photosynthesis-driven NAME biotransformation was evaluated. *In situ* substrate supply via a two-liquid phase system was tested to enhance and stabilize biocatalyst performance by overcoming reactant toxicity as well as mass transfer limitations. Finally, the reaction system is scaled from a glass tube to a stirred tank photo-bioreactor setting.

### 4.3 Materials and Methods

**Chemicals, bacterial strains, and plasmids.** Chemicals used in this study are given in **Chapter 2**. Syn6803\_BGT, i.e., *Synechocystis* sp. PCC 6803 harboring the alkane monooxygenase system AlkBGT on plasmid pAH042, has been constructed in **Chapter 3**. Cloning procedures of this and further plasmids and strains used in this study are given in **Chapter 2 (Table 2.1)**.

**Cultivation of *Synechocystis* sp. PCC 6803.** If not stated otherwise, shake flask cultivation of *Synechocystis* sp. PCC 6803 was performed as described in **Chapter 2** (YBG11 medium, 50 mM HEPES, 20 mL in 100 mL baffled Erlenmeyer flasks, 30 °C, 150 rpm, 2.5 cm amplitude, 50  $\mu\text{E m}^{-2} \text{s}^{-1}$ , LED, ambient  $\text{CO}_2$  (0.04%), 75% humidity). Kanamycin was used at a final concentration of 50  $\mu\text{g mL}^{-1}$ . Gene expression was induced using 2 mM IPTG or 0.025% (v/v) DCPK. If required, 50 mM  $\text{NaHCO}_3$  were supplied to the medium before sterile filtration (0.2  $\mu\text{m}$ ). Nitrogen source-free YBG11 medium was supplemented with 0.17  $\mu\text{M}$   $\text{CoCl}_2 \cdot 6 \text{H}_2\text{O}$  instead of  $\text{Co}(\text{NO}_3)_2 \cdot 6 \text{H}_2\text{O}$ . The correlation factor 0.2246 was used for the conversion of  $\text{OD}_{750}$  values to cell dry weight (CDW) concentrations in  $\text{g}_{\text{CDW}} \text{L}^{-1}$  (**Chapter 2, Figure 2.2**).

Cultivation of Syn6803\_BGT cells in the stirred tank photo-bioreactor Labfors 5 Lux (Infors AG, Bottmingen, Switzerland) was performed using 3 L YBG11 medium inoculated to an  $\text{OD}_{750}$  of 0.08 using pre-cultures obtained via the standard cultivation protocol described above. Cultivation in photo-bioreactors was performed at a light intensity of 50  $\mu\text{E m}^{-2} \text{s}^{-1}$  from 0 to 30 h, 75  $\mu\text{E m}^{-2} \text{s}^{-1}$  from 30 to 48 h and 100  $\mu\text{E m}^{-2} \text{s}^{-1}$  from 48 to 96 h. The agitation speed was set to 300 rpm. The aeration rate was set to 3  $\text{L min}^{-1}$  (1 vvm) from 0 to 48 h and 5  $\text{L min}^{-1}$  (1.7 vvm) from 48 to 96 h using compressed air. The applied light spectrum is shown in **Figure 10.2**.

**Biotransformation procedures.** Whole-cell oxyfunctionalization activity assays were performed with cells cultivated as described above. Gene expression was induced two days after inoculation. At defined time-points, cells were harvested by centrifugation (5000g, 4 °C, 10 min) and resuspended in YBG11 medium (facultatively amended with nitrate, ammonium, and  $\text{NaHCO}_3$ ) to a final biomass concentration of ca. 2  $\text{g}_{\text{CDW}} \text{L}^{-1}$ . Exact biomass concentrations were determined via  $\text{OD}_{750}$  measurement. Long-term oxyfunctionalization assays (> 30 min) were performed in YBG11 medium supplemented with 50  $\mu\text{g mL}^{-1}$  kanamycin and 2 mM IPTG. Aliquots of 1 mL were transferred to 11 mL screw cap glass tubes and pre-adapted for 10 min at 30 °C, 220 rpm (2.5 cm amplitude), and the chosen light intensity (typically 30  $\mu\text{E m}^{-2} \text{s}^{-1}$ ). The biotransformation reaction was started by adding 10 mM NAME (5  $\mu\text{L}$  of 2 M stock in ethanol) or DINP containing different NAME concentrations. The reaction was quenched at defined time-points either by adding 1 mL ice-cold diethyl ether containing 200  $\mu\text{M}$  hexadecane as internal standard (followed by extraction

for GC analysis) or, in case of two-liquid phase biotransformations, by cold centrifugation (4640g, 4 °C, 5 min).

Whole-cell oxyfunctionalization in the stirred tank photo-bioreactor Labfors 5 Lux (Infors AG, Bottmingen, Switzerland) was performed with cells derived from a 3 L photo-bioreactor culture three days after inoculation. Cells were harvested via centrifugation (4640g, 4 °C, 20 min) and resuspended in 0.6 L YBG11 medium containing 50 mM NaHCO<sub>3</sub>, 50 µg mL<sup>-1</sup> kanamycin, and 2 mM IPTG, resulting in a final biomass concentration of 1.6 g<sub>CDW</sub> L<sup>-1</sup>. This cell suspension was returned into the photo-bioreactor followed by pre-conditioning at 30 °C, 300 rpm (impeller) and 100 µE m<sup>-2</sup> s<sup>-1</sup> irradiation for 30 min. An aeration rate of 1.8 L min<sup>-1</sup> (2.2 vvm) with compressed air was chosen to ensure proper mixing of the two phases applied. The biotransformation was started by adding 0.21 L of DINP containing different NAME concentrations (10, 25, or 50% (v/v)). Samples were withdrawn at regular time intervals and immediately centrifuged (17000g, 4 °C, 10 min) to quench the reaction, separate the phases, and remove the cells.

**Analytical procedures.** Reactants (H-NAME, NAME, and NA) from aqueous phase samples were extracted using equal amounts of ice-cold diethyl ether containing 200 µM hexadecane as internal standard. The ether phase was separated by centrifugation (17000g, 4 °C, 10 min) and dried over anhydrous Na<sub>2</sub>SO<sub>4</sub>, and subjected to GC analysis as described in **Chapter 3**. Reactants (H-NAME, NAME and NA) dissolved in DINP were diluted 10-fold in ice-cold diethyl ether containing 200 µM hexadecane as internal standard. The ether phase was dried over anhydrous Na<sub>2</sub>SO<sub>4</sub> and used for GC analysis. Separation via GC was performed as described in **Chapter 3** with the modification that a pre-column (deactivated silica guard column, 2 m x 0.53 mm, Thermo Fisher Scientific, Milan, Italy), an integrated backflush system and a split ratio of 3 was applied. 1.5 min after injection, a backflush through the pre-column was applied.

## 4.4 Results

### 4.4.1 Enhanced biocatalyst growth results in decreased biotransformation activities

As reported in **Chapter 3**, the recombinant strain Syn6803\_BGT is capable of hydroxylating NAME to H-NAME driven by photosynthetically derived O<sub>2</sub>. To investigate factors influencing whole-cell biocatalyst performance in more detail, the impact of growth/ expression conditions on the specific hydroxylation activity was analyzed. Standard growth conditions comprised an ambient CO<sub>2</sub> concentration of 0.04% and a light intensity of 50 µE m<sup>-2</sup> s<sup>-1</sup> and resulted in a maximal specific activity of 2.1 ± 0.1 U g<sub>CDW</sub><sup>-1</sup> (**Table 4.1, Figure 10.3**). CO<sub>2</sub> availability and light intensity are the primary factors defining the cyanobacterial growth rate (Beardall and Raven, 2013). In the following experiment, CO<sub>2</sub> concentrations and light intensity were increased during cell growth to 2% and 100 µE m<sup>-2</sup> s<sup>-1</sup>, respectively. Only the

combined increase in CO<sub>2</sub> and light intensity significantly enhanced the growth rate in the exponential phase from 0.054 to 0.077 h<sup>-1</sup> (**Table 4.1, Figure 10.3**). In all cases, linear growth was observed after 48 h (time-point of induction of *alkBGT* expression), which increased from 0.065 to 0.086 and 0.130 OD<sub>750</sub> h<sup>-1</sup> upon elevation of the CO<sub>2</sub> level (2%) and both CO<sub>2</sub> level (2%) and light intensity (100 μE m<sup>-2</sup> s<sup>-1</sup>), respectively. However, the maximum hydroxylation activity decreased by a factor of two from 2.1 to 1.1 U g<sub>CDW</sub><sup>-1</sup> (**Table 4.1, Figure 10.3**). Next to an altered AlkBGT biosynthesis efficiency, changes in cell physiology may have caused this activity decrease.

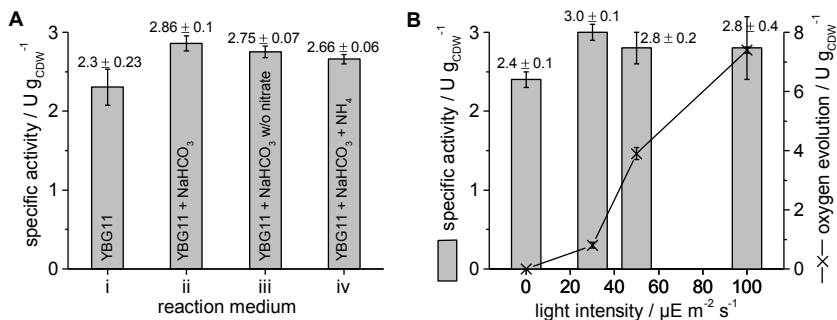
**Table 4.1:** Cell growth rates and maximum oxyfunctionalization activities of Syn6803\_BGT cultivated under different conditions.

Growth conditions	Exp. growth rate (until 48 h) / h <sup>-1</sup>	Linear growth rate (after 48 h) / OD <sub>750</sub> h <sup>-1</sup>	Expression time / h	Maximum specific activity / U g <sub>CDW</sub> <sup>-1</sup>
50 μE, amb. CO <sub>2</sub>	0.054	0.065	24	2.1 ± 0.1
50 μE, 2% CO <sub>2</sub>	0.059	0.086	24	1.4 ± 0.1
100 μE, amb. CO <sub>2</sub>	0.059	0.063	7	2.2 ± 0.1
100 μE, 2% CO <sub>2</sub>	0.077	0.130	6	1.1 ± 0.1

Two days after inoculation, gene expression was induced using 2 mM IPTG. Standard oxyfunctionalization assays were performed at different time-points after induction of gene expression (YBG11, 2 g<sub>CDW</sub> L<sup>-1</sup>, 30 μE m<sup>-2</sup> s<sup>-1</sup>). Expression time for maximum specific activities is given. Average values and standard deviations of two independent biological replicates are given. Amb. = ambient, U = unit = μmol min<sup>-1</sup>, CDW = cell dry weight.

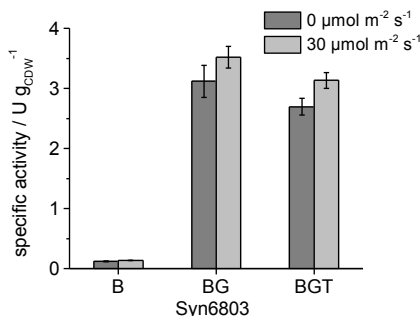
#### 4.4.2 NaHCO<sub>3</sub> supply but not light intensity influence NAME hydroxylation during single phase biotransformation

To investigate the impact of reaction conditions on the NAME hydroxylation activity, different growth media as well as light intensities were tested during whole-cell biotransformations. First, the medium composition was changed with respect to carbon and nitrogen content from i) standard YBG11 medium to ii) YBG11 + NaHCO<sub>3</sub>, iii) YBG11 + NaHCO<sub>3</sub> w/o nitrate, and iv) YBG11 + NaHCO<sub>3</sub> + ammonium w/o nitrate. The supplementation of YBG11 with NaHCO<sub>3</sub> resulted in a 26% increase of the specific activity (**Figure 4.1 A**). The omission of nitrate as well as its replacement by ammonium, while maintaining NaHCO<sub>3</sub> supplementation, resulted in a slight activity decrease. Therefore, YBG11 + NaHCO<sub>3</sub> was used as reaction medium for NAME hydroxylation in the following experiments with variable light intensities. In the absence of light, cells showed a relatively high specific activity of 2.4 ± 0.1 U g<sub>CDW</sub><sup>-1</sup>, as it has been observed before under non-optimized conditions (**Figure 4.1 B**) (**Chapter 3**). An increase in light intensity up to 250 μE m<sup>-2</sup> s<sup>-1</sup> resulted in strongly increasing O<sub>2</sub> evolution rates, but only a slight increase in specific hydroxylation activities with a maximum of 3.0 ± 0.1 U g<sub>CDW</sub><sup>-1</sup> reached at 30 μE m<sup>-2</sup> s<sup>-1</sup> (**Figure 4.1 B, Figure 10.4**).



**Figure 4.1:** Impact of medium composition (A) and light intensity (B) on the specific oxyfunctionalization activity of Syn6803\_BGT. Cells were cultivated under standard conditions (YBG11, ambient CO<sub>2</sub>, 50 μE m<sup>-2</sup> s<sup>-1</sup>). Two days after inoculation, *alkBGT* expression was induced and cultivation was continued for 24 h. Oxyfunctionalization assays were performed using a biomass concentration of 2 g<sub>CDW</sub> L<sup>-1</sup>. (A) Assays were performed using given medium composition at 30 μE m<sup>-2</sup> s<sup>-1</sup> using light tubes at light source. (B) Oxyfunctionalization assays were performed in YBG11 medium supplemented with NaHCO<sub>3</sub> at given light intensities using LEDs as light source. Oxygen evolution rates were determined in gas tight glass chambers as described in **Chapter 3** (2 g<sub>CDW</sub> L<sup>-1</sup>, YBG11). Average values and standard deviations of two independent biological replicates are given. U = unit = μmol min<sup>-1</sup>, CDW = cell dry weight.

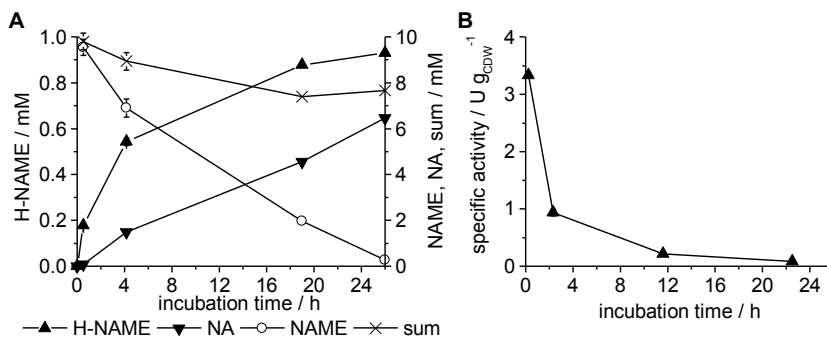
As expected from the native localization of AlkB (Benson *et al.*, 1979), membrane fractionation and Western blot analysis revealed that the monooxygenase AlkB is localized in the cytoplasmic membrane of the cyanobacterial cells (**Figure 10.5**), which may not be optimal for efficient electron transfer. Interestingly, experiments with AlkB containing *Synechocystis* sp. PCC 6803 strains lacking AlkT or AlkGT revealed that electron transfer to AlkB strictly depends on AlkG but not on NADH-dependent AlkT (**Figure 4.2**). Obviously, AlkT can be replaced by endogenous AlkG reduction, with even slightly higher rates in the absence of AlkT. Thus, electron transfer via NADH, which does not constitute a primary electron shuttle in phototrophic metabolism (Mellor *et al.*, 2017), can be circumvented. Overall, these results indicate that, under the applied reaction conditions, the electron supply capacity of photosynthetic water oxidation does not limit the oxyfunctionalization performance of Syn6803\_BGT and that electron supply via carbohydrate catabolism, which may involve storage compounds such as glycogen, can substantially contribute to this electron supply.



**Figure 4.2:** Whole-cell NAME biotransformation activity of *Synechocystis* sp. PCC 6803 cells harboring AlkB (pAH044), AlkB (pAH047), or AlkBGT (pA042). Cells were cultivated at standard conditions (YBG11, ambient  $\text{CO}_2$ ,  $50 \mu\text{E m}^{-2} \text{s}^{-1}$ ). Gene expression was induced two days after inoculation for 24 h. Oxyfunctionalization assays were performed at the given light conditions ( $2 \text{g}_{\text{CDW}} \text{L}^{-1}$ , YBG11 +  $\text{NaHCO}_3$ ). Average values and standard deviations of two independent biological replicates are given. U = unit =  $\mu\text{mol min}^{-1}$ , CDW = cell dry weight.

#### 4.4.3 Diisononyl phthalate (DINP) as carrier solvent overcomes substrate toxicity for *Synechocystis* sp. PCC 6803

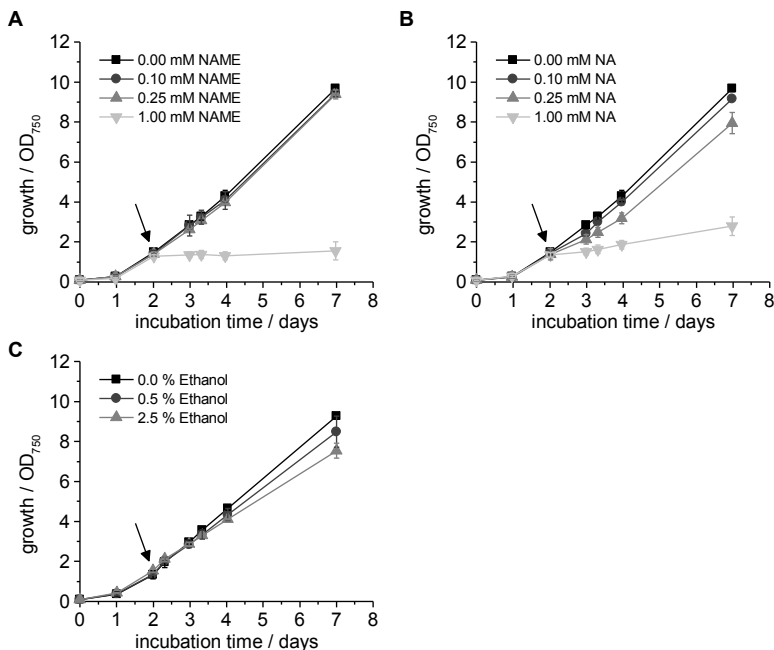
So far, the biocatalytic performance of Syn6803\_BGT has been investigated in short-term assays, hiding potential biocatalyst stability issues. Long-term NAME hydroxylation experiments revealed a fast decrease in specific activity, resulting in a final specific product yield on biomass of  $0.5 \text{mmol g}_{\text{CDW}}^{-1}$  (Figure 4.3, Table 4.2).



**Figure 4.3:** Long-term NAME biotransformation with Syn6803\_BGT. Cells were cultivated under standard conditions (YBG11, ambient  $\text{CO}_2$ ,  $50 \mu\text{E m}^{-2} \text{s}^{-1}$ ). Gene expression was induced two days after inoculation for 4 h before cells were harvested and applied for the biotransformation ( $2 \text{g}_{\text{CDW}} \text{L}^{-1}$ , YBG11 +  $\text{NaHCO}_3$ ,  $30 \mu\text{E m}^{-2} \text{s}^{-1}$ ). The biotransformation reaction was initiated by the addition of 10 mM NAME. Each data-point represents the average value of two independent biological samples. U = unit =  $\mu\text{mol min}^{-1}$ , CDW = cell dry weight.



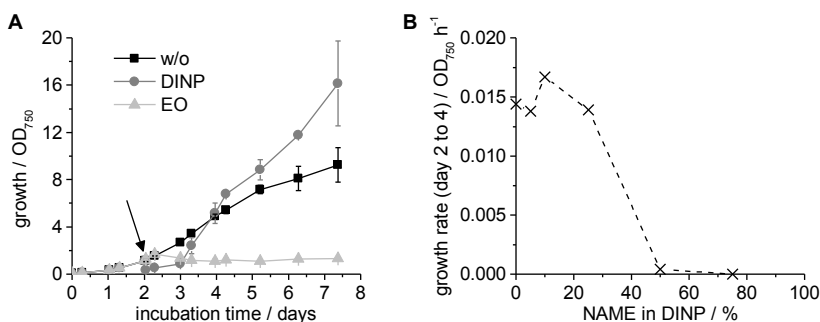
Beside its hydroxylation, NAME was hydrolyzed to nonanoic acid (NA) at a constant rate of  $2.3 \pm 0.1 \text{ U g}_{\text{CDW}}^{-1}$ , resulting in substrate depletion after 26 h of reaction. The biotransformation yield thus was restricted by limited substrate availability, which, however, cannot explain the fast activity decrease. The latter may be due to reactant toxicity. Thus, the impact of NAME and NA on growth of wildtype *Synechocystis* sp. PCC 6803 was investigated. The addition of 1 mM NAME or NA largely restricted cell growth (Figure 4.4). Obviously, low concentrations of NAME and NA lead to cell toxication which may have caused biocatalyst instability. In conclusion, both reactant toxicity and substrate hydrolysis constitute critical factors affecting the hydroxylation performance of Syn6803\_BGT.



**Figure 4.4:** Cell growth of *Synechocystis* sp. PCC 6803 (pAH032) (empty expression plasmid) at different NAME (A), NA (B), or ethanol (C) concentrations. Cells were cultivated under standard conditions (YBG11, ambient CO<sub>2</sub>, 50  $\mu\text{E m}^{-2} \text{s}^{-1}$ ). Addition of reactants is indicated by an arrow. NAME concentrations are calculated based on the volume of the aqueous phase, while the solubility limit of NAME is 133  $\mu\text{M}$ . Error bars represent the standard deviation of two independent biological replicates.

To realize efficient substrate supply while maintaining substrate concentrations low but constant, *in situ* substrate supply (ISSS) strategies can be followed (Hilker *et al.*, 2008; Schmöler *et al.*, 2012). Beside substrate feeding, two-phase approaches such as organic/aqueous two-liquid phase systems are promising, simultaneously allowing *in situ* product extraction (Leon *et al.*, 1998; Lye and Woodley, 1999). Thereby, a second organic liquid

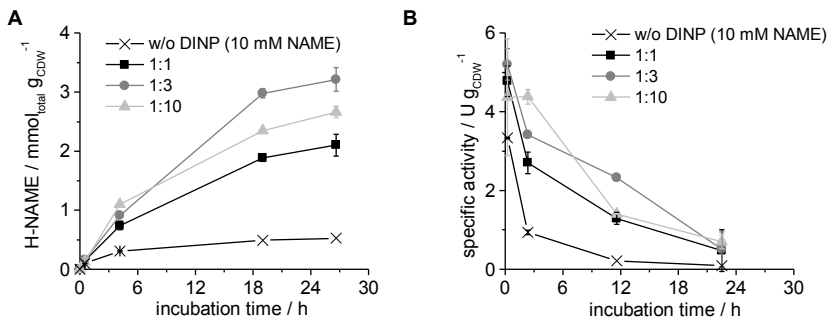
phase serves as substrate reservoir continuously providing the substrate at desired concentrations. So far, organic carrier phases were not applied for cyanobacterial processes. As information on the compatibility of organic carrier solvents with cyanobacterial growth is largely missing, such compatibility was tested for the two solvents ethyl oleate (EO) and diisononyl phthalate (DINP), which, together with similar phthalates, have proven highly suitable in bioprocesses based on heterotrophic bacteria (Bühler *et al.*, 2003b; Kuhn *et al.*, 2012b; Schrewe *et al.*, 2014; Willrodt *et al.*, 2014). With YBG11 medium as aqueous phase, these solvents were found to provide a similar partitioning behavior, with a partition coefficient  $P_{\text{org;aq}}$  of  $(24.5 \pm 3.5) \times 10^3$  for NAME. To test the compatibility of DINP and EO with wildtype *Synechocystis* sp. PCC 6803, the carrier solvents were added to cultures at a 1:3 organic/aqueous phase ratio two days after inoculation. EO was found to substantially impair cell growth, which was not the case for DINP (Figure 4.5 A). Thus, cell growth with DINP containing 0, 5, 10, 25, 50, or 75% (v/v) NAME was evaluated. Concentrations up to 25% (v/v) NAME dissolved in DINP were found not to affect the cyanobacterial cell growth rate and can thus be considered suitable for two-liquid phase setups (Figure 4.5 B, Figure 10.6).



**Figure 4.5:** Compatibility of the organic carrier solvents ethyl oleate (EO) and diisononyl phthalate (DINP) (**panel A**) and NAME dissolved in DINP at different concentrations (**panel B**) with *Synechocystis* sp. PCC 6803 cells lacking *alkBGT*. Cells were cultivated in YBG11 medium supplemented with (**panel A**) or without (**panel B**) NaHCO<sub>3</sub> under standard conditions (ambient CO<sub>2</sub>, 50 μE m<sup>-2</sup> s<sup>-1</sup>). Two days after inoculation, 7.5 or 15 mL aliquots were transferred into 100 or 250 mL shake flasks and supplemented with 2.5 or 5 mL organic phase, as indicated by the arrow in **panel A**. Cultivation was continued at a reduced shaking frequency of 100 rpm. **Panel B** shows growth rates after the addition of DINP containing different NAME concentrations, determined for day 2 to 4. Average values and standard deviations of two independent biological replicates are given.

#### 4.4.4 The two-liquid phase approach improves specific activity and product yield of Syn6803\_BGT

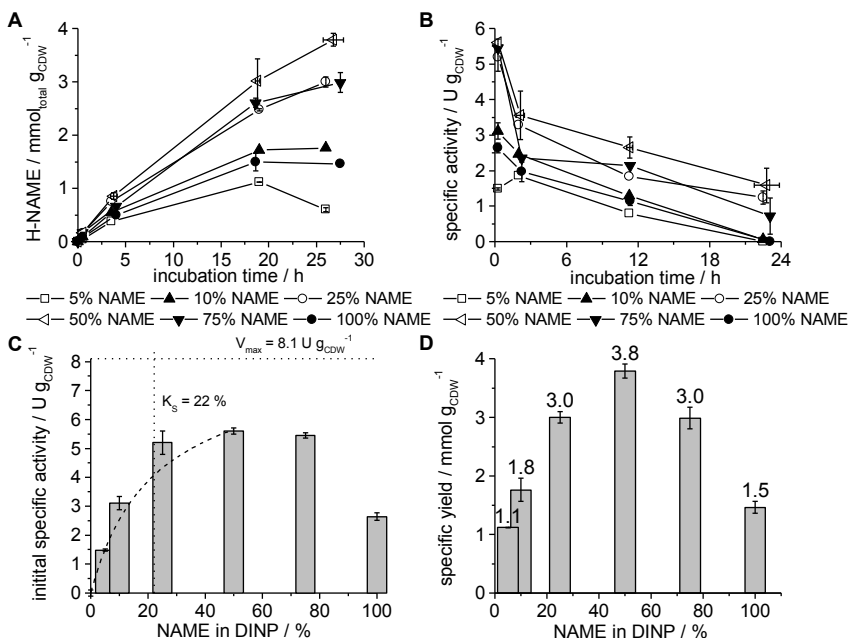
To investigate if and to what extent the two-liquid phase system improves whole-cell biocatalyst stability, DINP containing 25% (v/v) NAME was added to cyanobacterial cultures in different organic:aqueous phase ratios of 1:1, 1:3, and 1:10, and product formation was followed for 27 h. In all cases, initial specific activities as well as specific product yields were enhanced compared to the single aqueous phase system (**Figure 4.6, Table 4.2**). The best results were obtained using a phase ratio of 1:3, which enhanced the initial specific activity (from 3.3 to 5.2 U g<sub>CDW</sub><sup>-1</sup>) as well as the biotransformation stability, resulting in 6-fold increased specific product yields (**Table 4.2**). With a phase ratio of 1:10, the system appeared to become substrate mass transfer limited, whereas a high phase ratio of 1:1 lead to a reduced biocatalyst stability pointing to toxicity effects possibly mediated by direct contact of the cells with organic phase droplets and thus NAME, as it has been reported before for similar two-liquid phase systems (Bühler *et al.*, 2006; Park *et al.*, 2006; Schrewe *et al.*, 2011).



**Figure 4.6:** Impact of organic carrier solvent DINP containing 25% (v/v) NAME applied at different phase ratios on the long-term biotransformation stability with Syn6803\_BGT. Cells were cultivated under standard conditions in YBG11 medium for 2 days, induced with 2 mM IPTG for 4 h, harvested, and resuspended in YBG11 + 50 mM NaHCO<sub>3</sub> to a biomass concentration of 2 g<sub>CDW</sub> L<sup>-1</sup>. Biotransformations were initiated via the addition of 1, 0.33, or 0.1 mL of organic phase to 1 mL of cyanobacterial cultures in glass tubes. Average values and standard deviations are given for two independent biological replicates.

Elevated substrate concentrations have been found to be toxic and are thus expected to impair metabolism dependent whole-cell oxyfunctionalization activity and stability. Thus, the substrate concentration available in the aqueous phase was fine-tuned by applying different substrate concentrations (5%, 10%, 25%, 50%, 75%, and 100% (v/v) NAME) in the organic carrier solvent DINP added at an organic/aqueous phase ratio of 1:3. The substrate concentration applied significantly influenced the initial specific NAME hydroxylation rate,

which was highest at around  $5.5 \text{ U g}_{\text{CDW}}^{-1}$  with 25, 50, and 75% (v/v) NAME in DINP (**Figure 4.7**). Reduced hydroxylation rates at 5 and 10% (v/v) NAME indicated a substrate limitation, whereas high concentrations of 75 and 100% (v/v) NAME led to reduced initial activities and/or stabilities again indicating toxification of the cells.



**Figure 4.7:** Impact of different NAME concentrations within the organic carrier solvent DINP on the biotransformation performance of Syn6803\_BGT. Cells were cultivated, processed, and applied for long-term biotransformations as described in the legend of **Figure 4.6**. During biotransformations, different concentrations of NAME dissolved in DINP were applied at an organic:aqueous phase ratio of 1:3. **Panels A and B** show the courses of biomass-specific H-NAME accumulation and activities, respectively. **Panel C** shows initial specific activities calculated for the first 30 min of reaction. The dotted lines show the application of Michaelis-Menten kinetics for the data obtained with 5-50% NAME (v/v) in DINP. **Panel D** shows biomass-specific product yields. Average values and standard deviations of two independent biological replicates are given. U = unit =  $\mu\text{mol min}^{-1}$ , CDW = cell dry weight,  $V_{\text{max}}$  = maximal reaction velocity,  $K_s$  = apparent substrate uptake constant.

Up to 50% (v/v) NAME, initial activities exhibited a Michaelis-Menten type dependency on the substrate concentration with an apparent maximal reaction velocity  $V_{\text{max}}$  of  $8.1 \pm 0.5 \text{ U g}_{\text{CDW}}^{-1}$  and an apparent substrate uptake constant  $K_s$  of  $22.1 \pm 2.5\%$  (v/v) NAME in DINP ( $= 1 \text{ M}_{\text{org}} \triangleq 39 \mu\text{M}_{\text{aq}}$ ). The data obtained with higher substrate concentrations did not fit classical substrate inhibition kinetics ( $v = V_{\text{max}} * [S] / (K_s + [S] * (1 + [S] / K_i))$ ), pointing to toxification of the cells rather than enzyme inhibition as the cause for the reduced initial

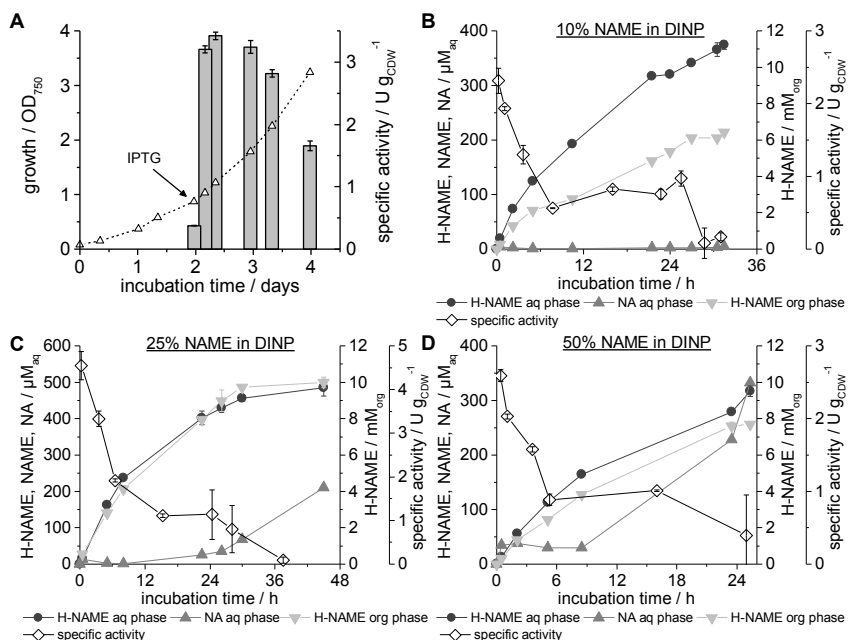
specific activities at high NAME concentrations. In conclusion, the application of NAME in DINP at a concentration of up to 50% (v/v) significantly increased biocatalyst performance enabling not only a high specific product yield of  $3.8 \pm 0.1 \text{ mmol g}_{\text{CDW}}^{-1}$ , but also an increase in specific activity.

#### **4.4.5 NAME hydroxylation in a 3 L stirred tank photo-bioreactor**

After successful stabilization of the NAME hydroxylation system, we set out to evaluate its scalability by transferring it from 1 mL glass tube- to a 3 L lab-scale stirred tank photo-bioreactor system. In contrast to cultivation and biotransformation in shake flasks and glass tubes, respectively, the photo-bioreactor setting provides an altered light input distribution, an aeration system continuously supplying compressed air into the medium, and stirring via impeller agitation, potentially affecting biocatalyst growth and physiology. First, the scaling of biocatalyst production was evaluated by growing the cells in the photo-bioreactor setting, induction 2 days after inoculation, and following oxyfunctionalization activity via short-term assays. During cultivation, the light intensity was increased after 30 and 48 h from 50 to 75 and 100  $\mu\text{E m}^{-2} \text{ s}^{-1}$ , respectively, and the aeration rate from 3 to 5  $\text{L min}^{-1}$  after 48 h to ensure optimal light and  $\text{CO}_2$  supply.

Initial growth rates ( $0.059 \text{ h}^{-1}$  from 0 to 32 h) in the photo-bioreactor were similar to those obtained in shake flasks (**Table 4.1**). The highest specific oxyfunctionalization activity ( $3.3 \pm 0.1 \text{ U g}_{\text{CDW}}^{-1}$ ) was achieved for a broad time range after induction, i.e., 4 up to 24 h (**Figure 4.8 A**), and was very similar to the maximal activity obtained with cells cultivated in shake flasks (**Figure 10.7**).

After the successful transfer of Syn6803\_BGT cultivation and induction to the photo-bioreactor scale, this transfer also was tested for the two-liquid phase biotransformation of NAME with Syn6803\_BGT. For two-liquid phase biotransformations in stirred tank photo-bioreactors, organic DINP phases containing 10, 25, or 50% (v/v) NAME were applied. The highest initial specific activity of  $4.5 \pm 0.3 \text{ U g}_{\text{CDW}}^{-1}$  was achieved with 25% (v/v) NAME in DINP, enabling a final biomass-specific product yield of  $2.6 \pm 0.1 \text{ mmol g}_{\text{CDW}}^{-1}$  after 45 h of biotransformation (**Figure 4.8, Table 4.2**). In comparison to the small scale experiments, biocatalyst performance with 10 and 25% (v/v) NAME in DINP was slightly reduced in terms of initial specific activity (by 10 - 20%) and final biomass-specific product yield (by 0 - 20%) (**Table 4.2**). With 50% (v/v) NAME in DINP, this performance was more significantly reduced (by 54 and 50% in terms of initial activity and specific yield, respectively) indicating that the bioreactor conditions promoted biocatalyst inactivation especially when high NAME concentrations were applied (Bühler *et al.*, 2002). Besides this, the successful scaling of biocatalyst growth and two-liquid phase biotransformation of NAME demonstrates the technical applicability of Syn6803\_BGT for two-liquid phase biotransformations in a stirred tank photo-bioreactor setting.



**Figure 4.8:** Syn6803\_BGT growth and NAME hydroxylation performance using different amounts of NAME dissolved in DINP in a stirred tank photo-bioreactor setting. Cells were cultivated in 3 L YBG11 medium at 50 (0 - 30 h), 75 (30 - 48 h), and 100  $\mu\text{E m}^{-2} \text{s}^{-1}$  (48 - 96 h), 300 rpm, and aeration with compressed air at 3 (0 - 48 h) and 5  $\text{L min}^{-1}$  (48 - 96 h). Gene expression was induced two days after inoculation. **Panel A** shows the growth curve and the course of specific activities determined in short-term activity assays ( $2 \text{ g}_{\text{CDW}}^{-1}$ , YBG11 +  $\text{NaHCO}_3$ ,  $30 \mu\text{E m}^{-2} \text{s}^{-1}$ ) for cells harvested at different time points. Specific activities are given as average values with standard deviations of two replicates. Photo-bioreactor-based biotransformations (**panels B-D**) were performed with cells harvested 24 h after induction and resuspended to  $1.6 \text{ g}_{\text{CDW}}^{-1}$  in 0.6 L of YBG11 medium containing 50 mM  $\text{NaHCO}_3$ . The biotransformation reaction was started by the addition of 0.21 L DINP containing 10, 25, and 50% (v/v) NAME (**panels B, C, and D**, respectively). Average values and standard deviations refer to two analytical replicates. org = measured in the organic phase, aq = measured in the aqueous phase, U = unit =  $\mu\text{mol min}^{-1}$ , CDW = cell dry weight.

## 4.5 Discussion

### 4.5.1 Substrate mass transfer, substrate hydrolysis, and reactant toxicity

Application of the two-liquid phase concept in principle may hamper biocatalysis with phototrophs due to shading. However, with phototrophic Syn6803\_BGT, two-liquid phase

**Table 4.1:** Overview on NAME biotransformation experiments with Syn6803\_BGT applying different NAME concentrations in the organic carrier solvent DINP in small-scale or photo-bioreactor settings.

NAME in DINP	org:aq phase ratio	NAME in aq phase <sup>1</sup> / $\mu\text{M}$	NA in aq phase <sup>2</sup> / $\mu\text{M}$	H-NAME / $\text{mmol}_{\text{total}} \text{L}_{\text{aq phase}}^{-1}$	Initial specific activity <sup>3</sup> / $\text{U g}_{\text{CDW}}^{-1}$	Initial hydrolysis rate <sup>3</sup> / $\text{U g}_{\text{CDW}}^{-1}$	Specific yield <sup>4</sup> / $\text{mmol}_{\text{total}} \text{g}_{\text{CDW}}^{-1}$
Tube							
10 mM	w/o DINP	$\leq 133^5$	1797 <sup>6</sup>	$0.9 \pm 0.1$	$3.3 \pm 0.1$	$2.3 \pm 0.1^{10}$	$0.5 \pm 0.1$
25% (v/v)	1:1	$58 \pm 4$	31	$3.7 \pm 0.3$	$4.8 \pm 0.4$	$0.10 \pm 0.01$	$2.1 \pm 0.2$
25% (v/v)	1:3	$54 \pm 5$	29	$5.7 \pm 0.3$	$5.2 \pm 0.4$	$0.47 \pm 0.01$	$3.2 \pm 0.2$
25% (v/v)	1:10	$53 \pm 3$	53	$4.7 \pm 0.1$	$4.4 \pm 1.5$	$1.74 \pm 0.12$	$2.7 \pm 0.1$
5% (v/v)	1:3	$10 \pm 1$	2	$2.1 \pm 0.1$	$1.5 \pm 0.1$	$0.06 \pm 0.01$	$1.1 \pm 0.01$
10% (v/v)	1:3	$22 \pm 1$	7	$3.3 \pm 0.3$	$3.1 \pm 0.2$	$0.15 \pm 0.01$	$1.8 \pm 0.2$
25% (v/v)	1:3	$44 \pm 4$	25	$5.7 \pm 0.2$	$5.2 \pm 0.4$	$0.36 \pm 0.01$	$3.0 \pm 0.1$
50% (v/v)	1:3	$81 \pm 5$	78	$7.3 \pm 0.1$	$5.6 \pm 0.1$	$0.92 \pm 0.01$	$3.8 \pm 0.1$
75% (v/v)	1:3	$120 \pm 11$	1797 <sup>6</sup>	$5.9 \pm 0.5$	$5.5 \pm 0.1$	$2.00 \pm 0.1$	$3.0 \pm 0.2$
100% (v/v)	1:3	$\leq 133^5$	1797 <sup>6</sup>	$2.8 \pm 0.3$	$2.6 \pm 0.1$	$5.23 \pm 0.01$	$1.5 \pm 0.2$
STR <sup>7</sup>							
10% (v/v) <sup>8</sup>	1:3	29 to 91	5	$2.6 \pm 0.1$	$2.3 \pm 0.2$	$0.13 \pm 0.02$	$1.7 \pm 0.1$
25% (v/v) <sup>9</sup>	1:3	64 to 133 <sup>5</sup>	$35 \pm 2 / 210 \pm 3$	$3.6 \pm 0.2 / 4.0 \pm 0.1$	$4.5 \pm 0.3$	$0.49 \pm 0.02$	$2.3 \pm 0.1 / 2.6 \pm 0.1$
50% (v/v)	1:3	83 to 133 <sup>5</sup>	$332 \pm 3$	$3.0 \pm 0.1$	$2.6 \pm 0.1$	$2.16 \pm 0.06$	$1.9 \pm 0.1$

Average values with standard deviations are given for independent biological or analytical replicates. org = organic, aq = aqueous, U = unit =  $\mu\text{mol min}^{-1}$ , CDW = cell dry weight. <sup>1</sup> Average value or, in case of experiments in photo-bioreactors, concentration ranges referring to the total biotransformation time, <sup>2</sup> highest value during biotransformation, <sup>3</sup> for the first 30 min of reaction, <sup>4</sup> calculated based on the total amount of product in aqueous and organic phases divided by the initially applied biomass assuming no growth, <sup>5</sup> solubility of NAME in water (Chemspider database structure 14846), <sup>6</sup> solubility of NA in water (Chemspider database structure 7866), <sup>7</sup> technical replicates, <sup>8</sup> 31.5 h of reaction time, <sup>9</sup> 26.2/ 45 h of reaction time, <sup>10</sup> rate calculated for 24 h

biotransformation resulted in up to 1.7-fold increased initial specific hydroxylation activities (**Table 4.2**). This can be ascribed to reduced cell toxification/ substrate inhibition by decreased aqueous phase NAME concentrations or to an enhanced substrate mass transfer to the cells, possibly involving direct substrate transfer from organic solvent droplets to the cells as it has been observed before (Bühler *et al.*, 2006; Park *et al.*, 2006; Schrewe *et al.*, 2011). Further, the presence of the organic phase significantly reduced substrate hydrolysis leading to only low final NA titers and thus, enabled higher product yields on substrate (**Table 4.2, Figure 10.8**). In whole-cell biocatalysis, cell toxification by hydrophobic reactants often affects biocatalyst and thus biotransformation performance. Hydrophobic compounds with  $\log P_{(\text{octanol/water})}$  values between 2 and 4 typically impair cell viability via intercalation into microbial membranes (Laane *et al.*, 1987; Sikkema *et al.*, 1994). Using the empirical equation for predicting the concentration leading to membrane dissociation as reported by Sikkema *et al.* (1994) and Kratzer *et al.* (2015) for heterotrophic microorganisms, NAME ( $\log P = 3.9$ ) and NA ( $\log P = 3.4$ ) are expected to become toxic at aqueous concentrations of 216 and 617  $\mu\text{M}$ , respectively (Kratzer *et al.*, 2015; Sikkema *et al.*, 1994). Our results show an impaired growth at concentrations of 1 mM NAME (solubility in water is 133  $\mu\text{M}$ ) and 100  $\mu\text{M}$  NA (**Figure 4.4**), indicating a higher sensitivity of *Synechocystis* sp. PCC 6803 compared to heterotrophic microorganisms. In addition to plasma membranes, phototrophic cells harbor thylakoid membranes containing the photosynthetic machinery of the light reaction. The disintegration of respective membranes may directly affect photosynthetic water oxidation and electron transport, and thus the energy metabolism and viability of phototrophic organisms. Consequently, *in situ* reactant supply and removal becomes highly important for the application of photoautotrophic whole-cell biocatalysts.

Overall, this study shows that the two-liquid phase concept can successfully be applied in light-dependent reaction setups based on phototrophic microorganisms, with benefits ranging from mass transfer over the handling of toxic compounds to the avoidance of side reactions.

### 4.5.2 Specific oxyfunctionalization activity

Factors possibly limiting the oxyfunctionalization activity of Syn6803\_BGT include  $\text{O}_2$  supply, substrate mass transfer to the cells, substrate transfer over the cellular membranes, cell integrity, the intracellularly available AlkB activity, and electron supply. Considering the enhanced  $\text{O}_2$  evolution rates measured with increasing light intensities (**Figure 4.1 B**) and the high NAME hydroxylation activities ( $100 \text{ U g}_{\text{CDW}}^{-1}$ ) achieved by recombinant *E. coli* containing AlkBGT (Schrewe *et al.*, 2011), limitations by  $\text{O}_2$  supply and substrate transfer over cellular membranes are improbable. The increase in specific activity in the presence of a second liquid organic phase indicated that substrate mass transfer to the cells and/ or substrate toxicity were critical factors. Besides and in parallel to NAME availability, the intracellular AlkBG(T) amount may constitute a limiting factor. Thus, excluding  $\text{O}_2$  as limiting

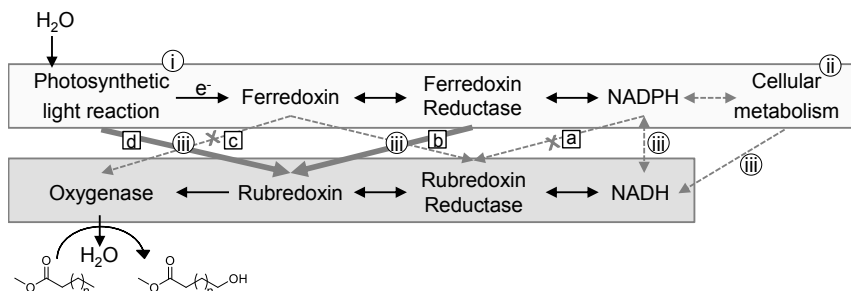


factor and knowing about the importance of controlled NAME supply as achieved via the two-liquid phase approach, intracellular AlkBGT synthesis and electron supply will be discussed in the following.

**AlkBGT synthesis.** In *E. coli* W3110 (pBT10), high specific oxyfunctionalization activities ( $100 \text{ U g}_{\text{CDW}}^{-1}$ ) involved *alkBGT* overexpression based on a high copy number plasmid (pCOM10) and the strong promoter system ( $P_{\text{alk}}$ ) of the *alk* operon of *P. putida* GPo1 (Schrewe *et al.*, 2011). The expression system applied in this study relies on a plasmid with a medium copy number in *Synechocystis* sp. PCC 6803 (RSF origin of replication, 10 - 30 copies per cell (Huang *et al.*, 2010)) and a promoter system ( $P_{\text{trc10}}$ ) showing low specific activities in *E. coli* W3110 in comparison to the  $P_{\text{alk}}$  promoter system (**Figure 10.9**). For Syn6803\_BGT, SDS-PAGE (**Figure 10.10**) revealed only low specific AlkB concentrations in comparison to the total protein amount and to the AlkB amount present in recombinant *E. coli* exhibiting high oxyfunctionalization activities ( $100 \text{ U g}_{\text{CDW}}^{-1}$ ) (Schrewe *et al.*, 2011). Duplication of the operon within the expression plasmid as a first strategy to increase the AlkBGT expression level did not result in increased AlkB concentrations and thus hydroxylation rates (**Figure 10.11**). Controlled and high level expression of recombinant genes in cyanobacteria still remains challenging (Camsund and Lindblad, 2014; Englund *et al.*, 2016). Thus, the development and application of more efficient expression systems for *Synechocystis* sp. PCC 6803 would be useful to facilitate *alkBG(T)* overexpression and thus possibly enhance oxyfunctionalization activities.

**The photosynthetic electron supply to AlkB.** In general, the efficiency of electron supply to AlkB is determined by 1) the electron activation rate in the course of the photosynthetic light reaction, 2) the competition for reduction equivalents with the primary cellular electron demand, and 3) the transport of electrons from the photosynthetic electron transport chain to AlkB (**Figure 4.9**). As discussed before, the presence of a second liquid organic phase enhanced specific oxyfunctionalization activities of Syn6803\_BGT, indicating a limitation in substrate availability in the single aqueous phase system. This and possibly the low AlkB amount within the cells obviously constituted the main limiting factors, which explains why increased photosynthetic water oxidation induced by increased light intensities (**Figure 4.9 i**) did not result in enhanced NAME oxyfunctionalization rates in single aqueous phase biotransformations (**Figure 4.1 B**). However, specific activities of Syn6803\_BGT slightly increased upon  $\text{NaHCO}_3$  supply (**Figure 4.1 A**). The primary cellular electron demand for, e.g.,  $\text{CO}_2$  fixation and nitrate assimilation, constitutes a major electron sink, which may compete with oxygenase catalysis, given a high capacity for the latter is present in the cell (**Figure 4.9 ii**). On the other hand, the presence of  $\text{NaHCO}_3$  may promote enhanced rates of photosynthetic water oxidation via different regulatory mechanisms and thus increase electron flux towards electron transfer shuttles such as ferredoxin, NADPH, or NADH. The

increased electron flux in turn may have caused the slight increase in NAME hydroxylation activity upon  $\text{NaHCO}_3$  supply. The observed oxyfunctionalization activity in the absence of light and thus water oxidation (**Figure 4.1 B**) suggests that electrons for oxygenase catalysis were derived from the catabolism of storage compounds under these conditions (**Figure 4.9**).



**Figure 4.9:** Possible electron transfer pathways from the photosynthetic electron transport chain to AlkB. The circles indicate the three factors determining the electron transfer efficiency: i) rate of water oxidation, ii) competition of oxygenase catalysis with cellular metabolism, and iii) transport of electrons from the photosynthetic electron transport chain to AlkB. *In vitro* studies showed that the rubredoxin reductase AlkT receives electrons primarily from NADH and not from NADPH (indicated by crossed arrow [a]) (Peterson *et al.*, 1967), whereas the replacement of AlkT with a NADPH-dependent spinach ferredoxin reductase (indicated by bold line [b]) was functional (McKenna and Coon, 1970). In addition, AlkB containing *Synechocystis* sp. PCC 6803 is shown to require the rubredoxin AlkG (indicated by crossed arrows [c]), but not AlkT for NAME oxyfunctionalization. This indicates that electron transfer to AlkG and finally AlkB either occurs directly from the photosynthetic electron transport chain (bold line [d]) or via endogenous ferredoxin reductases (bold line [b]).

Further, the native “NADH-AlkT-AlkG-AlkB” electron transfer pathway was bypassed quite efficiently in *Synechocystis* sp. PCC 6803 containing AlkBG but lacking AlkT (**Figure 4.2**) (Benson *et al.*, 1977; McKenna and Coon, 1970; Peterson *et al.*, 1966a). Thereby, AlkG, which was required for productive electron transfer to AlkB, may have received electrons either directly from the photosynthetic electron transport chain or via the action of endogenous ferredoxin reductases (**Figure 4.9**). Functional replacement of the NADH-dependent rubredoxin reductase AlkT by an NADPH-dependent spinach ferredoxin reductase has been shown in *in vitro* studies (McKenna and Coon, 1970). The same was reported for recombinant CYP450 enzymes actively coupling with ferredoxins/ ferredoxin reductases originating from phototrophic species *in vitro* and *in vivo* (Hara *et al.*, 1997; Jensen *et al.*, 2012; Mellor *et al.*, 2016). Identification and overexpression of enzymes involved in this electron transfer might be a powerful strategy to improve the coupling of oxyfunctionalization and photosynthetic metabolism. In addition to the availability of proteins involved in electron transfer and oxyfunctionalization, their localization also may determine

oxyfunctionalization efficiency. AlkB was found to be localized in the cytoplasmic membrane of the cyanobacterial cells, as could be expected from its native localization in *Pseudomonas putida* GpO1 (**Figure 10.5**) (Benson *et al.*, 1979). In contrast, the water oxidation and photosynthetic electron transfer are located in the thylakoid membranes (Vermaas, 2001). The spatial separation of AlkB and photosynthetic electron transfer chain might impair electron transfer to AlkB. Recent studies investigated the anchoring of a recombinant cytochrome P450 monooxygenase in cyanobacterial thylakoid membranes, allowing for photosynthesis coupled oxyfunctionalization of tyrosine to p-hydroxyphenyl-acetaldoxime (Lassen *et al.*, 2014a). Relocalization of AlkB to the thylakoid membrane might be another promising strategy to enhance electron supply to AlkB.

### 4.5.3 Scaling

Yet, process concepts specific for photosynthesis-driven biotransformations do not exist and are rare for H<sub>2</sub> production and product formation from CO<sub>2</sub> (Dasgupta *et al.*, 2010; Fresewinkel *et al.*, 2014). Light distribution, CO<sub>2</sub> supply, as well as substrate supply are critical process parameters to establish efficient reactor concepts. As a first step to evaluate scaling, the Syn6803\_BGT-catalyzed NAME hydroxylation in a two-liquid phase system was transferred from 1 mL glass tube to a 3 L stirred-tank photo-bioreactor, which proved to be successful. A similar biocatalyst performance as in the test tube system was achieved. However, specific yields were somewhat lower in comparison to the small-scale experiments, especially at high NAME concentrations in the organic phase (**Table 4.2**). The main difference to the small-scale setting was the mixing intensity, which was significantly higher in the stirred tank photo-bioreactor (2.2 vvm aeration, 300 rpm agitation). Direct contact of the cells with organic phase droplets, as discussed above as a possible reason for improved specific activities in the two-liquid phase system, may, on the other hand, promote biocatalyst toxification as also indicated by the adverse effect of high organic:aqueous phase ratios in small scale experiments (**Table 4.2**). The more intense mixing in the bioreactor leads to more frequent collision of cells with solvent droplets and thus can be expected to promote direct NAME transfer from the organic phase to the cells (Bühler *et al.*, 2006; Bühler *et al.*, 2002; Park *et al.*, 2006). Thus, mixing and the NAME concentration constitute critical parameters in stirred tank bioreactors. In addition to such toxification, a pH shift due to intense aeration, which promoted degassing of CO<sub>2</sub> derived from the NaHCO<sub>3</sub> in the medium (**Figure 10.12**), may have affected cell physiology and thus whole-cell biocatalyst performance. Beside pH control, strategies to overcome CO<sub>2</sub> degassing may become mandatory and include reduced agitation and the omission of aeration. Such oxyfunctionalization without aeration is enabled by the *in situ* O<sub>2</sub> generation via photosynthetic water oxidation (**Chapter 3, Chapter 7**).

### 4.6 Conclusions

Photoautotrophic organisms are promising biocatalysts for oxyfunctionalization catalysis as they are capable of supplying reduction equivalents as well as O<sub>2</sub> via photosynthetic water oxidation. The previously developed whole-cell biocatalyst Syn6803\_BGT was found to involve endogenous pathways and enzymes in the supply of electrons supporting oxygenase catalysis. This included AlkT-independent electron transfer to AlkG and electron supply via the catabolism of storage compounds. The whole-cell reaction system was stabilized via a two-liquid phase approach enabling bioprocess relevant time scales of >24 h. The application of DINP as organic carrier solvent not only stabilized NAME hydroxylation via the attenuation of NAME toxicity, but also increased the specific biocatalyst activity most likely via an improved substrate mass transfer and reduced by-product formation. Thereby, this study demonstrated feasibility of the two-liquid phase approach for photobiotechnology. This and the successful transfer of the light-driven two-liquid phase biotransformation to a 3 L stirred tank photobioreactor scale paves the way for the technical application of cyanobacteria as phototrophic host organisms for efficient oxyfunctionalization biocatalysis.

### 4.7 Acknowledgments

Victor de Lorenzo (Madrid, Spain) is acknowledged for the kind provision of the plasmid pSEVA251. The authors are grateful to Dr. Linde Debor for the membrane fractionation analysis and cloning of pAH044. The authors thank Tobias Kaufer for biocatalyst growth characterization and cloning of pAH047. The authors are grateful for the opportunity to use the facilities of the Centre for Biocatalysis (MiKat) at the Helmholtz Centre for Environmental Research, which is supported by European Regional Development Funds (EFRE -Europe funds Saxony) and the Helmholtz Association.

## **Chapter 5 Light-dependent and aeration-independent gram-scale hydroxylation of cyclohexane to cyclohexanol by CYP450 harboring *Synechocystis* sp. PCC 6803**

Adrian Hochkeppel contributed to the biochemical analysis of the recombinant strain and the assessment of the biotransformation performance of the recombinant strain in the stirred tank photobioreactor under exclusion of aeration, coordinated and supervised by Anna Hoschek and Jörg Toepel. Rohan Karande, Jörg Toepel, Bruno Bühler, and Andreas Schmid coordinated the project and corrected the manuscript.

Parts published in:

*Biotechnology Journal*, **2019**, DOI: 10.1002/biot.201800724

**5.1 Abstract**

Oxygenase-based whole-cell biocatalysis enables selective oxyfunctionalizations under mild conditions. Phototrophic organisms such as cyanobacteria are promising host systems for oxygenase catalysis as the photosynthetic water oxidation gives highly sustainable access to the required co-substrates that are activated reduction equivalents and O<sub>2</sub>. First studies have validated the functional coupling of oxygenase-enzyme systems to photosynthetic water oxidation. In this study, we developed a recombinant *Synechocystis* sp. PCC 6803 strain showing unprecedentedly high oxyfunctionalization activities for a photoautotrophic strain and evaluated its technical applicability. The strain functionally synthesizes a cytochrome P450 monooxygenase system originating from *Acidovorax* sp. CHX100 and enables the hydroxylation of cycloalkanes. For cyclohexane, the biocatalyst-specific reaction rate was found to be light-dependent reaching  $24.0 \pm 0.6 \text{ U g}_{\text{CDW}}^{-1}$  at a light intensity of  $150 \mu\text{E m}^{-2} \text{ s}^{-1}$ . *In situ* substrate supply via a two-liquid phase system increased the initial specific activity to  $39.2 \pm 0.7 \text{ U g}_{\text{CDW}}^{-1}$  and stabilized the biotransformation by preventing cell toxification. This resulted in a 10 times increased specific product yield compared to the single aqueous phase system up to  $4.5 \text{ g}_{\text{cyclohexanol}} \text{ g}_{\text{CDW}}^{-1}$ . Subsequently, the developed biotransformation system was successfully scaled from shake flask- to a 3 L stirred-tank photo-bioreactor setup. Thereby, the *in situ* generation of O<sub>2</sub> via photosynthetic water oxidation allowed non-aerated process operation, thus circumventing substrate evaporation as the most critical factor limiting process performance and stability. In summary, 2.6 g cyclohexanol were generated from water, light, and cyclohexane. This paper exemplifies the technical applicability of cyanobacteria for light-driven oxyfunctionalization reactions involving highly toxic and volatile substrates. The design of scalable biotransformation technologies for photoautotrophs may well develop into promising photosynthesis-driven bioprocesses.

## 5.2 Introduction

Since a few years, cyanobacteria have gained attention as valuable biocatalysts for biotransformation reactions such as the oxyfunctionalization of hydrocarbons to the respective value-added compounds (Böhmer *et al.*, 2017; Lassen *et al.*, 2014b; Mellor *et al.*, 2017). These whole-cell reaction systems utilize photosynthetic water oxidation as a source of activated reduction equivalents as well as O<sub>2</sub>, both co-substrates for oxygenase-catalyzed oxyfunctionalizations. Under high light conditions, the light reaction including water oxidation is considered not to limit growth, but rather has to be suppressed by phototrophic organisms in order to avoid damage by excessive buildup of reduction power, O<sub>2</sub>, and reactive oxygen species (Bailey and Grossman, 2008; Wilhelm and Selmar, 2011). The coupling of oxygenase catalysis to photosynthetic water oxidation provides a sink for reduction equivalents as well as O<sub>2</sub>, potentially enabling high oxyfunctionalization rates. Recently, several studies demonstrated the functional introduction of oxygenases into diverse photosynthetic organisms and their coupling to photosynthetic water oxidation (**Chapter 3**) (Berepiki *et al.*, 2016; Böhmer *et al.*, 2017; Lassen *et al.*, 2014a; Włodarczyk *et al.*, 2015), thus verifying the concept of photosynthesis-driven whole-cell oxyfunctionalization on laboratory scale. The applicability of cyanobacteria on technical scale, especially for the oxyfunctionalization of highly volatile and toxic substrates, however, has not been demonstrated, yet. Although the cultivation and reaction conditions of standard bioprocesses have to be modified by lighting systems to enable sufficient water oxidation, our recent study showed that established reaction engineering options such as two-liquid phase bioreactor setups are in principle applicable for photosynthetic biocatalysts (**Chapter 4**). The evaluation and intensification of such photosynthesis-driven bioprocessing for gram-scale hydroxylations, however, remains an open task.

Cyclohexanol constitutes an example for a high volume chemical produced via oxyfunctionalization, in this case from cyclohexane, and is of high commercial interest as a precursor for the synthesis of Nylon-6 and Nylon-6,6 building blocks (Schuchardt *et al.*, 1993). The current industrial production of cyclohexanol and cyclohexanone from cyclohexane involves the use of homogenous cobalt catalysts and high temperatures above 423 K and suffers from low selectivities (Schuchardt *et al.* 2001). Thus, numerous new heterogeneous chemocatalysts are under development. The enzymatic oxyfunctionalization of cyclohexane to cyclohexanol is a promising alternative route to the traditional chemical approaches as high selectivity can be achieved under mild conditions (Karande *et al.*, 2016a; Salamanca *et al.*, 2015). Cyclohexane reveals generic challenges for biocatalysis due to its low water solubility (650 µM), high volatility (0.15 atm m<sup>3</sup> mol<sup>-1</sup>), and high toxicity to microorganisms.

The focus of this work was to evaluate the potential of cyanobacteria as biocatalysts to meet these challenges and to develop a process setup suitable for cyclohexane oxidation. A recombinant *Synechocystis* sp. PCC 6803 strain harboring a cyclohexane monooxygenase, i.e., the cytochrome P450 monooxygenase from *Acidovorax* sp. CHX100 (Salamanca *et al.*, 2015), capable of hydroxylating cyclohexane at high rates was developed and evaluated regarding its oxyfunctionalization activity as well as stability under process conditions. An *in situ* substrate supply strategy involving a second liquid organic phase was followed, on the one hand, to attenuate cell toxification and thus improve process stability and, on the other hand, to improve substrate mass transfer and thus enhance productivity. Finally, the benefit of *in situ* O<sub>2</sub> generation via photosynthetic water oxidation for the conversion of volatile cyclohexane under non-aerated process conditions was evaluated in a 3L stirred tank photo-bioreactor setup.

### 5.3 Materials and Methods

**Chemicals, bacterial strains and plasmids.** Chemicals used in this study are given in **Chapter 2**. *Synechocystis* sp. PCC 6803 was transformed with the plasmid pAH050 harboring the cytochrome P450 enzyme system originating from *Acidovorax* sp. CHX100 resulting in the recombinant strain *Synechocystis* sp. PCC 6803 (pAH050) (hereinafter referred to as Syn6803\_CYP). Respective cloning was based on the broad-host-range vector pPMQAK1 (RSF origin of replication) involving transcriptional control by the P<sub>trc10</sub> promoter system (Huang *et al.*, 2010) (for cloning procedure see **Chapter 2**).

**Cultivation of *Synechocystis* sp. PCC 6803.** If not stated otherwise, shake flask cultivation of *Synechocystis* sp. PCC 6803 was performed as described in **Chapter 2** (YBG11 medium, 50 mM HEPES, 20 mL in 100 mL baffled Erlenmeyer flasks, 30 °C, 150 rpm, 2.5 cm amplitude, 50  $\mu\text{E m}^{-2} \text{s}^{-1}$ , LED, ambient CO<sub>2</sub> (0.04%), 75% humidity, start OD<sub>750</sub> ca. 0.08). Kanamycin was used at a final concentration of 50  $\mu\text{g mL}^{-1}$ . Gene expression was induced 2 days after inoculation using 2 mM IPTG for 24 h. If required, 50 mM NaHCO<sub>3</sub> were supplied to the medium before sterile filtration (0.2  $\mu\text{m}$ ). The correlation factor 0.2246 g<sub>CDW</sub> L<sup>-1</sup> OD<sub>750</sub><sup>-1</sup> was used for the conversion of OD<sub>750</sub> values to cell dry weight (CDW) concentrations in g<sub>CDW</sub> L<sup>-1</sup> (**Chapter 2, Figure 2.2**).

Cultivation of Syn6803\_CYP cells in the stirred tank photo-bioreactor Labfors 5 Lux (Infors AG, Bottmingen, Switzerland) was performed using 3 L YBG11 medium inoculated to an OD<sub>750</sub> of 0.08 using pre-cultures obtained via the standard cultivation protocol described above. Cultivation in photo-bioreactors was performed at a light intensity of 50  $\mu\text{E m}^{-2} \text{s}^{-1}$  from 0 - 30 h, 75  $\mu\text{E m}^{-2} \text{s}^{-1}$  from 30 - 48 h and 100  $\mu\text{E m}^{-2} \text{s}^{-1}$  from 48 to 96 h. The agitation speed was set to 300 rpm. The aeration rate was set to 3 L min<sup>-1</sup> (1 vvm) for 0 - 48 h and 5 L min<sup>-1</sup> (1.7 vvm) from 48 - 96 h using compressed air. The applied light spectrum is shown in **Figure 10.2**.



**Biotransformation procedures in shake flasks.** Standard oxyfunctionalization activity assays were performed by cultivating the cells as described above, harvesting by centrifugation (10 min, 5000g, rt) and resuspension in YBG11 medium (50 mM NaHCO<sub>3</sub>, 50 µg mL<sup>-1</sup> kanamycin, 2 mM IPTG) to a final biomass concentration of ca. 1 g<sub>CDW</sub> L<sup>-1</sup>. Aliquots of 10 mL culture were provided in 100 mL baffled screw cap shake flasks and pre-warmed for 10 min at 30 °C, 200 rpm (2.5 cm amplitude) and respective light intensity. The biotransformation reaction was started by adding 5 mM cyclohexane (5.17 µL of pure substrate). If cyclohexane was supplied via the gas phase, 25 mL culture was provided in 250 mL baffled screw cap shake flasks equipped with an open glass inlet containing 1 mL cyclohexane (**Figure 5.2 A**). The reaction was quenched at respective time-points by adding 600 µL reaction mixture to 600 µL ice-cold diethyl ether containing 200 µM of decane as internal standard before applied for GC analysis (see **GC analysis method 1**).

Two-liquid phase oxyfunctionalization was performed as described before, but with culture aliquots of 15 mL applied in 250 mL baffled screw cap shake flasks at 150 rpm (2.5 cm amplitude). The biotransformation reaction was started by adding 5 mL of the organic phase (5 - 20% cyclohexane in DINP). Samples from the organic phase were taken at respective time-points, quenched by centrifugation, and 10 times diluted in ice-cold diethyl ether containing 200 µM of decane as internal standards before applied for GC analysis (see **GC analysis method 2**).

**Biotransformation procedures in stirred tank photobioreactor.** Whole-cell oxyfunctionalization in the stirred tank photo-bioreactor Labfors 5 Lux (Infors AG, Bottmingen, Switzerland) was performed with cells derived from a 3 L photo-bioreactor culture three days after inoculation. Three days after inoculation, cells were harvested by centrifugation (4640, 4 °C, 20 min) and resuspended in 1.2 L YBG11 medium containing 50 mM NaHCO<sub>3</sub>, 50 µg mL<sup>-1</sup> kanamycin and 2 mM IPTG, to a biomass concentration of 0.5 - 0.8 g<sub>CDW</sub> L<sup>-1</sup>. Pre-conditioning in the photobioreactor was performed at 30 °C, 300 rpm (impeller), 150 µmol m<sup>-2</sup> s<sup>-1</sup>, and, if not stated otherwise, at 0.15 L min<sup>-1</sup> aeration with compressed air for ca. 30 min. The biotransformation reaction was started by adding 400 mL of DINP containing 5% (v/v) cyclohexane. Samples were taken at regular time intervals and quenched by immediate centrifugation (17000g, 4 °C, 10 min). Organic phase portions were diluted 10 times in ice-cold diethyl ether containing 200 µM decane, dried over anhydrous Na<sub>2</sub>SO<sub>4</sub>, and subjected to GC analysis (see **GC analysis method 2**). Reactants in the aqueous phase were extracted using equal amounts of ice-cold diethyl ether, followed by drying over anhydrous Na<sub>2</sub>SO<sub>4</sub> and GC analysis (see **GC analysis method 1**).

**Determination of org:aq partition coefficients under abiotic conditions in 1.5 mL reaction tubes.** Partitioning of cyclohexane, cyclohexanol, cyclohexanone between YBG11 medium and DINP was determined using defined stock solutions in DINP (0.5 and 1 M for

cyclohexane, 1 and 5 mM for cyclohexanol and cyclohexanone). 600  $\mu\text{L}$  of this stock solution was mixed vigorously with 600  $\mu\text{L}$  of YBG11 medium for 5 min and incubated for 2 h at 30 °C and 2000 rpm (ThermoMixerC, Eppendorf, Wesseling-Berzdorf, Germany). Phases were separated by centrifugation (10 min, 17,000g, room temperature). The aqueous phase then was extracted using an equal volume of diethyl ether (containing 0.2 mM decane as an internal standard). The organic phase was diluted in diethyl ether (0.2 mM decane). Quantification was performed by GC-FID analysis (see **GC analysis methods 1 and 2**, respectively).

**GC analysis method 1 (Extracted aqueous phase sample).** Cyclohexane, cyclohexanol, and cyclohexanone extracted from aqueous phase samples using diethyl ether were quantified using a Trace 1310 gas chromatograph (Thermo Fisher Scientific, Waltham, USA) equipped with a TG-5MS capillary column (5% diphenyl / 95% dimethyl polysiloxane, 30 m, I.D.: 0.25 mm, film thickness: 0.25  $\mu\text{m}$ , ThermoFisher Scientific) and a flame ionization detector (FID) operated at 320 °C, 350  $\text{mL min}^{-1}$  air flow, 30  $\text{mL min}^{-1}$  makeup gas flow, and 35  $\text{mL min}^{-1}$  hydrogen gas flow. Nitrogen gas was applied as carrier gas at a constant flow rate of 1.5  $\text{mL min}^{-1}$ . The injection volume was set to 1  $\mu\text{L}$  injected by means of a PTV injector, programmed for a temperature gradient of 2 °C  $\text{s}^{-1}$  from 40-250 °C. A split ratio of 7 was applied. The oven temperature profile was: 1) 40 °C for 1 min, 2) 40-80 °C at 10 °C  $\text{min}^{-1}$ , 3) 80-250 °C at 100 °C  $\text{min}^{-1}$ , and 4) 250 °C for 2 min.

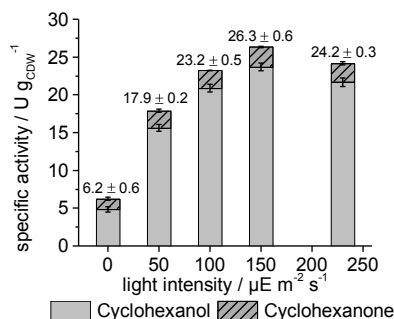
**GC analysis method 2 (Samples containing organic carrier solvent DINP).** Cyclohexane, cyclohexanol, and cyclohexanone dissolved in DINP were quantified using a Trace 1310 gas chromatograph (Thermo Fisher Scientific) equipped with the same column as used in method 1, a pre-column (deactivated silica guard column, 2 m x 0.53 mm, Thermo Fisher Scientific, Milan, Italy), an integrated backflush system, and a flame ionization detector (FID) operated as described for method 1. Nitrogen gas was applied as carrier gas at a constant flow of 1.5  $\text{mL min}^{-1}$ . The injection volume was set to 1  $\mu\text{L}$  injected by means of a PTV injector operating at the following temperature gradient: 1) 2 min at 250 °C, 2) 14.5 °C  $\text{s}^{-1}$  from 250 to 400 °C, and 3) 400 °C for 5 min. A split ratio of 3 was applied. 2 min after injection, a backflush through the pre-column was applied. The oven temperature profile was: 1) 40 °C for 2 min, 2) 40-70 °C with 25 °C  $\text{min}^{-1}$ , 3) 70-90 °C with 3 °C  $\text{min}^{-1}$ , 4) 90-310 °C with 100 °C  $\text{min}^{-1}$  and 5) 310 °C for 5 min.

## 5.4 Results

### 5.4.1 Syn6803\_CYP is active and shows light-dependent activity

Karande et al. 2016 reported the functional expression of the CYP450 monooxygenase genes from *Acidovorax* sp. CHX100 in recombinant *Pseudomonas taiwanensis* VLB120, enabling efficient cyclohexane hydroxylation driven by reduction equivalents derived from

chemoheterotrophic citrate catabolism. With the aim to drive this reaction by reduction equivalents (and  $O_2$ ) derived from photosynthetic water oxidation, the genes encoding this three-component monooxygenase system (composed of CYP = CYP450 monooxygenase component, FnR = FAD-ferredoxin reductase, and Fn = ferredoxin) were introduced into the cyanobacterium *Synechocystis* sp. PCC 6803 by means of the expression plasmid pAH050 (for cloning procedure see supplemental information). CYP450 synthesis in the resulting strain Syn6893\_CYP was verified by SDS-PAGE analysis, whereas protein bands for Fn and FnR could not be identified (**Figure 10.13**). At a light intensity of  $50 \mu E m^{-2} s^{-1}$ , Syn6803\_CYP catalyzed cyclohexane hydroxylation at a rate of  $17.9 \pm 0.2 U g_{CDW}^{-1}$ , proving the successful construction of a biocatalytically active strain.



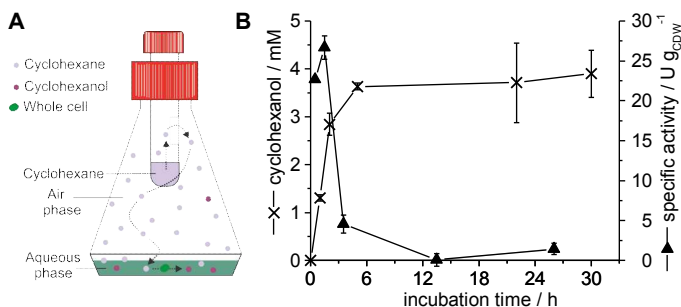
**Figure 5.1:** Cyclohexane hydroxylation activity of Syn6803\_CYP in dependence of the light intensity applied. Cyclohexane oxidation to cyclohexanol (grey bars) and overoxidation of cyclohexanol to cyclohexanone (dashed grey bars) is presented. For whole-cell oxyfunctionalization assays, cells were cultivated in YBG11 medium and resuspended in YBG11 supplemented with  $NaHCO_3$  to a biomass concentration of ca.  $1 g_{CDW} L^{-1}$ . Assays were performed with 10 mL of cell suspension in 100 mL screw capped and baffled shake flasks at  $30^\circ C$ , 200 rpm (2.5 cm amplitude), and the indicated light-intensities. Reactions were started by adding cyclohexane to a concentration of 5 mM with respect to the aqueous phase volume and stopped after 10 min by quenching with diethylether. Each column represents average values and standard deviations of two independent biological replicates.

Increased light intensities resulted in enhanced oxyfunctionalization activities, with a maximum specific activity of  $26.3 \pm 0.6 U g_{CDW}^{-1}$  at  $150 \mu E m^{-2} s^{-1}$  (**Figure 5.1**). Overoxidation of cyclohexanol to cyclohexanone was observed at a portion of ca. 10%. An increase of the light-intensity above  $150 \mu E m^{-2} s^{-1}$  did not result in higher, but in slightly decreased specific oxyfunctionalization activities, most likely due to photo-inhibition effects (Aro *et al.*, 1993; Nagy *et al.*, 1995). In the absence of light, cells showed a basal oxyfunctionalization activity of  $6.2 \pm 0.6 U g_{CDW}^{-1}$  and indicated the supply of reduction equivalents via the catabolism of storage compounds such as glycogen as it has been observed previously (**Chapter 4**). These results clearly show that Syn6803\_CYP-catalyzed cyclohexane hydroxylation was

light-dependent and profited from increasing rates of water oxidation up to a light intensity of  $150 \mu\text{E m}^{-2} \text{s}^{-1}$ .

#### 5.4.2 Syn6803\_CYP activity is stable for 2 h before decreasing rapidly

For the development of efficient whole-cell oxyfunctionalization processes, beside high biocatalyst activities, biocatalyst and thus process stability constitutes a crucial aspect. In order to assess the long-term performance of Syn6803\_CYP, the reaction system was amended with a glass container containing 1 mL of pure cyclohexane for continuous substrate supply via the gas phase (Figure 5.2 A).

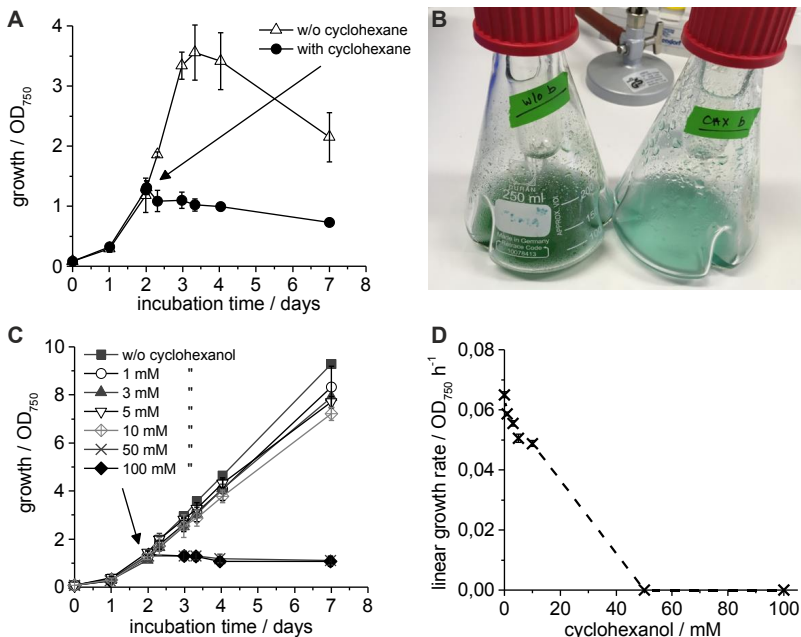


**Figure 5.2:** Long-term oxyfunctionalization by Syn6803\_CYP with cyclohexane supplied via the gas phase. The experiment was performed using freshly cultivated cells resuspended in 25 mL YBG11 (+NaHCO<sub>3</sub>, Km, IPTG) to a biomass concentration of ca  $1 \text{ g}_{\text{CDW}} \text{ L}^{-1}$  in 250 mL screw capped baffled shake flasks equipped with an open glass inlet (A). The reaction was started by adding 1 mL of pure cyclohexane into the glass inlet, followed by cultivation at  $30 \text{ }^\circ\text{C}$ , 150 rpm (2.5 cm amplitude), and  $150 \mu\text{E m}^{-2} \text{s}^{-1}$ . A) Figure adapted from Karande et al. (2016). B) Each data point represents average values of two biological replicates with standard deviations.

At a light intensity of  $150 \mu\text{E m}^{-2} \text{s}^{-1}$ , the cells showed similar cyclohexanol formation and thus initial specific activity ( $24.0 \pm 0.6 \text{ U g}_{\text{CDW}}^{-1}$  for cyclohexanol production) as obtained upon 5 mM cyclohexane addition (Figure 5.2 B, Table 5.1). In the setting applied, cyclohexanol formation was accompanied by overoxidation to cyclohexanone at a comparatively low rate ( $0.2 \pm 0.1 \text{ U g}_{\text{CDW}}^{-1}$ ). The hydroxylation activity remained constant for 2 h, then rapidly decreased, and was virtually lost after 5 h of reaction. This activity loss might have been caused by toxification or inhibition by the substrate cyclohexane and/or the product cyclohexanol. The final specific yield on biomass accounted for  $4.1 \pm 0.4 \text{ mmol g}_{\text{CDW}}^{-1}$ .

### 5.4.3 Cyclohexane provided via gas phase leads to toxification of *Synechocystis* sp. PCC 6803, which can be attenuated applying a two-liquid phase system

To evaluate the impact of cyclohexane and cyclohexanol on cyanobacterial viability, we investigated the growth behavior of *Synechocystis* sp. PCC 6803 carrying the empty vector pAH032 upon reactant exposure.

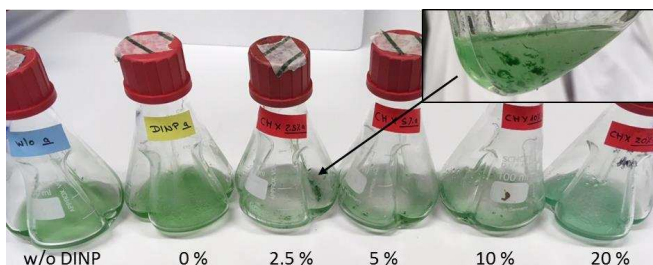


**Figure 5.3:** Impact of cyclohexane and cyclohexanol on *Synechocystis* sp. PCC 6803 (pAH032) (empty plasmid) growth. Cells were cultivated under standard cultivation conditions as described in the material and methods section. **A + B**) Cyclohexane toxicity: After 2 days (indicated by arrow), the cultures were harvested and resuspended in YBG11 medium (+ 50 mM NaHCO<sub>3</sub>). Aliquots of 25 mL were applied in 250 mL screw cap baffled shake flasks equipped with an open glass inlet containing 1 mL cyclohexane. **B**) Cultures after 7 days of incubation. Left flask: control without cyclohexane, right flask: with cyclohexane. **C + D**) Cyclohexanol toxicity: After 2 days (indicated by arrow), 1 - 100 mM cyclohexanol was added to the aqueous phase. **D**) Cell growth rates determined in the linear growth phase (days 2-7). Average values and standard deviations of two independent biological replicates are given.

The application of cyclohexane in saturating concentrations (via glass inlet, solubility in water: 650  $\mu$ M) completely inhibited cell growth and led to a culture color change from green to blue indicating the lysis of cyanobacterial cells (**Figure 5.3 A, B**) (Harada *et al.*, 2009). The product cyclohexanol inhibited cell growth at concentrations above 10 mM (**Figure 5.3 C, D**).

The maximum product concentration achieved with cyclohexane provided in the gas phase did not exceed 4 mM (**Figure 5.2 B**). These results point out that cyclohexane toxicity constitutes a critical factor limiting Syn6803\_CYP whole-cell biocatalyst stability.

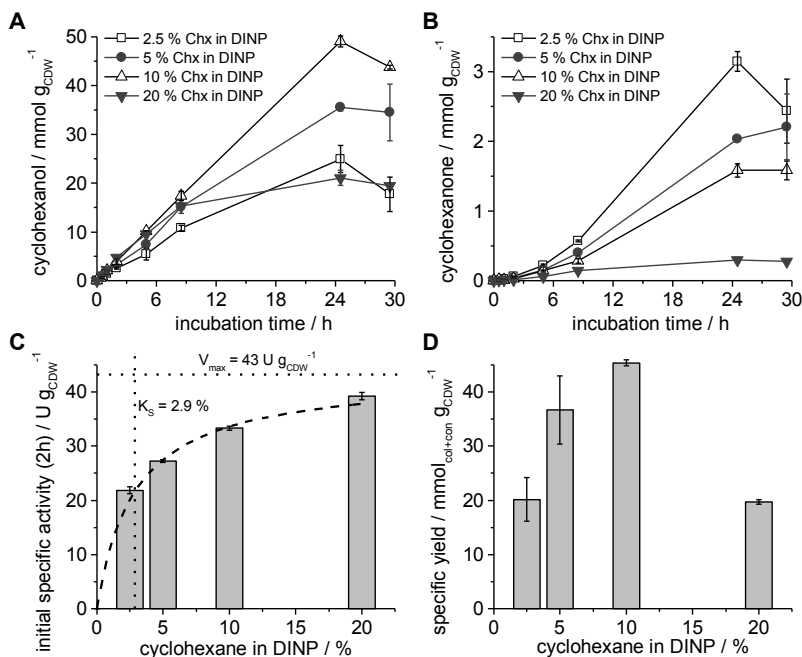
Substrate toxicity-related biocatalyst instability can be overcome via continuous substrate supply applying a feeding regime or a second liquid or solid phase. Respective concepts are widely established for heterotrophic strains to overcome mass transfer and toxicity issues (Hilker *et al.*, 2008; Schmörlzer *et al.*, 2012). The compatibility of the second liquid phase DINP with *Synechocystis* sp. PCC 6803 has successfully been demonstrated in our previous study enabling cell growth and stabilization of the whole-cell biotransformation of toxic nonanoic acid methyl ester (**Chapter 4**). The organic-aqueous partition coefficient  $P_{\text{org,aq}}$  for cyclohexane in a DINP/YBG11 two-liquid phase system was determined to be  $1775 \pm 214$  and can be considered appropriate for a 2-liquid phase biotransformation approach. Thus, the impact of cyclohexane dissolved in DINP on growth of *Synechocystis* sp. PCC 6803 containing the empty vector pAH032 was tested. Applying 2.5, 5, and 10% (v/v) of cyclohexane in DINP led to cell agglomeration (hindering  $OD_{750}$  determination) and to a visually observable increase in agglomerated biomass concentration (**Figure 5.4**). In contrast, 20% (v/v) of cyclohexane in DINP did not lead to such agglomeration and growth, but resulted in a culture color change from green to blue as observed before upon addition of cyclohexane via the gas phase. Overall, 2.5 - 10% (v/v) of cyclohexane in DINP appeared to constitute a feasible organic phase for two-liquid phase biotransformations.



**Figure 5.4:** Effect of cyclohexane dissolved in the organic carrier solvent DINP on cultures of *Synechocystis* sp. PCC 6803 (pAH032) (empty vector). Cells were cultivated under standard conditions for 2 days, before cultures were harvested and resuspended in YBG11 (+ 50 mM  $\text{NaHCO}_3$ ). Aliquots of 7.5 mL were applied in 100 mL screw capped baffled shake flasks. To each shake flask, 2.5 mL of DINP containing 0, 2.5, 5, 10, or 20% (v/v) cyclohexane were added, and cultivation was continued for another 5 days.

### 5.4.4 Two-liquid phase approach enhances biotransformation stability and the specific activity of Syn6803\_CYP

Next, the biocatalytic performance of Syn6803\_CYP in two-liquid phase systems was evaluated applying DINP phases containing 2.5, 5, 10, or 20% (v/v) cyclohexane at an organic:aqueous phase ratio of 1:3. The product formation performance was found to depend on the substrate concentration applied (**Figure 5.5 A, B**). The initial specific activity was constant for 2 h in all cases and increased with increasing substrate concentration (**Figure 5.5 C**).



**Figure 5.5:** Two-liquid phase biotransformation of cyclohexane using Syn6803\_CYP in shaking flasks. After 2 days of cultivation under standard conditions, oxygenase gene expression was induced by adding 2 mM IPTG, and cultivation was continued for 1 day. Then, cells were harvested, resuspended in YBG11 (NaHCO<sub>3</sub>, Km, IPTG) to a biomass concentration of ca. 1 g<sub>CDW</sub> L<sup>-1</sup>, and applied in aliquots of 18.75 mL in 250 mL screwed capped baffled shake flasks. Biotransformations were performed at 30 °C, 150 rpm (2.5 cm amplitude), and 150 μE m<sup>-2</sup> s<sup>-1</sup> and were started by adding 6.25 mL DINP containing 2.5, 5, 10, or 20% (v/v) cyclohexane. After phase separation, cyclohexanol and cyclohexanone concentrations were determined in the organic phase. Aqueous concentrations were calculated based on the separately determined partitioning coefficients P<sub>org:aq</sub> for cyclohexanol (2.1 ± 0.1) and cyclohexanone (4.4 ± 0.7). Average values and standard deviations of two biological replicates are given.

The highest specific activity of  $39.2 \pm 0.7 \text{ U g}_{\text{CDW}}^{-1}$  was observed with 20% (v/v) cyclohexane in DINP, being 1.5 times higher than the activity obtained without organic carrier solvent (**Table 5.1**). This indicated an enhanced substrate mass transfer possibly via a direct contact of the cells with organic phase droplets (Bühler *et al.*, 2006; Park *et al.*, 2006) or substrate toxicity/inhibition in the absence of an organic phase. High cyclohexane levels led to impaired biocatalyst stability resulting in a comparatively low specific product (cyclohexanol + cyclohexanone) yield on biomass (**Figure 5.5 D**). The highest specific yield on biomass ( $45.4 \pm 0.5 \text{ mmol g}_{\text{CDW}}^{-1}$ ) was obtained using 10% (v/v) cyclohexane in DINP, constituting a 10 times increase compared to the single phase biotransformation (**Table 5.1**).

With increasing cyclohexane concentrations, cyclohexanol over-oxidation decreased indicating a competition of cyclohexane and cyclohexanol for the active site of the oxygenase (**Figure 5.5 B**). The initial specific whole-cell activity exhibited a Michaelis-Menten-type dependency on the cyclohexane concentration applied, with an apparent  $V_{\text{max}}$  of  $43.2 \pm 2.2 \text{ U g}_{\text{CDW}}^{-1}$  and an apparent  $K_{\text{S}}$  of  $2.9 \pm 0.5\%$  (v/v) cyclohexane in DINP. These kinetic characteristics of the whole-cell photobiocatalyst can be considered highly promising for technical scale biotransformations in photobioreactors.

### 5.4.5 Non-aerated bioprocessing facilitates gram-scale hydroxylation of cyclohexane in a stirred tank photo-bioreactor

After successful stabilization of the cyclohexane oxyfunctionalization reaction, scaling from shake flasks to a stirred tank photo-bioreactor was conducted. For this purpose, cells were cultivated and induced in photobioreactors containing 3 L YBG11 medium, followed by harvesting and resuspension in 1.2 L YBG11 (+  $\text{NaHCO}_3$ ). The reaction was started by adding 0.4 L DINP containing 5% (v/v) cyclohexane to the photo-bioreactor setup aerated with compressed air. Within the first 5 h of reaction time, the specific cyclohexane oxyfunctionalization rate of  $24.6 \pm 0.4 \text{ U g}_{\text{CDW}}^{-1}$  was similar to that obtained in shake flasks, proving scalability to stirred tank photo-bioreactor setups (**Figure 5.6 A**). However, after 5 h of biotransformation, the biocatalyst activity started to decrease, resulting in a specific yield on biomass of  $18 \text{ mmol g}_{\text{CDW}}^{-1}$  after 24 h of reaction, half of the value achieved in shake flask experiments (**Table 5.1**). The partition coefficients for all reactants were similar to those determined in shake flasks and small reaction tubes (**Figure 10.14**, **Table 10.1**). Although the aeration rate of  $0.15 \text{ L min}^{-1}$  was low, the substrate steadily evaporated over time, resulting in continuously decreasing substrate concentrations in both organic and aqueous phases. According to the cyclohexane hydroxylation kinetics estimated for the two-liquid phase system (**Figure 5.5 C**), this decreasing substrate concentration can be considered the cause for the decrease in specific activities. In addition, degassing of  $\text{CO}_2$  originating from the dissolved  $\text{NaHCO}_3$  leads to a pH increase (**Figure 10.15 A**), which may have contributed to the activity decrease.



**Table 5.1:** Process data obtained from biotransformation experiments using Syn6803\_CYP in shake flasks and stirred tank photo-bioreactors.

Biotransformation condition	Chx in org phase <sup>a</sup> / M	Chx in aq phase <sup>a</sup> / $\mu\text{M}$	Initial specific activity (2h) <sup>b</sup> / $\text{U g}_{\text{CDW}}^{-1}$	Specific yield / $\text{mmol}_{\text{Col+Cone}} \text{g}_{\text{CDW}}^{-1}$	Overoxidation / % <sub>Cone</sub> in product
<u>Shake flask</u>					
5 mM Chx	-	88 <sup>c</sup>	23.7 $\pm$ 0.5 <sup>e</sup>	-	~ 10
Chx via gas phase	-	654 <sup>d</sup>	24.0 $\pm$ 0.6	4.1 $\pm$ 0.4	0.7 $\pm$ 0.1
2.5% (v/v) Chx in DINP	0.23	131	21.9 $\pm$ 0.6	20.2 $\pm$ 4.0	12.1 $\pm$ 0.1
5% (v/v) Chx in DINP	0.46	261	27.2 $\pm$ 0.3	36.7 $\pm$ 6.3	6.0 $\pm$ 0.3
10% (v/v) Chx in DINP	0.93	522	33.3 $\pm$ 0.3	45.4 $\pm$ 0.5	3.5 $\pm$ 0.3
20% (v/v) Chx in DINP	1.85	654 <sup>d</sup>	39.2 $\pm$ 0.7	19.7 $\pm$ 0.4	1.4 $\pm$ 0.1
<u>Photo-bioreactor</u>					
5% (v/v) Chx in DINP, with aeration	0.38 $\rightarrow$ 0.06	273 $\rightarrow$ 32	26.3 $\pm$ 0.6	20.0 $\pm$ 0.5	9.3 $\pm$ 0.1
5% (v/v) Chx in DINP, w/o aeration	0.42 $\rightarrow$ 0.34	150 $\rightarrow$ 244	34.9 $\pm$ 0.3	49.4 $\pm$ 0.3	4.6 $\pm$ 0.1

Chx = cyclohexane, Col = cyclohexanol, Cone = cyclohexanone.

<sup>a</sup> For shake flask experiments, theoretical numbers based on the molarity of 9.27 M for pure cyclohexane and its partition coefficient of  $P_{\text{org:aq}} = 1775$  in the DINP-YBG11 system are given.

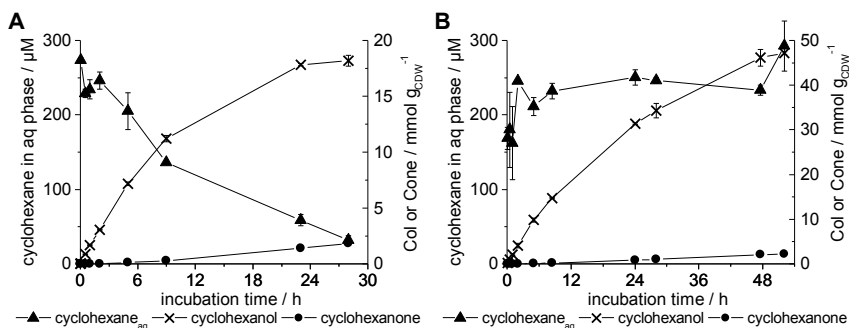
<sup>b</sup> The specific activity given is based on the cyclohexanol and cyclohexanone concentrations determined in both phases.

<sup>c</sup> Concentrations calculated based on Henry coefficient for cyclohexane (0.15 atm m<sup>3</sup> mol<sup>-1</sup>) and the gas:aq phase ratio of 9:1.

<sup>d</sup> The value for the solubility of cyclohexane in water is given (McAuliffe, 1966).

<sup>e</sup> The specific activity in the first 10 min of reaction is given.

To stabilize the substrate availability throughout the biotransformation, a bioreactor experiment without aeration was performed. Surrendering aeration indeed stabilized pH and cyclohexane concentrations in both phases, while the oxygen partial pressure stayed well above 100% of saturation during the entire process (**Figure 10.15 B**). The productive biotransformation time was significantly prolonged with a slow activity decrease up to 52 h, resulting in a specific yield of nearly 50 mmol g<sub>CDW</sub><sup>-1</sup> (**Figure 5.6 B**, **Table 5.1**). The final product titer of 31.5 ± 0.3 and 11.5 ± 0.1 mM in the organic and aqueous phases, respectively, resulted in a total product amount of 2.6 g cyclohexanol. These results clearly emphasize the scalability of the process, whereby the handling of the volatile substrate cyclohexane is simplified by *in situ* O<sub>2</sub> supply via photosynthetic water oxidation.



**Figure 5.6:** Two-liquid phase biotransformation of cyclohexane using Syn6803\_CYP in a stirred-tank photo-bioreactor with (A) and without (B) aeration. Cells were applied at a concentration of 0.8 (A) and 0.5 g<sub>CDW</sub> L<sup>-1</sup> (B) in YBG11 (+ NaHCO<sub>3</sub>, Km, IPTG) as described in the materials in methods section. Biotransformations were performed at 30 °C, 150 μE m<sup>-2</sup> s<sup>-1</sup>, 300 rpm agitation, and 0.15 L min<sup>-1</sup> aeration with compressed air (only for A), using 1.2 L aqueous cell suspension and 0.4 L organic phase consisting of 5% (v/v) cyclohexane in DINP. Col = cyclohexanol, Cone = cyclohexanone.

## 5.5 Discussion

Cyclohexanol is a key synthon mostly used in the production of polymer building blocks such as ε-caprolactone, ε-caprolactam, and adipic acid with an annual production in the million tons range (Schuchardt *et al.*, 1993; Weissermel and Arpe, 2008). However, the chemical synthesis of cyclohexanol is still challenging because of low selectivities (Schuchardt *et al.*, 2001). Biocatalysis provides an interesting alternative for the oxidation of cyclohexane providing high selectivities under mild conditions. In 2014, Salamanca *et al.* isolated the strain *Acidovorax* sp. CHX100, capable of growing on cyclohexane as sole carbon source, from a wastewater plant (Salamanca and Engesser, 2014). Characterization of this strain and subsequent recombinant gene overexpression in *Pseudomonas taiwanensis* VLB120 led to the identification of a novel cytochrome P450 monooxygenase system, which efficiently

catalyzes the oxidation of cyclohexane to cyclohexanol (Karande *et al.*, 2016a; Salamanca *et al.*, 2015).

### 5.5.1 Light dependency

In this study, we present the cyanobacterium *Synechocystis* sp. PCC 6803 as an efficient alternative host system enabling light-driven cytochrome P450 catalysis, i.e., cyclohexane oxyfunctionalization, with water as cheap and readily available source for reduction equivalents and O<sub>2</sub>. Thereby, such light-driven oxyfunctionalization profits from the efficient electron supply via the photosynthetic electron transport chain to ferredoxin and NADP<sup>+</sup> (Wilhelm and Selmar, 2011; Wilhelm and Wild, 1984). This is in contrast to photosynthesis-driven production of chemicals such as ethanol or lactate from CO<sub>2</sub>, which suffers from the low rate of CO<sub>2</sub> fixation by RuBisCO (Bathellier *et al.*, 2018; Knoot *et al.*, 2018). Overall, efficient coupling of redox enzymes with the photosynthetic light reaction enables high oxyfunctionalization rates that compete with or even outperform established heterotrophic biocatalysts (**Chapter 7**). With its electron transfer components ferredoxin and ferredoxin reductases, the CYP450 enzyme system applied in this study in principle depends on NADH as electron donor. However, not NADH but NADPH is the primary carrier of activated electrons produced in the photosynthetic light reaction. This discrepancy together with the high oxyfunctionalization rate obtained and its strong light-dependency indicates trapping of activated electrons directly from the photosynthetic electron transport chain via native or *Acidovorax* ferredoxin or from NADPH via native ferredoxin reductase. This electron transfer appears to be quite efficient given the comparatively high specific oxygenation activities achieved rivaling those reached with heterotrophic host strains (Schrewe *et al.*, 2013). Efficient integration of heterologous enzyme systems into photosynthetic redox metabolism by adjusting the electron transferring pathways represents an important research field for the development of efficient photobiocatalytic processes (Khanna and Lindblad, 2015; Lassen *et al.*, 2014b).

### 5.5.2 Reactant toxicity

Next to biocatalyst design, the physicochemical properties of reactants often constrain the biocatalytic process performance and necessitate an adequate bioprocess design (Kim *et al.*, 2007; Willrodt *et al.*, 2015b). In this study, the applied substrate cyclohexane and the product cyclohexanol feature logP<sub>OW</sub> values (logarithm of the partition coefficient in an octanol/water mixture) of 3.4 and 1.2, respectively. It has been shown that chemical compounds with logP<sub>OW</sub> values between 2 and 4 typically are toxic to microorganisms (Laane *et al.*, 1987; Sikkema *et al.*, 1994). These compounds damage bacterial membrane integrity, resulting in the impairment of microbial activity. Membrane permeabilization-induced loss of biocatalytic activity upon cyclohexane exposure has been reported, e.g., for the typically solvent-tolerant

strain *Pseudomonas taiwanensis* VLB120 (Karande *et al.*, 2016a) and thus constitutes a key aspect for the photobiocatalytic reaction system investigated in this study. Via *in situ* substrate supply by means of a two-liquid phase system, the substrate concentration was kept below 654  $\mu\text{M}$ , which can be considered critical according to the empirical considerations reported by Sikkema *et al.* 1994 and Kratzer *et al.* 2015 for microbial cell toxification by hydrophobic substances (Kratzer *et al.*, 2015; Sikkema *et al.*, 1994). Thus, growth as well as the cyclohexane hydroxylation activity of Syn6803\_CYP were stabilized by overcoming cell toxification.

### 5.5.3 Substrate volatility

During scale-up from shake flask to the stirred tank photo-bioreactor, a second physicochemical property of the substrate, namely its high volatility, constrained process durability. At a low aeration rate of 0.1 vvm, cyclohexane continuously evaporated from the reaction system and thus became the factor limiting the bioconversion rate and the final product yield. By omitting aeration, cyclohexane loss was largely avoided, enabling an increase of the biomass-specific product yield by a factor of 2.5 (Figure 5.6, Table 5.1). Such process management was possible, as  $\text{O}_2$  together with activated electrons, both key substrates for the oxyfunctionalization reaction, was continuously provided via photosynthetic water oxidation (Chapter 3). In conclusion, the use of a cyanobacterial host strain enables oxygenase catalysis without aeration and thus the efficient conversion of a volatile substrate.

### 5.5.4 Productivity

The production of fine-chemicals at industrially relevant scales necessitates productivities of at least 1 - 10  $\text{g L}^{-1} \text{h}^{-1}$  (Straathof *et al.*, 2002). With an average productivity of 0.04  $\text{g L}^{-1} \text{h}^{-1}$ , the reaction system developed in this study requires further improvement by a factor of at least 25. Comparison of process parameters of the Syn6803\_CYP-based whole-cell biotransformation of cyclohexane with an established *E. coli* driven process for the epoxidation of styrene reveals that the biotransformation durability of 52 h and the product yield on biomass with 4.9  $\text{g g}_{\text{CDW}}^{-1}$  are already valuable (Table 5.2) (Kuhn *et al.*, 2010b). In addition, hydroxylation coupled to the metabolism of the heterotrophic host strains depends on an organic compound such as glucose as source of reduction equivalents, representing a significant environmental and cost factor (Kuhn *et al.*, 2012b; Kuhn *et al.*, 2010b). Photosynthesis-driven processes make use of inexpensive carbon ( $\text{CO}_2$ ) and electron ( $\text{H}_2\text{O}$ ) sources for biocatalyst and product synthesis and thus augur well for the development of economically viable processes involving redox chemistry for the production of chemicals and fuels. The specific cyclohexane oxyfunctionalization rates obtained here were equal or even higher than those reported for *Pseudomonas* sp. VLB120 harboring the very same CYP enzyme system (24.0 and 39  $\text{U g}_{\text{CDW}}^{-1}$  in aqueous and 2-liquid phase systems, respectively,

**Table 5.2:** Comparison of process performance parameters of photosynthesis- or heterotrophically driven biocatalytic oxyfunctionalizations and possible improvement strategies for the biotransformation catalyzed by Syn6803\_CYP.

Parameter	Syn6803_CYP <sup>a</sup>	<i>E. coli</i> JM101 (pSPZ10) <sup>b</sup>	Possible improvement strategies for Syn6803_CYP
Volume aq phase / L	1.2	1	Scaling
Volume org phase / L	0.4	1	Scaling
Substrate in org phase	5% Chx in DINP	8% styrene in BEHP	-
Maximum specific activity / U g <sub>CDW</sub> <sup>-1</sup>	34.9 ± 0.3	60	Increase of oxygenase expression levels, improved coupling to electron transport chain
Applied biomass concentration / g <sub>CDW</sub> L <sup>-1</sup>	0.5	5.4 – 39.3	Prolonged growth phase, improvement of growth conditions (CO <sub>2</sub> , light)
Durability / h	52	8	-
Glucose consumed / g	-	113.7	-
Average productivity / g L <sub>aq</sub> <sup>-1</sup> h <sup>-1</sup>	0.04	11.08	Increase of biomass concentration, increase of specific activity
Specific yield / g g <sub>CDW</sub> <sup>-1</sup>	4.9	1.85	Continuous bioprocessing
Titer / g L <sub>aq</sub> <sup>-1</sup>	2.2	72.6	Increase of biomass concentration
Total product / g	2.6	72.6	Scaling

aq = aqueous, org = organic, U =  $\mu\text{mol min}^{-1}$ , CDW = cell dry weight, Chx = cyclohexane, BEHP = bis(2-ethylhexyl)phthalate.

<sup>a</sup> this study; <sup>b</sup> *E. coli* JM101 catalyzing the oxyfunctionalization of styrene to styrene oxide (Kuhn *et al.*, 2010b)

vs. 20-25 U g<sub>CDW</sub><sup>-1</sup> in *P. taiwanensis* VLB120, Karande *et al.* 2016). However, the specific biocatalyst activity and especially the cell concentration in bioreactor settings still require engineering efforts (see possible improvement strategies in **Table 5.2**). The cultivation of cyanobacteria at cell densities of up to 50 g<sub>CDW</sub> L<sup>-1</sup> is possible using systems with enhanced CO<sub>2</sub> and light supply (Apel *et al.*, 2017; Bähr *et al.*, 2016; Dasgupta *et al.*, 2010). With the reaction system developed in this study (39 U g<sub>CDW</sub><sup>-1</sup>), such a cell concentration would already enable a cyclohexanol productivity of ~ 12 g L<sup>-1</sup> h<sup>-1</sup>. Further increase in productivity may be achieved by enhancing the specific oxyfunctionalization activities. An enoate reductase has been shown to trap electrons derived from the photosynthetic metabolism at a rate of up to 123 U g<sub>CDW</sub><sup>-1</sup> (Köninger *et al.*, 2016). In theory, the photosynthetic light reaction provides activated reduction equivalents at high rates of up to 850 U g<sub>CDW</sub><sup>-1</sup> (assumptions: k<sub>cat</sub> of PSII: 1000 s<sup>-1</sup>, 1% PSII g<sub>CDW</sub><sup>-1</sup>, 350 kDa) (Dismukes *et al.*, 2009; Shen, 2015). With this high specific activity and a biomass concentration of 50 g<sub>CDW</sub> L<sup>-1</sup>, productivities of ~ 255 g L<sup>-1</sup> h<sup>-1</sup> are in theory possible and illustrate the potential of phototrophic organisms as hosts for hosts for oxyfunctionalization biocatalysis.

### 5.5.5 Scalability

For the development of eco-efficient bioprocesses, high productivities have to be accomplished at scale. In this study, a scale-up evaluation was performed based on the established stirred-tank bioreactor concept. Especially the generation of excess O<sub>2</sub> during biotransformation without aeration, effecting a pO<sub>2</sub> between 100 and 150% of air saturation throughout the entire process time, demonstrates the high capacity and suitability of photosynthetic biocatalysts for oxyfunctionalization bioprocesses, especially for those involving volatile substrates. However, efficient light supply constitutes a big challenge and a possible limitation for the further scaling of the stirred-tank bioreactor setup. To achieve high cell concentrations and thus high productivities, light intensities have to be increased, and/or additional light sources have to be installed within the reactor system. Alternatively, other reactor concepts such as biofilm-based capillary reactors can be applied (David *et al.*, 2015). Capillary reactors enable the establishment of a high irradiation surface area to volume ratio, facilitate continuous bioprocessing, and thus constitute a promising technology for photosynthesis-driven bioprocesses.

### 5.6 Conclusions

Photosynthetic water oxidation catalyzed by photoautotrophic microorganisms encompasses a high potential for efficient biocatalytic oxyfunctionalization, providing activated reduction equivalents as well as O<sub>2</sub> at high rates. The present study reports on the establishment of a recombinant CYP450 harboring cyanobacterium enabling an unprecedentedly high light-driven oxyfunctionalization activity. The specific cyclohexane hydroxylation rates achieved

compare well to those of established heterotrophic strains. Further, the two-liquid phase concept enabled stable bioprocessing for 52 h, and *in situ* O<sub>2</sub> generation allowed for a non-aerated process operation mode and thus gram-scale production of cyclohexanol from the volatile substrate cyclohexane. The reported concepts for biocatalyst and process engineering augur well for the future application of cyanobacteria for the ecologically as well as economically remunerative production of fine and even bulk chemicals via biotransformation reactions.

### **5.7 Acknowledgments**

The authors are grateful for using the facilities of the Centre for Biocatalysis (MiKat) at the Helmholtz Centre for Environmental Research which is supported by European Regional Development Funds (EFRE -Europe funds Saxony) and the Helmholtz Association.





## **Chapter 6 Super-high cell density cultivation of *Synechocystis* sp. PCC 6803 in a mixed-trophies biofilm-based capillary reactor**

Ingeborg Heuschkel performed biofilm experiments for the assessment of Syn6803\_CYP catalytic activities. Katja Bühler, Rohan Karande, Bruno Bühler and Andreas Schmid coordinated the project and corrected the manuscript.

Parts published in:

*Bioresource Technology*, **2019**, 282, 171 - 178

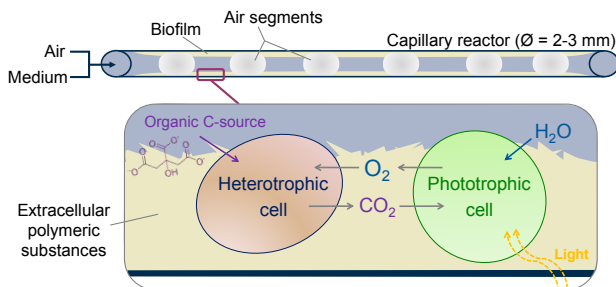
### **6.1 Abstract**

Cultivation of photoautotrophic organisms at high cell densities for photobiocatalytic applications still challenges the reactor and photobioprocess design. Reactor technologies providing high surface to volume ratios, such as biofilm-coated capillary reactors, are considered highly promising as they facilitate efficient light input and thus cell growth. However, in enclosed reactor systems O<sub>2</sub> accumulates to high concentrations in the course of oxygenic photosynthesis, leading to oxidative stress and cell growth inhibition. In this study, we present an improved cultivation concept based on the co-cultivation of the photoautotrophic strain *Synechocystis* sp. PCC 6803 with the chemoheterotrophic O<sub>2</sub>-respiring organism *Pseudomonas* sp. VLB120 in a biofilm-based capillary reactor. The chemoheterotrophic organism facilitated enhanced cyanobacterial surface coverage and reduced oxidative stress by the respiration of O<sub>2</sub>. Eventually, the mixed-trophies cultivation technology enabled growth of cyanobacterial biofilms to super-high cell densities of up to 48 g<sub>BDW</sub> L<sup>-1</sup> and was demonstrated to be accessible for the biocatalytic oxyfunctionalization of hydrocarbons.

## 6.2 Introduction

The application of photoautotrophic organisms for biocatalytic purposes constitutes a promising technology for the eco-efficient production of fuels and value-added chemicals. In contrast to chemoheterotrophic organisms, phototrophic microorganisms such as algae and cyanobacteria rely on water, light, and CO<sub>2</sub> as abundant sources for electrons, energy, and carbon, respectively. Yet, the cultivation of photobiocatalysts at high cell densities (HCD) still challenges the reactor and bioprocess design (Lima-Ramos *et al.*, 2014). Reactor technologies providing high surface to volume ratios, such as capillary reactors (Karande *et al.*, 2014; Wohlgemuth *et al.*, 2015), are highly promising for the cultivation of HCD phototrophic organisms, as they facilitate efficient light input and distribution. Applying the microbial catalyst in a biofilm format further exploits this technology, featuring self-immobilization, regeneration and high biomass retention and allowing a continuous process operation (Halan *et al.*, 2012; Rosche *et al.*, 2009). The capillary biofilm-based reactor concept was already successfully applied to heterotrophic microorganisms and was recently adapted to the cultivation of the cyanobacterium *Synechocystis* sp. PCC 6803 (David *et al.*, 2015). However, as a consequence of photosynthetic water oxidation, cultivation of photoautotrophic organisms in enclosed reactor setups quickly becomes hampered by the local supersaturation of oxygen in the system (Huang *et al.*, 2017; Weissman *et al.*, 1988). Such growth inhibiting effects were also observed for the biofilm-based cultivation of *Synechocystis* sp. PCC 6803 by David *et al.* 2015. Thus, the stable cultivation of HCD photoautotrophic organisms in the capillary biofilm reactor necessitates solutions to extract excess oxygen from the liquid phase. Technical approaches aim at the elimination of supersaturated O<sub>2</sub> concentrations by facilitating gas exchange from the aqueous medium to the gaseous environment (Weissman *et al.*, 1988). In that line, the insertion of air segments into the constant medium flow of the cyanobacterial-coated capillary reactor (**Figure 6.1 top**) most likely also stabilized the biofilm development of *Synechocystis* sp. PCC 6803 in David *et al.* 2015.

In this communication, we present an alternative and biologically-inspired concept to reduce aqueous phase oxygen concentrations by the co-cultivation of a chemoheterotrophic O<sub>2</sub>-respiring organism (*Pseudomonas* sp. VLB120). The use of two microbial species with complementary metabolic activities results in an O<sub>2</sub>-optimized microenvironment and thus reduced oxidative stress to the cells (**Figure 6.1 bottom**). Eventually, the mixed-trophies biofilm-based capillary reactor setting enables the retention of super-high biomass. Furthermore, the HCD cultivation system allows the biotechnological application of recombinant photobiocatalysts for the light-driven oxyfunctionalization of cyclohexane.



**Figure 6.1:** *Top:* Scheme of a segmented-flow capillary reactor. *Bottom:* Basic principle of proto-cooperation between two microbial species with complementary metabolic activities (chemoheterotrophic and photoautotrophic). Cells of both species are embedded in extracellular polymeric substances and form a three-dimensional biofilm on the inner surface of the capillary. O<sub>2</sub> respiration rates (chemoheterotrophic strain) and O<sub>2</sub> evolution rates (photoautotrophic strain) could balance the O<sub>2</sub> environment.

### 6.3 Materials and methods

**Chemicals and bacterial strains.** Chemicals, construction and cloning of plasmids and strains used in this study are described in **Chapter 2**. *Synechocystis* sp. PCC 6803 and *Pseudomonas* sp. VLB120 harboring the empty expression plasmid pAH032 contain a kanamycin resistance cassette and are hereinafter referred to as Syn6803\_Km and Ps\_Km. *Synechocystis* sp. PCC 6803 and *Pseudomonas* sp. VLB120 harboring pAH050 contain a cyclohexane monooxygenase CYP enzyme system and are hereinafter referred to as Syn6803\_CYP and Ps\_CYP. *Synechocystis* sp. PCC 6803 harboring pAH042 contain the alkane monooxygenase system AlkBGT and is hereinafter referred to as Syn6803\_BGT. *Pseudomonas* sp. VLB120 harboring pAH049 contains a cyclohexanone Baeyer-Villiger monooxygenase and is hereinafter referred to as Ps\_BVMO.

**Pre-cultivation of *Synechocystis* sp. PCC 6803 strains.** Cells were grown in YBG11 medium supplemented with 50 mM NaHCO<sub>3</sub> (see medium composition below). Pre-cultures were inoculated in 20 mL medium in a 100 mL baffled shake flask using 200 µL of cryo-stock and cultivation was carried out at 30 °C, 50 µE m<sup>-2</sup> s<sup>-1</sup> (LED), ambient CO<sub>2</sub> (0.04%), 150 rpm (2.5 cm amplitude), and 75% humidity in an orbital shaker (Multitron Pro shaker, Infors, Bottmingen, Switzerland) for 4 days. From this pre-culture, main-cultures were inoculated starting with an OD<sub>750</sub> of 0.08 and cultivation was continued for another 4 days.

**YBG11 medium composition (50 mM NaHCO<sub>3</sub>, w/o citrate):** 1.49 g L<sup>-1</sup> NaNO<sub>3</sub>, 0.074 g L<sup>-1</sup> MgSO<sub>4</sub> · 7 H<sub>2</sub>O, 0.031 g L<sup>-1</sup> K<sub>2</sub>HPO<sub>4</sub>, 10 mL L<sup>-1</sup> YBG11 trace elements (100x), 0.019 g L<sup>-1</sup> Na<sub>2</sub>CO<sub>3</sub>, 50 mM HEPES (pH 7.2); YBG11 trace elements (100x): 3.6 g L<sup>-1</sup> CaCl<sub>2</sub> · 2 H<sub>2</sub>O, 0.28 g L<sup>-1</sup> boric acid, 0.11 g L<sup>-1</sup> MnCl<sub>2</sub> · 4 H<sub>2</sub>O, 0.02 g L<sup>-1</sup> ZnSO<sub>4</sub> · 7 H<sub>2</sub>O, 0.039 g L<sup>-1</sup>

$\text{Na}_2\text{MoO}_4 \cdot 2 \text{H}_2\text{O}$ ,  $0.007 \text{ g L}^{-1}$   $\text{CuSO}_4 \cdot 5 \text{H}_2\text{O}$ ,  $0.005 \text{ g L}^{-1}$   $\text{Co}(\text{NO}_3)_2 \cdot 6 \text{H}_2\text{O}$ ,  $0.16 \text{ g L}^{-1}$   $\text{FeCl}_3 \cdot 6 \text{H}_2\text{O}$ ,  $0.6 \text{ g L}^{-1}$   $\text{Na}_2\text{EDTA} \cdot 2 \text{H}_2\text{O}$ ,  $4.2 \text{ g L}^{-1}$   $\text{NaHCO}_3$  (Shcolnick *et al.*, 2007).

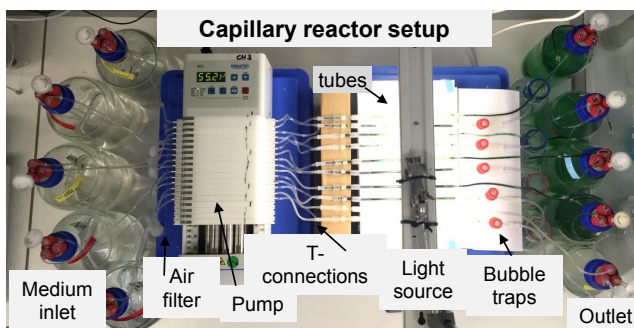
**Pre-cultivation of *Pseudomonas* sp. VLB120 strains.** Overnight cultures were inoculated from a cryo-stock using 5 mL LB medium and grown at  $30^\circ\text{C}$  and 200 rpm (2.5 cm amplitude) in an orbital shaker (Multitron Pro shaker, Infors, Bottmingen, Switzerland) (Sambrook and Russell, 2001). Pre-cultures were inoculated by adding 200  $\mu\text{L}$  of this overnight-culture to 20 mL M9 medium ( $5 \text{ g L}^{-1}$  citrate, US\* trace elements) and growth was continued for 24 h (Emmerling *et al.*, 2002). Main-cultures were cultivated for 8 h in 50 mL M9 medium ( $5 \text{ g L}^{-1}$  citrate, US\* trace elements) in 250 mL baffled shake flasks starting with an  $\text{OD}_{450}$  of 0.2.

**Pre-mixing of bacterial strains.** 20 mL of each main culture (*Synechocystis* sp. PCC 6803, *Pseudomonas* sp.VLB120) were centrifuged (5000g, rt, 7 min), washed with 20 mL YBG11 and resuspended in 40 mL YBG11 medium. Optical densities after resuspension were  $\text{OD}_{750} = 2.2$  and  $\text{OD}_{450} = 2.4$ , respectively. 10 mL of *Synechocystis* sp. PCC 6803 were mixed with 10 mL of *Pseudomonas* sp. VLB120 in a 100 mL baffled shake flask and cultivation was continued at  $30^\circ\text{C}$ ,  $50 \mu\text{E m}^{-2} \text{ s}^{-1}$  (LED), ambient  $\text{CO}_2$  (0.04%), 150 rpm (2.5 cm amplitude), and 75% humidity in an orbital shaker (Multitron Pro shaker, Infors, Bottmingen, Switzerland) for 24 h. Single species control cultures were mixed with 10 mL of YBG11 medium.

**Technical setting of the capillary reactor system.** For biofilm cultivation, a capillary reactor system adapted from David *et al.* 2015 was applied (**Figure 6.2**) (David *et al.*, 2015). Serological pipettes functioned as capillaries for biofilm growth (1 mL, trimmed to a capillary volume of 1.2 mL by cutting the tip and the intake area; inner diameter of 3 mm, 16.6 cm length, Labsolute, Th. Geyer GmbH & Co. KG, Renningen, Germany). YBG11 medium (supplemented with 50 mM  $\text{NaHCO}_3$ , with or without  $0.4 \text{ g L}^{-1}$  citrate) was supplied via Tygon tubing (LMT-55, 2.06 mm inner diameter, 0.88 mm wall thickness; Ismatec, Wertheim, Germany) using a peristaltic pump (ISM939D; Ismatec, Wertheim, Germany). Air segments were supplied via Tygon tubing connected by a T-connector to the capillary reactor system. Injection ports were introduced in front of the capillaries for inoculation using a syringe. Fluorescence-light tubes were used as light source ( $50 \mu\text{E m}^{-2} \text{ s}^{-1}$  measured at the center of capillaries) with a light spectrum shown in **Chapter 2**. Gas exchange at medium inlet, for air segments, and at medium outlet was enabled through sterile filters ( $0.2 \mu\text{m}$ ). Cultivation was performed at rt ( $\sim 26^\circ\text{C}$ ).

**Inoculation of the capillary reactor system.** The capillaries of the reactor system were inoculated with single- and mixed-species cultures, respectively, by purging ca. 5 mL of each culture through the injection port. Medium flow was started 15 – 24 h after inoculation at a

rate of  $\sim 55 \mu\text{L min}^{-1}$ . If indicated, air segments were introduced 9 days after inoculation at a rate of  $\sim 55 \mu\text{L min}^{-1}$ , resulting in an increased overall flow rate of  $\sim 110 \mu\text{L min}^{-1}$  in these capillaries.



**Figure 6.2:** Technical setup of the capillary reactor system.

**O<sub>2</sub> quantification in gas and in liquid phase.** For O<sub>2</sub> gas analysis of air segments, bubble traps (sealed with a septum) were introduced downstream of capillaries one day before measurement to enable gas equilibrium. 100  $\mu\text{L}$  of gas phase were sampled from the bubble trap using a gas-tight syringe (Hamilton Company, Reno, Nevada, USA) and O<sub>2</sub> was quantified using gas chromatography (GC Trace 1310, Thermo Fisher Scientific, Waltham, USA) equipped with a TG-BOND Msieve 5A capillary column (30 m, I.D.: 0.32 mm, film thickness: 30  $\mu\text{m}$ , ThermoFisher Scientific, Waltham, USA) and a thermal conductivity detector (TCD) operating at 100  $^{\circ}\text{C}$  with a filament temperature of 300  $^{\circ}\text{C}$ , and a reference gas flow of 4  $\text{mL min}^{-1}$ . Argon gas was applied as carrier gas with a constant flow of 5  $\text{mL min}^{-1}$ . The injection temperature was set to 50  $^{\circ}\text{C}$  and a split ratio of 2 was applied. The oven temperature was kept constant at 35  $^{\circ}\text{C}$  for 3 min. O<sub>2</sub> concentrations in the liquid medium were quantified using a Clark-type flow-through sensor (OX-500 Oxygen Microsensor, Unisense, Aarhus, Denmark) equipped with a microsensor amplifier (Microsensor multimeter, Unisense, Aarhus, Denmark).

**Quantification of citrate concentration in the liquid phase using HPLC.** Samples were collected from the capillary outlet, centrifuged (17000g, 5 min, rt), and the supernatant was applied for high pressure liquid chromatography (Dionex Ultimate 300, Thermo Fisher Scientific, Waltham, USA) equipped with a ligand exchange column (HyperREZ XP Carbohydrate H+, 30 cm length, 7.7 mm diameter, 8  $\mu\text{m}$  particle size, ThermoFisher Scientific, Waltham, USA) and a variable wavelength detector operating at 210 nm. The column oven temperature was kept constant at 40  $^{\circ}\text{C}$ . 16 mM H<sub>2</sub>SO<sub>4</sub> was applied as carrier solvent at a flow rate of 0.75  $\text{mL min}^{-1}$ .

**Syn6803\_CYP activity measurement in the Syn6803\_CYP + Ps\_CYP mixed-species biofilm setup.** *CYP* gene expression was induced 36 days after inoculation by the addition of 2 mM IPTG to the supplied YBG11 medium. At day 37, cyclohexane was delivered in saturating concentrations via air and medium phase. For this purpose the air and medium flow was passed through a silicone tube, dipped into liquid cyclohexane allowing the cyclohexane to diffuse through the silicone tube into the medium and air stream.

**Ps\_BVMO activity measurement in the Ps\_BVMO + Syn6803\_BGT mixed-species biofilm setup.** *BVMO* gene expression was induced 15 days after inoculation using 2 mM of IPTG supplied with the YBG11 medium. At day 16, BVMO activity was measured by adding 5 mM of cyclohexanone to the YBG11 medium flow.

**Quantification of cyclohexanol and caprolactone using gas chromatography (GC).**

Samples were collected from the reactor outflow and quenched with equal volumes of ice-cold diethyl ether, vortexed for 2 min, and centrifuged (17,000g, 2 min, rt). The ether phase was removed and dried over anhydrous Na<sub>2</sub>SO<sub>4</sub>. Quantification of caprolactone and cyclohexanol was performed using gas chromatography (GC Trace 1310, Thermo Fisher Scientific, Waltham, USA) equipped with a TG-5MS capillary column (5% diphenyl / 95% dimethyl polysiloxane, 30 m, I.D.: 0.25 mm, film thickness: 0.25 µm, Thermo Fisher Scientific, Waltham, USA) and a flame ionization detector (FID) operating at 320 °C, 350 mL min<sup>-1</sup> air flow, 30 mL min<sup>-1</sup> makeup gas flow and 35 mL min<sup>-1</sup> hydrogen gas flow. Nitrogen gas was applied as carrier gas with a constant flow of 1.5 mL min<sup>-1</sup>. The injection volume was set to 1 µL using a PTV injector, programmed with a temperature gradient of 10 °C s<sup>-1</sup> from 90 - 300 °C. A split ratio of 11 was applied. For cyclohexanol quantification, the temperature profile of the oven was: 1) 40 °C for 1 min, 2) 40 – 80 °C with 10 °C min<sup>-1</sup>, 3) 80 – 250 °C with 100 °C min<sup>-1</sup>, and 4) 250 °C for 2 min. The oven temperature profile for caprolactone quantification was: 1) 40 °C for 3 min, 2) 40 – 170 °C with 15 °C min<sup>-1</sup>, 3) 170 – 300 °C with 100 °C min<sup>-1</sup>, and 4) 300 °C for 1 min.

**Quantification of cell number, cell volume, and biofilm dry weight.** For biomass harvest purposes, the reactor experiment was actively stopped by terminating the medium supply. The biofilm coated capillaries were disassembled and the biomass was removed from the capillaries by scratching and resuspension into a defined volume of water. The resulting culture was mixed vigorously for 1 minute before cell number and cell volume quantification using coulter counter measurement (Multisizer 3, 20 µm aperture, Beckman Coulter, Brea, CA). *Synechocystis* sp. PCC 6803 and *Pseudomonas* sp. VLB120 cells were differentiated by particles size of 0.4 - 1.6 µm and 1.6 - 6 µm, respectively. For biofilm dry weight determination, the remaining biomass was concentrated by centrifugation (5000g, 20 °C, 7 min), transferred to pre-dried and pre-weighted glass tubes, centrifuged again (10000g, 4 °C, 7 min), and the remaining pellet dried at 60 °C for 1 week.

## 6.4 Results

To proof the technique of stably cultivating phototrophic microorganisms at high cell densities via a mixed-trophies biofilm-based capillary reactor, the two model strains *Synechocystis* sp. PCC 6803 and *Pseudomonas* sp. VLB120 were applied. *Synechocystis* sp. PCC 6803 is a well-known cyanobacterial model strain and widely used for studying photosynthesis-driven production of chemicals and fuels. *Pseudomonas* sp. VLB120 constitutes a chemoheterotrophic strain frequently applied for biocatalytic purposes with strong biofilm formation ability. First, single- and mixed-species of Syn6803\_Km and Ps\_Km were applied in the capillary reactor system. Six experimental setups using YBG11 medium (supplemented with 0.4 g L<sup>-1</sup> citrate if stated) for cell growth and without or with additional air segments were conducted. After five weeks of biofilm maturation, O<sub>2</sub> concentration in the liquid and gas phase as well as citrate consumption was measured. Afterwards, the cultivation system was actively terminated and characterized regarding photo-pigment formation (macroscopic), bio-volume of each species (cell number and cell volume), and total biofilm dry weight.

### 6.4.1 Cultivation of single species *Synechocystis* results in low surface coverage and impaired biofilm development.

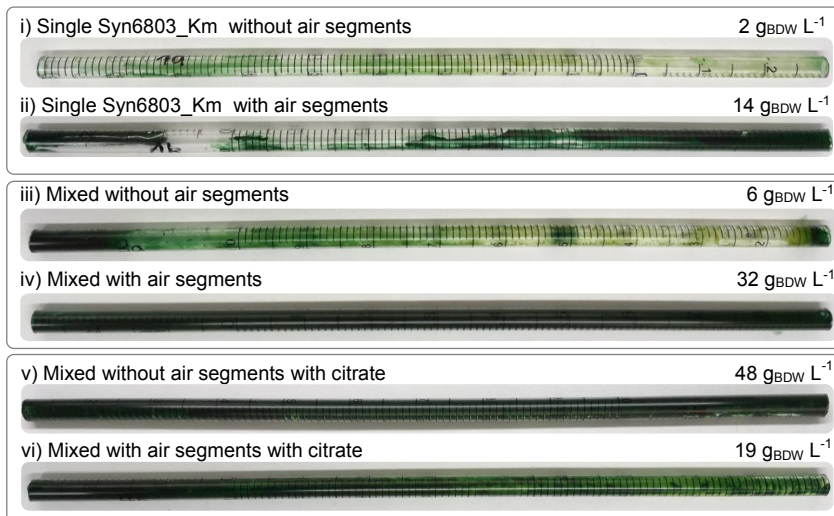
First, biofilm and O<sub>2</sub> formation in the capillary reactor were analyzed during cultivation of single species Syn6803\_Km. Cells cultivated without air segments resulted in weak biofilm formation with a low final biomass concentration of 2 g<sub>BDW</sub> L<sup>-1</sup> mainly located in the first part of the capillary tube (**Figure 6.3i**, **Table 6.1**, **Figure 6.4i**). In addition, photo-pigment formation seemed to be impaired indicated by a yellow/ light green outer appearance of the biofilm. O<sub>2</sub> concentrations measured in the aqueous phase were 3 fold above the saturation limit at ambient conditions (746 μM, **Table 6.1**, **Figure 6.4i**). The application of air segments promoted cyanobacterial growth resulting in a lush green colored biofilm and increased final biomass concentrations of 14 g<sub>BDW</sub> L<sup>-1</sup> (**Figure 6.3ii**). In contrast to single phase cultivation, the use of air segments facilitated O<sub>2</sub> extraction from the liquid phase into the gas segments, reflected by an increased O<sub>2</sub> concentration of 24% measured in the gas phase in comparison to ambient O<sub>2</sub> concentration (21%) (**Table 6.1**). In general, surface coverage of single species Syn6803\_Km grown biofilm was inhomogeneous.

### 6.4.2 Co-cultivation of *Synechocystis* with *Pseudomonas* sp. VLB120 enhances cyanobacterial surface coverage and promotes biofilm formation to high cell densities.

In a next setting, Ps\_Km was co-cultivated with Syn6803\_Km. After five weeks of cultivation without air segments visible surface coverage was slightly enhanced in comparison to single species cultivation (**Figure 6.3iii** vs. **Figure 6.3i**). This resulted in three-times higher final



biofilm dry weight of  $6 \text{ g}_{\text{BDW}} \text{ L}^{-1}$ , mainly consisting of cyanobacterial cells (98.3%) (**Table 6.1**).  $\text{O}_2$  concentrations measured in the aqueous phase were, as expected, above the solubility limit at ambient conditions (**Table 6.1**, **Figure 6.4iii**). As observed before, the use of air segments resulted in extraction of  $\text{O}_2$  into the air phase and promoted lush green cyanobacterial biofilm formation throughout the length of the capillary (**Figure 6.3iv**, **Table 6.1**). Overall, the co-cultivation of Syn6803\_Km with Ps\_Km promoted biofilm formation to a high final biofilm concentration of  $32 \text{ g}_{\text{BDW}} \text{ L}^{-1}$  mainly consisting of cyanobacterial cells (99.3%) (**Table 6.1**, **Figure 6.4iv**).



**Figure 6.3:** Pictures of capillary reactors taken five weeks after inoculation. Syn6803\_Km = *Synechocystis* sp. PCC 6803 pAH032, Ps\_Km = *Pseudomonas* VLB120 pAH032, Mixed = Syn6803\_Km + Ps\_Km, BDW = biofilm dry weight.

### 6.4.3 Citrate respiration relieves oxidative stress and supports the formation of super-high density cyanobacterial biofilm.

In the following experiments, mixed-trophies cultivation was conducted as described above, but using YBG11 medium supplemented with citrate to promote  $\text{O}_2$  respiration by Ps\_Km. After five weeks of cultivation, the capillaries were entirely coated with rich green biofilm (**Figure 6.3v + vi**). Without air segments, respiration of citrate by Ps\_Km decreased the  $\text{O}_2$  concentration in the aqueous phase to anoxic conditions (**Table 6.1**, **Figure 6.4v**). As already observed before, the relief of supersaturating  $\text{O}_2$  concentrations, in this case via Ps\_Km respiration, had a positive impact on the cyanobacterial biofilm development. The cyanobacterial surface coverage was high and resulted in a final biofilm concentration of  $48 \text{ g}_{\text{BDW}} \text{ L}^{-1}$  consisting of 85% cyanobacterial cells (**Table 6.1**). Upon the addition of air

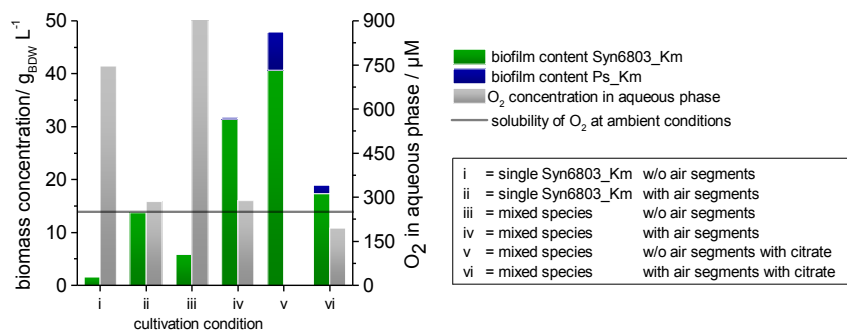
segments, O<sub>2</sub> was again stripped into the gas phase (**Figure 6.4vi**). Surprisingly, the final biofilm dry weight was reduced to 19 g<sub>BDW</sub> L<sup>-1</sup> (92% cyanobacterial cells) (**Figure 6.3vi, Table 6.1**).

**Table 6.1:** Quantitative data obtained from single- and mixed-species biofilm cultivation in a tubular microreactor. Mixed-species = Co-culture of Syn6803\_Km and Ps\_Km, - Citrate = without organic carbon source, + Citrate = with 0.39 g L<sup>-1</sup> citrate as carbon source, - Air = without air segments, + Air = with air segments.

Experimental setup	O <sub>2</sub> in gas phase / %	O <sub>2</sub> in aq. phase <sup>[1]</sup> / μM	Citrate consumption / g L <sup>-1</sup>	Biofilm dry weight <sup>[2]</sup> / g L <sup>-1</sup>		
				Ps.	Syn.	total
Single Syn6803_Km						
i) - Air - Citrate	-	746	-	-	1.5	1.5
ii) + Air - Citrate	23.9	284	-	-	13.7	13.7
Mixed-species						
iii) - Air - Citrate	-	923	-	0.1	5.8	5.9
iv) + Air - Citrate	24.1	287	-	0.2	31.4	31.6
Mixed-species						
v) - Air + Citrate	-	0	0.27	7.2	40.6	47.8
vi) + Air + Citrate	16.3	194	0.39	1.5	17.3	18.8

[1] Solubility of O<sub>2</sub> (at 26 °C, salinity of 3.5 g kg<sup>-1</sup>, 21% O<sub>2</sub> in gas phase): ~250 μM; aqueous phase O<sub>2</sub> concentrations of experiments performed with air segments are theoretical numbers relying on the partitioning between gas and aqueous phase.

[2] The biofilm dry weight is calculated based on 1.2 mL tube volume. Ps. and Syn. specific biofilm dry weights are calculated based on cell numbers and cell volumes and the respective total biofilm dry weight, assuming that both strains constitute equal biovolume to biofilm dry weight ratio.



**Figure 6.4:** Oxygen concentrations and final biofilm dry weight of single- and mixed-species cultivation of Syn6803\_Km and Ps\_Km grown in biofilm-based capillary reactor. Cultivation was performed using YBG11 medium without or with citrate supplementation and without or with air segments.

**6.4.4 The mixed-species biofilm-based capillary reactor setup enables biocatalytic reactions.**

Mixed-species cultivation significantly enhanced cyanobacterial biofilm development and retention of HCD cyanobacterial biofilm. In order to test the new developed cultivation method for biocatalytic purposes, an exemplary whole-cell reaction was performed using recombinant strains harboring a cyclohexane CYP monooxygenase enzyme system. Syn6803\_CYP was co-cultivated with Ps\_CYP using air segments for O<sub>2</sub> extraction and YBG11 medium without organic carbon source to focus on photobiocatalytic hydroxylation activity. After 5 weeks of cultivation, CYP gene expression was induced using IPTG and cyclohexane was delivered to the biofilm via substrate saturated air- and medium flow. Cyclohexanol quantification of samples from the reactor outlet showed titers of 1.1 mM corresponding to a productivity of 7.5 g L<sub>tube</sub><sup>-1</sup> day<sup>-1</sup> (**Table 6.2**). The reaction was most likely catalyzed by the cyanobacterial strain, as no organic carbon source for the Ps\_CYP cell growth and cofactor regeneration was present and cultivation under light exclusion resulted in reduced product formation (data not shown). Thus, we could proof the accessibility of the cyanobacterial cells in the grown biofilm for biocatalytic purposes.

**Table 6.2:** Exemplary biocatalytic reactions conducted with recombinant strains applied in the mixed-species biofilm based capillary reactor system. Syn\_CYP = *Synechocystis* sp. PCC 6803 pAH050, Ps\_CYP = *Pseudomonas* sp. VLB120 pAH050, Ps\_BVMO = *Pseudomonas* sp. VLB120 pAH049, Syn6803\_BGT = *Synechocystis* sp. PCC 6803 pAH042; + Citrate = with 0.46 g L<sup>-1</sup> citrate as carbon source, + Air = with air segments.

Recombinant biocatalytic strains	Reaction conditions	Reaction	Product concentration in reactor outlet	Productivity
Syn6803_CYP + Ps_CYP	- Citrate + Air	Cyclohexane → Cyclohexanol	1.1 mM	7.5 g L <sub>tube</sub> <sup>-1</sup> day <sup>-1</sup>
Ps_BVMO + Syn6803_BGT	+ Citrate + Air	Cyclohexanone → Caprolactone	2.5 mM	19.4 g L <sub>tube</sub> <sup>-1</sup> day <sup>-1</sup>

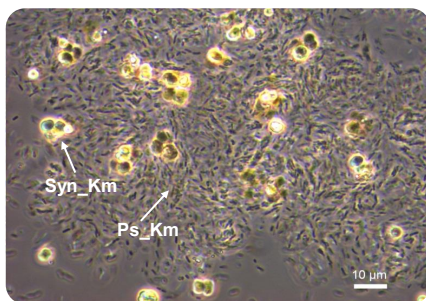
In a second reaction setup, two further recombinant strains, namely Syn6803\_BGT and Ps\_BVMO, were co-cultivated using air segments and YBG11 supplemented with citrate to promote chemoheterotrophic biocatalysis. After 15 days of cultivation, *AlkBGT* and *BVMO* gene expression was induced using IPTG and either pure NAME was supplied as additional organic phase or 5 mM of cyclohexanone were added to the cultivation medium. Analysis of the reactor outlet revealed no catalytic activity for Syn6803\_BGT. This might be explained by insufficient protein synthesis or insufficient coupling of the photosynthetic metabolism with the heterologous enzyme system under the applied cultivation and reaction conditions, as already observed for biotransformations using suspended cultures (**Chapter 4**). In contrast, the chemoheterotrophic strain Ps\_BVMO catalyzed the Baeyer-Villiger oxidation of

cyclohexanone to caprolactone. The final titer of 2.5 mM caprolactone corresponds to a catalytic rate of ca.  $19 \text{ g L}_{\text{tube}}^{-1} \text{ day}^{-1}$  (Table 6.2). Eventually, the mixed-species biofilm-based capillary reactor system enabled the biocatalytic functionality of both, the phototrophic biocatalysts and heterotrophic species.

## 6.5 Discussion

In nature, oxygenic phototrophs and aerobic heterotrophs are embedded in a complex matrix of extracellular polymeric substances (EPS) to form stable microbial mats (Prieto-Barajas *et al.*, 2017). In such mats, the microbial consortium interacts in close cooperation, and thereby profits from complementary metabolic activities and taps new resources. In wastewater treatment plants microalgal/ cyanobacterial biofilms are applied in undefined consortia, e.g. for effluent oxygenation, heavy metal removal, and recycling of nitrogen and phosphorous (Barros *et al.*, 2018). The here presented technology exploits the concept of microbial mats in a defined and minimized biofilm system. The co-cultivation of the chemoheterotrophic, aerobic microorganism *Pseudomonas* sp. VLB120 strongly enhanced biofilm formation, maturation and surface coverage of the photoautotrophic cyanobacterium *Synechocystis* sp. PCC 6803. This phenomenon may be attributed to proto-cooperation, which is the beneficial but not essential interaction of organisms, and is described for the here applied cultivation system by the following sections.

***Pseudomonas* sp. VLB120 supports *Synechocystis* sp. PCC 6803 cell attachment.** In principle, both strains produce EPS and thus facilitate biofilm formation. Using microscopy analysis of the harvested biofilm, the embedding of Syn6803\_Km and Ps\_Km in a biofilm matrix was visible (Figure 6.5). However, also during cultivation without organic carbon source the presence of *Pseudomonas* had a positive impact on *Synechocystis* biofilm formation although the cultivation conditions did not support *Pseudomonas* growth (0.6% of total cell fraction) (Figure 6.3iii, Table 6.1). Most likely, the few observed *Pseudomonas* cells survived on EPS or cell debris of *Synechocystis* and in turn improved the cyanobacterial surface attachment e.g., via conditioning of the capillary surface. Unexpectedly, the application of air segments reduced growth of *Pseudomonas*. This might be explained by a hydrodynamic stress response of the cells induced by high fluidic and interfacial stresses in the capillary, which might require more energy for *Pseudomonas* cell maintenance and EPS formation. This was reflected by a higher specific citrate consumption of  $0.26 \text{ g g}_{\text{PsBDW}}^{-1}$  in comparison to  $0.04 \text{ g g}_{\text{PsBDW}}^{-1}$  in single phase flow (Table 6.1). Thus, future optimization of the cultivation setting may involve the reduction of hydrodynamic stress e.g., via a reduced rate of air flow.



**Figure 6.5:** Microscopic image of a mixed-species biofilm containing *Synechocystis* sp. PCC 6803\_Km (Syn\_Km) and *Pseudomonas* VLB120\_Km (Ps\_Km), harvested from a capillary reactor. Scale bar equal to 10  $\mu\text{m}$ .

**Oxidative stress impairs cyanobacterial biofilm growth and can be relieved by O<sub>2</sub> respiration.** During single phase cultivation supersaturating O<sub>2</sub> concentrations were measured which went along with impaired biofilm formation (**Figure 6.4**). High O<sub>2</sub> concentrations can enhance the formation of radical oxygen species, which are side products generated during electron transport in oxygenic photosynthesis. Most likely these extreme O<sub>2</sub> concentrations led to oxidative stress and thus growth inhibition of Syn6803\_km, resulting in visible photo-pigment reduction (yellowish/ light green outer appearance of the strain) observed towards the end of the capillary tube (Latifi *et al.*, 2009; Narainsamy *et al.*, 2016; Weissman *et al.*, 1988). In contrast, the introduction of air segments as well the respiration of O<sub>2</sub> by *Pseudomonas* decreased the aqueous phase O<sub>2</sub> concentration to ambient or even anoxic levels, thus relieved oxidative stress and resulted in rich green, HCD biofilm (**Figure 6.4**). Overall, the dual trophies approach enabled the cultivation of photobiocatalysts in a stable and super-high cell density format which is currently a key-bottleneck in photo-biotechnology. Furthermore, the applied biotransformation of cyclohexane to cyclohexanol demonstrated the applicability of the developed cultivation technology for biotechnological purposes.

**The mixed-trophies capillary reactor system supports the application of chemoheterotrophic biocatalysts.** Continuous production of chemicals using *Pseudomonas* sp. VLB120 in biofilm-based capillary reactors was already investigated in several studies (Gross *et al.*, 2010; Karande *et al.*, 2016b). As for many O<sub>2</sub>-dependent bioprocesses, oxygen mass transfer constitutes a main process limitation also during cultivation in such reactor systems. The introduction of air segments into the medium flow increases oxygen availability, but again becomes limited after a specific length of the capillary tube (Karande *et al.*, 2014). In contrast, coupling photosynthetic O<sub>2</sub> generation with bacterial respiration relieves the process limitation of O<sub>2</sub>-dependent bioprocesses in theory

independent of the tube length as long as light is available (**Chapter 7**). Already some decades ago the phenomenon of *in situ* O<sub>2</sub> supply was transferred from nature to productive biotechnology utilizing defined co-cultures of algae and bacteria (Adlercreutz *et al.*, 1982; Adlercreutz and Mattiasson, 1982; Cheirsilp *et al.*, 2011; Papone *et al.*, 2012). Yet, this research either focused on immobilized cells embedded in artificial polymers such as alginate, or cell suspensions. In this study, growth of *Pseudomonas* sp. VLB120 in the capillary reactor was 6.5 times and citrate respiration 9 times higher than without the use of air segments, but solely due to the *in situ* supply of O<sub>2</sub> originating from the co-cultured cyanobacterium (data for single species Ps\_Km not shown). Furthermore, Ps\_BVMO applied in the mixed-trophies reaction system was accessible for the hydroxylation of cyclohexanone to caprolactone and thus demonstrates the functionality of the developed technology also for chemoheterotrophic biocatalysis.

## 6.6 Conclusion

In a mixed-trophies biofilm it was possible to co-cultivate the photoautotrophic *Synechocystis* sp. PCC 6803 with *Pseudomonas* sp. VLB120 over a time-period of five weeks to a high cell density of max. 48 g<sub>BDW</sub> L<sup>-1</sup>. This is the first cultivation technology allowing the defined, continuous cultivation of a phototrophic organism at super-high cell densities. Furthermore, the strains applied in the capillary reactor setup enabled the biocatalytic conversion of hydrocarbons to respective oxyfunctionalized value-added products. The concept now faces further implementation, evaluation and optimization of biocatalytic approaches and scale-up for the eco-efficient production of fuels and value-added chemicals.

## 6.7 Acknowledgments

We acknowledge the use of the facilities of the Centre for Biocatalysis (MiKat) at the Helmholtz Centre for Environmental Research, which is supported by European Regional Development Funds (EFRE, Europe funds Saxony) and the Helmholtz Association.

## **Chapter 7      General discussion - *In situ* O<sub>2</sub> generation for biocatalytic oxyfunctionalization reactions**

Bruno Bühler and Andreas Schmid coordinated the project and corrected the manuscript.

Published in:

*ChemCatChem*, **2018**, 10 (23), 5366 - 5371

### 7.1 Abstract

O<sub>2</sub>-dependent whole-cell bioprocesses, such as C-H oxyfunctionalizations, are constrained by technically limited O<sub>2</sub> mass transfer and biocatalyst-inherent O<sub>2</sub> respiration. In large-scale bioprocesses, this restricts the maximum achievable productivity to 5.6 g<sub>product</sub> L<sup>-1</sup> h<sup>-1</sup> assuming a resting cell concentration of 9.4 g<sub>CDW</sub> L<sup>-1</sup>. This concept paper discusses strategies to enhance the O<sub>2</sub> availability for biocatalytic oxyfunctionalizations with a focus on the *in situ* generation of O<sub>2</sub> from water. This promising approach was addressed recently by the exploitation of microbial photosynthesis for light-driven C-H oxyfunctionalization. Via intracellular O<sub>2</sub> evolution, phototrophic biocatalysts increase the maximum achievable productivity well beyond technical boundaries. This fundamental advantage over O<sub>2</sub>-respiring biocatalysts now awaits scale-up evaluations, combining established cultivation technologies for phototrophic organisms with bioprocessing techniques for heterotrophic organisms.



## 7.2 Introduction

Oxygen-dependent reactions like regio- and enantiospecific hydrocarbon oxyfunctionalizations are of outstanding interest for the chemical and pharmaceutical industries (Bühler *et al.*, 2003a; Dong *et al.*, 2018; Hollmann *et al.*, 2011). For such reactions, efficient biocatalysis concepts have been developed that rely on oxygenases and electron supply via the metabolism of living microbial cells (Schmid *et al.*, 2001; Schrewe *et al.*, 2013; Wachtmeister and Rother, 2016). Commercial production of oxyfunctionalized fine and bulk chemicals necessitates a productivity of at least  $1 - 10 \text{ g L}^{-1} \text{ h}^{-1}$  (Straathof *et al.*, 2002; van Dien, 2013). To achieve this, biocatalysts are required that feature high specific activities of  $>100 \text{ U g}_{\text{CDW}}^{-1}$  and/ or can be operated at high cell concentrations of  $>10 \text{ g}_{\text{CDW}} \text{ L}^{-1}$ . With a cellular oxygenase content of up to 12.5% of dry biomass (Tufvesson *et al.*, 2010), the given whole-cell activity translates into an enzyme-specific activity of  $>0.8 \text{ U mg}_{\text{enzyme}}^{-1}$ . In comparison to other industrially applied enzymes (e.g., lipases), the nature of oxygenases often limits the productivity due to a low  $k_{\text{cat}}$  (typically in the range of  $0.2 - 75 \text{ s}^{-1}$ ) and limited enzyme stability (Duetz *et al.*, 2001; Lundemo and Woodley, 2015). Thus, high biomass concentrations are essential for the production of large volume chemicals or energy carriers. The maximum applicable biomass concentration of  $\text{O}_2$  respiring biocatalysts is constrained by the maximum net oxygen accumulation rate ( $= d\text{O}_2/dt$ ,  $\mu\text{mol}_{\text{O}_2} \text{ min}^{-1} \text{ L}^{-1} = \text{U L}^{-1}$ ) of the bioprocess setup, constituting a critical process boundary for  $\text{O}_2$ -dependent reactions (Duetz *et al.*, 2001; Garcia-Ochoa and Gomez, 2009; Law *et al.*, 2006; Marques *et al.*, 2010). In classical biotransformation processes performed with heterotrophic microbes, this boundary depends on i) the bioreactor-intrinsic oxygen transfer rate (OTR) and ii) the biocatalyst specific oxygen respiration rate (ORR):

$$d\text{O}_2/dt = \text{OTR} - \text{ORR}.$$

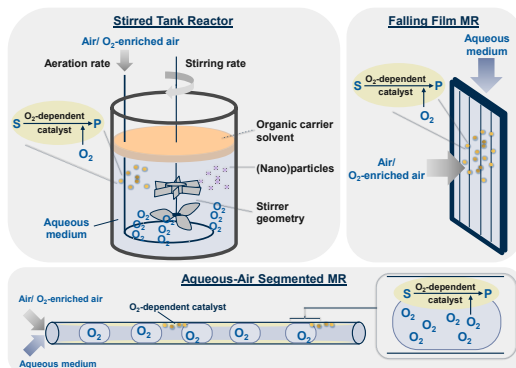
The OTR is a physical parameter defined by the gas-liquid mass transfer constant  $k_L$  ( $\text{m min}^{-1}$ ), the interfacial area  $a$  ( $\text{m}^2 \text{m}^{-3}$ ), and the difference between the  $\text{O}_2$  solubility  $C^*$  ( $\mu\text{mol L}^{-1}$ ) and the dissolved  $\text{O}_2$  concentration in the liquid phase  $C$  ( $\mu\text{mol L}^{-1}$ ):

$$\text{OTR} = k_L a (C^* - C).$$

As the  $\text{O}_2$  solubility in aqueous media is relatively low under atmospheric conditions ( $\sim 250 \mu\text{M}$  at  $25^\circ\text{C}$ , 1 atm, and a salinity of  $6 \text{ g kg}^{-1}$ ) (Garcia and Gordon, 1992; Garcia and Gordon, 1993), the mass transfer term  $k_L a$  is one of the most critical process parameters to be addressed during the scale-up of microbial bioprocesses (Marques *et al.*, 2010). It depends on the composition and physical properties of the gas and liquid phases (which also influence  $C^*$ ) and on the mixing applied. Technical solutions to enhance the net oxygen accumulation rate aim at an OTR increase via the optimization of the hydrodynamics in

bioreactor setups, that is, the bioreactor geometry or the operational conditions (**Figure 7.1**) (Garcia-Ochoa and Gomez, 2009). Examples concern either  $k_{L,a}$  or  $C^*$ :

- $k_{L,a}$ : increased aeration rate (Law *et al.*, 2006), improved mixing (stirrer speed, design), application of organic solvents (Kumar *et al.*, 2017; Shet *et al.*, 1997) or (nano)particles (Beenackers and van Swaaij, 1993; Olle *et al.*, 2006)
- $C^*$ : application of  $O_2$ -enriched air, increased pressure



**Figure 7.1:** Examples for technical solutions physically enhancing the  $O_2$  transfer rate in bioreactors. (**top left**) Standard stirred tank bioreactor (STR), (**top right**) falling film microreactor (FFMR), and (**bottom**) aqueous-air segmented microreactor (adapted with permission from Karande *et al.* 2014 Copyright 2018 John Wiley and Sons.) (Karande *et al.*, 2014).

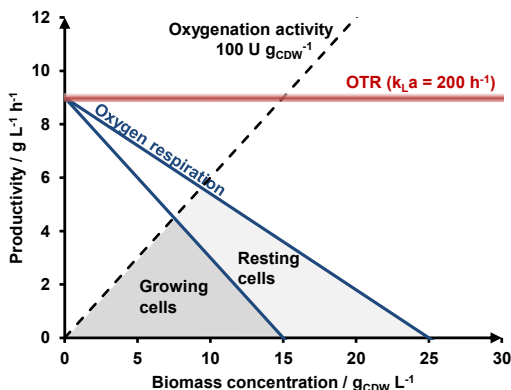
Further, the application of microreactors can significantly increase gas-liquid mass transfer by increasing the turbulence and thus  $k_{L,a}$  compared to reactors with a lower surface to volume ratio. This was shown for oxidations catalyzed by glucose oxidase or D-amino acid oxidase in falling film microreactors (Bolivar *et al.*, 2016; Illner *et al.*, 2014) and styrene epoxidation by recombinant *Pseudomonas* sp. VLB120 using air segments in multiphasic biofilm-coated microreactors (Karande *et al.*, 2014) (**Figure 7.1**).

Besides physical solutions to increase the net oxygen accumulation rate, approaches using oxygen donors other than  $O_2$  (namely  $H_2O$  and  $H_2O_2$ ) have been reported. After reviewing  $O_2$ -related technical constraints critical for the implementation of large-scale whole-cell oxygenation bioprocesses, new concepts for *in situ*  $O_2$  generation in the liquid phase will be discussed.

### 7.3 Constraints for standard large-scale whole-cell oxygenation bioprocesses

Successful scale-up of a bioprocess in a typically used stirred tank bioreactor (STR) depends on the power input available for  $O_2$  transfer. The maximum achievable  $k_{L,a}$  thus is scale-dependent. Considering bioreactor-intrinsic constraints, a maximum  $k_{L,a}$  of  $200\text{ h}^{-1}$  can be considered feasible for large-scale STRs ( $> 1\text{ m}^3$ ) at  $30\text{ }^\circ\text{C}$  and an assumed average pressure of 2.5 atm, enabling a maximum OTR of  $1500\text{ U L}^{-1}$  (Duetz *et al.*, 2001). This OTR

translates into a maximum productivity of  $9 \text{ g L}^{-1} \text{ h}^{-1}$  for a product with a molar mass of  $100 \text{ g mol}^{-1}$  (Figure 7.2).



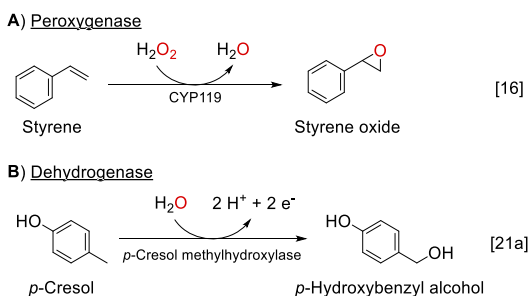
**Figure 7.2:** Maximum achievable productivity of  $\text{O}_2$ -dependent biocatalytic reactions as a function of the applied concentration of chemoheterotrophic whole-cell biocatalysts. The maximum applicable biomass concentration results from the bioreactor-intrinsic oxygen transfer rate (OTR) divided by the biocatalyst specific oxygen respiration rate and represents the biomass concentration, at which all  $\text{O}_2$  transferred into the aqueous medium is respired by the cells. The dashed line represents the productivity that can be achieved for a product with a molar mass of  $100 \text{ g mol}^{-1}$  at a reasonable biocatalyst-specific oxyfunctionalization rate of  $100 \text{ U g}_{\text{CDW}}^{-1}$ . The OTR is defined by the bioreactor-specific gas-liquid mass transfer term  $k_L a$  (estimated to be  $200 \text{ h}^{-1}$  in large scale reactors), the soluble  $\text{O}_2$  concentration ( $550 \text{ }\mu\text{M}$  at  $30 \text{ }^\circ\text{C}$  and  $2.5 \text{ atm}$ ) and the dissolved oxygen concentration ( $100 \text{ }\mu\text{M}$ ), forming an upper process boundary (red line). With increasing concentration of  $\text{O}_2$ -respiring biocatalysts, the net oxygen accumulation rate ( $d\text{O}_2/dt$ ) is reduced by the oxygen respiration rate ( $100 \text{ U g}_{\text{CDW}}^{-1}$  for growing,  $60 \text{ U g}_{\text{CDW}}^{-1}$  for non-growing resting cells), shifting the upper boundary towards lower productivities (blue lines).

The maximum net oxygen accumulation rate depends on the OTR and the ORR. Growing chemoheterotrophic microbes like *Escherichia coli* respire  $\text{O}_2$  at a specific rate of  $\sim 100 \text{ U g}_{\text{CDW}}^{-1}$  (Calhoun *et al.*, 1993; Duetz *et al.*, 2001; Park, 2007; Shet *et al.*, 1997). Thus,  $d\text{O}_2/dt$  is inversely proportional to the applied biocatalyst concentration. The maximum applicable biomass concentration is restricted to  $15 \text{ g}_{\text{CDW}} \text{ L}^{-1}$  at which all available  $\text{O}_2$  is used for respiration and the productivity for an  $\text{O}_2$  dependent reaction is thus reduced to zero (Figure 7.2) (Duetz *et al.*, 2001). Non-growing (resting) cells exhibit a lower energy demand (only for maintenance) and thus a lower respiration rate of  $\sim 60 \text{ U g}_{\text{CDW}}^{-1}$  (calculated based on a glucose uptake rate of  $0.62 \text{ mmol g}_{\text{CDW}}^{-1} \text{ h}^{-1}$  for resting *E. coli* JM101 with 6  $\text{O}_2$  molecules consumed per glucose molecule oxidized to  $\text{CO}_2$ ) (Julsing *et al.*, 2012a; van Beilen *et al.*, 2003). Their application thus increases the maximally applicable biomass concentration to

25 g<sub>CDW</sub> L<sup>-1</sup>. However, under aerobic conditions, the endogenous respiration remains indispensable for the application of chemoheterotrophic biocatalysts, enabling biocatalyst maintenance including, inter alia, protein regeneration. Careful adjustment of the biomass concentration is of utmost importance to maximize the productivity and avoid a limitation by O<sub>2</sub> (Baldwin and Woodley, 2006; Hilker *et al.*, 2006). For the industrial scale scenario defined above (molar mass<sub>product</sub> = 100 g mol<sup>-1</sup>, ORR = 60 - 100 U g<sub>CDW</sub><sup>-1</sup>, k<sub>La</sub> = 200 h<sup>-1</sup>, specific oxygenation activity = 100 U g<sub>CDW</sub><sup>-1</sup>), 7.5 and 9.4 g<sub>CDW</sub> L<sup>-1</sup> of growing and resting chemoheterotrophic biocatalysts allow a maximum achievable productivity of 4.5 and 5.6 g L<sup>-1</sup> h<sup>-1</sup>, respectively (**Figure 7.2**). *In situ* O<sub>2</sub> generation or the application of oxygen sources other than O<sub>2</sub> are promising strategies to overcome the restrictions by the traditional external O<sub>2</sub> supply and are discussed in the following.

#### 7.4 Use of alternative oxygen donors to overcome O<sub>2</sub> limitations

Enzymes that use oxygen sources other than O<sub>2</sub> represent an alternative to the use of catalysts based on oxygenases (**Figure 7.3**).



**Figure 7.3:** Examples for enzymes utilizing alternative oxygen donors for oxyfunctionalizations. Peroxygenase- (A) and dehydrogenase- (B) based enzyme systems make use of H<sub>2</sub>O<sub>2</sub> and H<sub>2</sub>O as oxygen donors, respectively.

Peroxygenases utilize H<sub>2</sub>O<sub>2</sub> as oxygen donor (Bormann *et al.*, 2015; Wang *et al.*, 2017). Cytochrome P450 CYP119, for instance, catalyzes the epoxidation of styrene to styrene oxide via a peroxide shunt pathway (**Figure 7.3 A**) (Koo *et al.*, 2000). Up to now, the variety of reactions catalyzed by peroxygenases is limited. Future exploration of novel peroxygenases with a more diverse reaction scope can be considered a promising approach for preparative oxyfunctionalization chemistry (Wang *et al.*, 2017). Importantly, the high reactivity of H<sub>2</sub>O<sub>2</sub> necessitates its well-controlled supply to the reaction system. *In situ* generation of H<sub>2</sub>O<sub>2</sub> by enzymatic, e.g., via glucose oxidase (van de Velde *et al.*, 2000), electrochemical, i.e., via a cathode (Lütz *et al.*, 2004), or photocatalytic, e.g., via Flavin/EDTA/ *hν* (Perez *et al.*, 2009; Zhang *et al.*, 2018), water oxidation successfully prevents the inactivation of the applied oxidoreductases (Bormann *et al.*, 2015). However, these

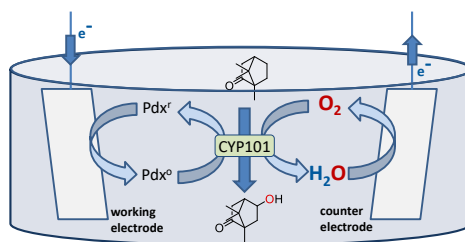
processes go along with  $O_2$  reduction and thus do not overcome the requirement for  $O_2$  dissolved in the aqueous phase.

In contrast, dehydrogenase-type enzymes such as molybdopterin-dependent hydroxylases use water as oxygen donor for the oxyfunctionalization of, however, rather activated carbon atoms (Hille *et al.*, 1998). The few examples showing the application of these enzymes for oxyfunctionalizations include the formation of *p*-hydroxybenzyl alcohol from *p*-cresol by the *p*-cresol methylhydroxylase or the hydroxylation of quinaldine to 4-hydroxyquinaldine using quinaldine 4-oxidase (**Figure 7.3 B**) (Hopper, 1978; Ütkür *et al.*, 2011).

Next to these enzymes, photochemically active catalysts such as ruthenium porphyrins have been developed relying on water as source of oxygen for the chemical oxyfunctionalization of olefins and sulfides (Fukuzumi *et al.*, 2012; Funiyu *et al.*, 2003; Inoue *et al.*, 2005; Inoue *et al.*, 1994; Li *et al.*, 2011; Pagliaro *et al.*, 2005).

### 7.5 *In situ* generation of $O_2$ in the liquid phase

Already in 1977, Hans Günter Schlegel developed the concept of “aeration without air” by investigating the controlled supply of  $H_2O_2$  to microbial cultures synthesizing catalases. Catalases enzymatically cleave  $H_2O_2$ , *in situ* releasing  $O_2$  that can be taken up by cells for respiration, and thus reduce the need for external aeration (Nies and Schlegel, 1984; Rosenberg *et al.*, 1992; Schlegel, 1977; Sonnleitner and Hahnemann, 1997; Sriram *et al.*, 1998).



**Figure 7.4:** Electrochemical *in situ*  $O_2$  generation for the hydroxylation of camphor to 5-exo hydroxyl camphor using CYP101 (Reipa *et al.*, 1997). Reduction equivalents were supplied from an antimony-doped tin oxide working electrode to CYP101 via putidaredoxin (Pdx).  $O_2$  was generated at the platinum counter electrode and the reactor was operated anaerobically using an argon purge. Figure adapted from Reipa *et al.*, 1997 Copyright (2018) National Academy of Sciences.

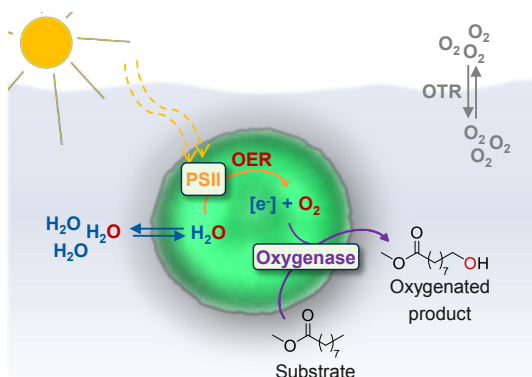
Using electrolysis, water can be used for the *in situ* generation of  $O_2$  (Wang *et al.*, 2016a). At an electric potential of at least 1.23 V, water is electrolyzed to  $O_2$  and  $H_2$ . Electrochemical *in situ*  $O_2$  generation in aqueous media has successfully been coupled to hydrocarbon oxyfunctionalization, e.g., the hydroxylation of camphor to 5-exo-hydroxycamphor or the epoxidation of styrene to styrene oxide using CYP101 (**Figure 7.4**) (Mayhew *et al.*, 2000;

Reipa *et al.*, 1997). From an energy perspective, the use of light energy for photocatalytic, photo-electrochemical, or photovoltaic-electrochemical water oxidation constitutes an economically and ecologically promising approach for the *in situ* generation of O<sub>2</sub> (Abe, 2010; Jiao *et al.*, 2015; Li, 2017). Whereas many photo-/electro-/chemical concepts focus on H<sub>2</sub> generation, the coupling of this O<sub>2</sub> generation principle with enzymatic oxyfunctionalizations has yet to be demonstrated on technical scale.

### 7.6 Exploitation of microbial photosynthesis for O<sub>2</sub>-dependent reactions

Following the principle of lichens (symbiosis of fungi with microalgae or cyanobacteria), Adlercreutz *et al.* reported in 1982 the co-immobilization of the algae *Chlorella pyrenoidosa* as natural O<sub>2</sub> producer with O<sub>2</sub>-respiring *Gluconobacter oxydans* (Adlercreutz *et al.*, 1982; Adlercreutz and Mattiasson, 1982). The defined mixed-cultures revealed a 5.4 times increased production of dihydroxyacetone from glycerol in comparison to the single species system without O<sub>2</sub>-evolving algae.

Recently, we successfully exploited the cyanobacterium *Synechocystis* sp. PCC 6803 for the intracellular coupling of the photosynthetic O<sub>2</sub> generation with the O<sub>2</sub>-dependent C-H oxyfunctionalization of a fatty acid methyl ester (**Figure 7.5**) (**Chapter 3**).



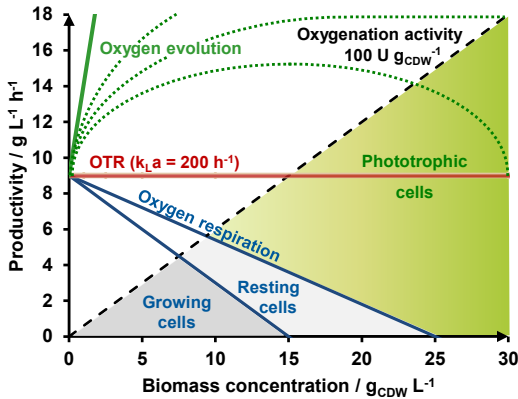
**Figure 7.5:** Microbial photosynthesis as source of O<sub>2</sub> for biocatalytic oxygenation. Phototrophic organisms like cyanobacteria oxidize water resulting in the intracellular formation of O<sub>2</sub> and reduction equivalents, both required for oxygenase catalysis. PSII = photosystem II, OER = oxygen evolution rate, OTR = oxygen transfer rate.

Photoautotrophic whole-cell biocatalysts rely on photosynthetic water oxidation rather than the oxidation of organic compounds and O<sub>2</sub> respiration for the supply of (bio)energy in the form of ATP and activated electrons (e.g., NAD(P)H). Thus, they are not only independent from extracellular O<sub>2</sub> supply for growth and maintenance, but even increase the overall O<sub>2</sub> supply.

The equation for the net oxygen accumulation rate then is expanded by the biocatalyst-specific oxygen evolution rate (OER), while the negative impact of the ORR becomes small as long as light is available and photosynthetic water oxidation takes place:

$$dO_2/dt = OTR - ORR + OER.$$

In this case, the net oxygen accumulation rate correlates directly with the applied photo-biocatalyst concentration enabling high productivities (Figure 7.6).



**Figure 7.6:** Maximally achievable productivity of  $O_2$ -dependent biocatalytic reactions as a function of the applied concentration of chemoheterotrophic as well as photoautotrophic whole-cell biocatalysts. The dashed black line represents the productivity that can be achieved for a product with a molar mass of  $100 \text{ g mol}^{-1}$  at a biocatalyst-specific oxyfunctionalization rate of  $100 \text{ U g}_{CDW}^{-1}$ . The oxygen transfer rate (OTR) is defined by the bioreactor specific gas-liquid mass transfer coefficient  $k_{L,a}$  (estimated to be  $200 \text{ h}^{-1}$  in large-scale bioreactors) and the soluble  $O_2$  concentration, in principle forming an upper process boundary (red line). With increasing concentration of  $O_2$ -respiring biocatalysts, the effective net oxygen accumulation rate ( $dO_2/dt$ ) is reduced by the biocatalysts specific oxygen respiration rate ( $100 \text{ U g}_{CDW}^{-1}$  for growing,  $60 \text{ U g}_{CDW}^{-1}$  for non-growing cells), shifting the upper boundary towards lower productivities (blue lines). By contrast, photosynthetically active whole-cell biocatalysts enhance  $dO_2/dt$  (green line) by their intrinsic  $O_2$  evolution rate (maximally  $850 \text{ U g}_{CDW}^{-1}$ ), thus theoretically supporting significantly higher productivities. The green area indicates the expanded operational space of phototrophic biocatalysts. The dashed green lines represent a limitation of  $dO_2/dt$  by the availability of light, which can be expected to occur at high cell densities due to shading effects and will depend on the reactor design.

This gives the photosynthetically active biocatalysts a sweeping advantage over  $O_2$ -respiring ones. The upper productivity limit is determined by the biocatalyst-specific oxyfunctionalization rate as long as this rate does not exceed the net oxygen accumulation rate. The OER at photosystem II (PSII) can in theory reach a maximum of  $850 \text{ U g}_{CDW}^{-1}$  (assumptions:  $k_{cat}$  of PSII:  $1000 \text{ s}^{-1}$ , 1% PSII  $\text{g}_{CDW}^{-1}$ , 350 kDa), (Dismukes *et al.*, 2009; Shen,

2015) being in line with maximally measured OERs ranging from 50 to 910 U g<sub>CDW</sub><sup>-1</sup> (Porankiewicz and Clarke, 1997; Thomas *et al.*, 1993; Touloupakis *et al.*, 2015; Wang *et al.*, 2012; Yao *et al.*, 2012; Zavřel *et al.*, 2016). However, it has to be considered that the OER at PSII depends on the available light intensity. Respiration and photorespiration (ribulose-1,5-bisphosphate oxygenation catalyzed by RuBisCO) may limit the maximum net O<sub>2</sub> accumulation rate, e.g., as a result of shading at high cell densities (indicated by dashed green lines in **Figure 7.6**) (Peterhansel *et al.*, 2010; Vermaas, 2001).

Altogether, O<sub>2</sub>-evolving microorganisms provide the basis to realize oxyfunctionalization productivities far in excess of those achievable in large-scale bioreactors with external O<sub>2</sub> supply (> 9 g L<sup>-1</sup> h<sup>-1</sup>). This requires the achievement of high specific oxygenation activities (≥ 100 U g<sub>CDW</sub><sup>-1</sup>) and cultivation of phototrophic biocatalysts to high cell densities (> 10 g<sub>CDW</sub><sup>-1</sup>) to be targeted via biocatalyst, bioreactor, and bioprocess engineering (Fresewinkel *et al.*, 2014). Such high productivities augur well for the production of large volume base chemicals or energy carriers. Classically, high amounts of photosynthetically-derived (algae) biomass are produced in open pond systems and are used for animal and human nutrition products, cosmetics, as well as for the extraction of high value molecules such as special fatty acids or pigments (Chaumont, 1993; Grobbelaar, 2009; Pulz, 2001; Singh and Sharma, 2012; Spolaore *et al.*, 2006; Weissman *et al.*, 1988). Meanwhile, also closed systems such as the tubular photo-bioreactor in Klötze, Germany (500 km total length and 700 m<sup>3</sup> volume) are developed successfully, producing 130-150 t dry biomass per year (Spolaore *et al.*, 2006). In contrast to biomass producing systems, production systems utilizing phototrophic microorganisms as biocatalyst hold altered requirements with respect to safety, process regulation/ control, biomass production, and product recovery. In order to develop technically and economically viable production processes with (recombinant) photoautotrophic biocatalysts, the well-established advances in microbial fermentation technologies have to be complemented by methodologies for the efficient cultivation of phototrophs with a main focus on light distribution and – at least during growth/ biocatalyst production – carbon dioxide mass transfer (Fresewinkel *et al.*, 2014). Recently, a number of promising cultivation concepts such as tubular, flat panel, and thin-layer reactors have been developed, enabling the generation of biomass concentrations of up to 50 g<sub>CDW</sub> L<sup>-1</sup> (Apel *et al.*, 2017; Bähr *et al.*, 2016; Dasgupta *et al.*, 2010). These technologies primarily focus on the generation of CO<sub>2</sub>-derived chemical products and now have to be transferred to biotransformation applications, such as the oxyfunctionalization of hydrocarbons (Lippi *et al.*, 2018). Beside biocatalyst growth to high concentrations (> 10 g<sub>CDW</sub> L<sup>-1</sup>), the technical reaction setting must allow efficient substrate mass transfer and high product titers including *in situ* product removal technologies for efficient post-process product recovery. The application of cyanobacterial biofilm-coated capillaries constitutes another promising technology, allowing



for continuous bioprocessing (David *et al.*, 2015; Strieth *et al.*, 2018). High surface to volume ratios enhance the light distribution and therefore allow increased phototrophic biocatalyst growth and consequently increased productivities. Algal biofilms (such as *Chlorella* sp.) were reported to grow to cell densities of ca. 25 g m<sup>-2</sup> on polystyrene foam (Johnson and Wen, 2010). Growing such dense biofilms in tubes with an inner diameter of 2 mm, as it was shown for *Synechocystis* sp. PCC 6803 (David *et al.*, 2015), in theory enable biomass concentrations of up to 100 g<sub>CDW</sub> L<sub>tube</sub><sup>-1</sup>. With such a high biomass concentration and a specific activity of 100 U g<sub>CDW</sub><sup>-1</sup>, the application of phototrophic biocatalysts overcoming O<sub>2</sub> limitation would theoretically allow an increase of productivities from 5.6 up to 30 g<sub>product</sub> L<sup>-1</sup> h<sup>-1</sup> (100 g mol<sup>-1</sup> molar mass of the product) for efficient light-dependent biocatalytic oxyfunctionalization at scale.

### **7.7 Conclusion**

The *in situ* generation of O<sub>2</sub> in the liquid phase has a large potential to overcome limitations of the productivity by the O<sub>2</sub> availability in O<sub>2</sub>-dependent whole-cell bioprocesses. Photosynthetically active biocatalysts that evolve O<sub>2</sub> *in situ* via the photosynthetic water splitting reaction, which simultaneously supplies oxygenases with activated electrons, can efficiently overcome limitations by O<sub>2</sub> mass transfer. Now, photo-bioreactor systems have to be developed that combine the technologies available for photo-biocatalyst cultivation and biotransformations. Photosynthesis has a great potential to considerably raise the productivity process boundary of biocatalytic oxyfunctionalizations in a highly eco-efficient way.

### **7.8 Acknowledgements**

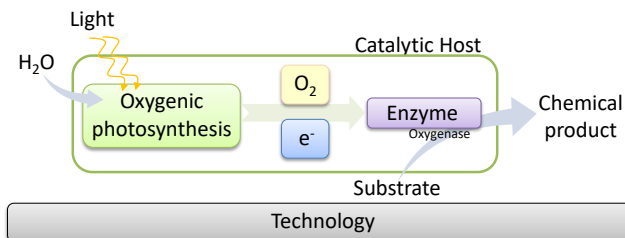
The authors are grateful to Christian Willrodt for helpful discussions and proofreading of the manuscript.



## **Chapter 8      Conclusions & Outlook**

## 8.1 Conclusions & Outlook

Biocatalysis targets the synthesis of fuels and chemical compounds using a biological system that is applied in a technological reaction setup (**Figure 8.1**). Oxygenic photosynthesis is a highly valuable driver for industrially relevant redox biotransformations such as the oxyfunctionalization of hydrocarbons (**Chapter 1**).



**Figure 8.1:** Conceptual design of photosynthesis-driven biotransformations. Redox enzymes (oxygenases) catalyze the conversion of substrates to the targeted oxyfunctionalized chemical products and are fueled with electrons and O<sub>2</sub> derived from oxygenic photosynthesis. The applied technological system encloses the catalytic host and facilitates the supply with sufficient light, nutrients, and substrates as well as product extraction.

Via photosynthetic water oxidation, reduction equivalents as well as O<sub>2</sub>, both co-substrates of oxygenases, are accessed by the energy of light. Isolated enzymes and chemoheterotrophic biocatalysts are frequently applied, while the photobiotechnological application of photoautotrophic organisms in redox biocatalysis is rare. This thesis aimed at the development and investigation of photosynthesis-driven oxyfunctionalization bioprocesses that go beyond the proof-of-concept catalyst development stage. An integrated bioprocess design concept (**Chapter 1**), comprising biocatalyst, reaction, and process engineering tools, was followed to conceptually evaluate the photosynthetic O<sub>2</sub> and electron supply as well as the technical application of cyanobacteria as phototrophic biocatalysts. The following sections conclude the main outcomes of this work and provide prospects for the design of eco-efficient oxyfunctionalization bioprocesses.

### ***Synechocystis* sp. PCC 6803 is a suitable biocatalytic host for oxyfunctionalizations.**

Integrated bioprocess development relied on the construction of two recombinant cyanobacterial strains. The alkane monooxygenase enzyme system AlkBGT, originating from *Pseudomonas putida* GPo1, and a CYP enzyme system, originating from *Acidovorax* sp. CHX100, were genetically introduced into *Synechocystis* sp. PCC 6803 resulting in Syn6803\_BGT (**Chapter 3**) and Syn6803\_CYP (**Chapter 5**). Both strains functionally catalyzed the hydroxylation of nonanoic acid methyl ester (NAME) to 9-hydroxynonanoic acid methyl ester (H-NAME) and cyclohexane to cyclohexanol, respectively. Biochemical analysis revealed that, in comparison to the total endogenous protein amount, Syn6803\_BGT and

Syn6803\_CYP synthesized the heterologous proteins at rather low concentrations (**Chapter 4**, **Chapter 5**). Although *Synechocystis* sp. PCC 6803 constitutes the model organisms for photoautotrophic biocatalysts, controlled overexpression of genes and thus the synthesis of the target proteins at high specific concentrations is hindered by the limited availability of promoter and plasmid systems. Therefore, future developments have to address the elaboration on these genetic engineering tools for improving the expression system function. Next to low heterologous protein levels, Syn6803\_BGT showed high catalytic activity towards the hydrolysis of the substrate NAME, resulting in the formation of the toxic reactant nonanoic acid (NA) (**Chapter 4**). Thus, the biocatalytic chassis may be engineered for the elimination of this side reaction. In a comparable study on several *E. coli* strains, the carboxylesterase BioH was identified as medium-chain length fatty acid methyl ester hydrolyzing enzyme and thus might be a potential target for a knock-out strategy in Syn6803\_BGT (Kadisich *et al.*, 2017a). The biocatalytic host system may also be changed to another cyanobacterial chassis potentially facilitating a reduced or even lacking side-reaction activity. Furthermore, phototrophic strains possessing accelerated growth rates for faster biocatalyst growth or enhanced solvent tolerance for improved reaction robustness would be relevant. A promising candidate for further evaluation is *Synechococcus elongatus* UTEX 2973 which was (re-) identified in 2015 and capable of growing at high rates with a doubling time of 2.1 h (in comparison 6.6 h for *Synechocystis* sp. PCC 6803) (Yu *et al.*, 2015a). Eventually, the complementation of above described strain engineering strategies with the application of further oxygenases, e.g., the Baeyer-Villiger cyclohexanone monooxygenase, but also of other redox enzymes, such as hydrogenases, will broaden the reaction and thus the product scope of photosynthesis-driven biotransformations.

**Photosynthetic water oxidation is a valuable source of O<sub>2</sub>.** Biocatalyst characterization followed the biocatalyst development with a focus on evaluating the possibilities of linking photosynthetic O<sub>2</sub> and electron sources to productive biocatalysis. Under exclusion of external O<sub>2</sub>, Syn6803\_BGT captured nearly 25% of photosynthetically generated O<sub>2</sub> for the hydroxylation of NAME (**Chapter 3**). In addition, *in situ* O<sub>2</sub> supply allowed the operation of bioreactors without aeration during Syn6803\_CYP biotransformation, preventing substrate (cyclohexane) evaporation and thus enhancing process stability (**Chapter 5**). The *in situ* generation of photosynthetically generated O<sub>2</sub> is a highly promising concept for redox biocatalysis, overcoming the need for external gas-liquid mass transfer (**Chapter 7**). O<sub>2</sub>-respiring catalyst restrict the maximum achievable productivity to 5.6 g L<sup>-1</sup> h<sup>-1</sup>. In contrast, O<sub>2</sub>-evolving photobiocatalysts possess the ability to shift this O<sub>2</sub>-boundary far in excess of the reactor intrinsic oxygen transfer rate of 9 g L<sup>-1</sup> h<sup>-1</sup> (traditional large-scale stirred tank bioreactor). In conclusion, cyanobacteria inherently provide a promising technological solution for otherwise O<sub>2</sub> limited, large-scale redox bioprocesses.

***In situ* extraction of O<sub>2</sub> potentially facilitates O<sub>2</sub>-sensitive bioprocesses.** The concept of *in situ* capturing photosynthetically generated O<sub>2</sub> overcomes gas-liquid mass transfer limitations. In addition, it also features a promising solution for photosynthesis-driven, but O<sub>2</sub>-sensitive bioprocesses. An example is the photosynthesis-driven production of hydrogen. Hydrogen with its high energy density is regarded as a favorable future zero-emission fuel gas. Production of hydrogen via coupling the photosynthetic water oxidation with hydrogenases constitutes a highly promising alternative technology to the power-demanding electrolysis of water. However, due to the inherent O<sub>2</sub> generation during photosynthetic water oxidation, photobiotechnological production of hydrogen suffers from O<sub>2</sub>-sensitive hydrogenases as well as the formation of explosive oxyhydrogen gas (Knallgas). Current approaches aim at the technical separation of the two gases or the identification and development of O<sub>2</sub>-resistant hydrogenases. In a patent application, we emphasize a novel approach of co-applying hydrogenases with oxygenases as O<sub>2</sub>-consuming enzyme (**Chapter 10.4**). Accumulating O<sub>2</sub> is *in situ* captured at its place of generation, potentially preventing hydrogenase inactivation and furthermore reducing the risk of oxy hydrogen gas formation.

**Photosynthetic water oxidation is a valuable source of activated reduction equivalents.** So far, cofactor regeneration constitutes a key parameter in standard enzymatic as well as whole-cell redox biocatalysis. The photosynthetic light reaction provides a rich source of electrons originating from water, accessed by the energy of light. By increasing the light intensity, and thus the photosynthetic water oxidation rate, cyclohexane oxyfunctionalization activities of Syn6803\_CYP were increased from 6 to 26 U<sub>gCDW</sub><sup>-1</sup> (**Chapter 5**). The rate of oxyfunctionalization equals the rate of heterotrophic biocatalysts harboring the very same enzyme system (Karande *et al.*, 2016a) and thus demonstrates the successful change of the cofactor regeneration system from a carbohydrate-based to a photosynthesis driven metabolism. The characterization of the electron flux (electron balance) from water oxidation at the photosystems PSII to the heterologous redox enzyme will provide an understanding of, and potential engineering targets for the interplay of the introduced electron sink within the photosynthetic metabolism. On the one hand, the electron flux towards the oxygenase may be enhanced, e.g., by the knock-out of competing, electron demanding reactions as described in the general introduction (**Chapter 1**). On the other hand, the pathway of electron supply may be optimized, e.g., by engineering the cofactor specificity from NADH to NADPH-dependent oxygenases, the overexpression of endogenous reductases coupling with the introduced redox enzyme, or fusion of the heterologous enzyme in spatial proximity to the photosynthetic machinery (e.g., PSII). Importantly, determination of redox potentials of the heterologous redox enzyme and the endogenous electron transferring enzymes is a powerful strategy to disclose potential electron-accessing points allowing for maximum efficient electron abstraction.

**Reaction engineering via two-liquid phase biotransformation stabilizes photosynthesis-driven C-H oxyfunctionalization.** Biotransformation of pure substrates with Syn6803\_BGT or Syn6803\_CYP revealed a substantial reactant toxicity and mass transfer challenges. These issues tremendously affected the specific oxyfunctionalization rate (productivity) and biotransformation stability (yield and titer). *In situ* substrate supply via the application of a 2-liquid phase cultivation setup successfully enhanced the reaction performance with respect to productivities, yields on biomass, and titers for both reaction systems (**Chapter 4, Chapter 5**). In the case of Syn6803\_BGT, the use of DINP as organic carrier phase additionally reduced the side-reaction of substrate hydrolysis, potentially enabling higher yields on the substrate. Eventually, for Syn6803\_CYP, the reaction engineering approach resulted in 1.5 times enhanced initial specific activities of ca.  $40 \text{ U g}_{\text{CDW}}^{-1}$  and a pro-longed biotransformation stability of  $> 24 \text{ h}$  resulting in 10 times increased final yields of  $4.5 \text{ g}_{\text{product}} \text{ g}_{\text{CDW}}^{-1}$ . Further reaction engineering may even improve these productivities and yields e.g., by improvement of growth and reaction conditions including medium optimization,  $\text{CO}_2$  and light supply. Furthermore, the consumption of materials as well as metabolic resources may be reduced by decoupling the biotransformation phase from growth. Bioprocesses based on heterotrophic whole-cells can benefit from the omission of growth-essential nutrients such as nitrogen or magnesium, thus preventing cell growth (Julsing *et al.*, 2012a; McIver *et al.*, 2008; Willrodt *et al.*, 2016). The physiological state of these resting cells possesses decreased metabolic competition for reduced cofactors and thus enables higher reaction rates for product formation. The concept of production decoupled from growth might be beneficial for photosynthesis driven oxyfunctionalization as well, although the exclusion of nutrients such as nitrogen might be detrimental to the photosynthetic functionality of cyanobacteria as degradation of phycobilisomes (chlorosis) was observed (Richaud *et al.*, 2001).

**Successful application of *Synechocystis* sp. PCC 6803 in a technical process setting.** The application of Syn6803\_BGT and Syn6803\_CYP in a technical process setting promoted the integrated development of a photobiocatalytic biotransformation process. Biocatalyst growth and gene expression were successfully transferred from a mL shake-flask to the multi-liter scale in a stirred-tank photobioreactor (**Chapter 4, Chapter 5**). Two-liquid phase biotransformations under process conditions without aeration enabled for the first time the photosynthesis-driven production of 2.6 g cyclohexanol from cyclohexane, water, and light. A further increase in total product amount will necessitate higher biomass concentrations, increased volumes and prolonged biotransformation times. Scaling of standard stirred tank bioreactors would result in decreased surface to volume ratios, resulting in impaired light distribution and thus photosynthetic activity. A highly promising technology for the cultivation of phototrophic organisms relies in the miniaturization of reaction systems. At the scale of a

capillary reactor, the surface to volume ratio and thus the light distribution to the phototrophic organisms is maximized, allowing for high photosynthetic and thus biocatalytic activities. The operation of a mixed-species biofilm in a capillary reactor setting enabled the continuous cultivation of *Synechocystis* sp. PCC 6803 at exceptionally high biomass concentrations of  $48 \text{ g}_{\text{CDW}} \text{ L}^{-1}$  (Chapter 6). The biofilm supporting, co-applied strain *Pseudomonas* sp. VLB120 enhanced the surface coverage and reduced oxidative stress by the respiration of  $\text{O}_2$ . The capillary reactor setting now faces the integration of recombinant protein activity and, subsequently, reaction engineering strategies for appropriate substrate supply and product removal, including downstream processing. Finally, numbering up is a promising strategy for scaling the reaction system, retaining the advantage of the miniaturized setting, i.e., high surface to volume ratio.

### 8.2 Concluding remarks

Combining the achievements of this thesis, comprising a specific initial activity of ca.  $40 \text{ U g}_{\text{CDW}}^{-1}$ , a cyanobacterial biomass concentration of  $41 \text{ g}_{\text{CDW}} \text{ L}^{-1}$ , and a biotransformation stability of 52 h in one bioprocess setting, would already facilitate industrially relevant productivities, titers and yields of ca.  $10 \text{ g L}^{-1} \text{ h}^{-1}$ ,  $500 \text{ g L}^{-1}$  and  $12.5 \text{ g g}_{\text{CDW}}^{-1}$ , respectively, for a  $100 \text{ g mol}^{-1}$  molecular weight product. This requires the retention of the high specific activities throughout the entire biotransformation time. Using a standard stirred tank photobioreactor, high biocatalyst concentrations need to be realized. In turn, the application of a biofilm-capillary reactor system necessitates the implementation of high specific oxyfunctionalization activities. In conclusion, oxygenic photosynthesis constitutes a highly promising driver for redox biocatalysis. Continuing the integration of biocatalyst-, reaction-, and process engineering will facilitate the successful development of photosynthesis-driven redox biotransformations. Eventually, photosynthesis as the billion years old milestone of natural evolution may develop into a milestone for the eco-efficient production of fuels and value-added chemicals.



**Chapter 9    References**

- Abe, R., 2010. Recent progress on photocatalytic and photoelectrochemical water splitting under visible light irradiation. *J. Photochem. Photobiol.*, **C**, **11**, 179-209.
- Adlercreutz, P., Holst, O., Mattiasson, B., 1982. Oxygen supply to immobilized cells: 2. Studies on a coimmobilized algae - bacteria preparation with *in situ* oxygen generation. *Enzyme Microb. Technol.* **4**, 395-400.
- Adlercreutz, P., Mattiasson, B., 1982. Oxygen supply to immobilized cells: 1. Oxygen production by immobilized *Chlorella pyrenoidosa*. *Enzyme Microb. Technol.* **4**, 332-336.
- Albers, S. C., Gallegos, V. A., Peebles, C. A., 2015. Engineering of genetic control tools in *Synechocystis* sp. PCC 6803 using rational design techniques. *J. Biotechnol.* **216**, 36-46.
- Anastas, P., Eghbali, N., 2010. Green chemistry: principles and practice. *Chem. Soc. Rev.* **39**, 301-312.
- Angermayr, S. A., Paszota, M., Hellingwerf, K. J., 2012. Engineering a cyanobacterial cell factory for production of lactic acid. *Appl. Environ. Microbiol.* **78**, 7098-7106.
- Apel, A., Pfaffinger, C., Basedahl, N., Mittwollen, N., Göbel, J., Sauter, J., Brück, T., Weuster-Botz, D., 2017. Open thin-layer cascade reactors for saline microalgae production evaluated in a physically simulated Mediterranean summer climate. *Algal Res.* **25**, 381-390.
- Aro, E.-M., Virgin, I., Andersson, B., 1993. Photoinhibition of photosystem II. Inactivation, protein damage and turnover. *Biochim. Biophys. Acta, Bioenerg.* **1143**, 113-134.
- Austin, R. N., Groves, J. T., 2011. Alkane-oxidizing metalloenzymes in the carbon cycle. *Metalomics*. **3**, 775-87.
- Bachmann, B. J., 1996. Derivations and genotypes of some mutant derivatives of *Escherichia coli* K-12. *Escherichia coli and Salmonella: cellular and molecular biology*, 2nd ed. ASM Press, Washington, DC. 2460-2488.
- Bähr, L., Wüstenberg, A., Ehwald, R., 2016. Two-tier vessel for photoautotrophic high-density cultures. *J. Appl. Phycol.* **28**, 783-793.
- Bailey, S., Grossman, A., 2008. Photoprotection in cyanobacteria: regulation of light harvesting. *Photochem. Photobiol.* **84**, 1410-1420.
- Balcerzak, L., Lipok, J., Strub, D., Lochyński, S., 2014. Biotransformations of monoterpenes by photoautotrophic micro-organisms. *J. Appl. Microbiol.* **117**, 1523-1536.
- Baldwin, C. V., Woodley, J. M., 2006. On oxygen limitation in a whole cell biocatalytic Baeyer-Villiger oxidation process. *Biotechnol. Bioeng.* **95**, 362-369.
- Barros, A. C., Gonçalves, A. L., Simões, M., 2018. Microalgal/cyanobacterial biofilm formation on selected surfaces: the effects of surface physicochemical properties and culture media composition. *J. Appl. Phycol.*, 1-13.
- Bathellier, C., Tcherkez, G., Lorimer, G. H., Farquhar, G. D., 2018. Rubisco is not really so bad. *Plant Cell Environ.* **41**, 705-716.
- Beardall, J., Raven, J. A., 2013. Limits to phototrophic growth in dense culture: CO<sub>2</sub> supply and light. *Springer*, Dordrecht.
- Beenackers, A., van Swaaij, W. P. M., 1993. Mass transfer in gas-liquid slurry reactors. *Chem. Eng. Sci.* **48**, 3109-3139.
- Benson, S., Fennewald, M., Shapiro, J., Huettner, C., 1977. Fractionation of inducible alkane hydroxylase activity in *Pseudomonas putida* and characterization of hydroxylase-negative plasmid mutations. *J. Bacteriol.* **132**, 614-621.
- Benson, S., Oppici, M., Shapiro, J., Fennewald, M., 1979. Regulation of membrane peptides by the *Pseudomonas* plasmid *alk regulon*. *J. Bacteriol.* **140**, 754-762.
- Berepiki, A., Hitchcock, A., Moore, C. M., Bibby, T. S., 2016. Tapping the unused potential of photosynthesis with a heterologous electron sink. *ACS Synth. Biol.* **5**, 1369-1375.
- Blank, L. M., Ebert, B. E., Buehler, K., Bühler, B., 2010. Redox biocatalysis and metabolism: molecular mechanisms and metabolic network analysis. *Antioxid. Redox. Sign.* **13**, 349-394.
- Blank, L. M., Ebert, B. E., Bühler, B., Schmid, A., 2008. Metabolic capacity estimation of *Escherichia coli* as a platform for redox biocatalysis: constraint-based modeling and experimental verification. *Biotechnol. Bioeng.* **100**, 1050-1065.

- Bloom, J. D., Meyer, M. M., Meinhold, P., Otey, C. R., MacMillan, D., Arnold, F. H., 2005. Evolving strategies for enzyme engineering. *Curr. Opin. Struc. Biol.* **15**, 447-452.
- Böhmer, S., Köninger, K., Gómez-Baraibar, A., Bojarra, S., Mügge, C., Schmidt, S., Nowaczyk, M. M., Kourist, R., 2017. Enzymatic oxyfunctionalization driven by photosynthetic water-splitting in the cyanobacterium *Synechocystis* sp. PCC 6803. *Catalysts*. **7**, 240.
- Bolivar, J. M., Krämer, C. E., Ungerböck, B., Mayr, T., Nidetzky, B., 2016. Development of a fully integrated falling film microreactor for gas–liquid–solid biotransformation with surface immobilized O<sub>2</sub>-dependent enzyme. *Biotechnol. Bioeng.* **113**, 1862-1872.
- Bordeaux, M., Galarneau, A., Drone, J., 2012. Catalytic, mild, and selective oxyfunctionalization of linear alkanes: current challenges. *Angew. Chem., Int. Ed.* **51**, 10712-10723.
- Bormann, S., Baraibar, A. G., Ni, Y., Holtmann, D., Hollmann, F., 2015. Specific oxyfunctionalisations catalysed by peroxygenases: opportunities, challenges and solutions. *Catal. Sci. Technol.* **5**, 2038-2052.
- Bornscheuer, U., Huisman, G., Kazlauskas, R., Lutz, S., Moore, J., Robins, K., 2012. Engineering the third wave of biocatalysis. *Nature*. **485**, 185-194.
- Bradford, M. M., 1976. A rapid and sensitive method for the quantitation of microgram quantities of protein utilizing the principle of protein-dye binding. *Anal. Biochem.* **72**, 248-254.
- Bühler, B., Bollhalder, I., Hauer, B., Witholt, B., Schmid, A., 2003a. Chemical biotechnology for the specific oxyfunctionalization of hydrocarbons on a technical scale. *Biotechnol. Bioeng.* **82**, 833-842.
- Bühler, B., Bollhalder, I., Hauer, B., Witholt, B., Schmid, A., 2003b. Use of the two-liquid phase concept to exploit kinetically controlled multistep biocatalysis. *Biotechnol. Bioeng.* **81**, 683-694.
- Bühler, B., Park, J. B., Blank, L. M., Schmid, A., 2008. NADH availability limits asymmetric biocatalytic epoxidation in a growing recombinant *Escherichia coli* strain. *Appl. Environ. Microbiol.* **74**, 1436-1446.
- Bühler, B., Schmid, A., 2004. Process implementation aspects for biocatalytic hydrocarbon oxyfunctionalization. *J. Biotechnol.* **113**, 183-210.
- Bühler, B., Straathof, A. J., Witholt, B., Schmid, A., 2006. Analysis of two-liquid-phase multistep biooxidation based on a process model: indications for biological energy shortage. *Org. Process Res. Dev.* **10**, 628-643.
- Bühler, B., Witholt, B., Hauer, B., Schmid, A., 2002. Characterization and application of Xylene Monooxygenase for multistep biocatalysis. *Appl. Environ. Microbiol.* **68**, 560-568.
- Burton, S. G., Cowan, D. A., Woodley, J. M., 2002. The search for the ideal biocatalyst. *Nat. Biotechnol.* **20**, 37-45.
- Calhoun, M. W., Oden, K. L., Gennis, R. B., de Mattos, M. J., Neijssel, O. M., 1993. Energetic efficiency of *Escherichia coli*: effects of mutations in components of the aerobic respiratory chain. *J. Bacteriol.* **175**, 3020-3025.
- Camsund, D., Lindblad, P., 2014. Engineered transcriptional systems for cyanobacterial biotechnology. *Frontiers in Bioengineering and Biotechnology*. **2**, 40.
- Carmichael, A. B., Wong, L. L., 2001. Protein engineering of *Bacillus megaterium* CYP102: the oxidation of polycyclic aromatic hydrocarbons. *Eur. J. Biochem.* **268**, 3117-3125.
- Carvalho, C. C., 2017. Whole cell biocatalysts: essential workers from nature to the industry. *Microb. Biotechnol.* **10**, 250-263.
- Chaudhari, R., Bhattacharya, A., Bhanage, B., 1995. Catalysis with soluble complexes in gas-liquid-liquid systems. *Catal. Today*. **24**, 123-133.
- Chaumont, D., 1993. Biotechnology of algal biomass production: a review of systems for outdoor mass culture. *J. Appl. Phycol.* **5**, 593-604.
- Cheirsilp, B., Suwannarat, W., Niyomdecha, R., 2011. Mixed culture of oleaginous yeast *Rhodotorula glutinis* and microalga *Chlorella vulgaris* for lipid production from industrial wastes and its use as biodiesel feedstock. *New Biotechnol.* **28**, 362-368.

- Chemspider database structure 7866, <http://www.chemspider.com/Chemical-Structure.7866.html>, accessed on 12.11.2018
- Chemspider database structure 14846, <http://www.chemspider.com/Chemical-Structure.14846.html>, accessed on 12.11.2018
- Chin, T., Sano, M., Takahashi, T., Ohara, H., Aso, Y., 2015. Photosynthetic production of itaconic acid in *Synechocystis* sp. PCC6803. *J. Biotechnol.* **195**, 43-45.
- Chmiel, H., 1991. Bioprozesstechnik. Band 2. Angewandte Bioverfahrenstechnik. *Gustav Fischer*, Stuttgart.
- Cornelissen, S., Julsing, M. K., Volmer, J., Riechert, O., Schmid, A., Bühler, B., 2013. Whole-cell-based CYP153A6-catalyzed (*S*)-limonene hydroxylation efficiency depends on host background and profits from monoterpene uptake via AlkL. *Biotechnol. Bioeng.* **110**, 1282-1292.
- Cornils, B., Herrmann, W. A., 2004. Aqueous-phase organometallic catalysis: concepts and applications. *John Wiley & Sons*, Weinheim.
- Dalton, H., 1980. Oxidation of hydrocarbons by methane monooxygenases from a variety of microbes. *Adv. Appl. Microbiol.* **26**, 71-87.
- Das, D., Veziroğlu, T. N., 2001. Hydrogen production by biological processes: a survey of literature. *Int. J. Hydrogen Energy.* **26**, 13-28.
- Dasgupta, C. N., Gilbert, J. J., Lindblad, P., Heidorn, T., Borgvang, S. A., Skjanes, K., Das, D., 2010. Recent trends on the development of photobiological processes and photobioreactors for the improvement of hydrogen production. *Int. J. Hydrogen Energy.* **35**, 10218-10238.
- David, C., Bühler, K., Schmid, A., 2015. Stabilization of single species *Synechocystis* biofilms by cultivation under segmented flow. *J. Ind. Microbiol. Biotechnol.* **42**, 1083-1090.
- David, C., Schmid, A., Adrian, L., Wilde, A., Buehler, K., 2018. Production of 1, 2-propanediol in photoautotrophic *Synechocystis* is linked to glycogen turn-over. *Biotechnol. Bioeng.* **115**, 300-311.
- de Bont, J. A., 1998. Solvent-tolerant bacteria in biocatalysis. *Trends Biotechnol.* **16**, 493-499.
- de Carvalho, C. C., 2011. Enzymatic and whole cell catalysis: finding new strategies for old processes. *Biotechnol. Adv.* **29**, 75-83.
- Dismukes, G. C., Brimblecombe, R., Felton, G. A., Pryadun, R. S., Sheats, J. E., Spiccia, L., Swiegers, G. F., 2009. Development of bioinspired Mn<sub>4</sub>O<sub>4</sub>-cubane water oxidation catalysts: lessons from photosynthesis. *Acc. Chem. Res.* **42**, 1935-1943.
- Dong, J., Fernández-Fueyo, E., Hollmann, F., Paul, C., Pasic, M., Schmidt, S., Wang, Y., Younes, S., Zhang, W., 2018. Biocatalytic oxidation reactions - a Chemist's perspective. *Angew. Chem.* **130**, 9380-9404.
- Duetz, W. A., van Beilen, J. B., Witholt, B., 2001. Using proteins in their natural environment: potential and limitations of microbial whole-cell hydroxylations in applied biocatalysis. *Curr. Opin. Biotechnol.* **12**, 419-425.
- Emmerling, M., Dauner, M., Ponti, A., Fiaux, J., Hochuli, M., Szyperski, T., Wüthrich, K., Bailey, J., Sauer, U., 2002. Metabolic flux responses to pyruvate kinase knockout in *Escherichia coli*. *J. Bacteriol.* **184**, 152-164.
- Englund, E., Liang, F., Lindberg, P., 2016. Evaluation of promoters and ribosome binding sites for biotechnological applications in the unicellular cyanobacterium *Synechocystis* sp. PCC 6803. *Sci. Rep.* **6**, 36640.
- Eş, İ., Vieira, J. D. G., Amaral, A. C., 2015. Principles, techniques, and applications of biocatalyst immobilization for industrial application. *Appl. Microbiol. Biotechnol.* **99**, 2065-2082.
- Evonik Industries AG, Biobased  $\omega$ -amino lauric acid - More flexibility in the production of high-performance plastics. Elements 45 - Quarterly Science Newsletter, 2013, pp. 13.
- Fasan, R., Chen, M. M., Crook, N. C., Arnold, F. H., 2007. Engineered alkane-hydroxylating cytochrome P450 BM3 exhibiting nativelike catalytic properties. *Angew. Chem., Int. Ed.* **46**, 8414-8418.

- Fasan, R., Crook, N. C., Peters, M. W., Meinhold, P., Buelter, T., Landwehr, M., Cirino, P. C., Arnold, F. H., 2011. Improved product-per-glucose yields in P450-dependent propane biotransformations using engineered *Escherichia coli*. *Biotechnol. Bioeng.* **108**, 500-510.
- Ferreira, E. M. A., Evaluation and improvement of *Synechocystis* sp. PCC 6803 tolerance to temperature and development of Synthetic Biology tools. *Universidade do Porto*, 2014.
- Fiedler, A. T., Fischer, A. A., 2017. Oxygen activation by mononuclear Mn, Co, and Ni centers in biology and synthetic complexes. *J. Biol. Inorg. Chem.* **22**, 407-424.
- Fresewinkel, M., Rosello, R., Wilhelm, C., Kruse, O., Hankamer, B., Posten, C., 2014. Integration in microalgal bioprocess development: design of efficient, sustainable, and economic processes. *Eng. Life Sci.* **14**, 560-573.
- Fukuzumi, S., Mizuno, T., Ojiri, T., 2012. Catalytic electron-transfer oxygenation of substrates with water as an oxygen source using manganese porphyrins. *Chem. - Eur. J.* **18**, 15794-15804.
- Funyu, S., Isobe, T., Takagi, S., Tryk, D. A., Inoue, H., 2003. Highly efficient and selective epoxidation of alkenes by photochemical oxygenation sensitized by a ruthenium (II) porphyrin with water as both electron and oxygen donor. *J. Am. Chem. Soc.* **125**, 5734-5740.
- Garcia-Ochoa, F., Gomez, E., 2009. Bioreactor scale-up and oxygen transfer rate in microbial processes: an overview. *Biotechnol. Adv.* **27**, 153-176.
- Garcia, H. E., Gordon, L. I., 1992. Oxygen solubility in seawater: Better fitting equations. *Limnol. Oceanogr.* **37**, 1307-1312.
- Garcia, H. E., Gordon, L. I., 1993. Erratum: Oxygen solubility in seawater: Better fitting equations. *Limnol. Oceanogr.* **38**, 656-656.
- Gavriilidis, A., Constantinou, A., Hellgardt, K., Hii, K. K. M., Hutchings, G. J., Brett, G. L., Kuhn, S., Marsden, S. P., 2016. Aerobic oxidations in flow: opportunities for the fine chemicals and pharmaceuticals industries. *React. Chem. Eng.* **1**, 595-612.
- Gemoets, H. P., Su, Y., Shang, M., Hessel, V., Luque, R., Noël, T., 2016. Liquid phase oxidation chemistry in continuous-flow microreactors. *Chem. Soc. Rev.* **45**, 83-117.
- Gibson, D. G., Young, L., Chuang, R. Y., Venter, J. C., Hutchison, C. A., 3rd, Smith, H. O., 2009. Enzymatic assembly of DNA molecules up to several hundred kilobases. *Nat. Methods.* **6**, 343-345.
- Girvan, H. M., Dunford, A. J., Neeli, R., Ekanem, I. S., Waltham, T. N., Joyce, M. G., Leys, D., Curtis, R. A., Williams, P., Fisher, K., 2011. Flavocytochrome P450 BM3 mutant W1046A is a NADH-dependent fatty acid hydroxylase: implications for the mechanism of electron transfer in the P450 BM3 dimer. *Arch. Biochem. Biophys.* **507**, 75-85.
- Glieder, A., Farinas, E. T., Arnold, F. H., 2002. Laboratory evolution of a soluble, self-sufficient, highly active alkane hydroxylase. *Nat. Biotechnol.* **20**, 1135-1139.
- Gofñi, G., Zöllner, A., Lisurek, M., Velázquez-Campoy, A., Pinto, S., Gómez-Moreno, C., Hannemann, F., Bernhardt, R., Medina, M., 2009. Cyanobacterial electron carrier proteins as electron donors to CYP106A2 from *Bacillus megaterium* ATCC 13368. *Biochim. Biophys. Acta, Proteins Proteomics.* **1794**, 1635-1642.
- Greene, J. F., Preger, Y., Stahl, S. S., Root, T. W., 2015. PTFE-membrane flow reactor for aerobic oxidation reactions and its application to alcohol oxidation. *Org. Process Res. Dev.* **19**, 858-864.
- Grobbelaar, J. U., 2009. Factors governing algal growth in photobioreactors: the "open" versus "closed" debate. *J. Appl. Phycol.* **21**, 489-492.
- Gross, R., Buehler, K., Schmid, A., 2013. Engineered catalytic biofilms for continuous large scale production of n-octanol and (S)-styrene oxide. *Biotechnol. Bioeng.* **110**, 424-436.
- Gross, R., Hauer, B., Otto, K., Schmid, A., 2007. Microbial biofilms: new catalysts for maximizing productivity of long-term biotransformations. *Biotechnol. Bioeng.* **98**, 1123-1134.
- Gross, R., Lang, K., Bühler, K., Schmid, A., 2010. Characterization of a biofilm membrane reactor and its prospects for fine chemical synthesis. *Biotechnol. Bioeng.* **105**, 705-717.
- Halan, B., Buehler, K., Schmid, A., 2012. Biofilms as living catalysts in continuous chemical syntheses. *Trends Biotechnol.* **30**, 453-465.

- Hanahan, D., 1983. Studies on transformation of *Escherichia coli* with plasmids. *J. Mol. Biol.* **166**, 557-580.
- Hara, M., Ohkawa, H., Narato, M., Shirai, M., Asada, Y., Karube, I., Miyake, J., 1997. Regeneration of NADPH by cactus chloroplasts: Coupling reaction with P450 monooxygenase. *J. Ferment. Bioeng.* **84**, 324-329.
- Harada, K.-I., Ozaki, K., Tsuzuki, S., Kato, H., Hasegawa, M., Kuroda, E. K., Arii, S., Tsuji, K., 2009. Blue color formation of cyanobacteria with  $\beta$ -cyclocitral. *J. Chem. Ecol.* **35**, 1295-1301.
- Harayama, S., Reikik, M., 1990. The meta cleavage operon of TOL degradative plasmid pWVO comprises 13 genes. *Mol. Gen. Genet.* **221**, 113-120.
- Harnastai, I. N., Gilep, A. A., Usanov, S. A., 2006. The development of an efficient system for heterologous expression of cytochrome P450s in *Escherichia coli* using *hemA* gene co-expression. *Protein Expression Purif.* **46**, 47-55.
- Hartmans, S., van der Werf, M., de Bont, J., 1990. Bacterial degradation of styrene involving a novel flavin adenine dinucleotide-dependent styrene monooxygenase. *Appl. Environ. Microbiol.* **56**, 1347-1351.
- Hayaishi, O., Katagiri, M., Rothberg, S., 1955. Mechanism of the pyrocatechase reaction. *J. Am. Chem. Soc.* **77**, 5450-5451.
- Heidorn, T., Camsund, D., Huang, H. H., Lindberg, P., Oliveira, P., Stensjo, K., Lindblad, P., 2011. Synthetic biology in cyanobacteria engineering and analyzing novel functions. *Methods Enzymol.* **497**, 539-579.
- Hibbert, E. G., Baganz, F., Hailles, H. C., Ward, J. M., Lye, G. J., Woodley, J. M., Dalby, P. A., 2005. Directed evolution of biocatalytic processes. *Biomol. Eng.* **22**, 11-19.
- Hilker, I., Baldwin, C., Alphand, V., Furstoss, R., Woodley, J., Wohlgemuth, R., 2006. On the influence of oxygen and cell concentration in an SFPR whole cell biocatalytic Baeyer-Villiger oxidation process. *Biotechnol. Bioeng.* **93**, 1138-1144.
- Hilker, I., Gutiérrez, M. C., Furstoss, R., Ward, J., Wohlgemuth, R., Alphand, V., 2008. Preparative scale Baeyer-Villiger biooxidation at high concentration using recombinant *Escherichia coli* and *in situ* substrate feeding and product removal process. *Nat. Protoc.* **3**, 546-554.
- Hille, R., Rétey, J., Bartlewski-Hof, U., Reichenbecher, W., Schink, B., 1998. Mechanistic aspects of molybdenum-containing enzymes. *FEMS Microbiol. Rev.* **22**, 489-501.
- Hisatomi, T., Kubota, J., Domen, K., 2014. Recent advances in semiconductors for photocatalytic and photoelectrochemical water splitting. *Chem. Soc. Rev.* **43**, 7520-7535.
- Hollmann, F., Arends, I. W., Buehler, K., Schallmeyer, A., Bühler, B., 2011. Enzyme-mediated oxidations for the chemist. *Green Chem.* **13**, 226-265.
- Hollmann, F., Taglieber, A., Schulz, F., Reetz, M. T., 2007. A light-driven stereoselective biocatalytic oxidation. *Angew. Chem., Int. Ed.* **46**, 2903-2906.
- Hong, H., Patel, D. R., Tamm, L. K., van den Berg, B., 2006. The outer membrane protein OmpW forms an eight-stranded  $\beta$ -barrel with a hydrophobic channel. *J. Biol. Chem.* **281**, 7568-7577.
- Hopper, D. J., 1978. Incorporation of [<sup>18</sup>O] water in the formation of *p*-hydroxybenzyl alcohol by the *p*-cresol methylhydroxylase from *Pseudomonas putida*. *Biochem. J.* **175**, 345-347.
- Huang, H. H., Camsund, D., Lindblad, P., Heidorn, T., 2010. Design and characterization of molecular tools for a Synthetic Biology approach towards developing cyanobacterial biotechnology. *Nucleic Acids Res.* **38**, 2577-2593.
- Huang, Q., Jiang, F., Wang, L., Yang, C., 2017. Design of photobioreactors for mass cultivation of photosynthetic organisms. *Engineering.* **3**, 318-329.
- Hudlicky, T., Reed, J. W., 2009. Applications of biotransformations and biocatalysis to complexity generation in organic synthesis. *Chem. Soc. Rev.* **38**, 3117-3132.
- Ihara, M., Nakamoto, H., Kamachi, T., Okura, I., Maeda, M., 2006a. Photoinduced hydrogen production by direct electron transfer from photosystem I cross-linked with cytochrome c3 to [NiFe]-hydrogenase. *Photochem. Photobiol.* **82**, 1677-1685.

- Ihara, M., Nishihara, H., Yoon, K. S., Lenz, O., Friedrich, B., Nakamoto, H., Kojima, K., Honma, D., Kamachi, T., Okura, I., 2006b. Light-driven hydrogen production by a hybrid complex of a [NiFe]-hydrogenase and the cyanobacterial photosystem I. *Photochem. Photobiol.* **82**, 676-682.
- Illner, S., Hofmann, C., Löb, P., Kragl, U., 2014. A falling-film microreactor for enzymatic oxidation of glucose. *ChemCatChem.* **6**, 1748-1754.
- Inoue, H., Funiyu, S., Shimada, Y., Takagi, S., 2005. Artificial photosynthesis via two-electron conversion: Photochemical oxygenation sensitized by ruthenium porphyrins with water as both electron and oxygen atom donor. *Pure Appl. Chem.* **77**, 1019-1033.
- Inoue, H., Okamoto, T., Kameo, Y., Sumitani, M., Fujiwara, A., Ishibashi, D., Hida, M., 1994. Photochemical epoxidation of cyclohexene sensitized by tetraphenylporphyrinatoantimony (V) in the presence of water acting both as an electron and an oxygen donor. *J. chem. Soc., Perkin Trans. 1.* 105-111.
- Jasniewski, A. J., Que Jr, L., 2018. Dioxygen activation by nonheme diiron enzymes: Diverse dioxygen adducts, high-valent intermediates, and related model complexes. *Chem. Rev.* **118**, 2554-2592.
- Jensen, K., Johnston, J. B., de Montellano, P. R., Møller, B. L., 2012. Photosystem I from plants as a bacterial cytochrome P450 surrogate electron donor: terminal hydroxylation of branched hydrocarbon chains. *Biotechnol. Lett.* **34**, 239-245.
- Jiao, Y., Zheng, Y., Jaroniec, M., Qiao, S. Z., 2015. Design of electrocatalysts for oxygen- and hydrogen-involving energy conversion reactions. *Chem. Soc. Rev.* **44**, 2060-2086.
- Johnson, M. B., Wen, Z., 2010. Development of an attached microalgal growth system for biofuel production. *Appl. Microbiol. Biotechnol.* **85**, 525-534.
- Jones, K. H., Smith, R. T., Trudgill, P. W., 1993. Diketocamphane enantiomer-specific "Baeyer-Villiger" monooxygenases from camphor-grown *Pseudomonas putida* ATCC 17453. *Microbiology.* **139**, 797-805.
- Julsing, M. K., Cornelissen, S., Bühler, B., Schmid, A., 2008. Heme-iron oxygenases: powerful industrial biocatalysts? *Curr. Opin. Chem. Biol.* **12**, 177-186.
- Julsing, M. K., Kuhn, D., Schmid, A., Bühler, B., 2012a. Resting cells of recombinant *E. coli* show high epoxidation yields on energy source and high sensitivity to product inhibition. *Biotechnol. Bioeng.* **109**, 1109-1119.
- Julsing, M. K., Schrewe, M., Cornelissen, S., Hermann, I., Schmid, A., Bühler, B., 2012b. Outer membrane protein AlkL boosts biocatalytic oxyfunctionalization of hydrophobic substrates in *Escherichia coli*. *Appl. Environ. Microbiol.* **78**, 5724-33.
- Kadisch, M., Schmid, A., Bühler, B., 2017a. Hydrolase BioH knockout in *E. coli* enables efficient fatty acid methyl ester bioprocessing. *J. Ind. Microbiol. Biotechnol.* **44**, 339-351.
- Kadisch, M., Willrodt, C., Hillen, M., Bühler, B., Schmid, A., 2017b. Maximizing the stability of metabolic engineering-derived whole-cell biocatalysts. *Biotechnol. J.* **12**, 1600170.
- Kantarci, N., Borak, F., Ulgen, K. O., 2005. Bubble column reactors. *Process Biochem.* **40**, 2263-2283.
- Karande, R., Debor, L., Salamanca, D., Bogdahn, F., Engesser, K. H., Buehler, K., Schmid, A., 2016a. Continuous cyclohexane oxidation to cyclohexanol using a novel cytochrome P450 monooxygenase from *Acidovorax* sp. CHX100 in recombinant *P. taiwanensis* VLB120 biofilms. *Biotechnol. Bioeng.* **113**, 52-61.
- Karande, R., Halan, B., Schmid, A., Buehler, K., 2014. Segmented flow is controlling growth of catalytic biofilms in continuous multiphase microreactors. *Biotechnol. Bioeng.* **111**, 1831-1840.
- Karande, R., Salamanca, D., Schmid, A., Buehler, K., 2017. Biocatalytic conversion of cycloalkanes to lactones using an in-vivo cascade in *Pseudomonas taiwanensis* VLB120. *Biotechnol. Bioeng.* **115**, 312-320.
- Karande, R., Schmid, A., Buehler, K., 2011. Miniaturizing biocatalysis: Enzyme-catalyzed reactions in an aqueous/organic segmented flow capillary microreactor. *Adv. Synth. Catal.* **353**, 2511-2521.
- Karande, R., Schmid, A., Buehler, K., 2016b. Applications of multiphase microreactors for biocatalytic reactions. *Org. Process Res. Dev.* **20**, 361-370.

- Khanna, N., Lindblad, P., 2015. Cyanobacterial hydrogenases and hydrogen metabolism revisited: recent progress and future prospects. *Int. J. Mol. Sci.* **16**, 10537-10561.
- Kim, P. Y., Pollard, D. J., Woodley, J. M., 2007. Substrate supply for effective biocatalysis. *Biotechnol. Prog.* **23**, 74-82.
- Knot, C. J., Ungerer, J., Wangikar, P. P., Pakrasi, H. B., 2018. Cyanobacteria: promising biocatalysts for sustainable chemical production. *J. Biol. Chem.* **293**, 5044-5052.
- Ko, S., Yang, Y.-H., Choi, K.-Y., Kim, B.-G., 2015. Rational design and directed evolution of CYP102A1 (BM3) for regio-specific hydroxylation of isoflavone. *Biotechnol. Bioprocess Eng.* **20**, 225-233.
- Königer, K., Gómez Baraibar, Á., Mügge, C., Paul, C. E., Hollmann, F., Nowaczyk, M. M., Kourist, R., 2016. Recombinant cyanobacteria for the asymmetric reduction of C=C bonds fueled by the biocatalytic oxidation of water. *Angew. Chem., Int. Ed.* **55**, 5582-5585.
- Koo, L. S., Tschirret-Guth, R. A., Straub, W. E., Moëne-Loccoz, P., Loehr, T. M., De Montellano, P. R. O., 2000. The active site of the thermophilic CYP119 from *Sulfolobus solfataricus*. *J. Biol. Chem.* **275**, 14112-14123.
- Kratzer, R., Woodley, J. M., Nidetzky, B., 2015. Rules for biocatalyst and reaction engineering to implement effective, NAD(P)H-dependent, whole cell bioreductions. *Biotechnol. Adv.* **33**, 1641-1652.
- Kuchner, O., Arnold, F. H., 1997. Directed evolution of enzyme catalysts. *Trends Biotechnol.* **15**, 523-530.
- Kuhn, D., Blank, L. M., Schmid, A., Bühler, B., 2010a. Systems biotechnology - Rational whole-cell biocatalyst and bioprocess design. *Eng. Life Sci.* **10**, 384-397.
- Kuhn, D., Bühler, B., Schmid, A., 2012a. Production host selection for asymmetric styrene epoxidation: *Escherichia coli* vs. solvent-tolerant *Pseudomonas*. *J. Ind. Microbiol. Biotechnol.* **39**, 1125-1133.
- Kuhn, D., Julsing, M. K., Heinzle, E., Bühler, B., 2012b. Systematic optimization of a biocatalytic two-liquid phase oxyfunctionalization process guided by ecological and economic assessment. *Green Chem.* **14**, 645-653.
- Kuhn, D., Kholiq, M. A., Heinzle, E., Bühler, B., Schmid, A., 2010b. Intensification and economic and ecological assessment of a biocatalytic oxyfunctionalization process. *Green Chem.* **12**, 815-827.
- Kumar, A., Narta, U. K., Azmi, W., 2017. The emergence of oxygen vectors in overcoming the challenges of oxygen transfer rate in aerobic bioprocesses. *Curr. Biochem. Eng.* **4**, 164-171.
- Kumar, K., Dasgupta, C. N., Nayak, B., Lindblad, P., Das, D., 2011. Development of suitable photobioreactors for CO<sub>2</sub> sequestration addressing global warming using green algae and cyanobacteria. *Bioresour. Technol.* **102**, 4945-4953.
- Laane, C., Boeren, S., Vos, K., Veeger, C., 1987. Rules for optimization of biocatalysis in organic solvents. *Biotechnol. Bioeng.* **30**, 81-87.
- Lacour, T., Ohkawa, H., 1999. Engineering and biochemical characterization of the rat microsomal cytochrome P4501A1 fused to ferredoxin and ferredoxin-NADP<sup>+</sup> reductase from plant chloroplasts. *Biochim. Biophys. Acta, Protein Struct. Mol. Enzymol.* **1433**, 87-102.
- Laden, B. P., Tang, Y., Porter, T. D., 2000. Cloning, heterologous expression, and enzymological characterization of human squalene monooxygenase. *Arch. Biochem. Biophys.* **374**, 381-388.
- Ladkau, N., Assmann, M., Schrewe, M., Julsing, M. K., Schmid, A., Bühler, B., 2016. Efficient production of the Nylon 12 monomer  $\omega$ -aminododecanoic acid methyl ester from renewable dodecanoic acid methyl ester with engineered *Escherichia coli*. *Metab. Eng.* **36**, 1-9.
- Laemmli, U. K., 1970. Cleavage of structural proteins during the assembly of the head of bacteriophage T4. *Nature.* **227**, 680-685.



- Lassen, L. M., Nielsen, A. Z., Olsen, C. E., Bialek, W., Jensen, K., Moller, B. L., Jensen, P. E., 2014a. Anchoring a plant cytochrome P450 via PsaM to the thylakoids in *Synechococcus* sp. PCC 7002: evidence for light-driven biosynthesis. *PLoS One*. **9**, e102184.
- Lassen, L. M., Nielsen, A. Z., Ziersen, B., Gnanasekaran, T., Moller, B. L., Jensen, P. E., 2014b. Redirecting photosynthetic electron flow into light-driven synthesis of alternative products including high-value bioactive natural compounds. *ACS Synth. Biol.* **3**, 1-12.
- Latifi, A., Ruiz, M., Zhang, C. C., 2009. Oxidative stress in cyanobacteria. *FEMS Microbiol. Rev.* **33**, 258-278.
- Law, H., Baldwin, C., Chen, B., Woodley, J., 2006. Process limitations in a whole-cell catalysed oxidation: sensitivity analysis. *Chem. Eng. Sci.* **61**, 6646-6652.
- Lee, N.-R., Yoon, J. W., Park, J.-B., 2011. Effect of lipopolysaccharide mutation on oxygenation of linoleic acid by recombinant *Escherichia coli* expressing CYP102A2 of *Bacillus subtilis*. *Biotechnol. Bioprocess Eng.* **16**, 7-12.
- Leon, R., Fernandes, P., Pinheiro, H., Cabral, J., 1998. Whole-cell biocatalysis in organic media. *Enzyme Microb. Technol.* **23**, 483-500.
- Li, F., Yu, M., Jiang, Y., Huang, F., Li, Y., Zhang, B., Sun, L., 2011. Chemical and photochemical oxidation of organic substrates by ruthenium aqua complexes with water as an oxygen source. *Chem. Commun.* **47**, 8949-8951.
- Li, H., Liao, J. C., 2013. Engineering a cyanobacterium as the catalyst for the photosynthetic conversion of CO<sub>2</sub> to 1, 2-propanediol. *Microb. Cell Fact.* **12**, 4.
- Li, R., 2017. Latest progress in hydrogen production from solar water splitting via photocatalysis, photoelectrochemical, and photovoltaic-photoelectrochemical solutions. *Chin. J. Catal.* **38**, 5-12.
- Liang, F., Englund, E., Lindberg, P., Lindblad, P., 2018a. Engineered cyanobacteria with enhanced growth show increased ethanol production and higher biofuel to biomass ratio. *Metab. Eng.* **46**, 51-59.
- Liang, Y., Wei, J., Qiu, X., Jiao, N., 2018b. Homogeneous oxygenase catalysis. *Chem. Rev.* **118**, 4912-4945.
- Lima-Ramos, J., Neto, W., Woodley, J. M., 2014. Engineering of biocatalysts and biocatalytic processes. *Top. Catal.* **57**, 301-320.
- Lin, B., Tao, Y., 2017. Whole-cell biocatalysts by design. *Microb. Cell Fact.* **16**, 106.
- Lippi, L., Bähr, L., Wüstenberg, A., Wilde, A., Steuer, R., 2018. Exploring the potential of high-density cultivation of cyanobacteria for the production of cyanophycin. *Algal Res.* **31**, 363-366.
- Lubner, C. E., Applegate, A. M., Knörzer, P., Ganago, A., Bryant, D. A., Happe, T., Golbeck, J. H., 2011. Solar hydrogen-producing bionanodevice outperforms natural photosynthesis. *Proc. Nat. Acad. Sci. U.S.A.* **108**, 20988-20991.
- Lundemo, M. T., Woodley, J. M., 2015. Guidelines for development and implementation of biocatalytic P450 processes. *Appl. Microbiol. Biotechnol.* **99**, 2465-2483.
- Luo, W., Deng, X.-X., Huo, J., Ruan, T., Gong, Z.-W., Yan, J.-B., Yang, Z.-H., Quan, C., Cui, Z.-F., 2018. Strengthening NADPH regeneration for improving photo-biocatalytic ketones asymmetric reduction reaction by *Synechocystis* through overexpression of FNR. *Catalysis Letters*. 1-9.
- Lütz, S., Steckhan, E., Liese, A., 2004. First asymmetric electroenzymatic oxidation catalyzed by a peroxidase. *Electrochem. Commun.* **6**, 583-587.
- Lye, G. J., Woodley, J. M., 1999. Application of *in situ* product-removal techniques to biocatalytic processes. *Trends Biotechnol.* **17**, 395-402.
- Lynch, R. M., Woodley, J. M., Lilly, M. D., 1997. Process design for the oxidation of fluorobenzene to fluorocatechol by *Pseudomonas putida*. *J. Biotechnol.* **58**, 167-175.
- Madigan, M. T., Martinko, J. M., 2006. Brock biology of microorganisms. *Pearson Prentice Hall*, Upper Saddle River.
- Marques, M. P., Cabral, J., Fernandes, P., 2010. Bioprocess scale-up: quest for the parameters to be used as criterion to move from microreactors to lab-scale. *J. Chem. Technol. Biotechnol.* **85**, 1184-1198.

- Martínez-García, E., Aparicio, T., Gofí-Moreno, A., Fraile, S., de Lorenzo, V., 2014. SEVA 2.0: an update of the Standard European Vector Architecture for de-/re-construction of bacterial functionalities. *Nucleic Acids Res.* **43**, D1183-D1189.
- Mason, H., Fowlks, W., Peterson, E., 1955. Oxygen transfer and electron transport by the phenolase complex<sup>1</sup>. *J. Am. Chem. Soc.* **77**, 2914-2915.
- Maswana, T., Phunpruch, S., Lindblad, P., Maneeruttanarungroj, C., 2018. Enhanced hydrogen production by optimization of immobilized cells of the green alga *Tetraspora* sp. CU2551 grown under anaerobic condition. *Biomass Bioenergy.* **111**, 88-95.
- Maurer, S. C., Kühnel, K., Kaysser, L. A., Eiben, S., Schmid, R. D., Urlacher, V. B., 2005. Catalytic hydroxylation in biphasic systems using CYP102A1 mutants. *Adv. Synth. Catal.* **347**, 1090-1098.
- Mayhew, M. P., Reipa, V., Holden, M. J., Vilker, V. L., 2000. Improving the cytochrome P450 enzyme system for electrode-driven biocatalysis of styrene epoxidation. *Biotechnol. Prog.* **16**, 610-616.
- McAuliffe, C., 1966. Solubility in water of paraffin, cycloparaffin, olefin, acetylene, cycloolefin, and aromatic hydrocarbons<sup>1</sup>. *J. Phys. Chem.* **70**, 1267-1275.
- McIver, A. M., Garikipati, S. J., Bankole, K. S., Gyamerah, M., Peeples, T. L., 2008. Microbial oxidation of naphthalene to cis-1, 2-naphthalene dihydrodiol using naphthalene dioxygenase in biphasic media. *Biotechnol. Prog.* **24**, 593-598.
- McKenna, E. J., Coon, E. J., 1970. Enzymatic omega oxidation: IV. Purification and properties of the omega hydroxylase of *Pseudomonas oleovorans*. *J. Biol. Chem.*
- Mellor, S. B., Nielsen, A. Z., Burow, M., Motawia, M. S., Jakubauskas, D., Moller, B. L., Jensen, P. E., 2016. Fusion of ferredoxin and cytochrome P450 enables direct light-driven biosynthesis. *ACS Chemical Biology.* **11**, 1862-1869.
- Mellor, S. B., Vavitsas, K., Nielsen, A. Z., Jensen, P. E., 2017. Photosynthetic fuel for heterologous enzymes: the role of electron carrier proteins. *Photosynth. Res.* **134**, 329-342.
- Merkx, M., Kopp, D. A., Sazinsky, M. H., Blazyk, J. L., Müller, J., Lippard, S. J., 2001. Dioxxygen activation and methane hydroxylation by soluble methane monooxygenase: a tale of two irons and three proteins. *Angew. Chem., Int. Ed.* **40**, 2782-2807.
- Michal, G., 1999. Biochemical pathways. *Spektrum, Akad. Verlag*, New York.
- Mifsud, M., Gargiulo, S., Iborra, S., Arends, I. W., Hollmann, F., Corra, A., 2014. Photobiocatalytic chemistry of oxidoreductases using water as the electron donor. *Nat. Commun.* **5**, 3145.
- Mooney, A., Ward, P. G., O'Connor, K. E., 2006. Microbial degradation of styrene: biochemistry, molecular genetics, and perspectives for biotechnological applications. *Appl. Microbiol. Biotechnol.* **72**, 1-10.
- Murata, N., Omata, T., 1988. Isolation of cyanobacterial plasma membranes. *Methods in Enzymology.* **167**, 245-251.
- Nagy, L., Bálint, E., Barber, J., Ringler, A., Cook, K. M., Maroti, P., 1995. Photoinhibition and law of reciprocity in photosynthetic reactions of *Synechocystis* sp. PCC 6803. *J. Plant Physiol.* **145**, 410-415.
- Nakamura, K., Yamanaka, R., 2002. Light mediated cofactor recycling system in biocatalytic asymmetric reduction of ketone. *Chem. Commun.*, 1782-1783.
- Narainsamy, K., Farci, S., Braun, E., Junot, C., Cassier-Chauvat, C., Chauvat, F., 2016. Oxidative-stress detoxification and signalling in cyanobacteria: the crucial glutathione synthesis pathway supports the production of ergothioneine and ophthalmate. *Molecular microbiology.* **100**, 15-24.
- Neeli, R., Roitel, O., Scrutton, N. S., Munro, A. W., 2005. Switching pyridine nucleotide specificity in P450 BM3 mechanistic analysis of the W1046H and W1046A enzymes. *J. Biol. Chem.* **280**, 17634-17644.
- Ng, A. H., Berla, B. M., Pakrasi, H. B., 2015. Fine-tuning of photoautotrophic protein production by combining promoters and neutral sites in the cyanobacterium *Synechocystis* sp. Strain PCC 6803. *Appl. Environ. Microbiol.* **81**, 6857-6863.
- Ni, Y., Holtmann, D., Hollmann, F., 2014. How green is biocatalysis? To calculate is to know. *ChemCatChem.* **6**, 930-943.

- Niederholtmeyer, H., Wolfstadter, B. T., Savage, D. F., Silver, P. A., Way, J. C., 2010. Engineering cyanobacteria to synthesize and export hydrophilic products. *Appl Environ Microbiol.* **76**, 3462-3466.
- Nies, D., Schlegel, H., 1984. Use of catalase from *Escherichia coli* in model experiments for oxygen supply of microorganisms with hydrogen peroxide. *Biotechnol. Bioeng.* **26**, 737-741.
- Noble, M. A., Miles, C. S., Chapman, S. K., Lysek, D. A., MacKay, A. C., Hanzlik, R. P., Munro, A. W., 1999. Roles of key active-site residues in flavocytochrome P450 BM3. *Biochem. J.* **339**, 371-379.
- Nyberg, M., Heidorn, T., Lindblad, P., 2015. Hydrogen production by the engineered cyanobacterial strain *Nostoc* PCC 7120 DeltahupW examined in a flat panel photobioreactor system. *J. Biotechnol.* **215**, 35-43.
- Okeefe, D. P., Tepperman, J. M., Dean, C., Leto, K. J., Erbes, D. L., Odell, J. T., 1994. Plant expression of a bacterial cytochrome-P450 that catalyzes activation of a sulfonylurea pro-herbicide. *Plant Physiology.* **105**, 473-482.
- Oliver, J. W. K., Atsumi, S., 2014. Metabolic design for cyanobacterial chemical synthesis. *Photosynth. Res.* **120**, 249-261.
- Olle, B., Bucak, S., Holmes, T. C., Bromberg, L., Hatton, T. A., Wang, D. I., 2006. Enhancement of oxygen mass transfer using functionalized magnetic nanoparticles. *Ind. Eng. Chem. Res.* **45**, 4355-4363.
- Omata, T., Murata, N., 1983. Isolation and characterization of the cytoplasmic membranes from the blue-green alga (cyanobacterium) *Anacystis nidulans*. *Plant Cell Physiol.* **24**, 1101-1112.
- Omata, T., Murata, N., 1984. Isolation and characterization of three types of membranes from the cyanobacterium (blue-green alga) *Synechocystis* PCC 6714. *Arch. Microbiol.* **139**, 113-116.
- Osterberg, P. M., Niemeier, J. K., Welch, C. J., Hawkins, J. M., Martinelli, J. R., Johnson, T. E., Root, T. W., Stahl, S. S., 2014. Experimental limiting oxygen concentrations for nine organic solvents at temperatures and pressures relevant to aerobic oxidations in the pharmaceutical industry. *Org. Process Res. Dev.* **19**, 1537-1543.
- Ozkan, A., Kinney, K., Katz, L., Berberoglu, H., 2012. Reduction of water and energy requirement of algae cultivation using an algae biofilm photobioreactor. *Bioresour. Technol.* **114**, 542-548.
- Pade, N., Erdmann, S., Enke, H., Dethloff, F., Dühning, U., Georg, J., Wambutt, J., Kopka, J., Hess, W. R., Zimmermann, R., 2016. Insights into isoprene production using the cyanobacterium *Synechocystis* sp. PCC 6803. *Biotechnol. Biofuels.* **9**, 89.
- Pagliari, M., Campestrini, S., Ciriminna, R., 2005. Ru-based oxidation catalysis. *Chem. Soc. Rev.* **34**, 837-845.
- Panke, S., de Lorenzo, V., Kaiser, A., Witholt, B., Wubbolts, M. G., 1999. Engineering of a stable whole-cell biocatalyst capable of (S)-styrene oxide formation for continuous two-liquid-phase applications. *Appl. Environ. Microbiol.* **65**, 5619-5623.
- Panke, S., Held, M., Wubbolts, M. G., Witholt, B., Schmid, A., 2002. Pilot-scale production of (S)-styrene oxide from styrene by recombinant *Escherichia coli* synthesizing styrene monooxygenase. *Biotechnol. Bioeng.* **80**, 33-41.
- Panke, S., Witholt, B., Schmid, A., Wubbolts, M. G., 1998. Towards a biocatalyst for (S)-styrene oxide production: characterization of the styrene degradation pathway of *Pseudomonas* sp. strain VLB120. *Appl. Environ. Microbiol.* **64**, 2032-2043.
- Papone, T., Kookkhunthod, S., Leesing, R., 2012. Microbial oil production by monoculture and mixed cultures of microalgae and oleaginous yeasts using sugarcane juice as substrate. *World Acad. Sci. Eng. Technol.* **64**, 1127-1131.
- Park, J. B., 2007. Oxygenase-based whole-cell biocatalysis in organic synthesis. *J. Microbiol. Biotechnol.* **17**, 379-392.
- Park, J. B., Bühler, B., Habicher, T., Hauer, B., Panke, S., Witholt, B., Schmid, A., 2006. The efficiency of recombinant *Escherichia coli* as biocatalyst for stereospecific epoxidation. *Biotechnol. Bioeng.* **95**, 501-512.

- Pattanaik, B., Lindberg, P., 2015. Terpenoids and their biosynthesis in cyanobacteria. *Life*. **5**, 269-293.
- Payne, A. H., Hales, D. B., 2004. Overview of steroidogenic enzymes in the pathway from cholesterol to active steroid hormones. *Endocr. Rev.* **25**, 947-970.
- Pazmino, D. T., Winkler, M., Glieder, A., Fraaije, M. W., 2010. Monooxygenases as biocatalysts: classification, mechanistic aspects and biotechnological applications. *J. Biotechnol.* **146**, 9-24.
- Perez, D. I., Grau, M. M., Arends, I. W., Hollmann, F., 2009. Visible light-driven and chloroperoxidase-catalyzed oxygenation reactions. *Chem. Commun.*, 6848-6850.
- Peterhansel, C., Horst, I., Niessen, M., Blume, C., Kebeish, R., Kürkcüoğlu, S., Kreuzaler, F., 2010. Photorespiration. *Arabidopsis Book*. **8**, e0130.
- Petersen, M., Abdullah, Y., Benner, J., Eberle, D., Gehlen, K., Hücherig, S., Janiak, V., Kim, K. H., Sander, M., Weitzel, C., 2009. Evolution of rosmarinic acid biosynthesis. *Phytochemistry*. **70**, 1663-1679.
- Peterson, J. A., Basu, D., Coon, M. J., 1966a. Enzymatic omega oxidation: I. Electron carriers in fatty acid and hydrocarbon hydroxylation. *J. Biol. Chem.* **241**, 5162-5164.
- Peterson, J. A., Basu, D., Coon, M. J., 1966b. Enzymatic  $\omega$ -oxidation I. Electron carriers in fatty acid and hydrocarbon hydroxylation. *J. Biol. Chem.* **241**, 5162-5164.
- Peterson, J. A., Kusunose, M., Kusunose, E., Coon, M. J., 1967. Enzymatic  $\omega$ -oxidation II. Function of rubredoxin as the electron carrier in  $\omega$ -hydroxylation. *J. Biol. Chem.* **242**, 4334-4340.
- Pflug, S., Richter, S. M., Urlacher, V. B., 2007. Development of a fed-batch process for the production of the cytochrome P450 monooxygenase CYP102A1 from *Bacillus megaterium* in *E. coli*. *J. Biotechnol.* **129**, 481-488.
- Piera, J., Bäckvall, J. E., 2008. Catalytic oxidation of organic substrates by molecular oxygen and hydrogen peroxide by multistep electron transfer—a biomimetic approach. *Angew. Chem., Int. Ed.* **47**, 3506-3523.
- Porankiewicz, J., Clarke, A. K., 1997. Induction of the heat shock protein ClpB affects cold acclimation in the cyanobacterium *Synechococcus* sp. strain PCC 7942. *J. Bacteriol.* **179**, 5111-5117.
- Prieto-Barajas, C. M., Valencia-Cantero, E., Santoyo, G., 2017. Microbial mat ecosystems: Structure types, functional diversity, and biotechnological application. *Electron. J. Biotechnol.* **31**, 48-56.
- Pulz, O., 2001. Photobioreactors: production systems for phototrophic microorganisms. *Appl. Microbiol. Biotechnol.* **57**, 287-293.
- Reipa, V., Mayhew, M. P., Vilker, V. L., 1997. A direct electrode-driven P450 cycle for biocatalysis. *Proc. Nat. Acad. Sci. U.S.A.* **94**, 13554-13558.
- Richaud, C., Zabulon, G., Joder, A., Thomas, J.-C., 2001. Nitrogen or sulfur starvation differentially affects phycobilisome degradation and expression of the *nblA* gene in *Synechocystis* strain PCC 6803. *J. Bacteriol.* **183**, 2989-2994.
- Ringborg, R. H., Woodley, J., 2016. The application of reaction engineering to biocatalysis. *React. Chem. Eng.* **1**, 10-22.
- Rosche, B., Li, X. Z., Hauer, B., Schmid, A., Buehler, K., 2009. Microbial biofilms: a concept for industrial catalysis? *Trends Biotechnol.* **27**, 636-643.
- Rosenberg, M., Švitel, J., Šturdik, E., Rosenbergova, I., 1992. Gluconic acid production by *Aspergillus niger* with oxygen supply by hydrogen peroxide. *Bioprocess Eng.* **7**, 309-313.
- Rosenthal, K., Oehling, V., Dusny, C., Schmid, A., 2017. Beyond the bulk: disclosing the life of single microbial cells. *FEMS Microbiol. Rev.* **41**, 751-780.
- Ruffing, A. M., 2011. Engineered cyanobacteria: teaching an old bug new tricks. *Bioeng. Bugs.* **2**, 136-149.
- Ruffing, A. M., 2014. Improved free fatty acid production in cyanobacteria with *Synechococcus* sp. PCC 7002 as host. *Front. Bioeng. Biotechnol.* **2**, 17.
- Ruijsenaars, H. J., Sperling, E. M., Wiegerinck, P. H., Brands, F. T., Wery, J., de Bont, J. A., 2007. Testosterone 15 $\beta$ -hydroxylation by solvent tolerant *Pseudomonas putida* S12. *J. Biotechnol.* **131**, 205-208.

- Salamanca, D., Engesser, K.-H., 2014. Isolation and characterization of two novel strains capable of using cyclohexane as carbon source. *Environ. Sci. Pollut. Res.* **21**, 12757-12766.
- Salamanca, D., Karande, R., Schmid, A., Dobslaw, D., 2015. Novel cyclohexane monooxygenase from *Acidovorax* sp. CHX100. *Appl. Microbiol. Biotechnol.* **99**, 6889-6897.
- Salomon, E., Bar-Eyal, L., Sharon, S., Keren, N., 2013. Balancing photosynthetic electron flow is critical for cyanobacterial acclimation to nitrogen limitation. *Biochim. Biophys. Acta.* **1827**, 340-347.
- Sambrook, J., Russell, D., 2001. Molecular cloning - A laboratory manual. *Cold Spring Harbour Laboratory Press, New York*.
- Sander, R., 2015. Compilation of Henry's law constants (version 4.0) for water as solvent. *Atmos. Chem. Phys.* **15**.
- Sardessai, Y. N., Bhosle, S., 2004. Industrial potential of organic solvent tolerant bacteria. *Biotechnol. Prog.* **20**, 655-660.
- Savakis, P., Tan, X., Du, W., Branco dos Santos, F., Lu, X., Hellingwerf, K. J., 2015. Photosynthetic production of glycerol by a recombinant cyanobacterium. *J. Biotechnol.* **195**, 46-51.
- Schaffer, S., Haas, T., 2014. Biocatalytic and fermentative production of  $\alpha$ ,  $\omega$ -bifunctional polymer precursors. *Org. Process Res. Dev.* **18**, 752-766.
- Scheps, D., Honda Malca, S., Richter, S. M., Marisch, K., Nestl, B. M., Hauer, B., 2013. Synthesis of  $\omega$ -hydroxy dodecanoic acid based on an engineered CYP153A fusion construct. *Microb. Biotechnol.* **6**, 694-707.
- Schewe, H., Holtmann, D., Schrader, J., 2009. P450 BM-3-catalyzed whole-cell biotransformation of  $\alpha$ -pinene with recombinant *Escherichia coli* in an aqueous-organic two-phase system. *Appl. Microbiol. Biotechnol.* **83**, 849-857.
- Schewe, H., Kaup, B.-A., Schrader, J., 2008. Improvement of P450 BM-3 whole-cell biocatalysis by integrating heterologous cofactor regeneration combining glucose facilitator and dehydrogenase in *E. coli*. *Appl. Microbiol. Biotechnol.* **78**, 55-65.
- Schlegel, H., 1977. Aeration without air: oxygen supply by hydrogen peroxide. *Biotechnol. Bioeng.* **19**, 413-424.
- Schmid, A., Dordick, J., Hauer, B., Kiener, A., Wubbolts, M., Witholt, B., 2001. Industrial biocatalysis today and tomorrow. *Nature.* **409**, 258-268.
- Schmidt, T. G., Koepke, J., Frank, R., Skerra, A., 1996. Molecular interaction between the Strep-tag affinity peptide and its cognate target, streptavidin. *J. Mol. Biol.* **255**, 753-766.
- Schmölzer, K., Mädje, K., Nidetzky, B., Kratzer, R., 2012. Bioprocess design guided by *in situ* substrate supply and product removal: process intensification for synthesis of (S)-1-(2-chlorophenyl) ethanol. *Bioresour. Technol.* **108**, 216-223.
- Schneider, S., Wubbolts, M. G., Oesterheld, G., Sanglard, D., Witholt, B., 1999. Controlled regioselectivity of fatty acid oxidation by whole cells producing cytochrome P450 BM-3 monooxygenase under varied dissolved oxygen concentrations. *Biotechnol. Bioeng.* **64**, 333-341.
- Schrewe, M., Julsing, M. K., Bühler, B., Schmid, A., 2013. Whole-cell biocatalysis for selective and productive C-O functional group introduction and modification. *Chem. Soc. Rev.* **42**, 6346-6377.
- Schrewe, M., Julsing, M. K., Lange, K., Czarnotta, E., Schmid, A., Bühler, B., 2014. Reaction and catalyst engineering to exploit kinetically controlled whole-cell multistep biocatalysis for terminal FAME oxyfunctionalization. *Biotechnol. Bioeng.* **111**, 1820-1830.
- Schrewe, M., Magnusson, A. O., Willrodt, C., Bühler, B., Schmid, A., 2011. Kinetic analysis of terminal and unactivated C-H bond oxyfunctionalization in fatty acid methyl esters by monooxygenase-based whole-cell biocatalysis. *Adv. Synth. Catal.* **353**, 3485-3495.
- Schuchardt, U., Cardoso, D., Sercheli, R., Pereira, R., Da Cruz, R. S., Guerreiro, M. C., Mandelli, D., Spinacé, E. V., Pires, E. L., 2001. Cyclohexane oxidation continues to be a challenge. *Appl. Catal., A.* **211**, 1-17.

- Schuchardt, U., Carvalho, W. A., Spinacé, E. V., 1993. Why is it interesting to study cyclohexane oxidation? *Synlett*. **1993**, 713-718.
- Schuler, M. A., 2011. P450s in plant–insect interactions. *Biochim. Biophys. Acta, Proteins Proteomics*. **1814**, 36-45.
- Schüürmann, J., Quehl, P., Festel, G., Jose, J., 2014. Bacterial whole-cell biocatalysts by surface display of enzymes: toward industrial application. *Appl. Microbiol. Biotechnol.* **98**, 8031-8046.
- Shcolnick, S., Shaked, Y., Keren, N., 2007. A role for mrgA, a DPS family protein, in the internal transport of Fe in the cyanobacterium *Synechocystis* sp. PCC6803. *Biochim. Biophys. Acta, Bioenerg.* **1767**, 814-819.
- Shen, J. R., 2015. The structure of photosystem II and the mechanism of water oxidation in photosynthesis. *Annu. Rev. Plant Biol.* **66**, 23-48.
- Shet, M. S., Fisher, C. W., Estabrook, R. W., 1997. The function of recombinant cytochrome P450s in intact *Escherichia coli* cells: the 17 alpha-hydroxylation of progesterone and pregnenolone by P450c17. *Arch. Biochem.* **339**, 218-225.
- Shi, Z., Zhang, C., Tang, C., Jiao, N., 2012. Recent advances in transition-metal catalyzed reactions using molecular oxygen as the oxidant. *Chem. Soc. Rev.* **41**, 3381-3430.
- Sikkema, J., de Bont, J. A., Poolman, B., 1994. Interactions of cyclic hydrocarbons with biological membranes. *J. Biol. Chem.* **269**, 8022-8028.
- Simpson, H. D., Alphand, V., Furstoss, R., 2001. Microbiological transformations: 49. Asymmetric biocatalysed Baeyer–Villiger oxidation: improvement using a recombinant *Escherichia coli* whole cell biocatalyst in the presence of an adsorbent resin. *J. Mol. Catal. B: Enzym.* **16**, 101-108.
- Singh, R., Sharma, S., 2012. Development of suitable photobioreactor for algae production–A review. *Renewable Sustainable Energy Rev.* **16**, 2347-2353.
- Sonnleitner, B., Hahnemann, U., 1997. Robust oxygen supply by controlled addition of hydrogen peroxide to microbial cultures. *Bioprocess Eng.* **17**, 215-219.
- Spolaore, P., Joannis-Cassan, C., Duran, E., Isambert, A., 2006. Commercial applications of microalgae. *J. Biosci. Bioeng.* **101**, 87-96.
- Sriram, G., Manjula Rao, Y., Suresh, K., Sureshkumar, G., 1998. Oxygen supply without gas–liquid film resistance to *Xanthomonas campestris* cultivation. *Biotechnol. Bioeng.* **59**, 714-723.
- Stanier, R. Y., Kunisawa, R., Mandel, M., Cohen-Bazire, G., 1971. Purification and properties of unicellular blue-green algae (order *Chroococcales*). *Bacteriol. Rev.* **35**, 171-205.
- Straathof, A. J., Panke, S., Schmid, A., 2002. The production of fine chemicals by biotransformations. *Curr. Opin. Biotechnol.* **13**, 548-556.
- Strieth, D., Ulber, R., Muffler, K., 2018. Application of phototrophic biofilms: from fundamentals to processes. *Bioprocess Biosyst. Eng.* **41**, 295-312.
- Ströhle, F. W., Kranen, E., Schrader, J., Maas, R., Holtmann, D., 2016. A simplified process design for P450 driven hydroxylation based on surface displayed enzymes. *Biotechnol. Bioeng.* **113**, 1225-1233.
- Suzuki, M., Hayakawa, T., Shaw, J., Rekik, M., Harayama, S., 1991. Primary structure of xylene monooxygenase: similarities to and differences from the alkane hydroxylation system. *J. Bacteriol.* **173**, 1690-1695.
- Thomas, B. A., Bricker, T. M., Klotz, A. V., 1993. Post-translational methylation of phycobilisomes and oxygen evolution efficiency in cyanobacteria. *Biochim. Biophys. Acta, Bioenerg.* **1143**, 104-108.
- Tomaszewski, B., Lloyd, R. C., Warr, A. J., Buehler, K., Schmid, A., 2014. Regioselective biocatalytic aromatic hydroxylation in a gas–liquid multiphase tube-in-tube reactor. *ChemCatChem*. **6**, 2567-2576.
- Touloupakis, E., Cicchi, B., Torzillo, G., 2015. A bioenergetic assessment of photosynthetic growth of *Synechocystis* sp. PCC 6803 in continuous cultures. *Biotechnol. Biofuels*. **8**, 133.
- Touw, D. S., Patel, D. R., van Den Berg, B., 2010. The crystal structure of OprG from *Pseudomonas aeruginosa*, a potential channel for transport of hydrophobic molecules across the outer membrane. *PLoS one*. **5**, e15016.

- Tufvesson, P., Lima-Ramos, J., Nordblad, M., Woodley, J. M., 2010. Guidelines and cost analysis for catalyst production in biocatalytic processes. *Org. Process Res. Dev.* **15**, 266-274.
- Ütkür, F. Ö., Gaykawad, S., Bühler, B., Schmid, A., 2011. Regioselective aromatic hydroxylation of quinaldine by water using quinaldine 4-oxidase in recombinant *Pseudomonas putida*. *J. Ind. Microbiol. Biotechnol.* **38**, 1067-1077.
- van Beilen, J. B., Duetz, W. A., Schmid, A., Witholt, B., 2003. Practical issues in the application of oxygenases. *Trends Biotechnol.* **21**, 170-177.
- van Beilen, J. B., Holtackers, R., Luscher, D., Bauer, U., Witholt, B., Duetz, W. A., 2005. Biocatalytic production of perillyl alcohol from limonene by using a novel *Mycobacterium* sp. cytochrome P450 alkane hydroxylase expressed in *Pseudomonas putida*. *Appl. Environ. Microbiol.* **71**, 1737-1744.
- van Beilen, J. B., Wubbolts, M. G., Witholt, B., 1994. Genetics of alkane oxidation by *Pseudomonas oleovorans*. *Biodegradation.* **5**, 161-174.
- van de Velde, F., Lourenço, N. D., Bakker, M., van Rantwijk, F., Sheldon, R. A., 2000. Improved operational stability of peroxidases by coimmobilization with glucose oxidase. *Biotechnol. Bioeng.* **69**, 286-291.
- van Den Berg, B., Black, P. N., Clemons, W. M., Rapoport, T. A., 2004. Crystal structure of the long-chain fatty acid transporter FadL. *Science.* **304**, 1506-1509.
- van der Woude, A. D., Gallego, R. P., Vreugdenhil, A., Veetil, V. P., Chroumpi, T., Hellingwerf, K. J., 2016. Genetic engineering of *Synechocystis* PCC6803 for the photoautotrophic production of the sweetener erythritol. *Microb. Cell Fact.* **15**, 60.
- van Dien, S., 2013. From the first drop to the first truckload: commercialization of microbial processes for renewable chemicals. *Curr. Opin. Biotechnol.* **24**, 1061-1068.
- Varman, A. M., Xiao, Y., Pakrasi, H. B., Tang, Y. J., 2013. Metabolic engineering of *Synechocystis* sp. strain PCC 6803 for isobutanol production. *Appl. Environ. Microbiol.* **79**, 908-914.
- Veetil, V. P., Angermayr, S. A., Hellingwerf, K. J., 2017. Ethylene production with engineered *Synechocystis* sp. PCC 6803 strains. *Microb. Cell Fact.* **16**, 34.
- Vermaas, W. F., 2001. Photosynthesis and respiration in cyanobacteria. *Encyclopedia of Life Sciences.* **1**, 1-7.
- Volmer, J., Neumann, C., Bühler, B., Schmid, A., 2014. Engineering of *Pseudomonas taiwanensis* VLB120 for constitutive solvent tolerance and increased specific styrene epoxidation activity. *Appl. Environ. Microbiol.*, 6539-6548.
- Volmer, J., Schmid, A., Bühler, B., 2015. Guiding bioprocess design by microbial ecology. *Curr. Opin. Microbiol.* **25**, 25-32.
- Vorachek-Warren, M. K., Ramirez, S., Cotter, R. J., Raetz, C. R., 2002. A triple mutant of *Escherichia coli* lacking secondary acyl chains on lipid A. *J. Biol. Chem.* **277**, 14194-14205.
- Wachsen, O., Himmler, K., Cornils, B., 1998. Aqueous biphasic catalysis: where the reaction takes place. *Catal. Today.* **42**, 373-379.
- Wachtmeister, J., Rother, D., 2016. Recent advances in whole cell biocatalysis techniques bridging from investigative to industrial scale. *Curr. Opin. Biotechnol.* **42**, 169-177.
- Wang, J., Cui, W., Liu, Q., Xing, Z., Asiri, A. M., Sun, X., 2016a. Recent progress in cobalt-based heterogeneous catalysts for electrochemical water splitting. *Adv. Mater.* **28**, 215-230.
- Wang, Q. J., Singh, A., Li, H., Nedbal, L., Sherman, L. A., Whitmarsh, J., 2012. Net light-induced oxygen evolution in photosystem I deletion mutants of the cyanobacterium *Synechocystis* sp. PCC 6803. *Biochim. Biophys. Acta, Bioenerg.* **1817**, 792-801.
- Wang, Y., Lan, D., Durrani, R., Hollmann, F., 2017. Peroxygenases en route to becoming dream catalysts. What are the opportunities and challenges? *Curr. Opin. Chem. Biol.* **37**, 1-9.
- Wang, Y., Sun, T., Gao, X., Shi, M., Wu, L., Chen, L., Zhang, W., 2016b. Biosynthesis of platform chemical 3-hydroxypropionic acid (3-HP) directly from CO<sub>2</sub> in cyanobacterium *Synechocystis* sp. PCC 6803. *Metab. Eng.* **34**, 60-70.

- Watts, K. T., Mijts, B. N., Schmidt-Dannert, C., 2005. Current and emerging approaches for natural product biosynthesis in microbial cells. *Adv. Synth. Catal.* **347**, 927-940.
- WBCSD, 2000. Eco-efficiency. Creating more value with less impact. *World Business Council for Sustainable Development, Geneva*.
- Weissermel, K., Arpe, H.-J., 2008. Industrial organic chemistry. *VCH, New York*.
- Weissman, J. C., Goebel, R. P., Benemann, J. R., 1988. Photobioreactor design: mixing, carbon utilization, and oxygen accumulation. *Biotechnol. Bioeng.* **31**, 336-344.
- Wen, X., Du, K., Wang, Z., Peng, X., Luo, L., Tao, H., Xu, Y., Zhang, D., Geng, Y., Li, Y., 2016. Effective cultivation of microalgae for biofuel production: a pilot-scale evaluation of a novel oleaginous microalga *Graesiella* sp. WBG-1. *Biotechnol. Biofuels.* **9**, 123.
- Whitehouse, C. J., Bell, S. G., Wong, L.-L., 2012. P450 BM3 (CYP102A1): connecting the dots. *Chem. Soc. Rev.* **41**, 1218-1260.
- Wijffels, R. H., Kruse, O., Hellingwerf, K. J., 2013. Potential of industrial biotechnology with cyanobacteria and eukaryotic microalgae. *Curr. Opin. Biotechnol.* **24**, 405-413.
- Wilhelm, C., Selmar, D., 2011. Energy dissipation is an essential mechanism to sustain the viability of plants: the physiological limits of improved photosynthesis. *J. Plant Physiol.* **168**, 79-87.
- Wilhelm, C., Wild, A., 1984. The variability of the photosynthetic unit in *Chlorella* II. The effect of light intensity and cell development on photosynthesis, P-700 and cytochrome f in homocontinuous and synchronous cultures of *Chlorella*. *J. Plant Physiol.* **115**, 125-135.
- Willrodt, C., David, C., Cornelissen, S., Bühler, B., Julsing, M. K., Schmid, A., 2014. Engineering the productivity of recombinant *Escherichia coli* for limonene formation from glycerol in minimal media. *Biotechnol. J.* **9**, 1000-1012.
- Willrodt, C., Hoschek, A., Bühler, B., Schmid, A., Julsing, M. K., 2015a. Coupling limonene formation and oxyfunctionalization by mixed-culture resting cell fermentation. *Biotechnol. Bioeng.* **112**, 1738-1750.
- Willrodt, C., Hoschek, A., Bühler, B., Schmid, A., Julsing, M. K., 2016. Decoupling production from growth by magnesium sulfate limitation boosts de novo limonene production. *Biotechnol. Bioeng.* **113**, 1305-1314.
- Willrodt, C., Karande, R., Schmid, A., Julsing, M. K., 2015b. Guiding efficient microbial synthesis of non-natural chemicals by physicochemical properties of reactants. *Curr. Opin. Biotechnol.* **35**, 52-62.
- Włodarczyk, A., Gnanasekaran, T., Nielsen, A. Z., Zulu, N. N., Mellor, S. B., Luckner, M., Thofner, J. F., Olsen, C. E., Mottawie, M. S., Burow, M., Pribil, M., Feussner, I., Moller, B. L., Jensen, P. E., 2015. Metabolic engineering of light-driven cytochrome P450 dependent pathways into *Synechocystis* sp. PCC 6803. *Metab. Eng.* **33**, 1-11.
- Wohlgemuth, R., Plazl, I., Žnidaršič-Plazl, P., Gernaey, K. V., Woodley, J. M., 2015. Microscale technology and biocatalytic processes: opportunities and challenges for synthesis. *Trends Biotechnol.* **33**, 302-314.
- Wójcikowski, J., Basińska, A., Daniel, W. A., 2014. The cytochrome P450-catalyzed metabolism of levomepromazine: a phenothiazine neuroleptic with a wide spectrum of clinical application. *Biochem. Pharmacol.* **90**, 188-195.
- Woodley, J., Titchener-Hooker, N., 1996. The use of windows of operation as a bioprocess design tool. *Bioprocess Eng.* **14**, 263-268.
- Woodley, J. M., 2018. Integrating protein engineering with process design for biocatalysis. *Phil. Trans. R. Soc. A.* **376**, 20170062.
- Xue, Y., Zhang, Y., Grace, S., He, Q., 2013. Functional expression of an *Arabidopsis* p450 enzyme, p-coumarate-3-hydroxylase, in the cyanobacterium *Synechocystis* PCC 6803 for the biosynthesis of caffeic acid. *J. Appl. Phycol.* **26**, 219-226.
- Yacoby, I., Pochekailov, S., Toporik, H., Ghirardi, M. L., King, P. W., Zhang, S., 2011. Photosynthetic electron partitioning between [FeFe]-hydrogenase and ferredoxin: NADP<sup>+</sup>-oxidoreductase (FNR) enzymes in vitro. *Proc. Nat. Acad. Sci. U.S.A.* **108**, 9396-9401.
- Yamanaka, R., Nakamura, K., Murakami, A., 2011. Reduction of exogenous ketones depends upon NADPH generated photosynthetically in cells of the cyanobacterium *Synechococcus* PCC 7942. *AMB Express.* **1**, 24.

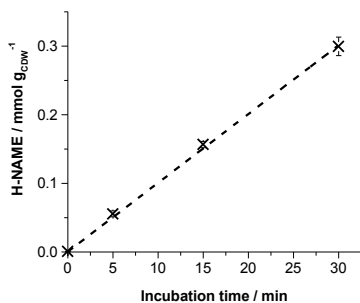


- Yamanaka, R., Nakamura, K., Murakami, M., Murakami, A., 2015. Selective synthesis of cinnamyl alcohol by cyanobacterial photobiocatalysts. *Tetrahedron Lett.* **56**, 1089-1091.
- Yao, D. C., Brune, D. C., Vavilin, D., Vermaas, W. F., 2012. Photosystem II component lifetimes in the cyanobacterium *Synechocystis* sp. strain PCC 6803 small Cab-like proteins stabilize biosynthesis intermediates and affect early steps in chlorophyll synthesis. *J. Biol. Chem.* **287**, 682-692.
- Yim, S.-K., Kim, D.-H., Jung, H.-C., Pan, J.-G., Kang, H.-S., Ahn, T., Yun, C.-H., 2010. Surface display of heme-and flavin-containing cytochrome P450 BM3 in *Escherichia coli*: a whole cell biocatalyst for oxidation. *J. Microbiol. Biotechnol.* **20**, 712-717.
- Yu, J., Liberton, M., Cliften, P. F., Head, R. D., Jacobs, J. M., Smith, R. D., Koppenaar, D. W., Brand, J. J., Pakrasi, H. B., 2015a. *Synechococcus elongatus* UTEX 2973, a fast growing cyanobacterial chassis for biosynthesis using light and CO<sub>2</sub>. *Sci. Rep.* **5**, 8132.
- Yu, K., Liu, C., Kim, B.-G., Lee, D.-Y., 2015b. Synthetic fusion protein design and applications. *Biotechnol. Adv.* **33**, 155-164.
- Yu, Y., You, L., Liu, D., Hollinshead, W., Tang, Y. J., Zhang, F., 2013. Development of *Synechocystis* sp. PCC 6803 as a phototrophic cell factory. *Mar. Drugs.* **11**, 2894-2916.
- Zavřel, T., Knoop, H., Steuer, R., Jones, P. R., Červený, J., Trtílek, M., 2016. A quantitative evaluation of ethylene production in the recombinant cyanobacterium *Synechocystis* sp. PCC 6803 harboring the ethylene-forming enzyme by membrane inlet mass spectrometry. *Bioresour. Technol.* **202**, 142-151.
- Zhang, W., Fernández-Fueyo, E., Ni, Y., van Schie, M., Gacs, J., Renirie, R., Wever, R., Mutti, F. G., Rother, D., Alcalde, M., 2018. Selective aerobic oxidation reactions using a combination of photocatalytic water oxidation and enzymatic oxyfunctionalizations. *Nat. Catal.* **1**, 55-62.
- Zhu, Y., Zhang, Q., Li, S., Lin, Q., Fu, P., Zhang, G., Zhang, H., Shi, R., Zhu, W., Zhang, C., 2013. Insights into caerulomycin A biosynthesis: A two-component monooxygenase CrmH-catalyzed oxime formation. *J. Am. Chem. Soc.* **135**, 18750-18753.



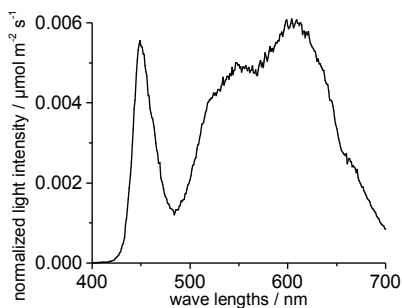
**Chapter 10    Appendix**

## 10.1 Supporting information to Chapter 3

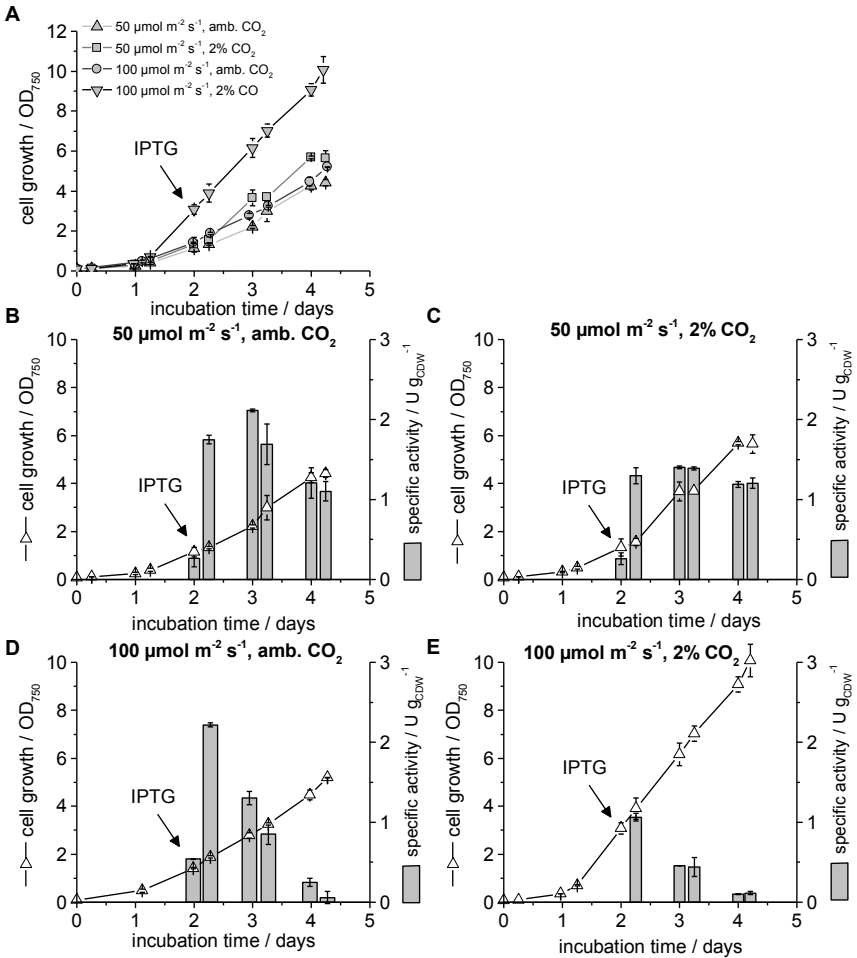


**Figure 10.1:** Product formation of recombinant *E. coli* W3110 (pAH042). The specific activity was  $10.0 \pm 0.1 \text{ U } g_{CDW}^{-1}$ , calculated for a reaction time of 30 min. Average values and standard deviations of two independent biological replicates are given.

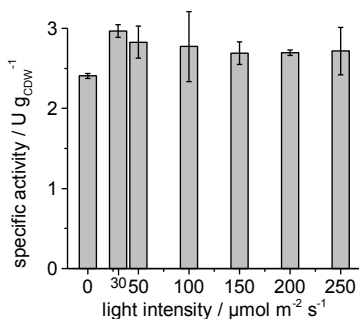
## 10.2 Supporting information to Chapter 4



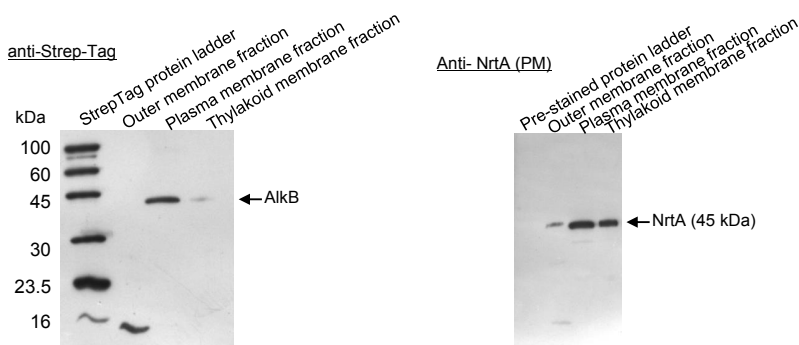
**Figure 10.2:** Normalized light spectrum of the stirred tank photo-bioreactor (Labfors 5 Lux, Infors AG, Bottmingen, Switzerland) used for the cultivation of *Synechocystis* sp. PCC 6803.



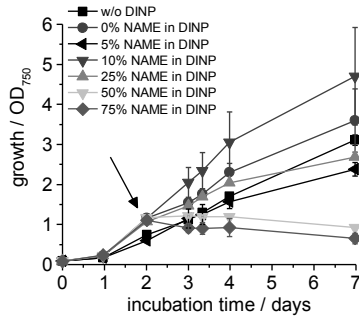
**Figure 10.3:** Influence of cell growth conditions on specific NAME oxyfunctionalization activity of Syn6803\_BGT. Cells were cultivated at indicated growth conditions, harvested at given time-points and standard oxygenation activity assays ( $2 \text{ g}_{\text{CDW}} \text{ L}^{-1}$ , YBG11,  $30 \mu\text{E m}^{-2} \text{ s}^{-1}$ ) were performed.



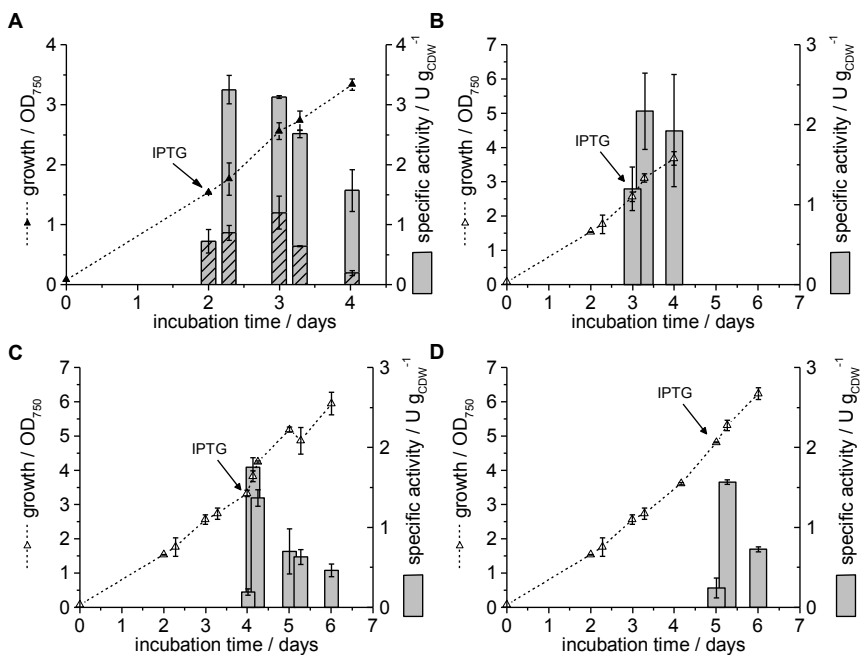
**Figure 10.4:** Impact of light intensity on NAME biotransformation activity of Syn6803\_BGT. Cells were cultivated under standard conditions (YBG11,  $50 \mu\text{E m}^{-2} \text{s}^{-1}$ , ambient  $\text{CO}_2$ ). Two days after inoculation, gene expression was induced for 24 h. Oxyfunctionalization assays were performed at given light intensities ( $2 \text{ g}_{\text{CDW}} \text{L}^{-1}$ , YBG11 +  $\text{NaHCO}_3$ ).



**Figure 10.5:** Membrane fractionation analysis of Syn6803\_BGT. Cells were cultivated and induced in a stirred tank photo-bioreactor as described in the materials and methods section of **Chapter 4**, disrupted by French press and applied for sucrose density gradient centrifugation as described in **Chapter 2**. Subsequently, Western blot analysis was performed for Strep-tag identification.  $10 \mu\text{g}$  of each protein fraction was loaded on SDS gel. Strep-tag protein ladder (IBA GmbH, Göttingen, Germany) or a pre-stained protein ladder (PageRuler Prestained Protein Ladder 26616, Thermo Fisher Scientific, Waltham, USA) were used. NrtA = Nitrate transport protein (localized in plasma membranes of *Synechocystis* sp. PCC 6803).

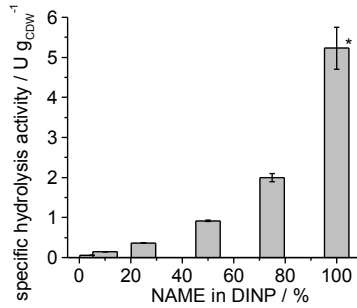


**Figure 10.6:** Cell growth of *Synechocystis* sp. PCC 6803 (pAH032) (empty expression plasmid) upon addition of DINP containing different NAME concentrations. Cells were cultivated under standard conditions for two days before aliquots of 7.5 mL were applied to fresh 100 mL shake flasks. Then, 2.5 mL of organic carrier solvent containing different NAME concentrations were added to the cultures (indicated by the arrow, organic:aqueous phase ratio of 1:3), and cultivation was continued under standard conditions with a reduced shaking frequency of 100 rpm (2.5 cm amplitude). Average values and standard deviations of two independent biological replicates are given.

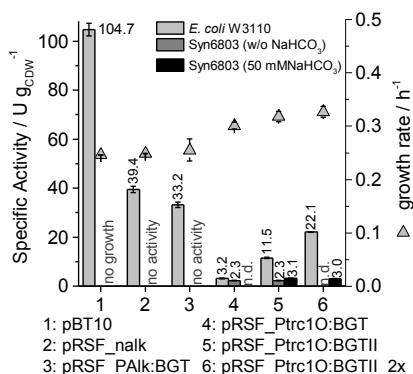


**Figure 10.7:** Dependency of the oxyfunctionalization activity of Syn6803\_BGT on gene expression time. Cells were cultivated under standard conditions (YBG11, 50  $\mu$ E, ambient  $CO_2$ ), induced after 2, 3, 4, or 5 days (panels **A**, **B**, **C**, and **D**, respectively), and harvested at defined time points to determine oxyfunctionalization activities in short-term assays ( $2 g_{CDW} L^{-1}$ , YBG11 +  $NaHCO_3$ , 30  $\mu$ E  $m^{-2} s^{-1}$ ). Non-induced cells (dashed bars) served as a control. Error bars represent the standard deviation of two independent biological replicates.

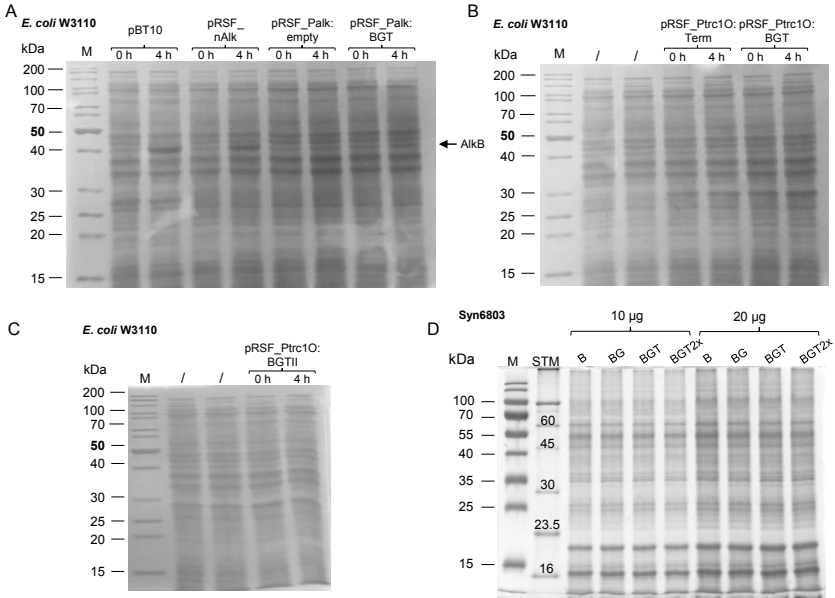




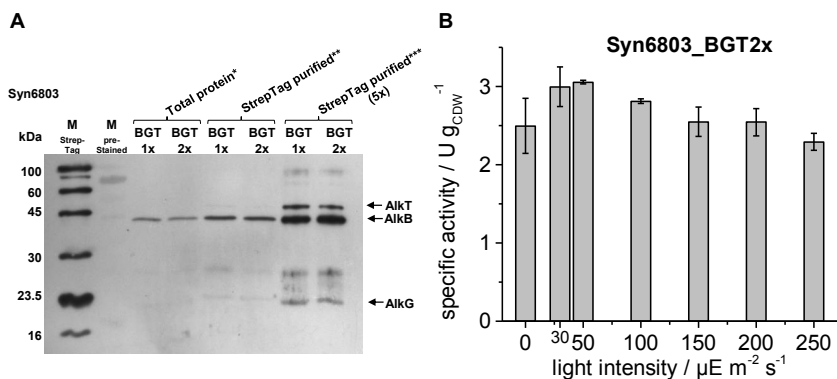
**Figure 10.8:** Impact of different NAME concentrations within the organic carrier solvent DINP on the NAME hydrolysis activity of Syn6803\_BGT. Cells were cultivated under standard conditions (YBG11, ambient CO<sub>2</sub>, 50 μE m<sup>-2</sup> s<sup>-1</sup>) and applied for long-term NAME biotransformations (YBG11 + NaHCO<sub>3</sub>, 2 g<sub>CDW</sub> L<sup>-1</sup>, 30 μE m<sup>-2</sup> s<sup>-1</sup>) using different concentrations of NAME dissolved in DINP added at an organic:aqueous phase ratio of 1:3. Initial specific activities were calculated for the first 30 min of reaction. Average values and standard deviations of two independent biological replicates are given. \* Only one biological replicate available; standard deviation of 10% was assumed. U = unit = μmol min<sup>-1</sup>, CDW = cell dry weight.



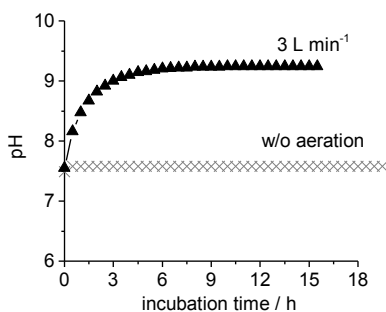
**Figure 10.9:** Analysis of expression system components used for the heterologous expression of *alkBGT* in *E. coli* W3110 and *Synechocystis* sp. PCC 6803 (Syn6803). Specific oxyfunctionalization activities of *E. coli* W3110 strains are based on 15 min resting-cell assays (performed as described in **Chapter 3**). Specific oxyfunctionalization activities of Syn6803 strains are based on 30 min standard reaction assays in YBG11 medium either without NaHCO<sub>3</sub> or with 50 mM NaHCO<sub>3</sub>, as indicated. pRSF\_nAlk (=pAH010) constitutes a broad host range vector (RSF origin of replication) encoding the *alkBFG* and *alkST* operons in their native configuration under control of the P<sub>alk</sub> regulatory system of *Pseudomonas putida* GPo1. pRSF\_PAIk:BGT (= pAH039) constitutes a broad host range vector (RSF origin of replication) with the *alkBGT* genes in a single operon under control of the P<sub>alk</sub> regulatory system. pRSF\_Ptrc10:BGT (= pAH038) constitutes a broad host range vector (RSF origin of replication) containing the *alkBGT* genes in a single operon under control of the P<sub>trc10</sub> promoter system. pRSF\_Ptrc10:BGTI (= pAH042) equals pAH038 with a Strep-tagII sequence added to the C-terminus of *alkB*, *alkG*, and *alkT*. pRSF\_Ptrc10:BGTII\_2x (= pAH048) equals pAH042 with a second *Ptrc10:BGTI* operon present in the same plasmid. “No growth” indicates that no colonies were formed upon transformation of *Synechocystis* sp. PCC 6803 with the respective plasmid. Growth rates are given for *E. coli* W3110 strains. The growth rates of recombinant *Synechocystis* sp. PCC 6803 did not vary between the strains. Average values and standard deviations of two independent biological replicates are given. U = unit = μmol min<sup>-1</sup>, CDW = cell dry weight.



**Figure 10.10:** SDS PAGE analysis of *E. coli* W3110 (**A** - **C**) and *Synechocystis* sp. PCC 6803 (= Syn6803) (**D**) harboring indicated plasmids. Cells were either disrupted by heat (*E. coli* W3110, 99 °C, 5 min) or using glass beads (Syn6803) as described in **Chapter 2**. Whole-cell protein fractions of 45 µg<sub>CDW</sub> (**A** - **C**) or protein fractions of 10 or 20 µg (**D**) were applied. **A**) pRSF\_nAlk = pAH010, pRSF\_Palk:empty = pAH008, pRSF\_Palk:BGT = pAH039, **B**) pRSF\_Ptrc1O:Term = pAH032, pRSF\_Ptrc1O:BGT = pAH042, **C**) pRSF\_Ptrc1O:BGTII = pAH048, **D**) B = pAH044, BG = pAH047, BGT = pA042, BGT2x = pAH048. The expression systems located on respective plasmids are described in **Chapter 2**. M = unstained protein ladder (PageRuler Unstained Protein Ladder 26614, Thermo Fisher Scientific, Waltham, USA), STM = Strep-tag protein ladder (IBA GmbH, Göttingen, Germany).

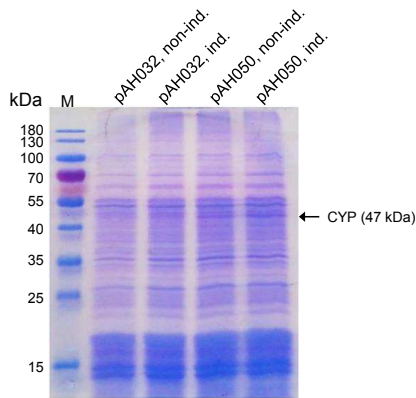


**Figure 10.11:** Western blot analysis and NAME oxyfunctionalization activities of recombinant *Synechocystis* sp. PCC 6803 harboring one (pAH042) or two (pAH048) *Ptc10:BGT* operons on the expression plasmid. Cells were cultivated under standard conditions (YBG11, ambient CO<sub>2</sub>, 50 μE m<sup>-2</sup> s<sup>-1</sup>). Gene expression was induced two days after inoculation. Cells were harvested 24 h after induction of gene expression and subjected to cell disruption, Strep-tag purification, and Western blot analysis as described in **Chapter 2** (panel **A**) or to oxyfunctionalization assays (as described in the materials and methods section of **Chapter 4**), of which the results are shown in panel **B** for the strain containing two operon copies (pAH048). \* 10 μg of total protein from supernatant after cell disruption, \*\* 20 μL of elution fraction after Strep-tag purification (Elution was performed in the same volume as loaden on Strep-tag purification column), \*\*\* 20 μL of 5x concentrated (via acetone precipitation) elution fraction.

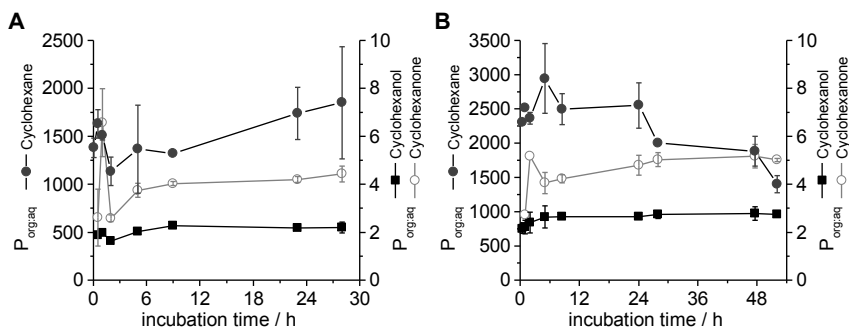


**Figure 10.12:** pH values measured in a stirred tank photo-bioreactor with standard YBG11 medium under abiotic conditions (30 °C, 300 rpm) with and without aeration, respectively.

## 10.3 Supporting information to Chapter 5



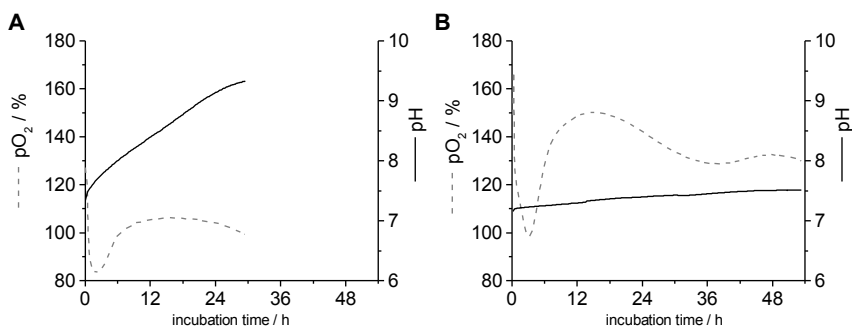
**Figure 10.13:** SDS-PAGE analysis of *Synechocystis* sp. PCC 6803 harboring the empty plasmid pAH032 or the expression vector pAH050 (Syn6803\_CYP). Samples were taken from cultures cultivated in YBG11 medium for 3 days, while gene expression was induced after 2 days using 2 mM IPTG when indicated (= ind.). Cell disruption was performed using glass beads as described in **Chapter 2**. The band corresponding to the CYP enzyme (47.3 kDa) is indicated by an arrow. Protein bands for ferredoxin (12.4 kDa) and ferredoxin reductase (42.7 kDa) could not be identified. Ind. = induced. Marker: PageRuler Prestained Protein Ladder 26616 (Thermo Fisher Scientific, Waltham, USA).



**Figure 10.14:** Partition coefficients for cyclohexane, cyclohexanol, and cyclohexanone during two-liquid phase biotransformation of cyclohexane using Syn6803\_CYP in aerated (A) and non-aerated (B) stirred tank photo-bioreactors.

**Table 10.1:** Partition coefficients obtained during biotransformation in stirred tank photo-bioreactors in comparison to those obtained from abiotic measurement (Eppendorf-tube).

	P <sub>org:aq</sub> (Chx)	P <sub>org:aq</sub> (C-ol)	P <sub>org:aq</sub> (C-one)
Abiotic (Eppendorf-tube)	1775 ± 214	2.1 ± 0.1	4.4 ± 0.7
STR with aeration	1502 ± 321	2.0 ± 0.2	4.0 ± 1.4
STR without aeration	2255 ± 496	2.6 ± 0.3	4.6 ± 0.7



**Figure 10.15:** pH and pO<sub>2</sub> courses during cyclohexane biotransformation using Syn6803\_CYP in aerated (A) and non-aerated (B) two-liquid phase stirred-tank photo-bioreactor setups. Biotransformation conditions were: 30 °C, 300 rpm, 150 μE m<sup>-2</sup> s<sup>-1</sup>, and, only for A, 0.15 L min<sup>-1</sup> aeration with compressed air.

## 10.4 Patent application WO2018/162465 A

(12) NACH DEM VERTRAG ÜBER DIE INTERNATIONALE ZUSAMMENARBEIT AUF DEM GEBIET DES PATENTWESENS (PCT) VERÖFFENTLICHTE INTERNATIONALE ANMELDUNG

(19) Weltorganisation für geistiges Eigentum  
Internationales Büro(43) Internationales Veröffentlichungsdatum  
13. September 2018 (13.09.2018)(10) Internationale Veröffentlichungsnummer  
WO 2018/162465 A1

WIPO | PCT

## (51) Internationale Patentklassifikation:

C12M 1/00 (2006.01) C12P 5/02 (2006.01)  
C12M 1/107 (2006.01) C12P 3/00 (2006.01)

(21) Internationales Aktenzeichen: PCT/EP2018/055449

(22) Internationales Anmeldedatum: 06. März 2018 (06.03.2018)

(25) Einreichungssprache: Deutsch

(26) Veröffentlichungssprache: Deutsch

(30) Angaben zur Priorität: 10 2017 104 648.8  
06. März 2017 (06.03.2017) DE

(71) Anmelder: HELMHOLTZ-ZENTRUM FÜR UMWELTFORSCHUNG GMBH - UFZ [DE/DE]; Permoserstr. 15, 04318 Leipzig (DE).

(72) Erfinder: SCHMID, Andreas; Trufanowstr. 17, 04105 Leipzig (DE). HOSCHEK, Anna; Blumenstr. 8, 04105 Leipzig (DE). BÜHLER, Bruno; Kirschbergstr. 12b, 04159 Leipzig (DE).

(74) Anwalt: GULDE &amp; PARTNER PATENT- UND RECHTSANWALTSKANZLEI MBB, Wallstr. 58/59, 10179 Berlin (DE).

(81) Bestimmungsstaaten (soweit nicht anders angegeben, für jede verfügbare nationale Schutzrechtsart): AE, AG, AL, AM, AO, AT, AU, AZ, BA, BB, BG, BH, BN, BR, BW, BY, BZ, CA, CH, CL, CN, CO, CR, CU, CZ, DE, DJ, DK, DM, DO, DZ, EC, EE, EG, ES, FI, GB, GD, GE, GH, GM, GT, HN, HR, HU, ID, IL, IN, IR, IS, JO, JP, KE, KG, KH, KN, KP, KR, KW, KZ, LA, LC, LK, LR, LS, LU, LY, MA, MD, ME, MG, MK, MN, MW, MX, MY, MZ, NA, NG, NI, NO, NZ, OM, PA, PE, PG, PH, PL, PT, QA, RO, RS, RU, RW, SA, SC, SD, SE, SG, SK, SL, SM, ST, SV, SY, TH, TJ, TM, TN, TR, TT, TZ, UA, UG, US, UZ, VC, VN, ZA, ZM, ZW.

(84) Bestimmungsstaaten (soweit nicht anders angegeben, für jede verfügbare regionale Schutzrechtsart): ARIPO (BW, GH, GM, KE, LR, LS, MW, MZ, NA, RW, SD, SL, ST, SZ, TZ, UG, ZM, ZW), eurasisches (AM, AZ, BY, KG, KZ, RU, TJ, TM), europäisches (AL, AT, BE, BG, CH, CY, CZ, DE, DK, EE, ES, FI, FR, GB, GR, HR, HU, IE, IS, IT, LT, LU, LV, MC, MK, MT, NL, NO, PL, PT, RO, RS, SE, SI, SK, SM, TR), OAPI (BF, BJ, CF, CG, CI, CM, GA, GN, GQ, GW, KM, ML, MR, NE, SN, TD, TG).

(54) Title: PROCESS FOR THE BIOREACTIVE EXTRACTION OF PRODUCED OXYGEN FROM A REACTION CHAMBER, AND USE OF PHOTOTROPHIC MICRO-ORGANISMS IN THE RECOVERY OF HYDROGEN

(54) Bezeichnung: VERFAHREN ZUR BIOREAKTIVEN EXTRAKTION ERZEUGTEN SAUERSTOFFS AUS EINEM REAKTIONSRaum, SOWIE VERWENDUNG VON PHOTOTROPHEN MIKROORGANISMEN BEI DER GEWINNUNG VON WASSERSTOFF

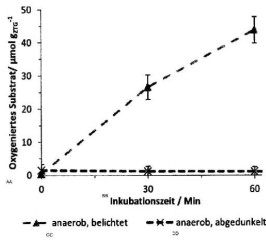


Fig. 1

AA Oxygenated substrate/  $\mu\text{mol l}^{-1}$   
 BB Incubation time/ Min  
 CC Anaerobic, irradiated  
 DD Anaerobic, shaded

(57) Abstract: The invention relates to a method for extracting oxygen from a reaction chamber, to the use of micro-organisms in a process of this type and to a photo-bioreactor for carrying out the method. According to the invention, the process comprises the steps - irradiating at least one phototrophic micro-organism with light under anaerobic conditions in a reaction chamber, and in-situ bonding of formed oxygen by means of the micro-organism, by the oxidation of an oxygen-salvaging substrate.

(57) Zusammenfassung: Die Erfindung betrifft ein Verfahren zur Extraktion von Sauerstoff aus einem Reaktionsraum, sowie eine Verwendung von Mikroorganismen in einem solchen Verfahren und einen Photobioreaktor zur Durchführung des Verfahrens. Erfindungsgemäß umfasst das Verfahren die Schritte - Bestrahlen zumindest eines phototrophen Mikroorganismus mit Licht unter anaeroben Bedingungen in einem Reaktionsraum, und-in situ Binden von entstehendem Sauerstoff mittels des Mikroorganismus durch Oxidation eines Sauerstoff-verwertenden Substrats.

[Fortsetzung auf der nächsten Seite]

WO 2018/162465 A1

**WO 2018/162465 A1** 

---

**Veröffentlicht:**

- mit internationalem Recherchenbericht (Artikel 21 Absatz 3)
- vor Ablauf der für Änderungen der Ansprüche geltenden Frist; Veröffentlichung wird wiederholt, falls Änderungen eingehen (Regel 48 Absatz 2 Buchstabe h)
- mit dem Sequenzprotokollteil der Beschreibung (Regel 5 Absatz 2 Buchstabe a)



WO 2018/162465

PCT/EP2018/055449

**Verfahren zur bioreaktiven Extraktion erzeugten Sauerstoffs aus einem Reaktionsraum, sowie Verwendung von phototrophen Mikroorganismen bei der Gewinnung von Wasserstoff**

Die Erfindung betrifft ein Verfahren zur bioreaktiven Extraktion erzeugten Sauerstoffs aus einem Reaktionsraum.

Stand der Technik

Wasserstoff gilt als Energieträger der Zukunft, da er einerseits eine hohe Energiedichte aufweist und andererseits eine umweltverträgliche Energiequelle darstellt. Er steht in unbegrenzten Mengen zu Verfügung und lässt sich durch verschiedene Verfahren aus Wasser gewinnen. Wasserstoff kann in einer Brennstoffzelle wieder in Strom und Wärme zurück gewandelt werden, als Endprodukt entsteht wiederum lediglich Wasser. Mittels Wasserstoff lassen sich zumindest theoretisch riesige Energiemengen auch langfristig zwischenspeichern.

Zur Herstellung von Wasserstoff sind insbesondere die Elektrolyse und die photokatalytische Wasserspaltung zu nennen.

Die Elektrolyse ist eine altbekannte und bewährte Methode zur Erzeugung von Wasserstoff. Mit Hilfe elektrischen Stroms wird Wasser in Wasserstoff und Sauerstoff zerlegt. Diese Methode ist zurzeit nur dann wirtschaftlich, wenn genügend günstiger Strom zur Verfügung steht.

Die photokatalytische Wasserspaltung - die Spaltung von Wasser in Wasserstoff und Sauerstoff mittels Sonnenlicht - stellt eine technologisch wichtige Alternative zur energieaufwendigen elektrolytischen Wasserspaltung dar. In diesem Fall werden in der Regel Algen oder Cyanobakterien eingesetzt, welche unter bestimmten Bedingungen während des Stoffwechselprozesses Wasserstoff an die Umgebung abgegeben können. So kann man in Algenreaktoren mittels Photosynthese Sonnenlicht und Wasser direkt in Wasserstoff umwandeln. Der enzymatische Prozess besteht aus zwei Schritten. Durch die photosynthetische Lichtreaktion erfolgt im ersten Schritt eine Aufteilung des Wassers in Protonen, Elektronen und molekularen Sauerstoff. Durch zum Beispiel Hydrogenasen werden die Protonen im zweiten Schritt zu molekularem Wasserstoff reduziert. Bei dieser oxygenen, das heißt Sauerstoff-freisetzenden Photosynthese, arbeiten zwei große, Cofaktor-haltige Proteinkomplexe, das Photosystem I (PSI) und das Photosystem II (PSII) zusammen. Das PSII spaltet mit Hilfe von Lichtenergie Wasser in Protonen, Sauerstoff und Elektronen und transferiert letztere über eine Elektronentransportkette auf das PSI.

WO 2018/162465

PCT/EP2018/055449

Die Kopplung der Hydrogenase mit dem Photosystem I, sowie dem Wasser-spaltenden Photosystem II der Mikroorganismen ermöglicht demzufolge die Herstellung von Wasserstoff aus Licht und Wasser, bei der lediglich Sauerstoff als „Abfallprodukt“ anfällt. Bei dem Aufeinandertreffen von Sauerstoff und Wasserstoff besteht durch die Bildung von Knallgas eine Explosionsgefahr. Zudem sind bekannte Hydrogenasen sauerstoffempfindlich. Es ist deshalb zunächst erforderlich, die Gase nach der Bildung schnell zu trennen, um die Explosionsgefahr (Entstehung von Knallgas) und die Degeneration der Hydrogenasen zu verringern. Das erfolgt zum Beispiel unter Verwendung Sauerstoff-resistenter Hydrogenasen (US 20090263846 A1), poröser Membranen (DE 102007002009 A1) oder zeitlicher Trennung von Sauerstoffbildung und Wasserstoffproduktion (US 4532210 A).

Diese Techniken besitzen wesentliche Nachteile, so unterdrücken die Sauerstoff-resistenten Hydrogenasen nicht die Bildung von Knallgas, die Membrantechnologie verhindert nicht die Inaktivierung eines Sauerstoff-sensitiven Enzymsystems und durch zeitliche Trennung von Sauerstoffbildung und Wasserstoffproduktion wird das Verfahren in eine produktive und nichtproduktive Phase geteilt. Demnach ist die photokatalytische Wasserstoffproduktion in großtechnischem Ausmaß an spezifische Bedingungen gebunden, die produktionstechnisch nicht oder nur unter hohem Kostenaufwand realisierbar sind.

Die Aufgabe der Erfindung besteht deshalb darin, ein Verfahren zur Wasserstoffproduktion bereitzustellen, das unerwünscht entstehenden molekularen Sauerstoff von der chemischen Produktion eines Zielprodukts trennt und die Nachteile des Standes der Technik, wie Explosionsgefahr durch Knallgasbildung, zwei Prozessphasen und Inaktivierung von Sauerstoff-sensitiven Enzymen, vermeidet. Insbesondere besteht die Aufgabe darin, umweltfreundliche, preiswerte und stabile Photokatalysatoren zu finden, die in der Lage sind, photosynthetisch entstehenden Sauerstoff während einer Wasserstoffproduktion zu binden.

Die Aufgabe wird durch ein Verfahren zur bioreaktiven Extraktion photokatalytisch erzeugten Sauerstoffs in einem Reaktionsraum erfüllt, das die folgenden Schritte umfasst:

- Bestrahlen zumindest eines phototrophen Mikroorganismus mit Licht unter anaeroben Bedingungen in einem Reaktionsraum, und
- in situ Binden von entstehendem Sauerstoff durch den Mikroorganismus.

Das erfindungsgemäße Verfahren überwindet technische Herausforderungen, die aufgrund von sauerstoffsensiblen Prozessen bzw. Edukten, Produkten und Enzymen entstehen. So können auch in sauerstoffproduzierenden enzymatischen Verfahren sauerstoffsensible Mikroorganismen und Enzyme eingesetzt werden, ohne dass die Leistungsfähigkeit beeinträchtigt wird. Prozesse, in denen sowohl Wasserstoff als auch Sauerstoff anfallen und

WO 2018/162465

PCT/EP2018/055449

die somit potenziell Knallgas produzieren, werden entschärft, da beide Reaktionspartner in situ getrennt werden.

Dies ist möglich, indem der Sauerstoff direkt am Ort seiner Entstehung eingefangen und enzymatisch gebunden wird. Damit ist der entstehende Sauerstoff direkt am Ort seiner Entstehung deaktiviert. Die Deaktivierung erfolgt beispielsweise durch die Oxidation eines ebenfalls im Reaktionsraum vorhandenen Substrats in Form einer chemischen Bindung des Sauerstoffs an das Substrat, aufgrund derer der Sauerstoff nicht wieder in den Reaktionsraum entlassen wird. Der Vorteil besteht daher insbesondere darin, dass der Sauerstoff nicht nur separiert oder maskiert ist, sondern chemisch deaktiviert ist. Somit weist der Reaktionsraum und insbesondere der Mikroorganismus bevorzugt ferner ein Sauerstoff verwertendes Substrat auf.

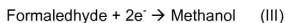
Darüber hinaus ermöglicht die Erfindung, die Sauerstoffdeaktivierung quantitativ zu regeln indem die sauerstoffverbrauchende Reaktion gesteuert wird. Somit kann ein zuvor definierter Betrag an Sauerstoff dem Reaktionsraum zur Verfügung gestellt werden, der im Bereich von 0 (entstehender Sauerstoff vollständig gebunden) bis 1 (kein Sauerstoff gebunden) liegt.

Durch geeignete Wahl des Substrats kann ferner ein oxidiertes Zielprodukt hergestellt werden, so dass die Bindung des im eigentlichen Zielprozess entstehenden störenden Sauerstoffs zu einem weiteren Wertschöpfungsschritt führt.

Vorliegend handelt es sich bei dem entstehenden Sauerstoff um molekular vorliegenden Sauerstoff.

Bevorzugt weist der Mikroorganismus ein sauerstoffumsetzendes Enzym auf oder produziert ein solches.

In weiter bevorzugter Ausführungsform ist das bevorzugte Zielprodukt Wasserstoff beziehungsweise Protonen, welche anschließend mit Elektronen zu Wasserstoffmolekülen reduziert werden. Alternativ ist das Zielprodukt Methanol, welches durch Reduktion von  $\text{CO}_2$  mit den aus der Wasserspaltung stammenden Elektronen erzeugt wird. In beiden Fällen handelt es sich um einen Brennstoff, der beispielsweise als Ausgangsprodukt für eine Brennstoffzellenreaktion eingesetzt wird. Diese Reaktionen werden beispielsweise durch drei Dehydrogenasen, welche zu der Klasse der Oxidoreduktasen gehören, katalysiert.



WO 2018/162465

PCT/EP2018/055449

Insbesondere weist der zumindest eine phototrophe Mikroorganismus daher ein Enzym ausgewählt aus der Gruppe Hydrogenase, Nitrogenase und/oder Oxidoreduktase auf.

Das Verfahren wird vorzugsweise in einem flüssigen, insbesondere wässrigen Medium durchgeführt. In bevorzugter Ausführungsform ist vorgesehen, in einem Prozess störenden Sauerstoff (O<sub>2</sub>) aus dem Reaktionsraum zu entfernen, der bei der photosynthetischen Lichtreaktion aus Wasser oder wässrigen Flüssigkeiten oder Lösungen unter Verwendung phototropher Mikroorganismen im Reaktionsraum entsteht. Dabei weist der phototrophe Mikroorganismus, mindestens ein sauerstoffumsetzendes Enzym auf oder produziert dieses. Gleichzeitig werden sauerstoffverwertende Substrate eingesetzt.

Vorteilhafterweise weist der Mikroorganismus neben der Hydrogenase, Nitrogenase und/oder Oxidoreduktase zumindest ein weiteres, sauerstoffumsetzendes Enzym auf. Insbesondere bei einer Kombination von Hydrogenase und einer Oxidoreduktase findet der Wasserstoff erzeugende und der Sauerstoffumsetzende Prozessschritt im gleichen Mikroorganismus und damit ohne räumliche Trennung statt. Der Sauerstoff wird direkt nach dessen Produktion umgesetzt und erfindungsgemäß deaktiviert. In bevorzugter Ausführungsform ist vorgesehen, dass das weitere Enzym eine Oxidoreduktase, insbesondere Oxidase und Oxygenase, ist.

Alternativ liegt im Reaktionsraum ein weiterer Mikroorganismus vor, der das weitere Enzym aufweist. Mit anderen Worten, weist bevorzugt ein Mikroorganismus Hydrogenase, Nitrogenase und/oder Oxidoreduktase als Wasserstoff-produzierendes Enzym und zusätzlich Oxidoreduktase als Sauerstoff-umsetzendes Enzym auf, oder zwei verschiedene im Reaktionsraum vorhandene Mikroorganismen weisen je eines dieser Enzyme auf. Vorliegend wird nur eine Kombination aus den genannten Enzymen explizit erwähnt, wobei auch sämtliche andere Kombinationen ausdrücklich vorgesehen sind. In der Ausführungsform verschiedener Mikroorganismen finden der sauerstoff erzeugende und der sauerstoffumsetzende Prozess nicht im selben Mikroorganismus, aber dennoch im selben Reaktionsraum statt. Der Vorteil besteht insbesondere darin, dass der sauerstoffumsetzende Prozess und damit das quantitative Maß an im Prozess vorhandenem Sauerstoff durch ein quantitatives Verhältnis der Mikroorganismen zueinander gesteuert werden kann.

Ferner ist bevorzugt, dass der Mikroorganismus selbst das Zielprodukt, also beispielsweise Wasserstoff oder Methanol, erzeugt. Mit anderen Worten, es wird in einer bevorzugten Ausführungsform des erfindungsgemäßen Verfahrens bei der Bestrahlung des zumindest einen phototrophen Mikroorganismus neben Sauerstoff auch Wasserstoff oder Methanol frei.

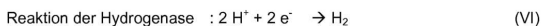
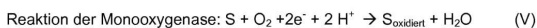
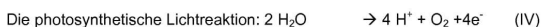
Somit sieht das erfindungsgemäße Verfahren in einer bevorzugten Ausführungsform vor, dass mindestens ein phototropher Mikroorganismus unter Lichteinwirkung mit Wasser oder

WO 2018/162465

PCT/EP2018/055449

einer wässrigen Flüssigkeit oder Lösung in Kontakt gebracht wird, wobei ein Mikroorganismus gewählt wird, der neben den Hydrogenasen weiterhin Oxidoreduktasen als Sauerstoff-umsetzende Enzyme aufweist oder produziert oder ein weiterer Mikroorganismus im gleichen Reaktionsraum gewählt wird, der Oxidoreduktasen als Sauerstoff-umsetzende Enzyme aufweist oder produziert.

Die Oxidoreduktase ist vorzugsweise ausgewählt aus der Gruppe der Oxidasen oder Oxygenasen, vorzugsweise Monooxygenasen, Dioxygenasen oder coenzym-unabhängige Oxygenasen. Eine Monooxygenase als Sauerstoff verbrauchendes Enzym sollte das Enzym der Wahl sein, wenn das stöchiometrische Gleichgewicht im Reaktionsraum von Interesse ist. Es ergibt sich folgendes Reaktionssystem:



Besonders bevorzugt sind Oxidoreduktasen vom AlkB-Typ, die in der Literatur als Katalysatoren zur Herstellung überwiegend von weniger stark oxidierten Produkten bekannt sind. Diese eignen sich besonders um aus Alkanen und deren Carbonsäuren bzw. Carbonsäureestern, überwiegend Produkte höherer Oxidationsstufen herzustellen. - Derartige Oxidoreduktasen sind ferner zur selektiven Oxidation von Alkanen und deren Carbonsäuren bzw. -estern befähigt, wobei zu erwartende Nebenprodukte, insbesondere an anderen als endständigen Kohlenstoffatomen oxidierte Alkane, nur in unerwartet geringem Ausmaß oder überhaupt nicht in nachweisbaren Mengen herzustellen.

Vorliegend werden die Substrate vorzugsweise unter Verwendung einer Oxidoreduktase vom AlkB-Typ in Anwesenheit von Sauerstoff oxidiert. AlkB stellt eine zunächst aus dem AlkBGT-System aus *Pseudomonas putida Gpo1* bekannt gewordene Oxidoreduktase dar, die von zwei weiteren Polypeptiden, AlkG und AlkT, abhängig ist. AlkT wird als FAD abhängige Rubredoxin-Reduktase charakterisiert, die Elektronen aus NADH an AlkG weitergibt. Bei AlkG handelt es sich um ein Rubredoxin, ein eisenhaltiges Redoxprotein, das als direkter Elektronendonator für AlkB fungiert. In einer bevorzugten Ausführungsform wird unter demselben Begriff "Oxidoreduktase des alkB-Typs" ein Polypeptid mit einer Sequenzhomologie von zunehmend bevorzugt wenigstens 75, 80, 85, 90, 92, 94, 96, 98 oder 99 % zur Sequenz des AlkB von *Pseudomonas putida Gpo1* (Datenbankcode: CAB54050.1; dieser Datenbankcode stammt aus dem Stand der Technik, nämlich aus der NCBI Datenbank, genauer dem am 15. November 2011 online verfügbaren Release) mit der Fähigkeit, die erfindungsgemäßen Substrate, wie Alkane und deren Carbonsäuren zu

WO 2018/162465

PCT/EP2018/055449

oxidieren. In einer besonders bevorzugten Ausführungsform handelt es sich bei der Oxidoreduktase vom AlkB-Typ um eine mit den AlkG (CAB54052.1)- und AlkT (CAB54063.1)-Polypeptiden aus *Pseudomonas putida Gpo1* funktionell zusammenwirkende, Alkane oxidierende Oxidoreduktase. In einer bevorzugtesten Ausführungsform handelt es sich bei der Oxidoreduktase vom AlkB-Typ um AlkB aus dem AlkBGT-System aus *Pseudomonas putida Gpo1* oder eine Variante davon.

Mit besonderem Vorteil werden Substrate eingesetzt, die nach der Oxidation als Edukte weiterverwendet werden und sogenannte *value added products* für das erfindungsgemäße Verfahren bilden oder aber solche, die im Reaktionsraum unerwünscht sind und durch die Oxidation deaktiviert werden. Somit ist neben der Produktion des Zielprodukts, wie Wasserstoff oder Methanol, auch die Sauerstoffumsetzung ein Zielprozess des Verfahrens. Es handelt sich dann nicht mehr nur um die Bindung von unerwünschtem Sauerstoff, der die Produktion des ersten Zielprodukts stört, sondern um die Bindung von entstehendem Sauerstoff zu einem zweiten Zielprodukt. Ein Einsatzbeispiel, in dem ein unerwünschtes Edukt durch das erfindungsgemäße Verfahren durch Oxidation deaktiviert wird ist die Schmutzwasseraufbereitung. Hier liegen verschiedene Substrate als unerwünschte Stoffe im Schmutzwasser vor. Das Schmutzwasser wird durch Oxidation dieser Substrate aufgereinigt. Je nach eingesetztem Mikroorganismus wird dabei als erwünschtes Nebenprodukt beispielsweise Wasserstoff als Brennstoff produziert.

In bevorzugter Ausführungsform fungieren im erfindungsgemäßen Verfahren Kohlenstoffverbindungen als Substrate, die zugesetzt werden oder die sich in der wässrigen Ausgangslösung befinden. Dabei handelt es sich vorzugsweise um Carbonsäuren oder Carbonsäureester mittelkettiger Alkane mit einer C<sub>3</sub>-C<sub>20</sub>, insbesondere C<sub>5</sub>-C<sub>15</sub>, vorzugsweise C<sub>7</sub>-C<sub>10</sub>-Kette. Ein besonders bevorzugtes Beispiel ist Methylnonanoat (C<sub>8</sub>H<sub>17</sub>-COOH-CH<sub>3</sub>).

Das erfindungsgemäße Verfahren sieht bevorzugt vor, dass als phototropher Mikroorganismus Algen, Purpurbakterien oder Cyanobakterien eingesetzt werden, wobei Cyanobakterien bevorzugt sind. Diese betreiben Photosynthese und weisen sauerstoffumsetzende Enzyme auf, produzieren diese oder sind in geeignetem Maße zur genetischen Modifizierung geeignet, um derartige Enzyme aufzuweisen oder zu produzieren.

Mit besonderem Vorteil wird als Mikroorganismus ein, insbesondere genetisch modifizierter, Cyanobakterienstamm eingesetzt, der das Alkan-Monooxygenase-Enzymsystem AlkBGT aufweist.

In besonders bevorzugter Ausgestaltung des erfindungsgemäßen Verfahrens wird der genetisch modifizierte Cyanobakterienstamm *Synechocystis sp.* PCC6803 als

WO 2018/162465

PCT/EP2018/055449

Mikroorganismus eingesetzt. Dieser weist das Alkan-Monooxygenase-Enzymssystem AlkBGT auf.

Somit betrifft ein weiterer Aspekt der Erfindung eine Cyanobakterienzelle umfassend eine Hydrogenase und die von *alkBGT* kodierte Alkanmonooxygenase der SEQ ID NO: 1 (aus *Pseudomonas putida GPO1*) oder einer Variante davon, insbesondere einem Enzym, das zu mindestens 80% mit der SEQ ID NO: 1 identisch ist.

Die Lehre der vorliegenden Erfindung kann nicht nur unter Verwendung der exakten Aminosäure- oder Nukleinsäuresequenzen der hierin beschriebenen biologischen Makromoleküle ausgeführt werden, sondern auch unter Verwendung von Varianten derartiger Makromoleküle, die durch Deletion, Addition oder Substitution einer oder mehr als einer Aminosäure oder Nukleinsäure erhalten werden können.

In einer bevorzugten Ausführungsform bedeutet der Begriff "Variante" einer Nukleinsäuresequenz oder Aminosäuresequenz, im Folgenden gleichbedeutend und austauschbar mit dem Begriff "Homologen" gebraucht, wie hierin verwendet, eine andere Nukleinsäure- oder Aminosäuresequenz, die mit Hinblick auf die entsprechende ursprüngliche Wildtyp-Nukleinsäure- oder -aminosäuresequenz eine Homologie, hier gleichbedeutend mit Identität verwendet, von 70, 75, 80, 85, 90, 92, 94, 96, 98, 99 % oder mehr Prozent aufweist, wobei bevorzugt andere als die das katalytisch aktive Zentrum ausbildende Aminosäuren oder für die Struktur oder Faltung essentielle Aminosäuren deletiert oder substituiert sind oder letztere lediglich konservativ substituiert sind, beispielsweise ein Glutamat statt einem Aspartat oder ein Leucin statt einem Valin. Es besteht keine Notwendigkeit, dass die Sequenz über ihre gesamte Länge eine entsprechend hohe Homologie aufweist, erfindungsgemäß können auch Fusionsproteine oder für solche kodierende Nukleinsäuren verwendet werden, die einen Teil mit entsprechender Homologie und/oder Aktivität aufweist. Der Stand der Technik beschreibt Algorithmen, die verwendet werden können, um das Ausmaß von Homologie von zwei Sequenzen zu berechnen, z. B. Arthur Lesk (2008), *Introduction to bioinformatics, 3rd edition*.

In einer weiteren bevorzugteren Ausführungsform der vorliegenden Erfindung weist die Variante einer Aminosäure- oder Nukleinsäuresequenz, bevorzugt zusätzlich zur oben genannten Sequenzhomologie, im Wesentlichen die gleiche enzymatische Aktivität des Wildtypmoleküls bzw. des ursprünglichen Moleküls auf. Zum Beispiel weist eine Variante eines als Protease enzymatisch aktiven Polypeptids die gleiche oder im Wesentlichen die gleiche proteolytische Aktivität wie das Polypeptidenzym auf, d.h. die Fähigkeit, die Hydrolyse einer Peptidbindung zu katalysieren. In einer besonderen Ausführungsform bedeutet der Begriff "im Wesentlichen die gleiche enzymatische Aktivität" eine Aktivität mit

WO 2018/162465

PCT/EP2018/055449

Hinblick auf die Substrate des Wildtyp-Polypeptids, die deutlich über der Hintergrundaktivität liegt oder/und sich um weniger als 3, bevorzugter 2, noch bevorzugter eine Größenordnung von den KM- und/oder kcat-Werten unterscheidet, die das Wildtyppolypeptid mit Hinblick auf die gleichen Substrate aufweist. In einer weiteren bevorzugten Ausführungsform umfasst der Begriff "Variante" einer Nukleinsäure- oder Aminosäuresequenz wenigstens einen aktiven Teil/oder Fragment der Nukleinsäure- bzw. Aminosäuresequenz.

Insbesondere in vorgenannter Ausführungsform wird als Substrat Methylnonanoat verwendet.

Ein weiterer Aspekt der Erfindung betrifft die Verwendung von phototrophen Mikroorganismen, die neben Hydrogenasen Oxidoreduktasen als Sauerstoff-umsetzende Enzyme aufweisen oder produzieren, bei der Gewinnung von Wasserstoff (H<sub>2</sub>) und Sauerstoff (O<sub>2</sub>) aus Wasser oder wässrigen Flüssigkeiten und Lösungen und zur simultanen in-situ Entfernung des Sauerstoffs (O<sub>2</sub>) unter Verwendung entsprechender Substrate, die mit dem Sauerstoff Produkte bilden. Bevorzugt betrifft die Erfindung die Verwendung von phototrophen Mikroorganismen, die neben Hydrogenasen Oxidoreduktasen als Sauerstoff-umsetzende Enzyme aufweisen oder produzieren in dem erfindungsgemäßen Verfahren.

Insbesondere bevorzugt ist die Verwendung des erfindungsgemäßen Verfahrens bei der Schmutzwasseraufbereitung. Hierbei wird ein Gemisch undefinierter organischer Substanzen, die im Sinne der Erfindung als Substrate wirken, für die sauerstoffverwendende Reaktion des Mikroorganismus zur Verfügung gestellt. Die Wahl einer nicht spezifischen, nichtselektiven Oxygenierungsreaktion ermöglicht die Oxidation und damit die Inaktivierung der im Abwasser auftretenden Schadstoffe. Dabei findet vorteilhafterweise gleichzeitig eine Erzeugung von Wasserstoffgas als Quelle für Energieerzeugung und eine Oxidation von gelöstem organischen Kohlenstoff im Abwasser statt.

Als Mikroorganismus wird vorzugsweise ein Algenstamm, ein Purpurbakterienstamm oder ein Cyanobakterienstamm verwendet. Besonders bevorzugt wird ein Stamm, der das Alkan-Monooxygenase-Enzymsystem AlkBGT aufweist, wie beispielsweise *Synechocystis sp. PCC6803*, eingesetzt.

Das erfindungsgemäße Verfahren wird bevorzugt im Photobioreaktor durchgeführt. Somit betrifft ein weiterer Aspekt der Erfindung einen Photobioreaktor zur Ausführung des erfindungsgemäßen Verfahrens, insbesondere umfassend den genetisch modifizierten Cyanobakterienstamm *Synechocystis sp. PCC6803*, der das Alkan-Monooxygenase-Enzymsystem AlkBGT aufweist oder produziert. Hierbei liegt der Mikroorganismus, insbesondere der Bakterienstamm als Biofilm vor.



WO 2018/162465

PCT/EP2018/055449

Photobioreaktoren sind Fermenter, in denen die phototrophen Mikroorganismen zum Beispiel Algen, Cyanobakterien und Purpurbakterien kultiviert werden, in denen also entweder das Wachstum und die Vermehrung dieser Zellen ermöglicht wird oder die Produktion unterschiedlicher Substanzen mittels phototropher Zellen gefördert wird. Im Unterschied zu konventionellen biotechnischen Fermentationsprozessen sind phototrophe Vorgänge lichtabhängig. Um den Zellen einen aktiven Stoffwechsel zu ermöglichen, werden sie möglichst optimal sowohl mit Licht als auch mit verschiedenen Nährlösungen bzw. gelösten Substraten versorgt.

Die Photobioreaktoren variieren erheblich in Material und Konstruktionsweise. Ihnen allen gemein ist, dass sie auf Basis ihrer Konstruktion eine optimale Lichtversorgung der Mikroorganismen gewährleisten sollen. Auf dem Markt befinden sich zum Beispiel Reaktoren, die mit Kunststoff-Beuteln oder Schläuchen arbeiten oder Systeme die mit flachen Behältern oder Röhren die Biomasse in dünnen Schichten der Sonne exponieren.

Jeder Reaktor hat neben dem lichtdurchlässigen Photosyntheseteil auch einen Zulauf für CO<sub>2</sub> und Substrate und eine Einrichtung die Mikroorganismen zu ernten. Meist wird der Zustand und die Dichte der Kultur noch über eine sensible Mess-Elektronik detektiert, um regelnd eingreifen zu können.

Der Röhrenreaktor ist ein ausgereifter und bereits in Großanlagen verbauter Photobioreaktor. Die Mikroorganismensuspension wird in durchsichtigen Röhren aus Glas oder Plastik geführt und mittels einer Pumpe in Bewegung gehalten.

Der Helix- oder Coil-Reaktor ist im Grunde ein Röhrenreaktor, der allerdings keine Glasröhren einsetzt, sondern einen flexiblen Schlauch. Dieser wird dann kreisförmig angeordnet, die Prozessführung ähnelt dem Röhrenreaktor.

Der Beutel- oder Schlauch-Reaktor ist ein Photobioreaktor auf Basis von einzelnen Kompartimenten aus Kunststoffolie, oft hängend angeordnet. Es gibt hier auch Ansätze funktionale Kunststoffe einzusetzen und Ideen, die Beutel auf dem Wasser zu positionieren. Die Durchmischung erfolgt meist durch den CO<sub>2</sub>-Eintrag und ist damit relativ energieeffizient. Die Folie ist dabei nicht auf einen langfristigen Einsatz ausgerichtet, sondern wird von Zeit zu Zeit erneuert.

Beim Kessel-Reaktor wird ein üblicherweise säulenförmiger Flüssigkeitsbehälter eingesetzt, in dem die Algenbiomasse gezüchtet wird. Je nach Design des Behälters, wird über verschiedene Systeme Licht in den Behälter eingebracht. Dies kann Sonnenlicht sein, oder artifizielle Lichtquellen. Manche Ansätze nutzen dazu Linsensysteme und Lichtleiter. Eine

WO 2018/162465

PCT/EP2018/055449

Durchmischung kann über verschiedene Mechanismen erfolgen, wie zum Beispiel Gaseintrag oder Umwälzung durch Pumpen.

Im Flachplatten-Reaktor werden die Mikroorganismen dabei im Kulturmedium in flachen Schichten dem Licht ausgesetzt. Begrenzt wird der Reaktor durch Glas- oder Plastik-Platten, die Durchmischung erfolgt durch den Gaseintrag.

Im Dünnschicht-Reaktor, wird das Prinzip der Minimierung der Mikroorganismenschicht zur optimalen Lichtausbeute konsequent weiter verfolgt. Damit soll die Selbst-Überschattung dichter Suspensionen gemindert werden. Immobilisierte Mikroorganismen werden dabei auf einem Trägermaterial dem Licht exponiert.

Erfindungsgemäß werden bevorzugt Röhrenreaktoren eingesetzt.

Zusammenfassend ermöglicht die Erfindung eine Kombination zweier bislang unabhängiger Techniken, die photokatalytische Wasserstoffgasproduktion und die photokatalytische Sauerstoffreaktion. Simultan zur Herstellung von Wasserstoff als Biotreibstoff wird dabei ein Substrat oxidiert und dabei deaktiviert oder ein Mehrwertprodukt hergestellt.

Die vorliegende Erfindung wird weiterhin durch die folgenden Figuren und nicht beschränkenden Beispiele veranschaulicht, denen weitere Merkmale, Ausführungsformen, Aspekte und Vorteile der vorliegenden Erfindung entnommen werden können.

- **Figur 1:** graphische Darstellung einer Extraktion von photosynthetisch erzeugtem Sauerstoff durch das Alkan-Monooxygenase Enzymsystem AlkBGT, welches genetisch in den Cyanobakterien-Stamm *Synechocystis sp.* PCC6803 eingeführt wurde, in erfindungsgemäßer Durchführung.

Zur Durchführung des erfindungsgemäßen Verfahrens kommen verschiedene Bedingungen in Frage. Essentiell ist dabei lediglich die Anwesenheit von molekularem Sauerstoff als Oxidationsmittel.

Beispiel 1:

**Herstellung eines genetisch modifizierten Stamms - *Synechocystis sp.* PCC6803, enthaltend das Alkan-Monooxygenase Enzymsystem AlkBGT**

Die Einführung der Gene kodierend für das Alkan-Monooxygenase Enzymsystem AlkBGT erfolgte über einen Plasmid-basierten Ansatz (pRSF\_Ptrc10:BGTI1). Die folgenden Protokolle und Klonierungsschritte beschreiben die Konstruktion des Plasmides. In Tabelle 1

WO 2018/162465

PCT/EP2018/055449

sind die Stämme und Plasmide aufgeführt, welche während des Klonierungs-Verfahrens verwendet und erzeugt wurden.

Tabelle 1: Stämme/ Plasmid-Konstruktionen die während des Klonierungs-Verfahrens verwendet und erzeugt wurden.

Stamm/ Plasmid	Beschreibung	Referenz
<i>E. coli</i> DH5 $\alpha$	F <sup>-</sup> $\Phi$ 80 <i>lacZ</i> $\Delta$ M15 $\Delta$ ( <i>lacZYA-argF</i> ) U169 <i>recA1 endA1 hsdR17</i> (rK <sup>-</sup> , mK <sup>+</sup> ) <i>phoA</i> <i>supE44 <math>\lambda</math>B<sup>-</sup> thi<sup>-1</sup> gyrA96 relA1</i>	(Hanahan 1983)
<i>Synechocystis sp.</i> PCC6803	Geographische Ursprung: Kalifornien, USA Erhalten von der Pasteur Culture Collection of Cyanobacteria (PCC, Paris, Frankreich)	(Stanier et al. 1971)
pBT10	Alkane-Monooxygenase Expressionssystem ( <i>alkBFG</i> , <i>alkST</i> ) in pCOM10	(Schrewe et al. 2011)
pSB1AC3_Ptrc10:GFPmut3B	P <sub>Ptrc10</sub> Promoter, GFPmut3B Gen (BBa_E0040) in pSB1AC3	(Huang et al. 2010)
pSB1AC3_Ptrc10:Term	pSB1AC3 mit dem P <sub>Ptrc10</sub> Promoter aus pSB1AC3_Ptrc10:GFPmut3B via XbaI, diese Arbeit PstI (Gibson Klonierung)	
pSB1AC3_PrnpB:lacI	PrnpB (konstitutiver Promoter des <i>maseP</i> Gens) kontrollierend eine Variante des lac Repressors lacI in pSB1AC3	(Huang et al. 2010)
pSB1AC3_PrnpB:lacI_Ptrc10:Term	pSB1AC3_Ptrc10:Term mit PrnpB:lacI aus pSB1AC3_PrnpB:lacI via XbaI diese Arbeit (Restriktion, Ligation)	
pPMQAK1	Broad host range Plasmid, RSF ori, mob	(Huang et al.)

WO 2018/162465	PCT/EP2018/055449
	Gene 2010)
pMQAK1_PmpB:lacI_Ptrc1O:Term	pMQAK1 mit PmpB:lacI_Ptrc1O:Term aus pSB1AC3_PmpB:lacI_Ptrc1O:Term diese Arbeit via EcoRI, PstI (Restriktion, Ligation)
pMQAK1_PmpB:lacI_Ptrc1O:BGITII	pMQAK1_PmpB:lacI_Ptrc1O:Term mit <i>alkBGT</i> Genen aus pBT10 (Gene aufeinander folgend , optimierte RBS, C-terminaler Strep-tag II) via SpeI (Gibson Klonierung) diese Arbeit
pRSF_Ptrc1O:BGITII	pMQAK1_PmpB:lacI_Ptrc1O:BGITII mit zusätzlichem Terminator (biobrick #Bba_B0015 via XbaI (Gibson Klonierung) diese Arbeit

Als Teil des Klonierungsverfahrens wurden die folgenden Verfahrensschritte wie Restriktion, Amplifizierung u.s.w. wie im Folgenden angegeben durchgeführt.

Die Restriktions-Endonukleasen wurden von Thermo Scientific - Germany GmbH (Schwerte, Deutschland) bezogen und entsprechend der Empfehlung eingesetzt.

Eine Amplifizierung von DNA Fragmenten wurde durch polymere Kettenreaktion (PCR) bei Anwendung der Phusion High Fidelity (HF) DNA Polymerase von Thermo Scientific – Germany GmbH (Schwerte, Deutschland) über das empfohlene 3-Schritt Protokoll mit entsprechenden Primern (aufgeführt in Tabelle 2) durchgeführt. Entsprechende Anlagerungs- Temperaturen ( $T_{An}$ ) und Elongations-Zeiten ( $t_{Ei}$ ) sind im jeweiligen Verfahrensschritt unten beschrieben.

Eine gewünschte Overlap-Extension-PCR (OE-PCR) wurde durch Einsatz von je 50 ng der DNA Fragmente in einem 100  $\mu$ L Standard PCR-Ansatz durchgeführt. Entsprechende Primer wurden nach 5 PCR Zyklen zugegeben.

Plasmid-DNA wurde mittels FastAP Thermosensitive Alkaline Phosphatase von Thermo Scientific – Germany GmbH (Schwerte, Deutschland) entsprechend der Empfehlung dephosphoryliert.

WO 2018/162465

PCT/EP2018/055449

Anschließend erfolgte eine Aufreinigung von Plasmid-DNA und amplifizierter DNA-Fragmente über das PCR Clean-up Gel Extraktions-Kit von MACHERY-NAGEL GmbH & Co. KG (MACHEREY-NAGEL GmbH & Co. KG, Düren, Deutschland).

Gibson Klonierung erfolgte über eine einschrittige, isothermale, *in vitro* rekombinante Klonierungsmethode beschrieben durch Gibson et al. 2009 (Gibson et al. 2009).

Ligation erfolgte über die T4 DNA Ligase von Thermo Scientific – Germany GmbH (Schwerte, Deutschland) entsprechend der Empfehlung.

Schließlich erfolgte eine Verifizierung von PCR-amplifizierten DNA Sequenzen durch Sequenzierung über die Firma Eurofins MWG (Ebersberg, Deutschland).

Auf die in Tabelle 1 genannten bekannten Verfahren wird in der vorliegenden Arbeit Bezug mit der in Tabelle 1 vermerkten Referenz Bezug genommen.

Tabelle 2: Primer die während des Klonierungs-Verfahrens eingesetzt wurden.

Primer#	SEQ.- No.	Sequenz
PAH055	1	TCCGGCTCGTATAATGTGTGGAATTGTGAGCGGATAACA ATTTCACACATACTAGTACCAGGCATCAATAAAAACG
PAH056	2	TATAAACGCAGAAAGGCC
PAH057	3	TGATTTCTGGAATTCGCGGCCGCTTTCTAGATTGACAATT AATCATCCGGCTCGTATAATGTG
PAH058	4	ACACCTTGCCCCTTTTTTTCGCCGACTGCAGTATAAACG CAGAAAGGCC
PAH069	5	CTTTTCCTCGTAGAGCAC
PAH070	6	GAGCCACCCGCAGTTCGAAAAATAGTACTAGAGTAGTGG AGGTTACTAGATGGCAATCGTTGTTGTTG
PAH071	7	ATCAGGTAATTTTATACTCCC
PAH072	8	CTATTTTTCGAACTGCGGGTGGCTCCAAGCGCTCTTTTC CTCGTAGAGCAC
PAH073	9	CTTTCGTTTTATTTGATGCCTGGTACTATTTTTCGAACTG

WO 2018/162465

PCT/EP2018/055449

		CGGGTGGCTCCAAGCGCTATCAGGTAATTTTATACTCCC
PAH077	10	GGGAGGTATTGGACCGCATTGAACTCTAGTATATAAACG CAGAAAGGCC
PAH078	11	ACGAGCCGGATGATTAATTGTCAATCTAGAGCCAGGCAT CAAATAAAACG
SPAH017	12	CCATCAAACAGGATTTTCG
SPAH023	13	TGCCACCTGACGTCTAAGAA

Klonierungs-Verfahren

Konstruktion von pSB1AC3\_Ptrc1O:Term

Restriktion: pSB1AC3\_Ptrc1O:GFP (XbaI + PstI) → pSB1AC3 (XbaI, PstI)  
 Amplifizierung: Ptrc1O:Term part I von pSB1AC3\_Ptrc1O:GFP  
 (PAH055 + PAH056 → 186 BP, T<sub>An</sub>: 60°C, t<sub>Elong</sub>: 10 sec)  
 Ptrc1O:Term part II von part I  
 (PAH057 + PAH058 → 262 BP, T<sub>An</sub>: 72°C, t<sub>Elong</sub>: 10 sec)  
 Gibson Klonierung: pSB1AC3 (XbaI, PstI) + Ptrc1O:Term part II  
 → pSB1AC3\_Ptrc1O:Term

Konstruktion von pSB1AC3\_PmpB:lacI\_Ptrc1O:Term

Restriktion: pSB1AC3\_Ptrc1O:Term (XbaI)  
 Dephosphorylierung: pSB1AC3\_Ptrc1O:Term (XbaI) (FastAP, Thermo)  
 Restriktion: pSB1AC\_PmpB:lacI (XbaI + SpeI)  
 Ligation: pSB1AC3\_Ptrc1O:Term (XbaI) + PmpB:lacI (XbaI\_SpeI) (1:2)  
 → pSB1AC3\_PmpB:lacI\_Ptrc1O:Term

Verifizierung by PCR: Klone mit dem PmpB:lacI Fragment in gewünschter Richtung wurden durch PCR bestimmt (SPAH017 + SPAH023 → 500 BP, T<sub>An</sub>: 61°C, t<sub>Elong</sub>: 15 sec).

Konstruktion von pPMQAK1\_PmpB:lacI\_Ptrc1O:Term

Restriktion: pPMQAK1 (EcoRI + PstI)  
 Restriktion: pSB1AC3\_PmpB:lacI\_Ptrc1O:Term (EcoRI + PstI)  
 Ligation: pPMQAK1 (EcoRI, PstI) + PmpB:lacI\_Ptrc1O:Term (EcoRI, PstI) ( 1:5)  
 → pPMQAK1\_PmpB:lacI\_Ptrc1O:Term

WO 2018/162465

PCT/EP2018/055449

Konstruktion von pPMQAK1\_PrnB:lacI\_Ptrc1O:BGTI

Restriktion: pPMQAK1\_PrnB:lacI\_Ptrc1O:Term (Spel)

Amplifizierung: oAlkBII (PAH059 + PAH067 → 1283 BP,  $T_{An}$ : 65°C,  $t_{Elong}$ : 25 sec)  
 oAlkGII (PAH068 + PAH069 → 568 BP,  $T_{An}$ : 60°C,  $t_{Elong}$ : 25 sec)  
 oAlkTII (PAH070 + PAH071 → 1204 BP,  $T_{An}$ : 65°C,  $t_{Elong}$ : 25 sec)

OE-PCR: oAlkBII+ oAlkGII (PAH063 + PAH072 → 1859 BP,  $T_{An}$ : 65°C,  $t_{Elong}$ : 60 sec)

→ oBGII  
 oBGII + oAlkTII (PAH063 + PAH073 → 3096 BP,  $T_{An}$ : 57°C,  $t_{Elong}$ : 90 sec)

→ oBGTI

Gibson: pPMQAK1\_PrnB:lacI\_Ptrc1O:Term (Spel) + oBGT  
 → pPMQAK1\_PrnB:lacI\_Ptrc1O:BGTI

Konstruktion von pRSF\_Ptrc1O:BGTI

Restriktion: pPMQAK1\_PrnB:lacI\_Ptrc1O:BGTI (XbaI)

Amplifizierung: Term von pSB1AC3\_Ptrc1O:GFP  
 (PAH077 + PAH078 → 191 BP,  $T_{An}$ : 60°C,  $t_{Elong}$ : 5 sec)

Gibson: pPMQAK1\_PrnB:lacI\_Ptrc1O:oBGTI (XbaI) + Term  
 → pRSF\_Ptrc1O:BGTI

Wachstumsbedingungen für *Synechocystis sp.* PCC6803

*Synechocystis sp.* PCC6803 wurde in YBG11 medium, basierend auf Scholnick et al. 2007, bei Zugabe von 50 mM HEPES Puffer kultiviert (Scholnick et al. 2007). Als Selektionsdruck wurden 50 µg mL<sup>-1</sup> Kanamycin zugesetzt. Standard Kultivierungsbedingungen umfassen ein Kulturvolumen von 20 mL YBG11 medium in 100 mL Erlenmeyer Schüttelflaschen mit Schikane, welche in einem Orbitalschüttler (Multitron Pro shaker, Infors, Bottmingen, Schweiz) bei 150 rpm (2.5 cm Amplitude) eingesetzt wurden. Die Kultivierungstemperatur betrug 30°C, bei einer Lichtintensität von 50 µmol m<sup>-2</sup> s<sup>-1</sup> (LED), 0.04 % CO<sub>2</sub> und einer Luftfeuchtigkeit von 75 %. Das Wachstum wurde über die optische Dichte bei einer Wellenlänge von 750 nm über ein Spektrophotometer (Libra S11, Biochrom Ltd, Cambridge, UK) verfolgt. Vorkulturen wurden über 200 µL einer Cryostock-Lösung innokuliert und unter Standard-Bedingungen für 4 - 6 Tage kultiviert. Hauptkulturen wurden ausgehend von dieser

WO 2018/162465

PCT/EP2018/055449

Vorkultur mit einer Start-OD<sub>750</sub> von 0.08 innokuliert und für 3 Tage unter Standard-Bedingungen kultiviert bis die Genexpression für einen weiteren Tag durch Zugabe von 2 mM IPTG induziert wurde.

YBG11: 1.49 g L<sup>-1</sup> NaNO<sub>3</sub>, 0.074 g L<sup>-1</sup> MgSO<sub>4</sub> · 7 H<sub>2</sub>O, 0.305 g L<sup>-1</sup> K<sub>2</sub>HPO<sub>4</sub>, 10 mL L<sup>-1</sup> YBG11 Spurenelemente (100x), 0.019 g L<sup>-1</sup> Na<sub>2</sub>CO<sub>3</sub>, 50 mM HEPES (pH 7.2); YBG11 Spurenelemente (100x): 0.36 g L<sup>-1</sup> CaCl<sub>2</sub> · 2 H<sub>2</sub>O, 0.63 g L<sup>-1</sup> Zitronensäure, 0.28 g L<sup>-1</sup> Borsäure, 0.11 g L<sup>-1</sup> MnCl<sub>2</sub> · 4 H<sub>2</sub>O, 0.02 g L<sup>-1</sup> ZnSO<sub>4</sub> · 7 H<sub>2</sub>O, 0.039 g L<sup>-1</sup> Na<sub>2</sub>MoO<sub>4</sub> · 2 H<sub>2</sub>O, 0.007 g L<sup>-1</sup> CuSO<sub>4</sub> · 5 H<sub>2</sub>O, 0.003 g L<sup>-1</sup> Co(NO<sub>3</sub>)<sub>2</sub> · 6 H<sub>2</sub>O, 0.1 g L<sup>-1</sup> FeCl<sub>3</sub> · 6 H<sub>2</sub>O, 0.6 g L<sup>-1</sup> Na<sub>2</sub>EDTA · 2 H<sub>2</sub>O

Transformation von *Synechocystis* sp. PCC6803 durch Elektroporation

Transformation von *Synechocystis* sp. PCC6803 mit dem Plasmid pRSF\_Ptrc10:BG11 wurde über Elektroporation, basierend auf einer Methode nach Ferreira et al. 2014, durchgeführt (Universidade do Porto Ferreira 2014). Elektrokompente Zellen wurden ausgehend von einer 50 mL YBG11 Hauptkultur (in 100 mL Erlenmeyer Schüttelkolben mit Schikane) mit einer OD<sub>750</sub> von 0.5 – 1 hergestellt. Die Zellen wurden durch Zentrifugation geerntet (10 min, 3180 g, 4°C), dreimal mit je 10 mL HEPES Puffer (1 mM, pH 7.5) gewaschen und in 1 mL HEPES Puffer resuspendiert. Die elektrokompenten Zellen wurde nach Zugabe von 5 % (v/v) DMSO bei – 80°C gelagert. Zur Elektroporation wurden 0.2 – 1.0 µg Plasmid-DNA zu 60 µL elektrokompenten Zellen in eine Elektroporationsküvette (2 mm Elektrodenabstand) gegeben, bei 2500 V für 5 ms gepulst (12.5 kV cm<sup>-1</sup>) (Eppendorf Eporator, Eppendorf Vertrieb Deutschland GmbH, Wesseling-Berzdorf, Deutschland) und anschließend in 50 mL YBG11 Medium (in 100 mL Erlenmeyer Schüttelkolben mit Schikane) transferiert. Nach Kultivierung unter Standard-Bedingungen für 24 h wurden die Zellen durch Zentrifugation geerntet (10 min, 3180 g, RT), in 100 µL YBG11 Medium resuspendiert und auf BG11 Agarplatten mit 50 µg mL<sup>-1</sup> Kanamycin ausgestrichen ((Stanier et al. 1971). Einzelne Kolonien wurden nach 4 – 6 Tagen bei 30°C, 20-50 µmol m<sup>-2</sup> s<sup>-1</sup> Lichtintensität (Leuchtstoffröhren), 0.04 % CO<sub>2</sub> und 80 % Luftfeuchtigkeit (poly klima GmbH, Freising, Deutschland) auf frische BG11 Agarplatten transferiert und erneut inkubiert. Die Zellmasse einer Agarplatte wurde schließlich zur Innokulation einer 20 mL YBG11 Vorkultur genutzt.

BG11 Agarplatten: 1.5 g L<sup>-1</sup> NaNO<sub>3</sub>, 0.075 g L<sup>-1</sup> MgSO<sub>4</sub> · 7 H<sub>2</sub>O, 0.036 g L<sup>-1</sup> CaCl<sub>2</sub> · 2 H<sub>2</sub>O, 0.006 g L<sup>-1</sup> citric acid, 0.04 g L<sup>-1</sup> K<sub>2</sub>HPO<sub>4</sub>, 0.006 g L<sup>-1</sup> Eisen-Ammonium-Citrat, 0.001 g L<sup>-1</sup> Na<sub>2</sub>EDTA, 0.02 g L<sup>-1</sup> Na<sub>2</sub>CO<sub>3</sub>, 1 mL L<sup>-1</sup> BG11 Spurenelemente (1000x), 0.3 % Na<sub>2</sub>S<sub>2</sub>O<sub>3</sub>, 10 mM HEPES (pH 8), 1.5 % Agar; BG11 Spurenelemente (1000x) : 2.86 g L<sup>-1</sup> Borsäure, 1.8 g



WO 2018/162465

PCT/EP2018/055449

$L^{-1} MnCl_2 \cdot 4 H_2O$ ,  $0.22 g L^{-1} ZnSO_4 \cdot 7 H_2O$ ,  $0.39 g L^{-1} Na_2MoO_4 \cdot 2 H_2O$ ,  $0.08 g L^{-1} CuSO_4 \cdot 5 H_2O$ ,  $0.05 g L^{-1} Co(NO_3)_2 \cdot 6 H_2O$

Figur 1 zeigt eine Bio-reaktive Extraktion von photosynthetisch erzeugtem Sauerstoff durch das Alkan-Monooxygenase Enzymsystem AlkBGT, welches genetisch in den Cyanobakterien-Stamm *Synechocystis sp.* PCC6803 eingeführt wurde. Die photosynthetische Lichtreaktion wurde durch Beleuchtung (Lichtintensität von  $50 \mu mol m^{-2} s^{-1}$ ) induziert, während die Kontroll-Reaktion ohne Beleuchtung stattfand. Als oxygeniertes Produkt wurde terminal hydroxyliertes Methyl-Nonanoat detektiert. CDW = Zelltrockengewicht.

Hierzu wurde das Alkan-Monooxygenase Enzymsystem AlkBGT in den Cyanobakterien-Stamm *Synechocystis sp.* PCC6803 eingesetzt (über das Plasmid pRSF\_Ptrc10:BG1II, siehe Herstellung des modifizierten Stamms oben), welcher ein potentieller Biokatalysator zur photosynthetischen Wasserstoff Produktion ist. Nach Umsetzung des Reaktionssystems von aeroben zu anaeroben Bedingungen und nach Zugabe von Methyl-Nonanoat als Substrat, konnte die Bildung von oxygeniertem Produkt bei Beleuchtung detektiert werden (Figur 1).

Da bei Reaktionsbedingungen in Dunkelheit keine Produktbildung beobachtet wurde, weisen die Ergebnisse nach, dass der für die Reaktion gebrauchte Sauerstoff aus der photosynthetischen Lichtreaktion stammte. Die spezifische Aktivität betrug  $0,9 \pm 0,1 \mu mol_{\text{oxygeniertes Substrat}} \text{min}^{-1} g_{CDW}^{-1}$  für die ersten 30 Minuten. Die Sauerstoff-Bildungsrate bei gleicher Belichtungs-Intensität von  $50 \mu mol m^{-2} s^{-1}$  betrug  $3,7 \pm 0,5 \mu mol_{O_2} \text{min}^{-1} g_{CDW}^{-1}$  (ohne Substrat-Zugabe). Somit konnten mit dem nicht-optimierten Biokatalysator bereits nahezu 25 % des entstandenen Sauerstoffes enzymatisch abgefangen werden. Bei Betrachtung der möglichen Verdünnung des Sauerstoffes aus der wässrigen Phase in die Gasphase (wässrig:Gas Phasen-Verhältnis 1:10, dimensionslose Henry Volatilität  $H_{cc} = c_{aq}/c_{gas}$  für  $O_2$  in Wasser: 0.0297 bei  $25^\circ C$  (Sander 2015)) wird deutlich, dass der molekulare Sauerstoff bereits an der Stelle seiner Erzeugung abgefangen und in das Substrat eingebunden wurde, bevor es in die Gasphase entwichen ist. Eine Optimierung des Oxygenierungs-Systems (zum Beispiel durch Erhöhung des Enzymgehaltes in der Zelle), ist möglich und würde den Anteil an extrahiertem Sauerstoff erhöhen.

#### Beispiel 2:

Technische Anwendung - Rohrbündelreaktor Konzept

WO 2018/162465

PCT/EP2018/055449

Die technische Umsetzung der beschriebenen Erfindung erfolgt bevorzugt über ein Konzept, in dem ein beleuchteter Rohrbündelreaktor zur Anwendung kommt, welcher suspendierte oder immobilisierte phototrophe Zellen beinhaltet. Ein Scale-Up des Rohrbündelreaktors in einen technischen Maßstab erfolgt durch einfache Erhöhung der Anzahl an eingesetzter Mikrokapillare. Als spezielle Form immobilisierter Zellen wird ein Biofilm-basierter Aufbau gewählt, welcher sich bereits für die Cyanobakterien-Spezies *Synechocystis sp.* PCC6803 als realisierbar erwies (David, C., K. Buhler and A. Schmid (2015). "Stabilization of single species *Synechocystis biofilms* by cultivation under segmented flow." J Ind Microbiol Biotechnol 42(7): 1083-1089). Diese technische Umsetzung bietet ein kontinuierliches Produktionssystem, welches die photosynthetische Wasserspaltung, die Wasserstoff-Produktion, die Sauerstoff Extraktion, sowie die Substrat Oxidation beinhaltet. Die nachgelagerte Aufbereitung wird dann durch das Abfangen des molekularen Wasserstoffes über die Gasphase und, bei Einsatz von Abwasser als Substrat, durch Rückführung des behandelten Abwassers zum weiterführenden Aufbereitungsprozess ermöglicht. Wird hingegen ein kombinierter biokatalytischer Produktionsprozess beabsichtigt, ist eine Abtrennung des Produktes mit erhöhter Wertschöpfung zum Beispiel durch den Einsatz einer organischen Trägerphase durchzuführen. Die folgenden Beispiele enthalten Annahmen und Werte welche entsprechend der spezifischen Anwendung und der gewählten Rahmenbedingungen angepasst werden und zeigen das Potential der Erfindung.

#### Spezifische Aktivität bezüglich der Wasserspaltung durch das PSII

Die verwendeten Mikroorganismen weisen einen Gehalt von ca. 1% des Photosystems II auf, wobei das Photosystem II eine molare Masse von 350 kDa besitzt ( $g_{CDW}^{-1}$ , Molekulargewicht PSII (Shen, J. R. (2015). "The structure of photosystem II and the mechanism of water oxidation in photosynthesis." Annu Rev Plant Biol 66: 23-48). Der höchste in vitro gemessene Wert wird von Dismukes et al. (Dismukes, G. C., R. Brimblecombe, G. A. Felton, R. S. Pryadun, J. E. Sheats, L. Spiccia and G. F. Swiegers (2009). "Development of bioinspired  $Mn_4O_4$ -cubane water oxidation catalysts: lessons from photosynthesis." Acc Chem Res 42(12): 1935-1943.) mit  $1000 s^{-1}$  angegeben. Dies führt zu einer spezifischen Aktivität des PSII von  $1700 \mu mol_{H_2O\text{Spaltung}} \text{ pro Minute je } g_{CDW}^{-1}$ . Daraus ergibt sich bezüglich einer Wasserstoffproduktion, einem Sauerstoffverbrauch und einer Substartoxidierung durch den Organismus von  $850 \mu mol_{H_2/O_2/Substrat} \text{ pro Minute je } g_{CDW}^{-1}$ .

#### Produkt Ertrag durch einen Rohrbündelreaktor Prozess

Auf 20 000 Mikrokapillaren mit je 2 m Länge und 5 mm Durchmesser werden  $10 g_{CDW} L^{-1}$  Biomasse mit einer volumetrischen Produktivität von  $0.51 mol_{H_2/O_2/Substrat} L^{-1} h^{-1}$  eingesetzt.

WO 2018/162465

PCT/EP2018/055449

Es ergibt sich ein Gesamtvolumen von 785 L (39.3 mL Kapillare<sup>-1</sup>). Bei 2920 Sonnenstunden im Jahr (Licht Verfügbarkeit 8 h pro Tag, 365 Tage) produziert das System 1169 kmol Wasserstoff, sowie oxidiertes Substrat pro Jahr.

#### Energieertrag

Es gilt die Voraussetzung, dass der Prozess nicht durch die Hydrogenase limitiert ist. Auf Basis eines Molekulargewichts von 2 g/mol weist Wasserstoff eine volumetrische Produktaktivität von  $1.02 \text{ g}_{\text{H}_2} \text{ L}^{-1} \text{ h}^{-1}$ . Daraus ergibt sich ein Produktertrag von 2338 kg Wasserstoff pro Jahr von denen 60 % also 1402 kg rückgewonnen werden. Bei einem zugrunde gelegten Energiegehalt von 33.3 kWh je Kilogramm Wasserstoff (Wikipedia) kann mit dem erfindungsgemäßen Prozess eine Energie von 46 686 kWh pro Jahr generiert werden.

WO 2018/162465

PCT/EP2018/055449

Patentansprüche

1. Verfahren zur bioreaktiven Extraktion erzeugten Sauerstoffs aus einem Reaktionsraum, umfassend die folgenden Schritte:
  - Bestrahlen zumindest eines phototrophen Mikroorganismus unter anaeroben Bedingungen in einem Reaktionsraum, und
  - in situ Binden von entstehendem Sauerstoff mittels des Mikroorganismus durch Oxidation eines Sauerstoff-verwertenden Substrats.
2. Verfahren nach Anspruch 1, wobei der zumindest eine phototrophe Mikroorganismus, zumindest ein Sauerstoff-umsetzendes Enzym aufweist oder produziert.
3. Verfahren nach Anspruch 2, wobei das zumindest eine Enzym ausgewählt ist aus der Gruppe Hydrogenase, Nitrogenase und/oder Oxidoreduktase.
4. Verfahren nach einem der Ansprüche 1 bis 3, wobei bei der Bestrahlung des zumindest einen phototrophen Mikroorganismus neben Sauerstoff auch Wasserstoff oder Methanol frei wird.
5. Verfahren nach einem der vorhergehenden Ansprüche, dadurch gekennzeichnet, dass die Oxidoreduktasen ausgewählt sind aus der Gruppe der Oxidasen oder Oxygenasen, vorzugsweise Monooxygenasen, Dioxygenasen oder coenzym-unabhängige Oxygenasen.
6. Verfahren nach einem der vorhergehenden Ansprüche, wobei als phototropher Mikroorganismus Algen oder Cyanobakterien eingesetzt werden, vorzugsweise Cyanobakterien.
7. Verfahren nach einem der vorhergehenden Ansprüche, dadurch gekennzeichnet, dass als Mikroorganismus ein, insbesondere genetisch modifizierter, Cyanobakterienstamm eingesetzt wird, der das Alkan-Monooxygenase-Enzymsystem AlkBGT aufweist.

WO 2018/162465

PCT/EP2018/055449

8. Verfahren nach einem der vorhergehenden Ansprüche, dadurch gekennzeichnet, dass der genetisch modifizierte Cyanobakterienstamm *Synechocystis* sp. PCC6803 eingesetzt wird, der das Alkan-Monooxygenase-Enzymsystem AlkBGT aufweist oder produziert.
9. Verfahren nach Anspruch 8, dadurch gekennzeichnet, dass als Substrat Methylnonanoat verwendet wird.
10. Verwendung von phototrophen Mikroorganismen, die neben Hydrogenasen, Nitrogenasen oder Oxidoreduktasen als Wasserstoff-produzierendes Enzym zusätzlich Oxidoreduktasen als Sauerstoff-umsetzende Enzyme aufweisen oder produzieren, bei der Gewinnung von Wasserstoff (H<sub>2</sub>) oder Methanol und Sauerstoff (O<sub>2</sub>) aus Wasser oder wässrigen Flüssigkeiten und Lösungen und zur simultanen in-situ Entfernung des Sauerstoffs (O<sub>2</sub>) unter Verwendung entsprechender Substrate, die mit dem Sauerstoff Produkte bilden.
11. Photobioreaktor umfassend den genetisch modifizierten Cyanobakterienstamm *Synechocystis* sp. PCC6803, der das Alkan-Monooxygenase-Enzymsystem AlkBGT aufweist oder produziert.

WO 2018/162465

PCT/EP2018/055449

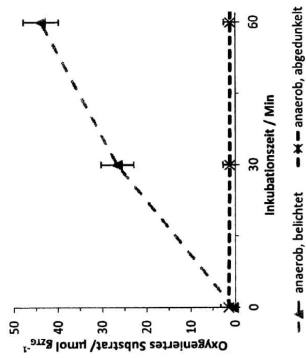


Fig. 1

ERSATZBLATT (REGEL 26)  
1/1

INTERNATIONAL SEARCH REPORT		International application No PCT/EP2018/055449
A. CLASSIFICATION OF SUBJECT MATTER INV. C12M1/00 C12M1/107 C12P5/02 C12P3/00 ADD.		
According to International Patent Classification (IPC) or to both national classification and IPC		
B. FIELDS SEARCHED		
Minimum documentation searched (classification system followed by classification symbols) C12M C12P		
Documentation searched other than minimum documentation to the extent that such documents are included in the fields searched		
Electronic data base consulted during the international search (name of data base and, where practicable, search terms used) EPO-Internal, BIOSIS, Sequence Search, EMBASE, WPI Data		
C. DOCUMENTS CONSIDERED TO BE RELEVANT		
Category*	Citation of document, with indication, where appropriate, of the relevant passages	Relevant to claim No.
X	DE 10 2010 015807 A1 (EVONIK DEGUSSA GMBH [DE]) 20 October 2011 (2011-10-20) claims 12-15; examples -----	11
A	RAINER GROSS ET AL: "Engineered catalytic biofilms for continuous large scale production of n -octanol and ( S )-styrene oxide", BIOTECHNOLOGY AND BIOENGINEERING, vol. 110, no. 2, 1 February 2013 (2013-02-01), pages 424-436, XP55490337, US ISSN: 0006-3592, DOI: 10.1002/bit.24629 -----	1-11
A	DE 10 2007 002009 A1 (SALVETZKI RALF [DE]) 26 June 2008 (2008-06-26) cited in the application -----	1-11
- / - -		
<input checked="" type="checkbox"/> Further documents are listed in the continuation of Box C.		<input checked="" type="checkbox"/> See patent family annex.
* Special categories of cited documents :		
*A* document defining the general state of the art which is not considered to be of particular relevance		*T* later document published after the international filing date or priority date and not in conflict with the application but cited to understand the principle or theory underlying the invention
*E* earlier application or patent but published on or after the international filing date		*X* document of particular relevance; the claimed invention cannot be considered novel or cannot be considered to involve an inventive step when the document is taken alone
*L* document which may throw doubts on priority claim(s) or which is cited to establish the publication date of another citation or other special reason (as specified)		*Y* document of particular relevance; the claimed invention cannot be considered to involve an inventive step when the document is combined with one or more other such documents, such combination being obvious to a person skilled in the art
*O* document referring to an oral disclosure, use, exhibition or other means		*8* document member of the same patent family
*P* document published prior to the international filing date but later than the priority date claimed		
Date of the actual completion of the international search  24 July 2018		Date of mailing of the international search report  01/08/2018
Name and mailing address of the ISA/ European Patent Office, P.B. 5818 Patentaan 2 NL - 2280 HV Rijswijk Tel: (+31-70) 340-2040, Fax: (+31-70) 340-3016		Authorized officer  Kania, Thomas

2

Form PCT/ISA/210 (second sheet) (April 2005)

page 1 of 2

INTERNATIONAL SEARCH REPORT		International application No PCT/EP2018/055449
C(Continuation). DOCUMENTS CONSIDERED TO BE RELEVANT		
Category*	Citation of document, with indication, where appropriate, of the relevant passages	Relevant to claim No.
A	NAGARAJAN DILLIRANI ET AL: "Recent insights into biohydrogen production by microalgae - From biophotolysis to dark fermentation", BIORESOURCE TECHNOLOGY, ELSEVIER, AMSTERDAM, NL, vol. 227, 30 December 2016 (2016-12-30), pages 373-387, XP029881857, ISSN: 0960-8524, DOI: 10.1016/J.BIORTECH.2016.12.104 -----	1-11
A	NADINE LADKAU ET AL: "The microbial cell-functional unit for energy dependent multistep biocatalysis", CURRENT OPINION IN BIOTECHNOLOGY., vol. 30, 1 December 2014 (2014-12-01), pages 178-189, XP055490341, GB ISSN: 0958-1669, DOI: 10.1016/j.copbio.2014.06.003 -----	1-11
X,P	ANNA HOSCHEK ET AL: "Overcoming the Gas-Liquid Mass Transfer of Oxygen by Coupling Photosynthetic Water Oxidation with Biocatalytic Oxyfunctionalization", ANGEWANDTE CHEMIE INTERNATIONAL EDITION, vol. 56, no. 47, 20 November 2017 (2017-11-20), pages 15146-15149, XP055490345, ISSN: 1433-7851, DOI: 10.1002/anie.201706886 the whole document -----	1-11
2		



## INTERNATIONAL SEARCH REPORT

Information on patent family members

International application No

PCT/EP2018/055449

Patent document cited in search report	Publication date	Patent family member(s)	Publication date
DE 102010015807 A1	20-10-2011	BR 112012027051 A2	06-12-2016
		CA 2796777 A1	27-10-2011
		CN 102947328 A	27-02-2013
		CN 106279380 A	04-01-2017
		DE 102010015807 A1	20-10-2011
		EP 2560987 A1	27-02-2013
		JP 5936601 B2	22-06-2016
		JP 2013528361 A	11-07-2013
		RU 2012148996 A	27-05-2014
		TW 201207105 A	16-02-2012
		US 2013052700 A1	28-02-2013
		WO 2011131420 A1	27-10-2011
-----			
DE 102007002009 A1	26-06-2008	NONE	
-----			

Form PCT/ISA/210 (patent family annex) (April 2006)

INTERNATIONALER RECHERCHENBERICHT		Internationales Aktenzeichen PCT/EP2018/055449
<b>A. KLASSIFIZIERUNG DES ANMELDUNGSGEGENSTANDES</b> INV. C12M1/00 C12M1/107 C12P5/02 C12P3/00 ADD.		
Nach der internationalen Patentklassifikation (IPC) oder nach der nationalen Klassifikation und der IPC		
<b>B. RECHERCHIERTE GEBIETE</b> Recherchierter Mindestprüfstoff (Klassifikationsystem und Klassifikationsymbole) C12M C12P		
Recherchierte, aber nicht zum Mindestprüfstoff gehörende Veröffentlichungen, soweit diese unter die recherchierten Gebiete fallen		
Während der internationalen Recherche konsultierte elektronische Datenbank (Name der Datenbank und evtl. verwendete Suchbegriffe) EPO-Internal, BIOSIS, Sequence Search, EMBASE, WPI Data		
<b>C. ALS WESENTLICH ANGESEHENE UNTERLAGEN</b>		
Kategorie*	Bezeichnung der Veröffentlichung, soweit erforderlich unter Angabe der in Betracht kommenden Teile	Betr. Anspruch Nr.
X	DE 10 2010 015807 A1 (EVONIK DEGUSSA GMBH [DE]) 20. Oktober 2011 (2011-10-20) Ansprüche 12-15; Beispiele	11
A	----- RAINER GROSS ET AL: "Engineered catalytic biofilms for continuous large scale production of n -octanol and ( S )-styrene oxide", BIOTECHNOLOGY AND BIOENGINEERING, Bd. 110, Nr. 2, 1. Februar 2013 (2013-02-01), Seiten 424-436, XP55490337, US ISSN: 0006-3592, DOI: 10.1002/bit.24629	1-11
A	----- DE 10 2007 002009 A1 (SALVETZKI RALF [DE]) 26. Juni 2008 (2008-06-26) in der Anmeldung erwähnt	1-11
----- -/-		
<input checked="" type="checkbox"/> Weitere Veröffentlichungen sind der Fortsetzung von Feld C zu entnehmen <input checked="" type="checkbox"/> Siehe Anhang Patentfamilie		
* Besondere Kategorien von angegebenen Veröffentlichungen : "A" Veröffentlichung, die den allgemeinen Stand der Technik definiert, aber nicht als besonders bedeutung anzusehen ist "E" frühere Anmeldung oder Patent, die bzw. das jedoch erst am oder nach dem internationalen Anmeldedatum veröffentlicht worden ist "L" Veröffentlichung, die geeignet ist, einen Prioritätsanspruch zweifelhaft erscheinen zu lassen, oder durch die das Veröffentlichungsdatum einer anderen im Recherchenbericht genannten Veröffentlichung belegt werden soll oder die aus einem anderen besonderen Grund angegeben ist (wie ausgeführt) "O" Veröffentlichung, die sich auf eine mündliche Offenbarung, eine Benutzung, eine Ausstellung oder andere Maßnahmen bezieht "P" Veröffentlichung, die vor dem internationalen Anmeldedatum, aber nach dem beanspruchten Prioritätsdatum veröffentlicht worden ist "T" Spätere Veröffentlichung, die nach dem internationalen Anmeldedatum oder dem Prioritätsdatum veröffentlicht worden ist und mit der Anmeldung nicht kollidiert, sondern nur zum Verständnis des der Erfindung zugrundeliegenden Prinzips oder der ihr zugrundeliegenden Theorie angegeben ist "X" Veröffentlichung von besonderer Bedeutung; die beanspruchte Erfindung kann allein aufgrund dieser Veröffentlichung nicht als neu oder auf erfindersicher Tätigkeit beruhend betrachtet werden "Y" Veröffentlichung von besonderer Bedeutung; die beanspruchte Erfindung kann nicht als auf erfindersicher Tätigkeit beruhend betrachtet werden, wenn die Veröffentlichung mit einer oder mehreren Veröffentlichungen dieser Kategorie in Verbindung gebracht wird und diese Verbindung für einen Fachmann nahelegend ist "8" Veröffentlichung, die Mitglied derselben Patentfamilie ist		
Datum des Abschlusses der internationalen Recherche		Absendedatum des internationalen Recherchenberichts
24. Juli 2018		01/08/2018
Name und Postanschrift der Internationalen Recherchenbehörde Europäisches Patentamt, P.B. 5818 Patentlaan 2 NL- 2280 HV Rijswijk Tel: (+31-70) 340-2040, Fax: (+31-70) 340-3016		Bevollmächtigter Bediensteter  Kania, Thomas

2

Formblatt PCT/ISA210 (Blatt 2) (April 2006)

INTERNATIONALER RECHERCHENBERICHT		Internationales Aktenzeichen PCT/EP2018/055449
C. (Fortsetzung) ALS WESENTLICH ANGESEHENE UNTERLAGEN		
Kategorie*	Bezeichnung der Veröffentlichung, soweit erforderlich unter Angabe der in Betracht kommenden Teile	Betr. Anspruch Nr.
A	NAGARAJAN DILLIRANI ET AL: "Recent insights into biohydrogen production by microalgae - From biophotolysis to dark fermentation", BIORESOURCE TECHNOLOGY, ELSEVIER, AMSTERDAM, NL, Bd. 227, 30. Dezember 2016 (2016-12-30), Seiten 373-387, XP029881857, ISSN: 0960-8524, DOI: 10.1016/J.BIORTECH.2016.12.104 -----	1-11
A	NADINE LADKAU ET AL: "The microbial cell-functional unit for energy dependent multistep biocatalysis", CURRENT OPINION IN BIOTECHNOLOGY., Bd. 30, 1. Dezember 2014 (2014-12-01), Seiten 178-189, XP055490341, GB ISSN: 0958-1669, DOI: 10.1016/j.copbio.2014.06.003 -----	1-11
X,P	ANNA HOSCHEK ET AL: "Overcoming the Gas-Liquid Mass Transfer of Oxygen by Coupling Photosynthetic Water Oxidation with Biocatalytic Oxyfunctionalization", ANGEWANDTE CHEMIE INTERNATIONAL EDITION, Bd. 56, Nr. 47, 20. November 2017 (2017-11-20), Seiten 15146-15149, XP055490345, ISSN: 1433-7851, DOI: 10.1002/anie.201706886 das ganze Dokument -----	1-11

2

Formblatt PCT/ISA210 (Fortsetzung von Blatt 2) (April 2006)

Seite 2 von 2

**INTERNATIONALER RECHERCHENBERICHT**

Angaben zu Veröffentlichungen, die zur selben Patentfamilie gehören

Internationales Aktenzeichen

PCT/EP2018/055449

Im Recherchenbericht angeführtes Patentdokument	Datum der Veröffentlichung	Mitglied(er) der Patentfamilie	Datum der Veröffentlichung
DE 102010015807 A1	20-10-2011	BR 112012027051 A2	06-12-2016
		CA 2796777 A1	27-10-2011
		CN 102947328 A	27-02-2013
		CN 106279380 A	04-01-2017
		DE 102010015807 A1	20-10-2011
		EP 2560987 A1	27-02-2013
		JP 5936601 B2	22-06-2016
		JP 2013528361 A	11-07-2013
		RU 2012148996 A	27-05-2014
		TW 201207105 A	16-02-2012
		US 2013052700 A1	28-02-2013
		WO 2011131420 A1	27-10-2011
-----			
DE 102007002009 A1	26-06-2008	KEINE	
-----			

---

## Curriculum vitae

### Personal data

---

Name: Anna Hoschek  
Date of birth: 12.11.1989 in Marl, Germany  
Nationality: German  
Family status: Single

### Education

---

11/ 2014 – 01/ 2019 **Ph. D. Student** at the Department of Solar Materials, Helmholtz-Centre for Environmental Research - UFZ, Leipzig, Germany, under supervision of Prof. Dr. Andreas Schmid and Prof. Dr. Bruno Bühler

10/ 2012 – 07/ 2014 **Studies in Chemical Biology**, Faculty of Chemistry and Chemical Biology, TU Dortmund University, Dortmund, Germany  
Degree: **Master of Science**

10/ 2009 – 09/ 2012 **Studies in Chemical Biology**, Faculty of Chemistry and Chemical Biology, TU Dortmund University, Dortmund, Germany  
Degree: **Bachelor of Science**

08/ 2006 – 10/ 2009 Hans-Böckler-vocational school, Marl, Germany  
Degree: State-certified **technical assistant in biology** (BTA)

08/ 2006 – 06/ 2009 Hans-Böckler-vocational school, Marl, Germany  
Degree: University entrance diploma (**Abitur**)

08/ 2000 – 06/ 2006 Maristen Realschule (Secondary school), Recklinghausen, Germany  
Degree: Secondary school certificate (**Fachoberschulreife**)

**Peer reviewed articles**

---

**Hoschek, A.**, Toepel, J., Hochkeppel, A., Karande, R., Bühler, B., Schmid, A., (2019)  
Light-dependent and aeration-independent gram-scale hydroxylation of cyclohexane to cyclohexanol by CYP450 harboring *Synechocystis* sp. PCC 6803  
*Biotechnol. J.*, DOI: 10.1002/biot.201800724

**Hoschek, A.**, Bühler, B., Schmid, A., (2019)  
Stabilization and scale-up of photosynthesis-driven  $\omega$ -hydroxylation of nonanoic acid methyl ester by two-liquid phase whole-cell biocatalysis  
*Biotechnol. Bioeng.*, DOI: 10.1002/bit.27006

**Hoschek, A.**, Heuschkel I., Schmid, A., Bühler, B., Karande, R., Bühler, K., (2019)  
Mixed-species biofilms for high-cell-density application of *Synechocystis* sp. PCC 6803 in capillary reactors for continuous cyclohexane oxidation to cyclohexanol  
*Bioresour. Technol.*, **282**, 171 – 178

**Hoschek, A.**, Schmid, A., Bühler, B., (2018)  
*In situ* O<sub>2</sub> generation for biocatalytic oxyfunctionalization reactions  
*ChemCatChem*, **10** (23), 5366 – 5371

**Hoschek, A.**, Bühler, B., Schmid, A., (2017)  
Overcoming the gas-liquid mass transfer of oxygen by coupling photosynthetic water oxidation with biocatalytic oxyfunctionalization  
*Angew. Chem.-Int. Edit.* **56** (47), 15146 – 15149

Willrodt, C., **Hoschek, A.**, Bühler, B., Schmid, A., Julsing, M.K., (2016)  
Decoupling production from growth by magnesium sulfate limitation boosts de novo limonene production  
*Biotechnol. Bioeng.* **113** (6), 1305 – 1314

Willrodt, C., **Hoschek, A.**, Bühler, B., Schmid, A., Julsing, M.K., (2015)  
Coupling limonene formation and oxyfunctionalization by mixed-culture resting cell fermentation  
*Biotechnol. Bioeng.* **112** (9), 1738 – 1750

**Patent applications**

---

Karande, R., Bühler, K., **Hoschek, A.**, Heuschkel, I., Schmid, A. (2018)  
Concept for stabilizing photoautotrophic biofilms for the continuous production of value added compounds and energy carriers.  
PCT/EP2018/074746

Schmid, A., **Hoschek, A.**, Bühler, B., (2017)  
Verfahren zur bioreaktiven Extraktion erzeugten Sauerstoffs aus einem Reaktionsraum, sowie Verwendung von phototrophen Mikroorganismen bei der Gewinnung von Wasserstoff  
Germany, DE 10 2017 104 648 A1; International, WO2018/162465

**Poster presentations**

---

**Hoschek, A., Bühler B. and Schmid A. (2018)**

Whole-cell oxygenation biocatalysis driven by photosynthesis

Metabolic Engineering 12

24. - 28. June 2018 Munich, Germany

**Hoschek, A., Bühler B. and Schmid A. (2017)**

Whole cell oxygenation biocatalysis driven by photosynthesis.

BioTrans 2017 - 13<sup>th</sup> International Symposium on Biocatalysis and Biotransformations

9. - 13. July 2017 Budapest, Ungarn

**Hoschek, A., Bühler B. and Schmid A. (2017)**

Whole cell oxygenation biocatalysis driven by photosynthesis.

Summer School Biotransformations 2017

16. - 19. July 2017 Hannover, Germany